UNIVERSIDAD MICHOACANA DE SAN NICOLAS DE HIDALGO

FACULTAD DE INGENIERIA ELECTRICA

DIVISION DE ESTUDIOS DE POSGRADO

NONLINEAR OSCILLATIONS ANALYSIS OF POWER SYSTEMS INCLUDING FACTS DEVICES BASED ON THE MODAL SERIES METHOD

By

Osvaldo Rodríguez Villalón

Thesis presented for the Degree of

DOCTOR IN SCIENCES
IN ELECTRICAL ENGINEERING

Thesis Advisor:
Ph.D. J. Aurelio Medina Rios

Morelia, Mich., June 2012

ACKNOWLEDGEMENTS

A goal such as a Doctoral degree is traduced in a personal and professional challenge, large hours of intensive work, complicated theorems, plenty of time in front of the computer, etc. but on the other side, in a bundle of great experiences that cannot be written and detailed in a final document.

My PhD degree would have not been possible without the invaluable help of many persons involved in different ways.

I would like to thank to Dr. Aurelio Medina for his encouragement, friendship, advices and support even when the situation seems very complicated.

Special thanks to my reviewers, specially to Dr. Claudio R. Fuerte for guided me at the beginning of my work and Dr. Jesus Rico for the large discussions on the interesting and unfinished topic of the nonlinear systems.

For other side, my best regards to the Universidad de Guanajuato for its support during my study leave and specially to Dr. Oscar Ibarra and M.E. René Jaime-Rivas, for their help.

Many thanks to the Departamento de Ingeniería Eléctrica, specially to Dr. Miguel Angel Hernández Figueroa for his invaluable support and trust in my project. Also special mention to my colleagues for pushing me to finish.

A very special mention to Dr. Arturo Roman Messina for his vital advisory and very interesting discussions during my study leave in Guadalajara. I really appreciate your time, friendship and uninterested help. Of course, my thankful with CINVESTAV-Guadalajara for the facilities.

The unforgettable 10 months that I spent in the beautiful Zurich, Switzerland were possible thanks to Professor Göran Andersson. All my thanks for the great opportunity and also for the interesting technical discussions. Also, my best acknowledgements to my colleagues from Power Systems Laboratory ETH Zurich, for their friendship and the warm environment during my study leave. Thanks for everyone.

Thanks to PROMEP for the study leave and scholarship; in the same way to CONACYT for the scholarship

To Universidad Michoacana de San Nicolás de Hidalgo, for its generosity and vision despite the people that very often tries to kidnap it.

My best to my colleagues and partners during my PhD studies at the DEP-FIE.

Finally, all my thanks to my beloved wife for her encouragement and patient during my large absences. At the end, the goal has been obtained.

To every person whose contribution for me and for my family was crucial and relevant.

THIS PAGE IS INTENTIONALLY LEFT BLANK

This work is dedicated to my dear children

Diana, Paola Isabel

and Darío

THIS PAGE IS INTENTIONALLY LEFT BLANK

ABSTRACT

This thesis describes the procedure followed to represent the nonlinear modal interaction of a power system dynamic based on the modal series method. The method is based on the multidimensional Laplace transform and theorems of association of variables. Through this systematic procedure it is possible to represent the nonlinear modal interaction of a nonlinear system. Furthermore, the method is capable of identifying nonlinear forced oscillations due to an arbitrary excitation function.

The procedure allows the computation of analytical approximate functions, which are independent of any resonance condition. In addition, the method is capable for representing nonlinear transfer functions, since the solution of the method is based on an uncoupled nonlinear system solved through Laplace transform.

The modal expansion procedure is extended to the case of higher order multidimensional nonlinear systems described by nonlinear differential equations. A detailed description about the analytical steps needed to form the method is exemplified by a third order nonlinear model. The proposed method is experimented with a synchronous machine-infinite busbar power system which allows a detailed description on the application of the higher order modal series method.

The method is studied through the 3 machines-9 buses and the New England 10 machines-39 buses test power systems, where the accuracy of the approach is verified through comparison with respect to the direct integration of the nonlinear dynamic system. The main nonlinear modal interactions are remarked, which clarify the behavior of the nonlinear oscillations

The study of the system when a UPFC is connected is analyzed. The closed form solution of the set of algebraic-differential equations is obtained by the modal series method. The nonlinear contribution and the modal interaction are considered through the analysis of nonlinear indices, and linear and nonlinear participation factors in a SMIB-UPFC test system.

THIS PAGE IS INTENTIONALLY LEFT BLANK

CONTENT

LIST OF SYMBOLS AND ACRONYMS

Nonlinear state variables vector	$\mathbf{x}$
Initial conditions of the nonlinear state variables vector	$\mathbf{x}_0$
Stable equilibrium point	$\mathbf{x}_{sep}$
Right eigenvectors	$\mathbf{U}$
Left eigenvectors	$\mathbf{V}$
Jordan canonical state variables vector	$\mathbf{y}$
Normal forms nonlinear state variable	z
Eigenvalue	λ
Nonlinear resonant coefficients	h_{2kl}^{j}
Nonlinear constant of the Dobson's nonlinear benchmark system	ε
Nonlinear second order coefficients	C_{kl}^{j}
Nonlinear third order coefficients	D_{pqr}^{j}
Multidimensional Laplace transform function	$F\left(s_1, s_2, \ldots, s_n\right)$
State matrix (Jacobian matrix)	$\mathbf{A}$
Hessian matrix (third order partial differential matrix)	$\mathbf{H}$
Rotor angle	δ
Rotor speed	ω
Mechanical power	P_m
Damping coefficient	D_m
Inertia constant	H
Direct axis	d
Quadrature axis	q
Quadature transient voltage	E'_q

Direct axis current and voltage	I_d, V_d
Field voltage	E_{fd}
Quadrature axis current and voltage	I_q, V_q
Reduced admittance matrix	$\mathbf{Y}_{RED}$
Modulation coefficient and angle of VSC shunt of the UPFC	m_E, δ_E
Modulation coefficient and angle of VSC series of the UPFC	m_B, δ_B
Reactance of the VSC shunt	x_E
Reactance of the VSC series	x_B
Voltage of VSC shunt	V_{SH}
Voltage of VSC series	V_{SERIES}
Stable equilibrium point	SEP
Unified power flow controller	UPFC
Normal Forms method	NF
Modal Series method	MS
Automatic voltage regulator	AVR
Voltage source converter	VSC

LIST OF FIGURES

LIST OF TABLES

THIS PAGE IS INTENTIONALLY LEFT BLANK

LIST OF PUBLICATIONS

Conference Proceedings Papers

- Osvaldo Rodriguez, Aurelio Medina, "*Nonlinear Transfer Function Based on Forced Response Modal Series Analysis*", accepted for presentation at the 2011 North American Power Symposium NAPS 2011, Boston, Massachusetts, August 4-6, 2011
- Rodriguez, Osvaldo; Medina, Aurelio; , "*Stressed power systems analysis by using higher order Modal Series method: A basic study*," Transmission and Distribution Conference and Exposition, 2010 IEEE PES , pp.1-7, 19-22 April 2010
- Osvaldo Rodríguez, Aurelio Medina, A. Román-Messina, Claudio R. Fuerte Esquivel, "*The Modal Series Method and Multi-Dimensional Laplace Transforms for the Analysis of Nonlinear Effects in Power Systems Dynamics*", IEEE General Meeting 2009, Calgary, Alberta, Canada, July 2009
- Osvaldo Rodríguez, C. R. Fuerte-Esquivel, Aurelio Medina, "*A Comparative Analysis of Methodologies for the Representation of Nonlinear Oscillations in Dynamic Systems*", IEEE Power Tech 2007, July 2007, Lausanne, Switzerland

Journal Papers

- Osvaldo Rodríguez, Aurelio Medina, "*Stressed Power System Analysis by Using Higher Order Modal Series Method*", submitted to the IEEE Transactions on Power Systems, February 2012
- Osvaldo Rodríguez, Aurelio Medina, A. Román-Messina, Claudio R. Fuerte Esquivel, "*A Methodology Based on Modal Series and Multi-Dimensional Laplace Transform for the Assessment of Nonlinear System Dynamics*", to be submitted to IEEE Transactions on Power Systems, July 2012
- Osvaldo Rodriguez, Aurelio Medina, "*Analytical Method of Nonlinear Transfer Function Based On Forced Response Modal Series Analysis*", to be submitted to Electric Power Systems Research, July 2012

- Osvaldo Rodríguez, Aurelio Medina, Göran Andersson, Claudio R. Fuerte Esquivel "*Damping Oscillations Analysis in Power Systems with UPFC's by Using Modal Series Technique*", to be submitted to Electric Power Systems Research, August 2012
- Osvaldo Rodríguez, Aurelio Medina, A.Roman-Messina, Claudio R. Fuerte-Esquivel, "*A Systematic Procedure Based on Modal Series for the Assessment of Nonlinear Electric Circuits*", to be submitted to the IEEE Transactions on Circuits and Systems Regular Papers, August 2012

1

INTRODUCTION

1.1 MOTIVATION

This doctoral research is focused on the application of a methodology, different than classical modal analysis that allows the interpretation of dynamic operation in power systems when subjected to small perturbations. The power systems present electromechanical oscillations principally due to changes in their structural aspect, which become into a different network topology. Small signal stability is based on small perturbations around a stable equilibrium point with short duration times (just a few time cycles) which increase such oscillations presenting low frequency characteristics. These oscillation effects are mainly due to power system commutations, load variations, switching devices operating in power systems, etc.

The oscillations phenomena have been strongly studied using methodologies based on modal analysis. However, the conventional modal analysis only incorporates the linear part in its analysis, leaving out of scope the nonlinear contribution to the dynamics, which is a part of almost any physical system such as power systems. The method of Normal Forms of vector fields (NF) and Modal Series (MS) method have important characteristics contained in their mathematical fundamentals, which identify them with respect to traditional modal analysis, due to the information of the so called nonlinear interaction that can be obtained.

The Modal Series method, as it will be described along this investigation, represents a serious alternative of solution for the analysis of nonlinear oscillations. It is based as in the same philosophy of the Normal Forms method, *i.e.* on Taylor series expansion from the nonlinear system. Through application of a linear transformation and Laplace theorems it is possible to determine an analytical closed form solution, explicitly containing nonlinear characteristics. Throughout the document, the mathematical fundaments in which the Modal Series method is based and the information concerning

on the nonlinear characteristics of the power system under study will be remarked. It is also important to consider that the Modal Series method may be able to be used in analysis of different physical systems with nonlinear features.

This doctoral research attempts to contribute to the analysis of nonlinear oscillations in power systems extending the Modal Series method and its applicability by using multidimensional Laplace transform, association of variables theorems, forced input response of the nonlinear system and incorporation of FACTS devices to the nonlinear dynamic power system modeling and analysis.

1.2 OVERVIEW OF THE STATE OF ART

Nonlinear oscillations in power systems have been studied for several years. Power systems have strong nonlinear characteristics which require the use of multiple analytical, numerical and mathematical strategies for their study. Such nonlinearities are mainly produced due to the nonlinear interaction between electrical and mechanical components of electric generators (which is studied through the swing equation), excitation limits and magnetic saturation, just for mentioning some of them. Electric loads may have high nonlinear characteristics; therefore representing a big source of nonlinear contribution, mostly due to the switching operation conditions and nonlinear characteristics of frequency and voltage.

An important problem addressed by the power systems industry is related to the low frequency electromechanical oscillations. These oscillations are identified depending on the frequency range and the existing devices in the system; *e.g.* oscillations associated with single generators are called local modes or plant modes (normally classified between 0.7 to 2.0 Hz); oscillations presented over a group of generators so called inter-area oscillations, in the range of 0.1 to 0.8 Hz [Klein *et al.* 1991].

The main analytical tool used for the analysis of low frequency phenomena in power systems has been the modal analysis, based on eigenvalues characteristics of the dynamic system [Rogers 2000]. The system is linearized around at a stable equilibrium point, which represents a stable dynamic operation situation. Under this analysis, the system operation is restricted to only consider the behavior due to the linear part, leaving out of scope the nonlinear contribution.

Despite the consideration of only linear characteristics of the system under study, the information obtained from modal analysis is of vital concern; *e.g.* frequency oscillations, damping rates and the extension to participation factors and mode shapes are very important to determine the stability of the power system and the nature of oscillations; taking place presented after a disturbance condition or any other operating condition considered. An important development, called selective modal analysis [Pérez-Arriaga *et al.* 1982] details the participation factors based on modal analysis, being one of the most relevant contributions in the area of modal analysis based on linear techniques.

In the same way, modal analysis has been carried out to prove local mode oscillations, interarea mode oscillations, detailed representation of large regions within interconnected power systems, excitation systems, speed governors, tuning of PSS, HVDC modulation, FACTS controllers, load characteristics, etc. [Kundur 1994] [Kundur and Wang 2002].

On the other side, since the modal analysis only assumes the linear contribution of a nonlinear system transformed to a linear one through a linearization process, one question emerges from this theory: how important may be the contribution of the nonlinear part to the nonlinear power system analysis? This can be the philosophy of including different methodologies, which model the power system adding the nonlinear part.

Working groups associated to the Task forces from IEEE and CIGRE have resumed main ideas in order to consider nonlinear analysis of power systems. The method of Normal Forms of nonlinear vector fields emerged as an important analytical tool to investigate the qualitative behavior of nonlinear dynamical systems in a general point of view [Kahn and Zarmi 1998] [Guckenheimer and Holmes 1986] [Arrowsmith and Place 1994] [Nayfeh 1993], and subsequently developed by the group of the University of Iowa for applications to power systems [Lin, *et al.* 1996] [Saha *et al.* 1997] [Jang *et al.* 1998] [Vittal *et al.* 1998]. More recently, other researchers have taken the Normal Forms as one of the main methods applied to the analysis of nonlinear dynamic power systems with several applications [Barocio and Messina 2003] [Barocio *et al.* 2004] [Liu, *et al.* 2005] [Betancourt *et al.* 2006]. Some other contributions are based on Volterra series analysis [Schetzen 1980], bifurcations theory [Abed and Varaiya 1984] [Ajjarapu and Lee 1992], and more recently through Hilbert transforms [Messina and Vittal 2006] [Liu *et al.* 2004] and modal analysis using the theory of normal modes [Betancourt *et al.* 2009] and bilinear systems [Arroyo *et al.* 2006].

In addition, in [Pariz *et al.* 2003] and [Schanechi, *et al.* 2003] the Modal Series method has been proposed as an alternative to the nonlinear analysis of dynamic systems. It is based on transforming a linearized system around a stable equilibrium point; a straightforward linear transformation allows to obtain a linear approximation of a nonlinear system. In the method of Modal Series, the resonance conditions are not of concern, so the system is solved for any set of eigenvalues.

1.2.1 Main Contributions on Normal Forms Method

The method of Normal Forms of vector fields has been utilized in order to analyze nonlinear oscillations in power systems. The method is based on two transformations: beginning with a linearization process around a stable equilibrium point, obtained through Taylor series expansion. An application of the Normal Forms technique to the linearized system, keeping the nonlinear characteristics given by the eigenvalues, allows an approximate solution of the dynamic system in

terms of the transformed variable to be obtained. This method has the great advantage of obtaining the simplest form of a set of ordinary differential equations of sequential transformations [Nayfeh 1993]. However, it has the disadvantage of having an wrong dynamic performance when a resonance condition is present in the system dependent on eigenvalues [Arrowsmith and Place 1994].

The method of Normal Forms has been used to study nonlinear modal interactions in power systems as well. Different components in the power system model have been included, which has opened the path to several studies of modal interactions. Interpretation of results in Normal Forms is often a challenging problem.

The methodology known as Normal Forms has been formalized by several authors [Chua and Kokubu, 1988] [Chua and Oka, 1988]. It was suggested as an alternative of solution for the nonlinear dynamic analysis problems. The normal form of a vector field is defined as the simplest member of an equivalent class of vector fields exhibiting the same qualitative behavior, where this family is obtained from a nonlinear transformation to a diagonalized system, with a set of different eigenvalues. It is possible to introduce a formal coordinate change (proposed by Poincaré), which may be stated as the Poincaré Normal Form Theorem, that is [Chua and Kokubu, 1988]:

"A formal vector field $\dot{x} = v(x)$ *(with* $x \in \mathbf{C}^n$*) can be transformed into the Poincaré normal form* $\dot{y} = \Lambda y + w(y)$, $y \in \mathbf{C}^n$ *by an appropriate formal coordinate transformation* $x = \psi(y)$, *where* Λ *denotes the Jacobian matrix of* $v(x)$ *at the origin and each component of* $w = (w_1, w_2, \ldots, w_n)$ *consists of all resonant monomial associated with the eigenvalue* λ_k *of* Λ *".*

This Poincaré transformation had established the basis to develop under the same platform the Normal Forms applications. More specific details on Normal Forms definitions and some other relevant implications are described in [Kahn and Zarmi 1998] and [Nayfeh 1993].

Now focusing on Normal Forms method applied to the power systems analysis, it results necessary to make a quick look to the proposal of [Vittal *et al.* 1991] where inclusion of higher order terms to identify interarea oscillations was considered. A stressed power system is analyzed using higher order expansion of the modal solution to detect modal interactions that contributes to the interarea mode phenomenon. However, the methodology described in the paper does not have the capacity to consider the modal interactions, mostly due to nonlinear contributions.

In the work [Lin *et al.* 1996] modal interaction in power systems under stress conditions and excitation controls is evaluated through Normal Forms. Emphasis on interarea oscillations was one of the main purposes of the paper. Thus, a new platform of analysis emerged, oriented to the analysis of nonlinear oscillations in power systems. For instance, [Thapar *et al.* 1997] applied Normal Forms to predict interarea separation due to large disturbances; indexes that identify and measure the modal

interaction were used. On the other side, stability boundary approximation over the postfault equilibrium point was suggested in [Saha *et al.* 1997] using Normal Forms. Unstable equilibrium points were determined over different scenarios of the power system.

Referring to interaction modal studies and generation control in power systems, the Normal Forms method has been introduced for the analysis of larger power systems [Jang *et al.* 1998]. The information obtained by the Normal Forms analysis is used to set generation system controllers. Also, the island creation due to strong disturbances and high stress conditions has been considered [Vittal *et al.* 1998].

As it was mentioned earlier, the selective modal analysis introduced the concept of participation factors. An extension to nonlinear modal interaction has been proposed by the concept of nonlinear participation factor, based on second order nonlinear terms in the Normal Forms method [Starret y Fouad 1998]. Oscillation frequencies resulting from modal interaction are described in such contribution.

The application of the method of Normal Forms to study modal interaction in power systems that includes static vars compensators has been developed [Barocio y Messina 2002]. In this contribution, it is demonstrated that the SVC connected to the system combined with an overload and stress constraint, takes influence on the nonlinear characteristic associated with the power system. Addition of FACTS devices to the electric system has been considered by other authors [Barocio and Messina 2002a], [Messina *et al.* 2003] y [Zou *et al.* 2005], where the modal interaction and interarea oscillations through Normal Forms, over systems with transmission controllers are analyzed.

A classical analysis oriented to modal resonance in power systems is presented by [Yorino *et al.* 1989]. In this interesting document, a generalized method to analize parametric resonance which can be reflected in the power system operation as a nonlinear oscillation is described in detail.

The analysis of factors that affect interpretation of results in the Normal Forms method, relative to the estimation of initial conditions or modal interaction that modifies nonlinear coefficients have been studied. In the contribution [Barocio *et al.* 2004], a detailed analysis of factors affecting interpretation of Normal Forms method results has been made; the modal resonance effect acting over the method and the problematic involved in the determination of initial conditions with respect to z variables has been analyzed. Now, referring to the work proposed by [Kshatriya *et al.* 2005], a methodology to validate initial conditions is studied. The method tries to move these initial conditions in order to find a better initial operation constraints, which leads to a favorable response with the Normal Forms method. The method is based on the determination of indexes which quantify the feasibility of initial conditions. In the interesting work [Dobson and Barocio 2004] a quantification of factors affecting modal analysis in the Normal Forms method is made. The changes presented along with the calculation

of nonlinear coefficients and indexes are analyzed; in fact, since these changes come from the nonlinear transformation, they affect not only modal interaction associated to the system, but also represent a possible reason of modal resonance.

Concerning modal resonance, several papers have dealt with this topic, which is a consequence of modal analysis. For instance, a classical analysis on modal resonance in power systems is represented in the paper proposed by [Yorino *et al.* 1989]. In this document, a detailed generalized method is described in order to analyze parametric resonance, which is reflected in the power system operation as a nonlinear oscillation. More recently, in [Betancourt *et al.* 2006] a study of modal resonance presented in the Normal Forms method has been considered.

Viewing some other contributions over Normal Forms method, other applications can be found, *e.g.* [Liu *et al.* 2005] [Liu *et al.* 2006] that have incorporated the Normal Forms method to assess the PSS placement estimating the nonlinear modal interaction. Both papers exhibited the usefulness of including nonlinear interaction, in order to design the power systems controllers. [Martínez *et al.* 2007] have proposed the structure preserving approach applied to the Normal Forms method, which allows to deal with the power system model represented by a set of differential-algebraic equations as a unique set of dynamic state variables.

From the extensive review of all works published, which deal with applications of the Normal Forms method to the analysis of nonlinear interaction in power systems, it can be concluded that the method has a strong mathematical background; it means a challenging issue and demanding from the computational point of view. Considering that the method of Normal Forms possesses a strong mathematical formalism and contributes with additional information of the nonlinear dynamic system behavior, not included with linear analysis, therefore it may be considered as a one of the main methods for the nonlinear analysis of power systems.

1.2.2 Earlier Proposition of Modal Series Method

Besides the widely described Normal Forms method, the Modal Series method proposed by [Pariz *et al.* 2003] and [Schanechi, *et al.* 2003] represents an alternative of the analysis of nonlinear oscillations oriented to the application in power systems. The authors in both contributions addressed in this method the inclusion of nonlinear modal interaction, thus obtaining a close form solution. According with the characteristics described by the original version of Modal Series proposal, using Modal Series it is possible to represent nonlinear dynamic systems, as well as stressed power systems; the method of solution has the great conceptual advantage of representing a nonlinear system as a rather straightforward generalization of the linear case, although it may be much more extended [Pariz *et al.* 2003].

In the same way as the Normal Forms method, the method of Modal Series in its original version is restricted to the polynomial nonlinearity; therefore, Taylor series of other nonlinearity types are required. This reason adjusts the necessity of applying a linearization process in order to obtain a polynomial form of the nonlinear system.

A second version of the Modal Series method proposed in [Schanechi, *et al.* 2003] states that the Modal Series method is introduced to represent the nonlinear system response and to obtain an approximated closed form expression for the zero input response of the nonlinear system. Also, the method extends the linear system theory concepts to facilitate the understanding and analysis of nonlinear systems. Both papers punctuate the possibility of obtaining a closed form solution, even under resonance conditions. Some indices that quantify the error introduced by modal interaction [Pariz *et al.* 2003] and proximity measure have been proposed [Schanechi, *et al.* 2003] as well.

Almost every work based on the Modal Series method has been focused on comparisons against Normal Forms method [Wu *et al.* 2007] [Rodríguez *et al.* 2007] and to study the effects of fault location over interarea oscillations in stressed power systems [Naghshbandy *et al.* 2010].

1.2.3 Discussion on the Necessity for Including Higher Order Terms

Taking into account the extensive work resumed by the Task Force on Assessing the Need to Include Higher Order Terms [Sanchez-Gasca *et al.* 2005] and all the work previously mentioned along this Chapter, based both in the Normal Forms and the Modal Series method; it results very convenient to introduce this discussion on why to include higher order terms. The modal analysis means the basis of nonlinear systems since their basic analysis is related to the small signal analysis for studying electromechanical oscillations resulting on a linear equivalent that is valuated in the neighborhood of a steady state operating point. The information obtained by modal analysis is so important, since it allows to get insight into the nature of the main characteristics concerning on oscillation frequency (*i.e.* complex eigenvalues) and damping ratio. Thus, modal interactions mainly defined by participation factors are obtained. However, what does it happen when these modal interactions are the result of combinations due to second and even higher order terms? These modes and their interactions have been called higher order modes and higher order modal interactions [Sanchez-Gasca *et al.* 2005].

Hence, there are some topics that have to be followed to describe these higher order modal interactions, such as physical significance, indentifying when it is viable the higher order analysis, computational requirements, range of applicability of higher order terms, analytical tools to account for higher order terms. In the same way, it has been shown that some oscillations frequencies may appear in stressed power systems which are not predictable by linear modal analysis [Pariz *et al.* 2003].

As it was described in Section 1.2.1, the Normal Forms method is one of the main methods used to establish a systematic procedure to include higher order terms. Nevertheless, different strategies have been explored. Modal Series method tries to compete with the Normal Forms method, taking into account some of the main characteristics of nonlinear analysis, incorporating its own mark of reference. When a power system becomes more stressed, nonlinear modal interaction may play an important role in the dynamic behavior of the power system. This will reduce the valid region of the linear modal method [Wu *et al.* 2007].

It must be remarked the contribution that under some constraints may represent the interaction of switching devices such as FACTS devices, which are ruled by the extension of nonconventional energy sources linked by VSC converters (*i.e.* UPFC'S, STATCOMS, VSC-HVDC links, etc.). Nonlinear effect of electromechanical devices interacting with commutation devices results in nonlinear interactions [Barocio 2003] following stressed conditions.

In conclusion, methodologies that qualitatively and quantitatively can measure the nonlinear contributions of a stressed power systems are necessary. So far, to incorporate such contributions Normal Forms have been more extensively used; few works based on the Modal Series method have been developed. Both alternatives provide closed forms solutions and nonlinear interaction indices, with their own particularities, advantages and disadvantages.

This research is mainly focused on an in depth description and formulation of the Modal Series method and its feasibility of application in power systems that operate under stressed conditions. Also, the forced response function in a nonlinear system is considered through Modal Series thus introducing the concept of nonlinear transfer function in power systems. Finally, the power system operation with a FACTS device (oriented to the UPFC analysis) is described.

1.3 GENERAL OBJECTIVE

This thesis has as a principal objective to characterize the nonlinear contribution to the power systems oscillations under small disturbances using the modal series method. For that purpose, the modal series method is deduced through the use of the multidimensional Laplace transform and association of variables theorems, that allow to determine an analytical solution to the dynamic power system model under analysis.

1.4 AIMS OF THIS DOCTORAL RESEARCH

- To describe in detail the step by step procedure followed to apply the Modal Series method to the study of nonlinear oscillations in power systems.
- To establish a comparison of Modal Series method against other methodologies, specifically with respect to the Normal Forms method to allows to make a judgment concerning the identification of advantages and disadvantages of the new proposal.
- To develop a formal mathematical description of the Modal Series method, emphasizing on its mathematical fundaments and institute its extension to incorporate the closed form solution when a system with forced oscillations is assumed.
- To incorporate the Multidimensional Laplace theorems and association of variables to get the closed form solutions on which the Modal Series approach is based. Also, Volterra series theory is incorporated due to interrelationship and applications oriented to nonlinear dynamic systems analysis.
- To apply the Modal Series method to define the transfer functions based on the nonlinear terms when are subjected to an input function.
- To extend applications of the Modal Series method to networks containing FACTS devices such as the UPFC. It is of concern the nature of nonlinear oscillations when FACTS devices interact with the power system.

1.5 MAIN CONTRIBUTIONS

The main contributions of this doctoral research are,

- Incorporation of multidimensional Laplace transform and association of variable theorems to the Modal Series method.
- The extension of the Modal Series method to the inclusion of higher order terms in the closed form analytical solution
- The incorporation of the control input function (forced nonlinear response) to the Modal Series method
- The introduction of the definition of nonlinear transfer function to the power systems analysis, which is derived from the higher order terms of the Modal Series when the nonlinear system is subject to a forced input (control function) response.
- The study of nature of power systems oscillations using the Modal Series method when the power system experiments a short time duration disturbance.
- The study of power systems that incorporate the UPFC device, analyzed by the Modal Series method and the assessment of nonlinear oscillations contributions.

1.6 THESIS OUTLINE

This doctoral thesis is organized as follows:

- In this Chapter and extensive description of the state of art related to the Normal Forms and Modal Series methods contributions has been given. Justification of this doctoral research has been remarked, as well as the main goals and contributions followed in this research.
- In the Chapter 2, the Normal Forms method is briefly reviewed, in addition to the revisit of the Modal Series method. Both methods are simulated and exemplified by a nonlinear benchmark system, for which the validation of initial conditions is tested. The main differences, advantages and disadvantages of both methods are emphasized.
- In the Chapter 3, the Modal Series method is redefined when the multidimensional Laplace transform and associations of variables are applied to get the closed form solution of a nonlinear dynamic system, for the case of an unforced response. The method is exemplified through the application to a simple power system (synchronous machine-infinite busbar); the procedure followed to incorporate the higher order terms in the Modal Series are described as well.
- The Chapter 4 is focused on the development of Modal Series method for the case of forced oscillations response incorporating the nonlinear transfer function definition. An analytical nonlinear system and a couple of low scale power system are utilized to exemplify the ability of the proposed extension.
- In the Chapter 5 the multimachine power system modeling used along the thesis is described in detail.
- The Chapter 6 is oriented to the detailed analysis of numerical applications of the Modal Series method to the study of two known test power systems. Emphasis is given on the contributions of nonlinear terms to the modal analysis and frequency contributions to power system oscillations.
- Chapter 7, incorporates the study of the UPFC, in which the usefulness of the Modal Series method for the assessment of nonlinear oscillations is described.
- Finally, in the Chapter 8 conclusions remarks and suggestions for future research work are given.

2

TOOLS FOR THE ANALYSIS OF NONLINEAR DYNAMIC SYSTEMS

The dynamic of nonlinear systems has been determined by different strategic tools of analysis. Based on the main characteristics provided by the modal analysis, other alternatives can be described, such as Normal Forms and Modal Series methods. This chapter describes in detail both methods, including the characteristics given by modal analysis. Nonlinear interaction, participation factors, nonlinear interaction indices are familiar concepts related with the scope of modal analysis and extended to the nonlinear analysis.

2.1 BACKGROUND ON NONLINEAR METHODS

The main idea followed by the methods which assume nonlinear contributions in nonlinear systems is based on considering such nonlinearities through either linear or nonlinear transformations from the original system. The underlying idea of Normal Forms theory is to find an analytical change of coordinates with the fixed point shifted to the origin such that the vector fields becomes simpler to study in terms of new variables [Arroyo 2007].

Dynamic formulation in power systems has been carried-out by sets of nonlinear differential equations, which are in general, autonomous systems. Consider the set of nonlinear differential equations, where n is the number of state variables, that is,

$$\dot{x}_j = f_j\left(x_1, x_2, \ldots, x_n\right) \qquad j = 1, 2, \ldots, n \tag{2.1}$$

Using matrix notation, (2.1) can be written as,

$$\dot{\mathbf{x}} = \mathbf{f}\left(\mathbf{x}\right) \tag{2.2}$$

The equilibrium points for Equation (2.2) must satisfy the equilibrium condition [Kundur 1994],

$$\mathbf{f}\left(\mathbf{x}_0\right) = 0 \tag{2.3}$$

where $\mathbf{x}_0$ is the state vector located at the equilibrium point

If functions f_i ($i = 1, 2, \ldots, n$) are linear, then the system is linear itself. A linear system has just one equilibrium point (conditioned to the existence of a non-singular state matrix). For nonlinear systems,

more than one equilibrium points exist which describe the behavior of the system dynamics and therefore provides important information concerning the system stability.

2.2 LINEARIZATION PROCESS

Due to the difficulty involved on estimating the nature of nonlinear power systems represented by a set of nonlinear differential equations of the form given by Equation (2.2), it is common to simplify the nonlinear system through the Taylor series expansion.

Being $\mathbf{x}_{sep}$ an stable equilibrium point, so that according to the condition previously established by (2.3), the general form of Taylor series expansion from a n state variables function $x = \left[x_1',\, x_2',\, \ldots,\, x_n'\right]^T$ for a small deviation or perturbation $\Delta x_1, \Delta x_2, \ldots, \Delta x_n$ of the system described by (2.1) is

$$\begin{aligned}\dot{x}_i = \dot{x}_{i\,sep} + \Delta\dot{x}_i = {} & f_i\left(\mathbf{x_{sep}} + \mathbf{\Delta x}\right) \\ = {} & f_i\left(\mathbf{x}_{sep}\right) + \frac{\partial f_i}{\partial x_1}\Delta x_1 + \frac{\partial f_i}{\partial x_2}\Delta x_2 + \ldots + \frac{\partial f_i}{\partial x_n}\Delta x_n \\ & + \frac{1}{2!}\frac{\partial^2 f_i}{\partial x_1 \partial x_1}\Delta x_1 \Delta x_1 + \frac{1}{2!}\frac{\partial^2 f_i}{\partial x_1 \partial x_2}\Delta x_1 \Delta x_2 + \ldots + \frac{1}{2!}\frac{\partial^2 f_i}{\partial x_1 \partial x_n}\Delta x_1 \Delta x_n \\ & + \frac{1}{2!}\frac{\partial^2 f_i}{\partial x_2 \partial x_1}\Delta x_2 \Delta x_1 + \frac{1}{2!}\frac{\partial^2 f_i}{\partial x_2 \partial x_2}\Delta x_2 \Delta x_2 + \ldots + \frac{1}{2!}\frac{\partial^2 f_i}{\partial x_2 \partial x_n}\Delta x_2 \Delta x_n \\ & + \ldots + \frac{1}{2!}\frac{\partial^2 f_i}{\partial x_n \partial x_{n-1}}\Delta x_n \Delta x_{n-1} + \frac{1}{2!}\frac{\partial^2 f_i}{\partial x_n \partial x_n}\Delta x_n \Delta x_n + O\left(\left|\mathbf{\Delta x}\right|^3\right)\end{aligned} \tag{2.4}$$

Expressing in matrix form, Equation (2.4) takes the form,

$$\dot{\mathbf{x}}_i = \mathbf{A_i x} + \frac{1}{2}\mathbf{x}^{\mathbf{T}}\mathbf{H}^{\mathbf{i}}\mathbf{x} + O\left(\left|\mathbf{x}\right|^3\right) \tag{2.5}$$

$O\left(\left|\mathbf{x}\right|^3\right)$ represents the residual terms of third order and higher.

With $i = 1, 2, \ldots, n$, and

$$\mathbf{A} = \left[\begin{array}{cccc} \frac{\partial f_1(\mathbf{x})}{\partial x_1} & \frac{\partial f_1(\mathbf{x})}{\partial x_2} & \cdots & \frac{\partial f_1(\mathbf{x})}{\partial x_n} \\ \frac{\partial f_2(\mathbf{x})}{\partial x_1} & \frac{\partial f_2(\mathbf{x})}{\partial x_2} & \cdots & \frac{\partial f_n(\mathbf{x})}{\partial x_n} \\ \vdots & \vdots & \ddots & \vdots \\ \frac{\partial f_n(\mathbf{x})}{\partial x_1} & \frac{\partial f_n(\mathbf{x})}{\partial x_2} & \cdots & \frac{\partial f_n(\mathbf{x})}{\partial x_n} \end{array}\right]_{|\mathbf{x}=\mathbf{x}_{sep}}$$ Jacobian Matrix (2.6)

$$\mathbf{H}^j = \left[\begin{array}{cccc} \dfrac{\partial f_i(\mathbf{x})}{\partial x_1 \partial x_1} & \dfrac{\partial f_i(\mathbf{x})}{\partial x_1 \partial x_2} & \cdots & \dfrac{\partial f_i(\mathbf{x})}{\partial x_1 \partial x_n} \\ \dfrac{\partial f_i(\mathbf{x})}{\partial x_2 \partial x_1} & \dfrac{\partial f_i(\mathbf{x})}{\partial x_2 \partial x_2} & \cdots & \dfrac{\partial f_i(\mathbf{x})}{\partial x_2 \partial x_n} \\ \vdots & \vdots & \ddots & \vdots \\ \dfrac{\partial f_i(\mathbf{x})}{\partial x_n \partial x_1} & \dfrac{\partial f_i(\mathbf{x})}{\partial x_n \partial x_2} & \cdots & \dfrac{\partial f_i(\mathbf{x})}{\partial x_n \partial x_n} \end{array}\right]^j_{\mathbf{x}=\mathbf{x}_{sep}} \quad \text{Hessian Matrix} \tag{2.7}$$

So far the system is linearized around a steady state equilibrium point. If a higher complex system is considered, it implies the addition of terms corresponding to third and higher order terms. Thus, the complexity of the model increases. In this research, the Taylor series is considered up to third order terms.

2.3 JORDAN CANONICAL FORM

The Taylor series expansion of the system given by (2.5) is still of nonlinear nature and cumbersome to analyze. For small signal stability analysis in power systems, it may be assumed that the network is located in the vicinity of an equilibrium steady state point. As a result of state variables coupling, it is difficult to separate those parameters with a significant influence on motion [Kundur 1994]. To eliminate this coupling, consider the linear transformation,

$$\mathbf{x} = \mathbf{U}\mathbf{y} \tag{2.8}$$

Being $(\lambda_1, \lambda_2, \ldots, \lambda_n)$ distinct eigenvalues of the state matrix $\mathbf{A}$ and $\mathbf{U} = (U_1, U_2, \ldots, U_n)$, $\mathbf{V} = (V_1, V_{2,} \ldots, V_n)$ the corresponding right and left eigenvectors, respectively, are normalized in such a way that $\mathbf{VU} = \mathbf{I}$. Substituting (2.8) in (2.5), the system is converted to its Jordan Canonical form, which is located around a steady state equilibrium point. Thus,

$$\mathbf{U}\dot{\mathbf{y}} = \mathbf{AUy} + \mathbf{U^T y^T HUY} + \left(O|\mathbf{x}|^3\right)$$

$$\dot{\mathbf{y}} = \mathbf{U^{-1}AUy} + \mathbf{U^{-1}U^T y^T HUy} + \left(O|\mathbf{x}|^3\right)$$

Assuming,

$$\mathbf{\Lambda} = \mathbf{U^{-1}AU} = \mathbf{V^T AU} = diag\left[\lambda_1, \lambda_2, \ldots, \lambda_n\right]$$

$$\dot{\mathbf{y}} = \mathbf{\Lambda y} + \mathbf{F}_2(\mathbf{y}) + \left(O|\mathbf{y}|^3\right) \tag{2.9}$$

where,

$$\mathbf{F}_2(y) = \frac{1}{2}\mathbf{U}^{-1}\begin{bmatrix} \mathbf{y^T U^T H^1 U y} \\ \mathbf{y^T U^T H^2 U y} \\ \vdots \\ \mathbf{y^T U^T H^n U y} \end{bmatrix} \tag{2.10}$$

Or [Thapar *et al*. 1997],

$$\dot{y}_j = \lambda_j y_j + \sum_{k=1}^{n}\sum_{l=1}^{n} C_{kl}^{j} y_k y_l \qquad j = 1,2,\ldots,n \tag{2.11}$$

where

$$C^j = \frac{1}{2}\sum_{p=1}^{n} V_{jp}^{T}\left[\mathbf{U^T H^P U}\right] = \left[C_{kl}^{j}\right] \tag{2.12}$$

also,

$$C_{kl}^{j} = \frac{1}{2}\sum_{p=1}^{n}\sum_{m=1}^{n}\sum_{o=1}^{n} V_{jp}^{T} H_{mo}^{p} U_{mk} U_{ol} \tag{2.13}$$

Referring to Equation (2.11), the first term is linearly coupled, however, the second term is coupled as well. Coefficients C_{kl}^{j} determine the size of contribution from mode *k* and *l* to the dynamic equation that governs the behavior of mode *j* [Barocio *et al.* 2004].

2.4 NORMAL FORMS. THEORETICAL BACKGROUND

2.4.1 Nonlinear Coordinates Transformation

According to Poincaré's Theorem, a power series, like that shown by (2.11), can be reduced to its linear form around at steady state equilibrium point applying a nonlinear transformation: If the eigenvalues obtained from the state matrix are non-resonant [Kshatriya *et al*. 2005], the normal transformation is given by [Thapar *et al*. 1997],

$$y = z + h_2(z) \tag{2.14}$$

which can be expressed as,

$$y_j = z_j + \sum_{k=1}^{n}\sum_{l=1}^{n} h_{2kl}^{j} z_k z_l \tag{2.15}$$

where h_2 is a function valuated on a complex vector, whose components are second order homogeneous polynomials with coefficients obtained in such a way that the system given by (2.15) is

as simple as possible. Vector $z \in C^n$ denotes the new coordinate system, so called Normal Form system [Barocio *et al*. 2004].

Substituting (2.15) in (2.11) yields,

$$\begin{aligned} \dot{y} &= \dot{z} + Dh_2(z)\dot{z} = \left[I + Dh_2(z)\right]\dot{z} \\ \left[I + Dh_2(z)\right]\dot{z} &= \Lambda\{z + h_2(z)\} + F_2(z + h_2(z)) \\ \dot{z} &= \left[I + Dh_2(z)\right]^{-1}\left\{\Lambda z + \Lambda h_2(z) + F_2(z + h_2(z)) + O\left(|z|^3\right)\right\} \end{aligned} \tag{2.16}$$

where $O\left(|z|^3\right)$ is an expression that contains residual terms of third and higher order. Furthermore,

$$Dh_2(z) = \begin{bmatrix} \frac{\partial h_1(z)}{\partial z_1} & \frac{\partial h_1(z)}{\partial z_2} & \cdots & \frac{\partial h_1(z)}{\partial z_n} \\ \frac{\partial h_2(z)}{\partial z_1} & \frac{\partial h_2(z)}{\partial z_2} & \cdots & \frac{\partial h_2(z)}{\partial z_n} \\ \vdots & \vdots & \ddots & \vdots \\ \frac{\partial h_n(z)}{\partial z_1} & \frac{\partial h_n(z)}{\partial z_2} & \cdots & \frac{\partial h_n(z)}{\partial z_n} \end{bmatrix} \tag{2.17}$$

Considering that,

$$\left(I + Dh_2(z)\right)^{-1} \approx I - Dh_2(z) \tag{2.18}$$

The Normal Form system is described as,

$$\dot{z} = \Lambda z + \Lambda h_2(z) - Dh_2(z)\Lambda z + F_2(z + h_2(z)) + O\left(|z|^3\right) \tag{2.19}$$

Normal Forms theory indicates that resonant terms may be always eliminated from the Normal Form [Barocio *et al*. 2004]. The linear transformation coefficients are given by,

$$h_{2kl}^{\ j} = \frac{C_{kl}^{j}}{\lambda_k + \lambda_l - \lambda_j} \tag{2.20}$$

If $\lambda_j = \lambda_k + \lambda_i$, it means that a modal resonance is presented and the corresponding nonlinear terms can not be eliminated.

Thus, the system (2.19) can be represented in the form,

$$\dot{z}_j = \lambda_j z_j + O\left(|z|^3\right) \tag{2.21}$$

If higher order terms are not considered, the time evolution of state variables in Normal Forms may be expressed as,

$$z_j = z_{j0} e^{\lambda_j t} \tag{2.22}$$

where z_{j0} is the initial condition of variable z_j in Normal Form.

The Normal Forms approximation (2.22) results in a simplified representation of the original system, where the answer is still a function of eigenvalues from the original system, and where it is possible to point out that the final solution is obtained as a *minimal system* (Normal Form). A critical aspect in the determination of Normal Forms transformation coefficients and thus in the system linearization is the resonance condition given by,

$$\lambda_k + \lambda_i - \lambda_j = 0 \tag{2.23}$$

If this resonance condition is met, it may be said that the system is involved on a modal resonance problem; therefore, it cannot be diagonalized. That means, it is not possible to determine a Normal Form from the original system. Factors that influence the modal resonance have been of special interest and previously analyzed [Dobson 2001].

2.4.2 Approximate Solution of the Normal Forms

Results may be expressed in their original domain by using the inverse transformations of the Normal Forms. Hence substituting $y = z + h_2(z)$ and $x = Uy$ in (2.15), results in,

$$y_j(t) = z_{j0} e^{\lambda_j t} + \sum_{k=1}^{n}\sum_{l=1}^{n} h_{2kl}^{j} z_{k0} z_{l0} e^{(\lambda_k + \lambda_l)t} \qquad j = 1,2,\ldots,n \tag{2.24}$$

$$x_i(t) = \sum_{j=1}^{n} U_{ij} z_{j0} e^{\lambda_j t} + \sum_{j=1}^{n} U_{ij}\left[\sum_{k=1}^{n}\sum_{l=1}^{n} h_{2kl}^{j} z_{k0} z_{l0} e^{(\lambda_k + \lambda_l)t}\right] \qquad i = 1,2,\ldots,n \tag{2.25}$$

where initial conditions on spaces *y* and *z* are obtained solving the set of nonlinear algebraic equations,

$$f(z_0) = y_0 - z_0 - h_2(z_0) = U^{-1}x_0 - z_0 - h_2(z_0) = 0 \tag{2.26}$$

It is important to note from Equations (2.24) and (2.25) that second order nonlinear coefficients h_{2kl}^{j} and initial conditions z_{k0}, z_{l0} are very important to determine the total response of the nonlinear systems for a particular state. The product $h_{2kl}^{j} z_{k0} z_{l0}$ is a measure of the extension for which the system is acting as a nonlinear one. Interpreting solutions in the Normal Forms method, emphasis is necessary to be given to the next constraints [Barocio *et al*. 2004]:

i) A simpler Normal Form is obtained removing elements from a finite series; inverse of a truncated series may result in an error on the initial conditions from the new truncated system.

ii) The system expressed by (2.26) may exhibit multiple solutions.

An exact prediction of the system response to a given perturbation requires of precise initial conditions calculation for each framework of the system. This implies that behavior prediction of the nonlinear system may be a hard and challenging work.

Some other important observations based on the expressions (2.24) and (2.25) are next resumed [Thapar *et al*. 1997],

- The solutions are obtained in terms of initial conditions previously fixed in the system, and they characterize the time domain evolution in terms of coefficients h_2 and the modal structure.
- Higher order terms are independent of mode combinations ($\lambda_k + \lambda_l$), and the size of coefficients h_2 with initial conditions z_{k0}, z_{l0}, determine the effect of modal combination of the final solution
- Product $h_{2kl}^{j} z_{k0} z_{l0}$ referred as coefficient interaction, determines the effect of higher order terms in the solution.

The method of Normal Forms is schematically illustrated in Figure 2.1, which shows the steps needed in order to transform the original nonlinear system through the linear and nonlinear transformations to the final Normal Form.

It is well known that the application of the method to obtain the initial conditions of the Normal Forms method may be cumbersome and sensitive to convergence problems, since it is based on a numerical solution of a set of nonlinear algebraic equations (Newton methods based on optimization process are preferable); the nonlinear transformation may have multiple solutions of z_0 for a given y_0 and the convergence value will depend on the assumed initial condition [Barocio *et al.* 2004].

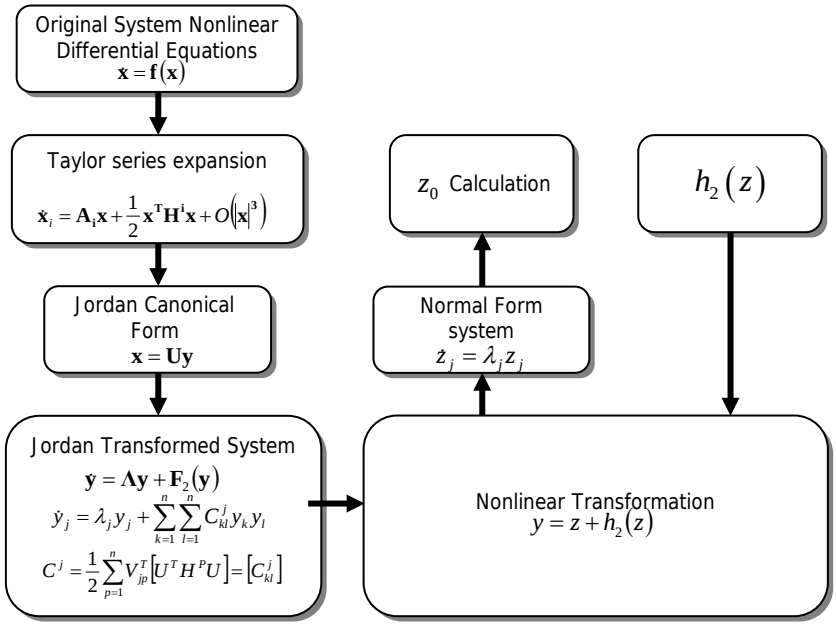

Figure 2.1 Flow chart showing the steps followed for the Normal Forms method

2.4.3 Determination of Initial Conditions for the Normal Forms Method

Due to importance of accurate determination of initial conditions in the method of Normal forms, which involves the calculation of state variables depending on whether linear and nonlinear transformation *x*, *y* and *z* are to be used, several strategies have been developed in order to calculate and validate the initial conditions under different constraints [Thapar *et al.* 1998], [Barocio *et al.* 2004], [Kshatriya *et al.* 2005]. One of the main difficulties related to the determination of such initial conditions is the combination of linear and nonlinear trnasformations. A critical aspect for the calculation of approximate analytical solutions closer to system behavior depends on z_0 initial conditions. Such initial conditions determination requires of the numerical solution of a set of nonlinear algebraic equations with complex coefficients [Barocio *et al.* 2004]. Conventional Newton methods commonly utilized to solve nonlinear equations have fast convergence speed properties but they require an initial point as nearest as possible to the solution point. Otherwise, a case of non-convergence problems is presented with these methods. Besides, the system may present multiple solutions that make difficult to interpret the final solution.

A methodology proposed by [Thapar *et al.* 1998] to obtain *z* initial conditions is based on the following procedure: close form solutions represent the evolution in the time domain of Jordan form variables and state variables at the postfault period. To obtain these solutions, initial conditions in terms of *z* variables must to calculated.

1. Updated variables X_{cl} are obtained at the end of the disturbance.
2. Stable equilibrium point at postfault conditions is obtained with X_{sep}
3. Initial conditions in terms of state variables with respect to the equilibrium point are determined as $X_0 = X_{cl} - X_{sep}$
4. These initial conditions are transformed, in order to get the initial conditions in Jordan form variables, that is, $Y_0 = U^{-1} X_0$
5. The nonlinear equations

$$f(z_0) = z_0 + h_2(z_0) - Y_0 = 0$$

are numerically solved to obtain initial conditions for z_{j0}. This is one of the most important steps in the application of the Normal Forms method when it is applied to power systems.

It is well known that sometimes this method to obtain initial conditions is not feasible and it is prompt to convergence problems since the nonlinear transformation has multiple solutions of z_0 for a

given y_0, and this convergence calculated value depends on the z_0 initial assumption [Barocio *et al.* 2004].

2.4.4 Nonlinearity Indexes

The rate of the transformed system nonlinearity has been proposed by [Thapar *et al.* 1997]. It is based on comparing the linear term obtained from linear equations solution against the approximate solutions obtained when second order terms are included. The interaction coefficient is defined as,

$$h^i_{2\,jk} z_{j0} z_{k0} \tag{2.27}$$

which quantifies the effects on the dynamic solution when second order terms are included.

In order to consider the nonlinear effect, according to the proposal by [Thapar *et al.* 1997], a comparison of the linear term from (2.22) and the linear term calculated from the Jordan canonical form is calculated. Difference between both solutions is given by,

$$\left|\left(y_j(0) - z_j(0)\right)e^{\lambda_j t}\right| \tag{2.28}$$

This term represents the difference between the linear part of the approximate solution with respect to the linear solution. Thus, in Equation (2.25) second order terms are added in order to include effects due to nonlinearities or difference between terms, where this linearity is introduced for the expression described by the Equation (2.28). This result in,

$$\left|\left(y_j(0) - z_j(0)\right)e^{\lambda_j t} + \sum_{k=1}^{n}\sum_{l=1}^{n} h^j_{2kl} z_{k0} z_{l0} e^{(\lambda_k + \lambda_l)t}\right| \tag{2.29}$$

According to Equation (2.29) two approximations may be performed [Thapar *et al.* 1997]:

a) The largest magnitude term is considered and it is assumed that all other terms are small compared to the largest one.

b) It is also noted that h^j_{2kl} is large if $\lambda_k + \lambda_i \approx \lambda_j$.

Hence, the nonlinear interaction index $I1$ for the mode *j* is given by,

$$I1(j) = \left|y_j(0) - z_j(0) + \max_{k,l}\left(h^j_{2kl} z_{k0} z_{l0}\right)\right| \tag{2.30}$$

where $\max_{k,l}\left(h^j_{2kl} z_{k0} z_{l0}\right)$ is complex when $\max_{k,l}\left|h^j_{2kl} z_{k0} z_{l0}\right|$ is presented; $y_j(0)$ and $z_j(0)$ are the Jordan canonical form and Normal Forms variables respectively, valuated at time $t = 0^+$. Index $I1$ provides a rate of the effect of nonlinear terms to the solution, comparing the nonlinear solution with respect to the second order solution [Vittal *et al.* 1998]. A normalized index of nonlinear interaction is given by [Barocio 2003] which relates the index $I1$ to mode *j*, hence,

$$\bar{I}1(j) = \frac{\left|y_j(0) - z_j(0)\right| + \left|\max_{k,l}\left(h_{2kl}^{j} z_{k0} z_{l0}\right)\right|}{\left|z_j(0)\right|} \tag{2.31}$$

Nonlinear interaction index $I2$ for mode *j* has been defined as,

$$I2(j) = \frac{\max_{k,l}\left(h_{2kl}^{j} z_{k0} z_{l0}\right)}{z_j(0)} \tag{2.32}$$

Index *I2* determines either nonlinear effects due to second order terms, which indicate a strong modal interaction, or second order terms that affects initial solution in variables *z*, that indicate the dominant fundamental mode [Vittal *et al*. 1998]. Another index of nonlinearity $I3$ has been proposed based on the theory of nonlinear distortion interference criteria in communications systems [Barocio 2003], that is,

$$I3(j) = \frac{\sqrt{\sum_{k=1}^{n}\sum_{l=k}^{n}\left|\left(h_{2kl}^{j} z_{k0} z_{l0}\right)\right|^2}}{\left|z_j(0)\right|} \tag{2.33}$$

2.4.5 Participation Factors

If the k^{th} state variable is excited whose magnitude is unity, $\mathbf{x}_0 = [0,\ldots,0,1,0,\ldots,0]$ yields

$$\mathbf{y}(t) = \mathbf{U}^{-1}\mathbf{x}(t)$$
$$y_i(0) = V_{ik}^{T} x_i(0)$$
$$\therefore \quad y_i(0) = V_{ik}^{T}$$

That is,

$$x_i(t) = \sum_{j=1}^{n} U_{ij} y_j(0) e^{\lambda_j t}$$

$$x_i(t) = \sum_{j=1}^{n} U_{ij} V_{ik}^{T} e^{\lambda_j t} \tag{2.34}$$

or,

$$x_i(t) = \sum_{j=1}^{n} p_{ki} e^{\lambda_j t} \tag{2.35}$$

Element $p_{ki} = U_{ki} V_{ik}^{T}$ is called *participation factor*. This is a size of relative participation of the k^{th} state variable in the i^{th} mode and viceversa [Pérez-Arriaga *et al.* 1982]. Since U_{ki} measures activity of x_k in the i^{th} mode and V_{ik} considers the contribution to this activity to the mode, the product p_{ki} measures the complete participation.

In matrix form, participation factors matrix is given as,

$$\mathbf{P}=\begin{bmatrix} U_{11}V_{11}^T & U_{12}V_{21}^T & \dots & U_{1n}V_{n1}^T \\ U_{21}V_{12}^T & U_{22}V_{22}^T & \dots & U_{2n}V_{n2}^T \\ \vdots & \vdots & \ddots & \vdots \\ U_{n1}V_{1n}^T & U_{n2}V_{2n}^T & \dots & U_{nn}V_{nn}^T \end{bmatrix} \tag{2.36}$$

2.5 THE INITIAL MODAL SERIES METHOD

Nonlinear modal analysis has been extensively used to study system dynamic behavior in a variety of nonlinear systems events. In this section, the Modal Series method will be summarized and the main results obtained on modal analysis reported. Their advantages as well as shortcomings are discussed, parting from the work reported in [Pariz *et al*. 2003] and [Schanechi, *et al*. 2003], where the concept of Modal Series analysis for the stressed and nonlinear power systems was introduced. The main objective of this section is to revisit the basic concepts on this field, since they represent the basis of further developments, carried out in this doctoral research.

2.5.1 Taylor Series Expansion and Jordan Canonical Form

Let us assume a nonlinear power system that can be modeled by a set on nonlinear ordinary differential equations of the form,

$$\dot{\mathbf{x}}=\mathbf{f}(\mathbf{x}) \tag{2.37}$$

where **x** is an *n*-dimensional vector of system states, and $\mathbf{f}: R^n \to R^n$ is a smooth vector field. The system is linearized expanding (2.37) in Taylor series around the initial equilibrium point, X_{sep}, resulting in,

$$\dot{x}_i = A_i X + \frac{1}{2}\sum_{k=1}^{n}\sum_{l=1}^{n} H_{kl}^{i} x_k x_l + \frac{1}{6}\sum_{p=1}^{n}\sum_{q=1}^{n}\sum_{r=1}^{n} P_{pqr}^{i} x_p x_q x_r + \dots \tag{2.38}$$

where A_i is the i^{th} row of the Jacobian matrix, being $\mathbf{A}=\left(\partial f / \partial X\right)\Big|_{X_{sep}}$; $H^i=\left(\partial^2 f_i / \partial X^2\right)\Big|_{X_{sep}}$ is the Hessian matrix, $P^i=\left(\partial^3 f_i / \partial X^3\right)\Big|_{X_{sep}}$ and so on. Also, the system has *n* distinct eigenvalues denoted as $\{\lambda_1 \quad \lambda_2 \quad \cdots \quad \lambda_n\}$ with associated right and left eigenvectors **U** and $\mathbf{V}=\mathbf{U}^{-1}$, respectively. Then, the linear change of coordinates $\mathbf{x}=\mathbf{U}\mathbf{y}$ transforms the system in Equation (2.38) into the equivalent set of differential equations of the form,

$$\dot{y}_j = \lambda_j y_j + \sum_{k=1}^{n}\sum_{l=1}^{n} C_{kl}^{j} y_k y_l + \sum_{p=1}^{n}\sum_{q=1}^{n}\sum_{r=1}^{n} D_{pqr}^{j} y_p y_q y_r + \dots \tag{2.39}$$

with $j = 1,...,n$, and

$$C_{kl}^{j} = \frac{1}{2}\sum_{p=1}^{n} V_{jp}^{T}\left[U^{T} H^{P} U\right] \tag{2.40}$$

$$D_{pqr}^{j} = \frac{1}{6}\sum_{P=1}^{n}\sum_{Q=1}^{n}\sum_{R=1}^{n} P_{pqr}^{j} V_{p}^{P} V_{q}^{Q} V_{r}^{R} \tag{2.41}$$

where V_p^P is the *p*th element of the *P*th left eigenvector [Schanechi, *et al*. 2003].

2.5.2 Modal Solutions

Several techniques to obtain closed form analytical solutions have been proposed in the literature, such as the whole contributions earlier described in detail in Chapter 1. This section is focused on the approach observed by [Pariz *et al*. 2003] and [Schanechi, *et al*. 2003].

Hence, following the Modal Series approach some considerations are necessary. Let the solution of (2.39) for initial condition Y_0 assume that the system solution to (2.39) can be expressed in the form [Schanechi, *et al*. 2003],

$$y_j(t) = f_j^1(t) + f_j^2(t) + f_j^3(t) + \ldots \tag{2.42}$$

with initial conditions,

$$f^1(0) = \left[\, f_1^1(0),\ f_2^1(0), \ldots,\ f_N^1(0)\right]^T = Y_0 \quad \text{and} \quad f_j^k(0) = 0 \quad \text{for each} \quad j \in \{1, 2, \ldots, N\} \quad \text{and} \quad k > 1,$$

where

$$\begin{aligned}
&\dot{f}_j^1 = \lambda_j f_j^1 \\
&\dot{f}_j^2 = \lambda_j f_j^2 + \sum_{k=1}^{n}\sum_{l=1}^{n} C_{kl}^{j} f_k^1 f_l^1 \\
&\dot{f}_j^3 = \lambda_j f_j^3 + \sum_{k=1}^{n}\sum_{l=1}^{n} C_{kl}^{j}\left(f_k^1 f_l^2 + f_k^2 f_l^1\right) + \sum_{p=1}^{n}\sum_{q=1}^{n}\sum_{r=1}^{n} D_{pqr}^{j} f_p^1 f_q^1 f_r^1 \\
&\vdots
\end{aligned} \tag{2.43}$$

Now, the method conveniently takes the procedure obtained by the method of small parameters. That is, the system is expanded considering a convenient scalar parameter ε such that $\varepsilon Y_0 \in \vartheta$, with $\vartheta = \upsilon \cap \psi$, ψ denotes the convergence of Maclaurin expansion of $y_j(Y_0, t)$ and $\upsilon \subseteq C^N$. All these variables represent the constraints involved on the necessary linear mapping to solve the system (2.39). From this approach, it may be said that Modal Series Method could be used as a formal method in circumstances that the convergence conditions are not met [Schanechi, *et al*. 2003], where the conditions are defined when the small parameter is small enough.

Equations (2.43) can be conveniently manipulated using the Laplace transform. Taking a two-dimensional Laplace transform of (2.43) we have

$$f_j^1(s) = \frac{f_j^1(0)}{(s-\lambda_j)} = \frac{y_{j0}}{(s-\lambda_j)} \tag{2.44}$$

$$f_j^2(s_1, s_2) = \sum_{k=1}^{n}\sum_{l=1}^{n} C_{kl}^j \frac{1}{(s_1+s_2-\lambda_j)} f_k^1(s_1) f_l^1(s_2) \tag{2.45}$$

where λ_j are the eigenvalues of the Jordan matrix.

These solutions are then transformed back to the original coordinates using the inverse Laplace transform. Taking the inverse Laplace transform on (2.44), it yields

$$f_j^1(t) = f_j^1(0) e^{\lambda_j t} = y_{j0} e^{\lambda_j t} \tag{2.46}$$

and from (2.45),

$$f_j^2(t) = \sum_{k=1}^{n}\sum_{l=1}^{n} C_{kl}^j f_k^1(0) f_l^1(0) S_{kl}^j(t)$$

or

$$f_j^2(t) = \sum_{k=1}^{n}\sum_{l=1}^{n} C_{kl}^j y_{k0} y_{l0} S_{kl}^j(t) \tag{2.47}$$

where,

$$S_{kl}^j(t) = \frac{1}{\lambda_k + \lambda_l - \lambda_j}\left(e^{(\lambda_k+\lambda_l)t} - e^{\lambda_j t}\right) \quad \text{for } (k,l,j) \notin R_2$$

$$S_{kl}^j(t) = te^{\lambda_j t} \quad \text{for } (k,l,j) \in R_2$$

Solving (2.39) for $y_j(t)$ up to order two leads to,

$$y_j(t) = f_j^1(t) + f_j^2(t)$$

$$y_j(t) = y_{j0} e^{\lambda_j t} + \sum_{k=1}^{n}\sum_{l=1}^{n} C_{kl}^j y_{k0} y_{l0} S_{kl}^j(t)$$

$$y_j(t) = \left(y_{j0} e^{\lambda_j t} - \sum_{k=1}^{n}\sum_{l=1}^{n} h_{2kl}^j y_{k0} y_{l0}\right) e^{\lambda_j t} + \sum_{k=1}^{n}\sum_{l=1}^{n} h_{2kl}^j y_{k0} y_{l0} e^{(\lambda_k+\lambda_l)t} \tag{2.48}$$

Then we have

$$x_i(t) = \sum_{j=1}^{n} L_{i,j}^{\text{modal}} e^{\lambda_j t} + \sum_{k=1}^{n}\sum_{l=1}^{n} S_{i,kl}^{\text{modal}} e^{(\lambda_k+\lambda_l)t} \tag{2.49}$$

where,

$$L_{i,j}^{\text{modal}} = \left(u_{ij} y_{j0} - \sum_{k=1}^{n}\sum_{l=1}^{n} u_{ij} h_{2kl}^j y_{k0} y_{l0}\right)$$

$$S_{i,kl}^{\text{modal}} = \sum_{k=1}^{n}\sum_{l=1}^{n} u_{ij} h_{2kl}^{j} y_{k0} y_{l0}$$

In the latter expression, the second-order nonlinear coefficients $h2_{kl}^{j}$ are defined as,

$$h_{2kl}^{j} = \frac{C_{kl}^{j}}{\lambda_k + \lambda_l - \lambda_j} \tag{2.50}$$

While these methods can be extended to multidimensional systems, numerical procedures may be difficult to apply. Moreover, the extension to higher-dimensional, forced oscillations is not immediately obvious. As a result, the method can be cumbersome and difficult to apply to general nonlinear systems with arbitrary excitations.

In what follows, we extend and generalize this approach to deal with multidimensional systems, considering the case of forced system responses. Emphasis is given to the rigorous determination of analytical closed form approximations to represent the system behavior.

In the notation above the upper number indicates the order associated to the term; *i.e.* at the y^1_j, number 1 means the first order terms of y_j variable, whilst in the y^2_j number 2 equals to the second order terms of y_j variable, and so on.

2.5.3 Initial Conditions in the Modal Series Method

One of the main advantages observed by the Modal Series method with respect to the Normal Forms method is that it does not need any nonlinear transformation for the calculation of the closed form solution of the nonlinear system.

This situation is reflected on the determination of the initial conditions over the different references in both methods. For instance, the Normal Forms method requires the procedure detailed earlier in Section 2.4.3. Initial conditions established in the original coordinates $\mathbf{x}_0$ are transformed to the Jordan canonical variables $\mathbf{y}_0$ and thus, the nonlinear variables $\mathbf{z}_0$ are calculated according to the numerical procedure above described.

Thus, the initial conditions in the Modal Series method are only defined by the linear transformation given by (2.8) as,

$$\mathbf{y}_0 = \mathbf{U}^{-1}\mathbf{x}_0 \tag{2.51}$$

which clearly shows that there is no need any numerical procedure to determine the initial state variables in the new referenced system. That means that the initial conditions only depends on the right eigenvectors characteristics.

2.6 PRINCIPAL DIFFERENCES BETWEEN NORMAL FORMS AND MODAL SERIES METHODS

Some differences between Normal Forms and Modal Series methods are of concern. These differences will be pointed-out here using an example based on a second order nonlinear system.

Consider the second order nonlinear system given by,

$$\begin{aligned} \dot{x}_1 &= f_1\left(x_1, x_2\right) \\ \dot{x}_2 &= f_2\left(x_1, x_2\right) \end{aligned} \tag{2.52}$$

with stable equilibrium points defined as,

$$\begin{aligned} f_1\left(x_1^{\,0}, x_2^{\,0}\right) &= 0 \\ f_2\left(x_1^{\,0}, x_2^{\,0}\right) &= 0 \end{aligned} \tag{2.53}$$

which is the general representation of the nonlinear system that will be developed over the next sections applying the Normal Forms and the Modal Series methods.

2.6.1 Normal Forms Solution

Based on equation (2.39) which links the relationship between the transformed variables with Jordan canonical form, the system (2.52) is linearized around stable equilibrium point defined by (2.53), resulting on,

$$\dot{\mathbf{y}} = \mathbf{A}\mathbf{y} + \mathbf{f}_2\left(\mathbf{y}\right) \tag{2.54}$$

where,

$$\mathbf{f}_2\left(\mathbf{y}\right) = \frac{1}{2}\mathbf{U}^{-1}\begin{bmatrix} \left(\mathbf{U}\mathbf{y}\right)^{\mathrm{T}}\mathbf{H}_2^1\mathbf{U}\mathbf{y} \\ \left(\mathbf{U}\mathbf{y}\right)^{\mathrm{T}}\mathbf{H}_2^2\mathbf{U}\mathbf{y} \end{bmatrix} = \frac{1}{2}\begin{bmatrix} \sum_{k=1}^{n}\sum_{l=1}^{n} C_{kl}^1 y_k y_l \\ \sum_{k=1}^{n}\sum_{l=1}^{n} C_{kl}^2 y_k y_l \end{bmatrix} \tag{2.55}$$

here C_{kl}^{j} is given by(2.40).

Applying the Normal Forms transformation given by (2.54) to the special case of a second order nonlinear system, with $z = \begin{bmatrix} z_1 & z_2 \end{bmatrix}^T$ and $h_2\left(z\right)$ defined as a complex polynomial vector, it gives,

$$h_2\left(z\right) = \begin{bmatrix} \sum_{k=1}^{n}\sum_{l=1}^{n} h_{2kl}^1 z_k z_l \\ \sum_{k=1}^{n}\sum_{l=1}^{n} h_{2kl}^2 z_k z_l \end{bmatrix} \tag{2.56}$$

At this step, the calculation of *z* is achieved with the approach described by (2.55). Finally, the Normal Forms solution is obtained as,

$$\begin{bmatrix} z_1(t) \\ z_2(t) \end{bmatrix} = \begin{bmatrix} z_1^0 e^{\lambda_1 t} \\ z_2^0 e^{\lambda_2 t} \end{bmatrix} \tag{2.57}$$

$$\begin{bmatrix} y_1(t) \\ y_2(t) \end{bmatrix} = \begin{bmatrix} z_1(t) \\ z_2(t) \end{bmatrix} + \begin{bmatrix} \sum_{k=1}^{n}\sum_{l=1}^{n} h_{2kl}^1 z_k^0 z_l^0 e^{(\lambda_k+\lambda_l)t} \\ \sum_{k=1}^{n}\sum_{l=1}^{n} h_{2kl}^2 z_k^0 z_l^0 e^{(\lambda_k+\lambda_l)t} \end{bmatrix} \tag{2.58}$$

$$\begin{bmatrix} x_1(t) \\ x_2(t) \end{bmatrix} = \begin{bmatrix} \Delta\delta(t) \\ \Delta\omega(t) \end{bmatrix} = \begin{bmatrix} u_{11} & u_{12} \\ u_{21} & u_{22} \end{bmatrix} \begin{bmatrix} y_1(t) \\ y_2(t) \end{bmatrix} \tag{2.59}$$

2.6.2 Modal Series Solution

In order to solve the nonlinear system by the Modal Series method, the Jordan canonical form transformed system is applied, *e.g.* from (2.54) we obtain,

$$y_j(t) = f_j^1(t) + f_j^2(t) \tag{2.60}$$

The full solution obtained for the second order nonlinear system is given by,

$$\begin{bmatrix} y_1(t) \\ y_2(t) \end{bmatrix} = \begin{bmatrix} f_1^1(t) \\ f_2^1(t) \end{bmatrix} + \begin{bmatrix} f_1^2(t) \\ f_2^2(t) \end{bmatrix} \tag{2.61}$$

where this time domain solution is carried-out with a function of the Jordan variables; that is,

$$\begin{bmatrix} y_1(t) \\ y_2(t) \end{bmatrix} = \begin{bmatrix} y_1^0 e^{\lambda_1 t} \\ y_2^0 e^{\lambda_2 t} \end{bmatrix} - \begin{bmatrix} \sum_{k=1}^{N}\sum_{l=1}^{N} h_{2kl}^1 y_k^0 y_l^0 e^{\lambda_1 t} \\ \sum_{k=1}^{N}\sum_{l=1}^{N} h_{2kl}^2 y_k^0 y_l^0 e^{\lambda_2 t} \end{bmatrix} + \begin{bmatrix} \sum_{k=1}^{N}\sum_{l=1}^{N} h_{2kl}^1 y_k^0 y_l^0 e^{(\lambda_k+\lambda_l)t} \\ \sum_{k=1}^{N}\sum_{l=1}^{N} h_{2kl}^2 y_k^0 y_l^0 e^{(\lambda_k+\lambda_l)t} \end{bmatrix} \tag{2.62}$$

$$\begin{bmatrix} x_1(t) \\ x_2(t) \end{bmatrix} = \begin{bmatrix} \Delta\delta(t) \\ \Delta\omega(t) \end{bmatrix} = \begin{bmatrix} u_{11} & u_{12} \\ u_{21} & u_{22} \end{bmatrix} \begin{bmatrix} y_1(t) \\ y_2(t) \end{bmatrix} \tag{2.63}$$

2.6.3 Summary of Main Differences Between Normal Forms and Modal Series Methods

- Both methods are based on representing a nonlinear system as a linear one, through Taylor series expansion around a stable equilibrium point.
- The Normal Forms method needs a pair of transformations: from original variables *x*, applying (2.8) the coordinates *y* are obtained, and then the nonlinear transformation given by (2.14) generates the uncoupled and minimal system, in terms of *z* variables. The Modal Series method only needs the transformation of *x* variables into the *y* variables. This step considerably reduces the computational effort.

- The Modal Series method is a potential alternative to the system solution even when a modal resonance is presented in the system [Schanechi, *et al*. 2003].
- The approach for obtaining a solution of the *z* variables (2.14) is not necessary in the Modal Series method. This represents a significant reduction in the numerical calculations since a set of nonlinear algebraic equations is usually a hard problem to solve.

2.7 CASE STUDY. FOURTH ORDER BENCHMARK NONLINEAR SYSTEM

2.7.1 Nonlinear Model Characteristics

The test system proposed in [Dobson 2001] is used to carry-out a linear iterative study of the results obtained through the application of both methods, *i.e.* Normal Forms and Modal Series respectively. The system consists of four nonlinear differential equations, which have the nonlinear condition handled by the ε constant.

$$\begin{bmatrix} \dot{x}_1 \\ \dot{x}_2 \\ \dot{x}_3 \\ \dot{x}_4 \end{bmatrix} = \begin{bmatrix} -1 & 1 & 1 & 0 \\ \mu & -1 & 0 & 1 \\ -1 & 0 & -1 & 1 \\ 0 & -1 & \mu & -1 \end{bmatrix} \begin{bmatrix} x_1 \\ x_2 \\ x_3 \\ x_4 \end{bmatrix} + \begin{bmatrix} 0 \\ \frac{1}{2}\varepsilon x_1^2 \\ 0 \\ 0 \end{bmatrix} \tag{2.64}$$

The Hessian Matrix is,

$$H_{jk}^{i} = 0 \text{ except } H_{11}^{2} = \varepsilon \tag{2.65}$$

and the eigenvalues are

$$\lambda_1 = -1 - \sqrt{\mu} + i\,, \quad \lambda_2 = -1 - \sqrt{\mu} - i \tag{2.66}$$

$$\lambda_3 = -1 + \sqrt{\mu} + i\,, \quad \lambda_4 = -1 + \sqrt{\mu} - i \tag{2.67}$$

The eigenvalues have a strong resonance in $-1+i$ when $\mu = 0$ [Dobson 2001]. Therefore, the parameter μ is assumed $\mu \neq 0$ to diagonalize the state matrix **A** of (2.64).

Hence, the right and left eigenvectors are,

$$\mathbf{U} = \frac{1}{\sqrt{2}\sqrt{1+\mu}} \begin{bmatrix} i & -i & 1 & 1 \\ -i\sqrt{\mu} & i\sqrt{\mu} & \sqrt{\mu} & \sqrt{\mu} \\ -1 & -1 & i & -i \\ \sqrt{\mu} & \sqrt{\mu} & i\sqrt{\mu} & -i\sqrt{\mu} \end{bmatrix} \tag{2.68}$$

$$\mathbf{V}=\mathbf{U}^{-1}=\frac{\sqrt{1+\mu}}{2\sqrt{2}}\begin{bmatrix} -i & \frac{i}{\sqrt{\mu}} & -1 & \frac{1}{\sqrt{\mu}} \\ i & \frac{-i}{\sqrt{\mu}} & -1 & \frac{1}{\sqrt{\mu}} \\ 1 & \frac{1}{\sqrt{\mu}} & -i & \frac{-i}{\sqrt{\mu}} \\ 1 & \frac{1}{\sqrt{\mu}} & i & \frac{i}{\sqrt{\mu}} \end{bmatrix} \tag{2.69}$$

Applying Jordan canonical form to the system (2.64) this is transformed into,

$$\begin{bmatrix} \dot{y}_1 \\ \dot{y}_2 \\ \dot{y}_3 \\ \dot{y}_4 \end{bmatrix}=\begin{bmatrix} \lambda_1 y_1 \\ \lambda_2 y_2 \\ \lambda_1^* y_3 \\ \lambda_2^* y_4 \end{bmatrix}+\frac{\varepsilon\left(y_1+y_2+y_3+y_4\right)^2}{8\sqrt{2}\sqrt{\mu}\sqrt{1+\mu}}\begin{bmatrix} 1 \\ -1 \\ 1 \\ -1 \end{bmatrix} \tag{2.70}$$

with

$$C_{jk}^{i}=\frac{\varepsilon(-1)^{i+1}}{8\sqrt{2}\sqrt{\mu}\sqrt{1+\mu}} \tag{2.71}$$

$$h_{2\,jk}^{\;\;i}=\frac{\varepsilon(-1)^{i+1}}{8\sqrt{2}\left(\lambda_j+\lambda_k-\lambda_i\right)\sqrt{\mu}\sqrt{1+\mu}} \tag{2.72}$$

Equations (2.68)-(2.72) are easily obtained using symbolic applications. For this case, Matlab® symbolic toolbox was used, and it is extensively applied in further case studies tested along this work.

2.7.2 Experiment Design

The main goal of this experiment is to demonstrate that the selected initial condition for the analysis may affect the final response. This constraint of initial conditions has been studied in detail in [Kshatriya 2003] and [Kshatriya *et al*. 2005] through determining error indexes defined under some validation criteria when the Normal Forms method is used. Our research only recalls the main idea from those mentioned works without emphasizing on these indexes. Based on the initial condition given by (2.73) and following the procedure described in Section 2.4.3, initial conditions for Jordan variables y_0 and therefore, for *z* variables are obtained.

Before applying Normal Forms and Modal Series, an arbitrary initial condition is selected [Kshatriya 2003],

$$\mathbf{x}=\begin{bmatrix}0.9 & 0.9 & 0.9 & 0.9\end{bmatrix}^T \tag{2.73}$$

with parameters $\mu=0.65$ and $\varepsilon=2.5$.

A comparison between Normal Forms, Modal Series and the so called direct numerical simulation is performed. This direct numerical simulation is conducted through the numerical solution of the set of nonlinear differential equations given by (2.64), solved by 4th order Runge-Kutta method.

The experiment is designed as follows:

- The system starts its simulation at instant $t = 0$ seconds, with initial conditions given for $\mathbf{x}_0$ according to (2.73).
- The first step is at the time instant $t = 0.5$ seconds. The state variables are calculated in this time instant and valuated, so obtaining the new initial conditions that will be used by the Normal Forms and the Modal Series methods.
- The second step is performed at t =1.0 second, again the state variables are calculated and used as the initial conditions of the Normal Forms and the Modal Series methods. This imply that the simulation with the nonlinear methods starts in the time instant snapshoted (0.5, 1.0, 1.5, …, 5 seconds).
- The subsequent time increments are valuated every 0.5 seconds up to 5 seconds, saving their values at each instant.

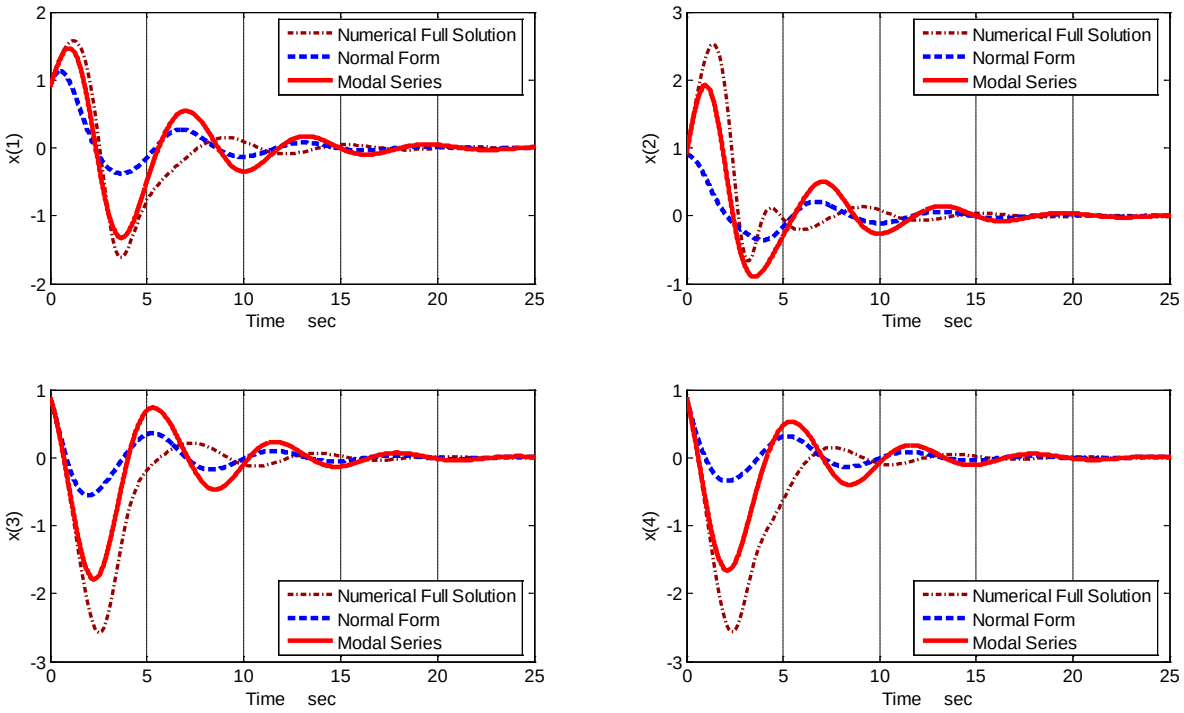

Figure 2.2. Time response comparison of NF and MS methods respect of Numerical solution for dynamic system, when the initial condition is snapshoted from $t = 0$ in time instant $t = 0$ sec

2.7.3 Simulation Results

Every figure is showing the four state variables involved in the experiment, *i.e.* $x(1)$, $x(2)$, $x(3)$ and $x(4)$, which have different dynamic. Thus, different initial conditions are presented when the simulation is evolving with time, observed when Normal Forms and Modal Series method are applied.

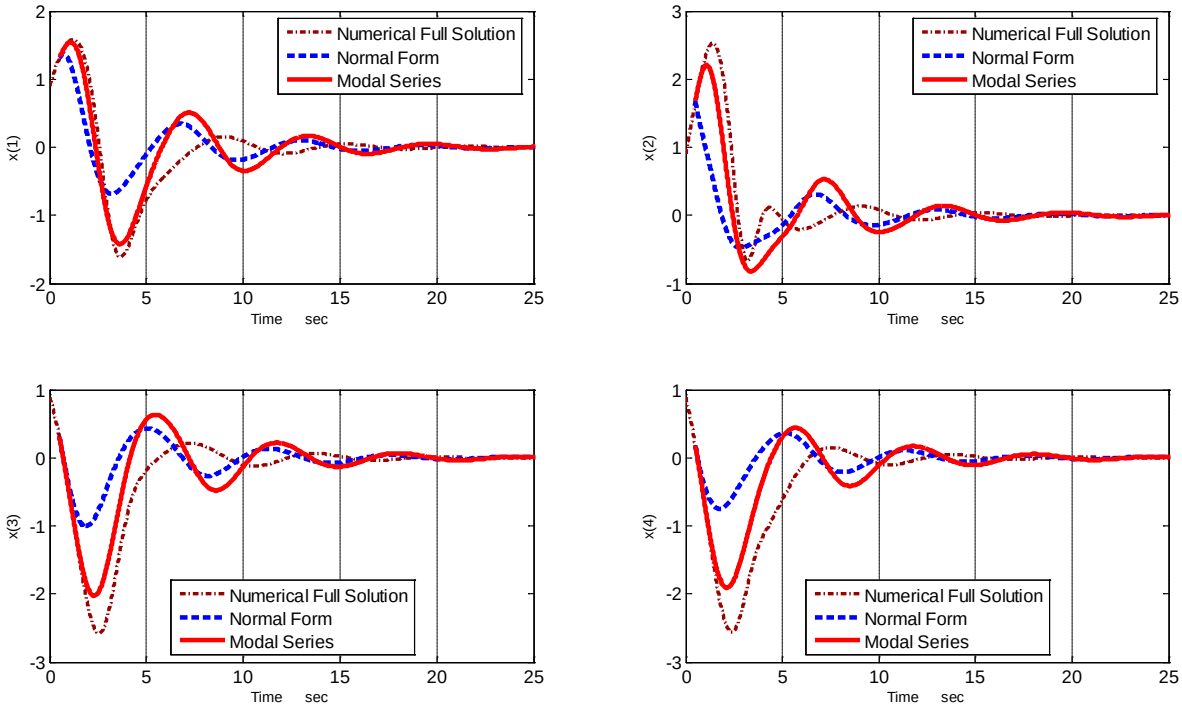

Figure 2.3. Time response comparison of NF and MS methods respect of Numerical solution for dynamic system, when the initial condition is snapshoted from $t = 0$ in time instant $t = 0.5$ sec

Figures 2.2 to 2.10 describe in detail this effect. The evolution of each state variable according to the process above described is shown. The experiment starts at $t = 0$ sec ; the state variables calculated by Normal Forms and Modal Series are compared against those obtained from the full numerical solution. Differences in both amplitude and phase angles are observed; nevertheless, the waveforms obtained through Normal Forms show the worse approximation, being their estimation the highest damping for all state variables (Figure 2.2). A quite similar behavior is observed in Figure 2.3 where the snapshot is at $t = 0.5$ sec . There are no important changes in the approximation of Normal Forms and Modal Series with respect to the direct numerical solution.

Now the experiment continues to the next snapshots at $t = 1.0$ sec and $t = 1.5$ sec . This is shown in Figures 2.4 and 2.5, where a good agreement can be observed between the Normal Forms and Modal

Series solutions, but still denoting differences in amplitude and phase angle with respect to the direct numerical approximation. Over the instant time snapshot $t = 1.5$ sec the Modal Series solution is closer to the numerical full solution leaving with more notorious differences in amplitude and phase angle to the solution obtained with the Normal Forms method. This situation is presented for the four state variables of the nonlinear system.

At instant $t = 2.5$ sec (Figure 2.6) the state variables obtained with Modal Series is nearer to the direct numerical solution. At $t = 2.5$ sec a large peak is obtained for the state variables using the Normal Forms method. After that, the time evolution is again closer to the rest of variables.

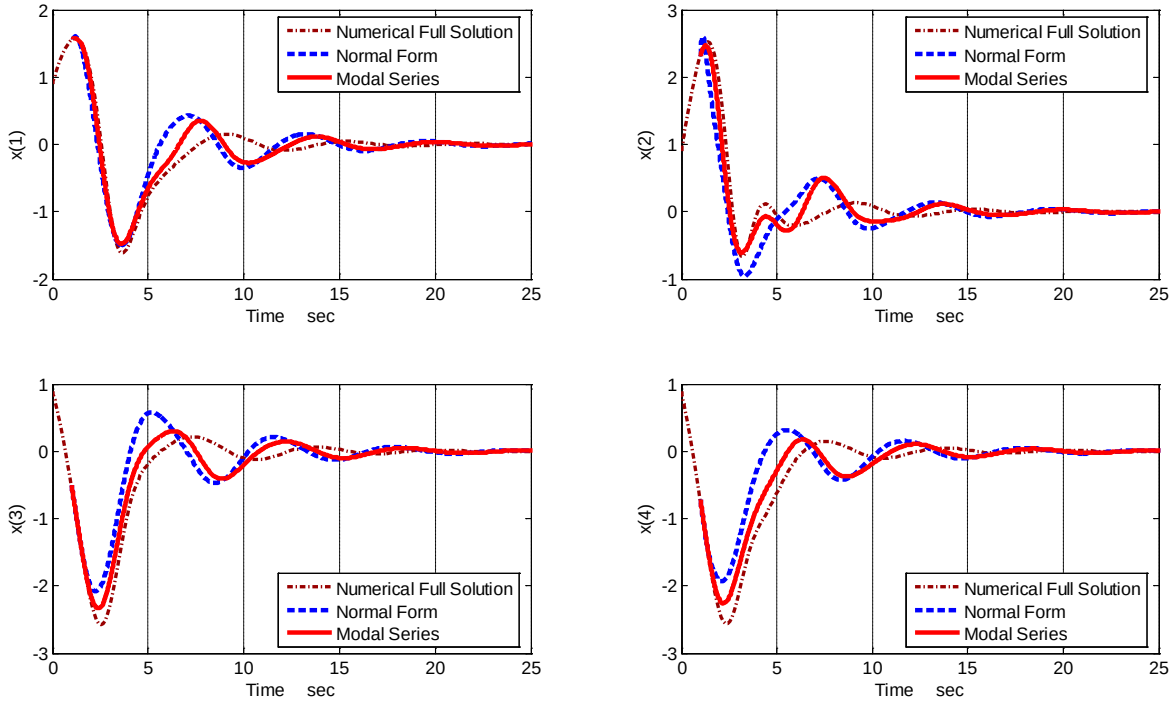

Figure 2.4. Time response comparison of NF and MS methods respect of Numerical solution for dynamic system, when the initial condition is snapshoted from $t = 0$ in time instant $t = 1.0$ sec

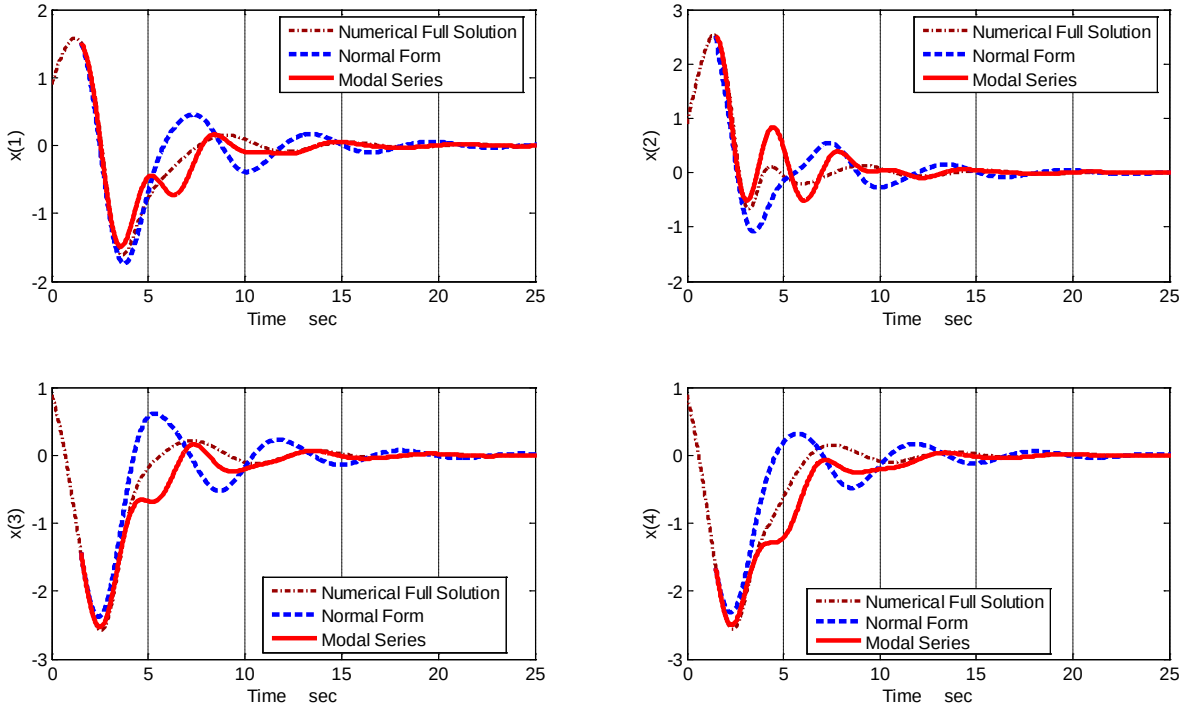

Figure 2.5. Time response comparison of NF and MS methods respect of Numerical solution for dynamic system, when the initial condition is snapshoted from $t = 0$ in time instant $t = 1.5$ sec

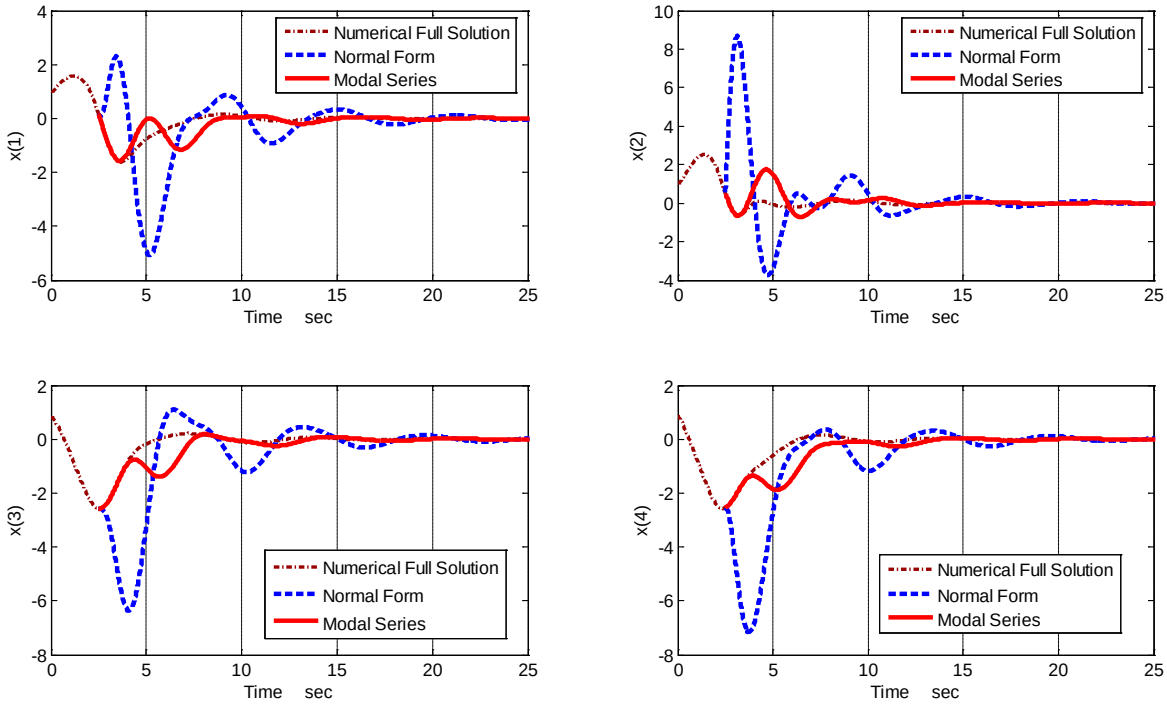

Figure 2.6. Time response comparison of NF and MS methods respect of Numerical solution for dynamic system, when the initial condition is snapshoted from $t = 0$ in time instant $t = 2.5$ sec

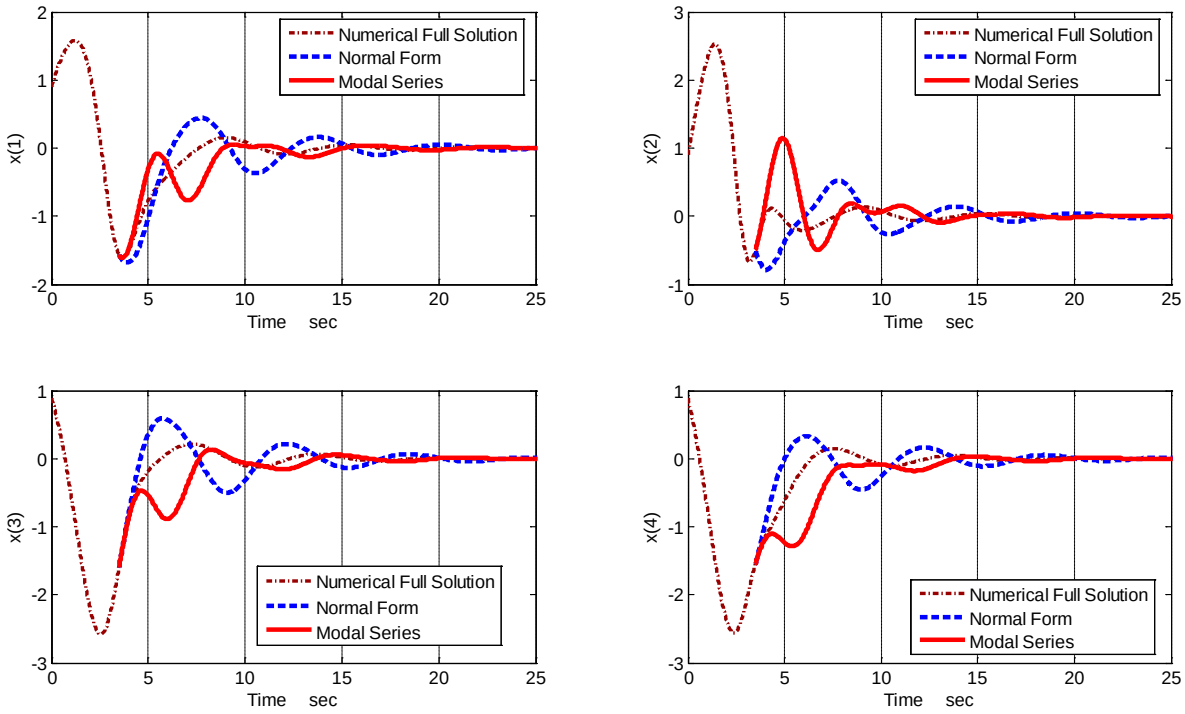

Figure 2.7. Time response comparison of NF and MS methods respect of Numerical solution for dynamic system, when the initial condition is snapshoted from $t = 0$ in time instant $t = 3.5$ sec

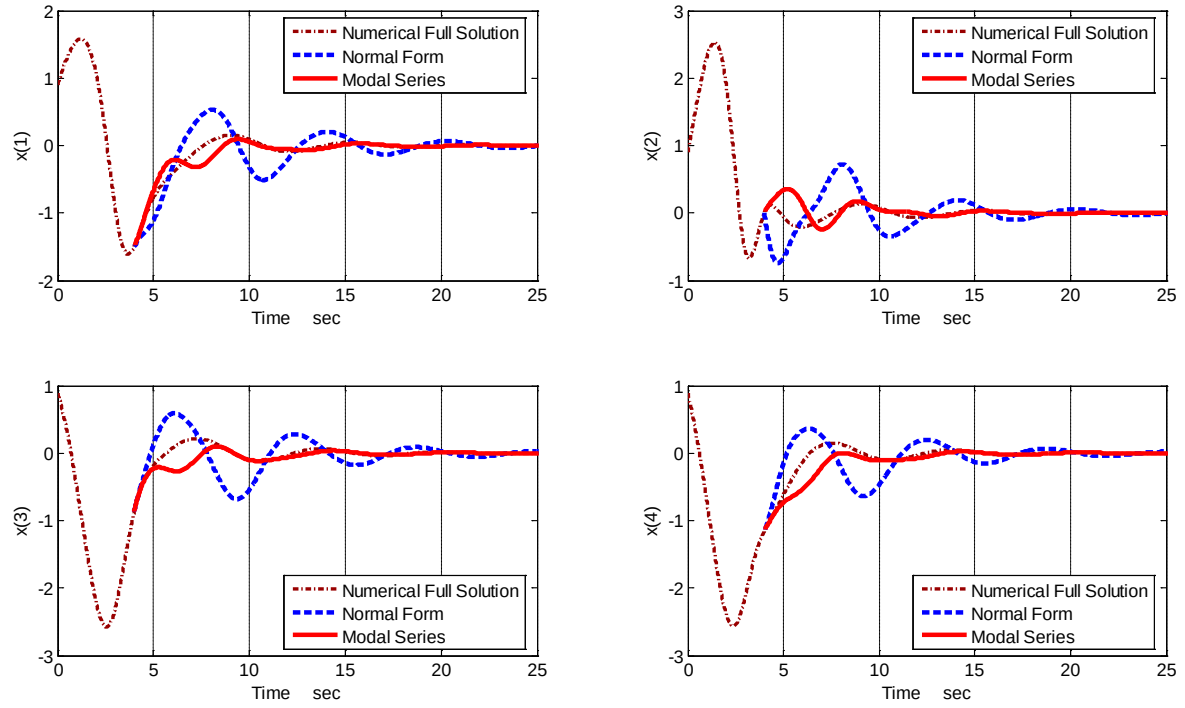

Figure 2.8. Time response comparison of NF and MS methods respect of Numerical solution for dynamic system, when the initial condition is snapshoted from $t = 0$ in time instant $t = 4.0$ sec

These sudden increases are mainly due to the numerical calculation of the new approximation of *z* variables in the Normal Forms nonlinear variables, once a Newton method has been applied in order to obtain the new approximation.

The experiment continues for the next time instants snapshots, *e.g.* $t = 3.5$ sec and $t = 4.0$ sec. A closer agreement between the Modal Series solution and the full numerical solution is observed, in both, amplitude and phase angle; mainly for the state variables $x(1)$, $x(3)$ and $x(4)$. The Normal Forms approximation is significantly deviated from the rest of trajectories, showing higher amplitude and completely different phase angle. These graphics can be observed from Figures 2.7 and 2.8.

After $t = 4.5$ sec, Figure 2.9 shows that the response of the three methods tends to be identical. They eventually reach the same trajectory, when the time is closer to $t = 5$ sec, as noticed from Figure 2.10. This fact is due to the state variables approach the vicinity of the equilibrium point condition, until this is reached at $t = 10$ sec.

Once the experiment was conducted through the time snapshots given by moving forward the initial approximation, it can be concluded that the Normal Forms method is more sensitive to changes in its initial approximation, to properly estimate a precise solution of the nonlinear dynamic system.

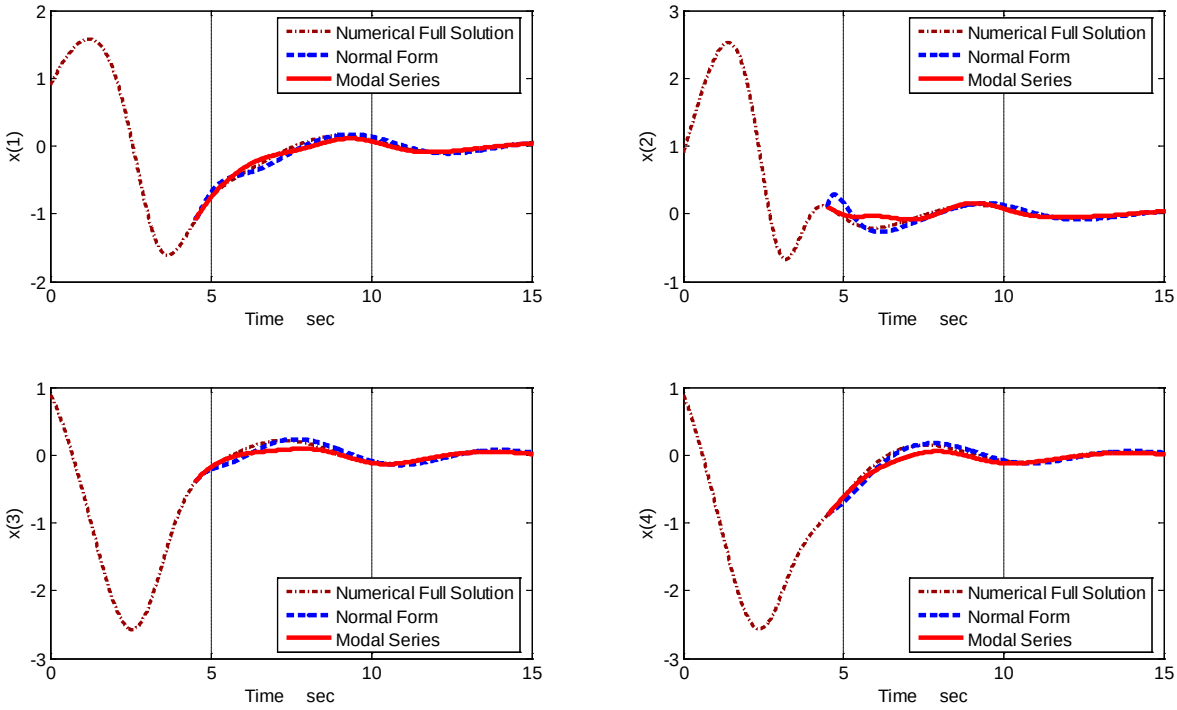

Figure 2.9. Time response comparison of NF and MS methods respect of Numerical solution for dynamic system, when the initial condition is snapshoted from $t = 0$ in time instant $t = 4.5$ sec

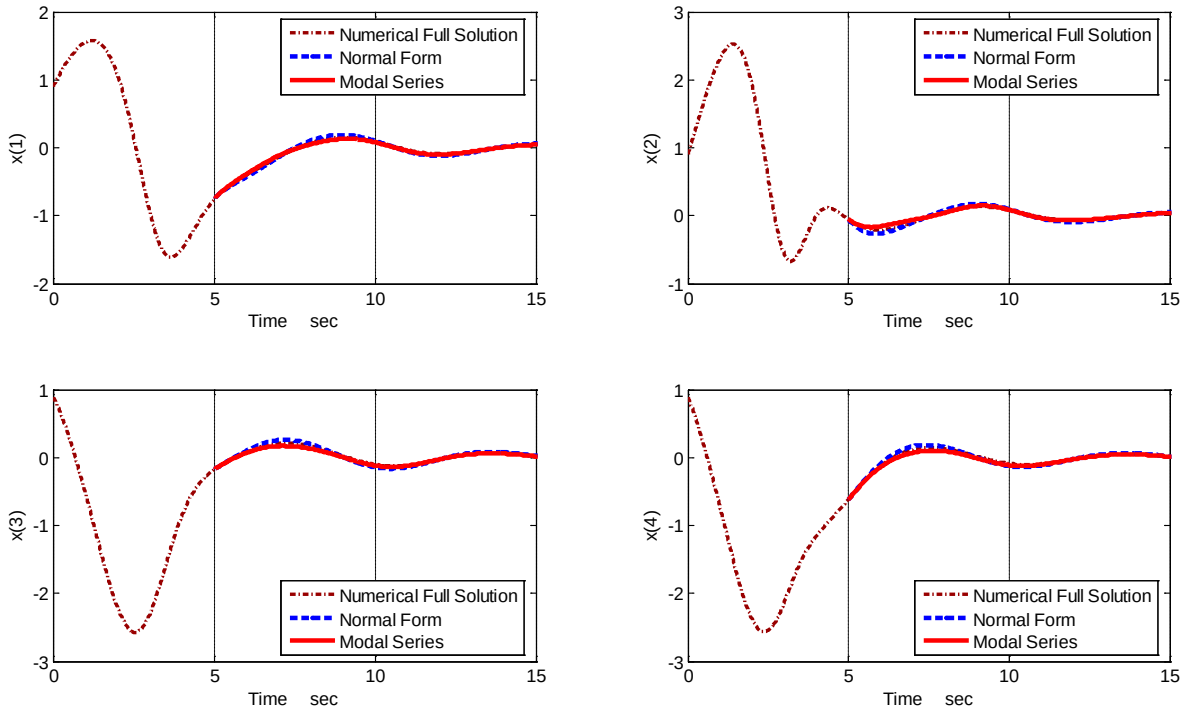

Figure 2.10. Time response comparison of NF and MS methods respect of Numerical solution for dynamic system, when the initial condition is snapshoted from $t = 0$ in time instant 5.0 seconds

The experiment demonstrated that Modal Series is less sensitive to the changes in initial conditions; however, it is important to establish a precise operating point, since the method is linearized around an equilibrium point. That means that while the initial estimation is closer to the stable equilibrium point, the solution is better approximated.

2.7.4 Change on Initial Conditions

Selecting a different initial condition, for instance, $x_0 = [0.45 \quad 0.4 \quad 0.4 \quad 0.4]$, may be considered a better option. Figure 2.11 shows the evolution of state variables under this constraint, where quite significant similitude between the responses using Normal Forms, Modal Series and direct numerical solution can be inferred. Nevertheless, it can be noticed that there are still considerable differences between Normal Forms waveforms, with respect to Modal Series and direct numerical solution waveforms obtained for each state variable. Basically the differences are only in amplitude, keeping the same phase shifting.

Different initial conditions for the same experiment may be proposed. Assuming $x_0 = [0.45 \quad 0.2 \quad 0.2 \quad 0.2]$ a better approximation of the three methods are obtained and shown in

Figure 2.12, where it is clearly observed that all the state variables obtained with the three different methods follow identical trajectories with a negligible difference.

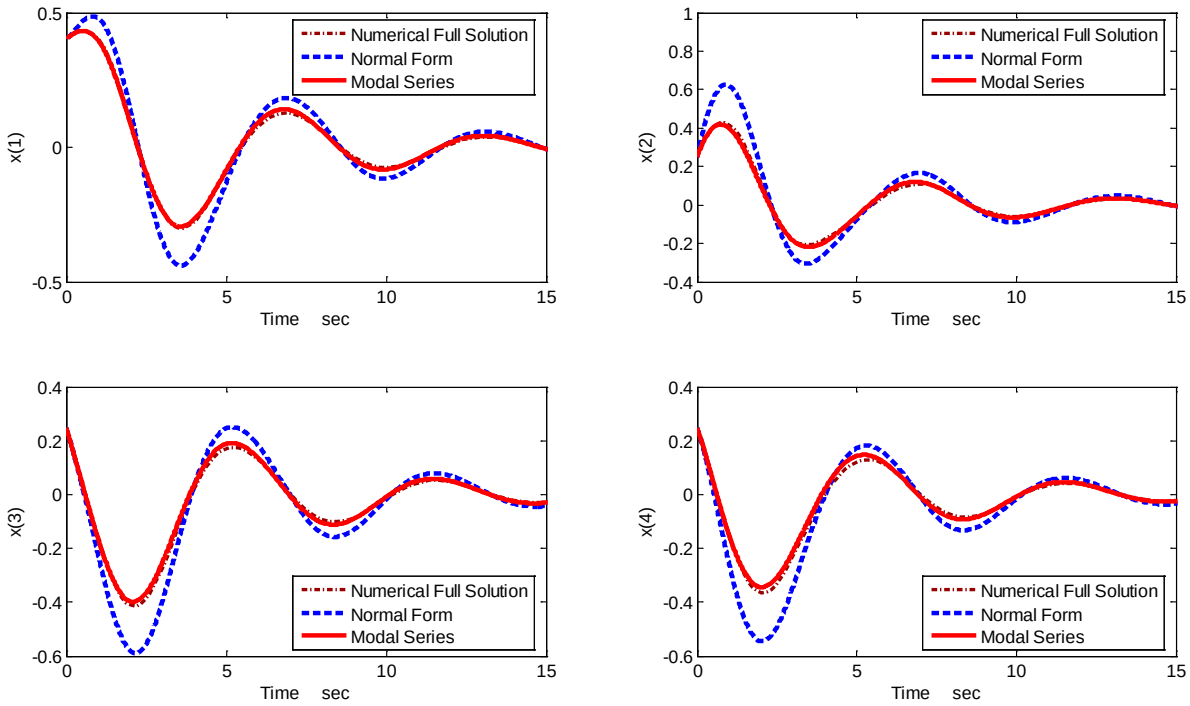

Figure 2.11. State variables response upon initial condition $x_0 = \begin{bmatrix} 0.45 & 0.4 & 0.4 & 0.4 \end{bmatrix}$ over time $t = 0$ sec

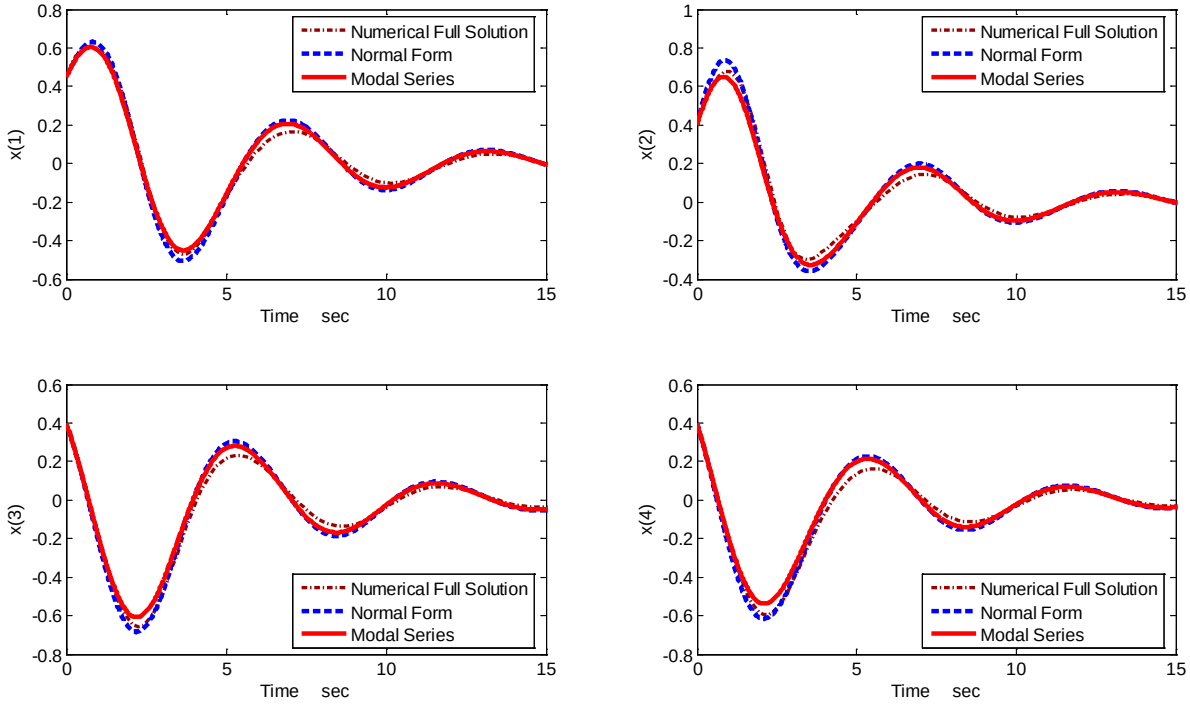

Figure 2.12. State variables response upon initial condition $x_0 = \begin{bmatrix} 0.45 & 0.2 & 0.2 & 0.2 \end{bmatrix}$ over time $t = 0$ sec

Hence, it can be said that these initial conditions mean the best starting point under the constraints previously defined for this experiment. Some other conditions may be analyzed varying the parameters associated to the nonlinear system.

Figures 2.13 through 2.18 show waveforms of state variables when variations on parameters ε and μ are made. Some important comments about this change can be drawn:

- In Figure 2.13, the nonlinear system parameters $\varepsilon = 2.5,\ \mu = 0.3250$ are varied, which represents a reduction on parameter μ, related to the real part of eigenvalues. An increment on the amplitude of the waveforms followed by the Modal Series method is observed.
- However, by keeping unchanged μ and increasing ε, the Modal Series approximation is closer to the direct numerical approximation than the Normal Forms response, as shown by Figure 2.14. Thus, it can be inferred that increasing the nonlinear characteristic, the Modal Series method approximates more closely the state variables behavior. The same result is observed in Figure 2.15, where an increase in the nonlinear parameter ε is combined with a decrease of μ.

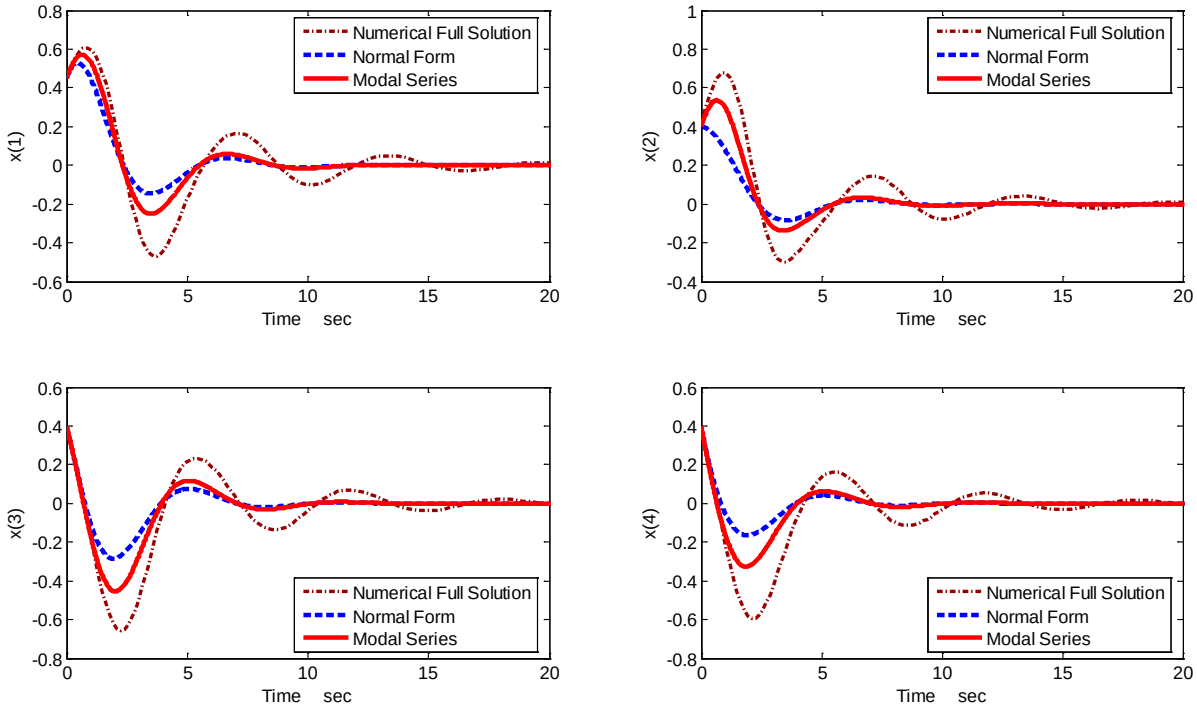

Figure 2.13. State variables for the case of parameters $\varepsilon = 2.5,\ \mu = 0.3250$ in the fourth order nonlinear benchmark system

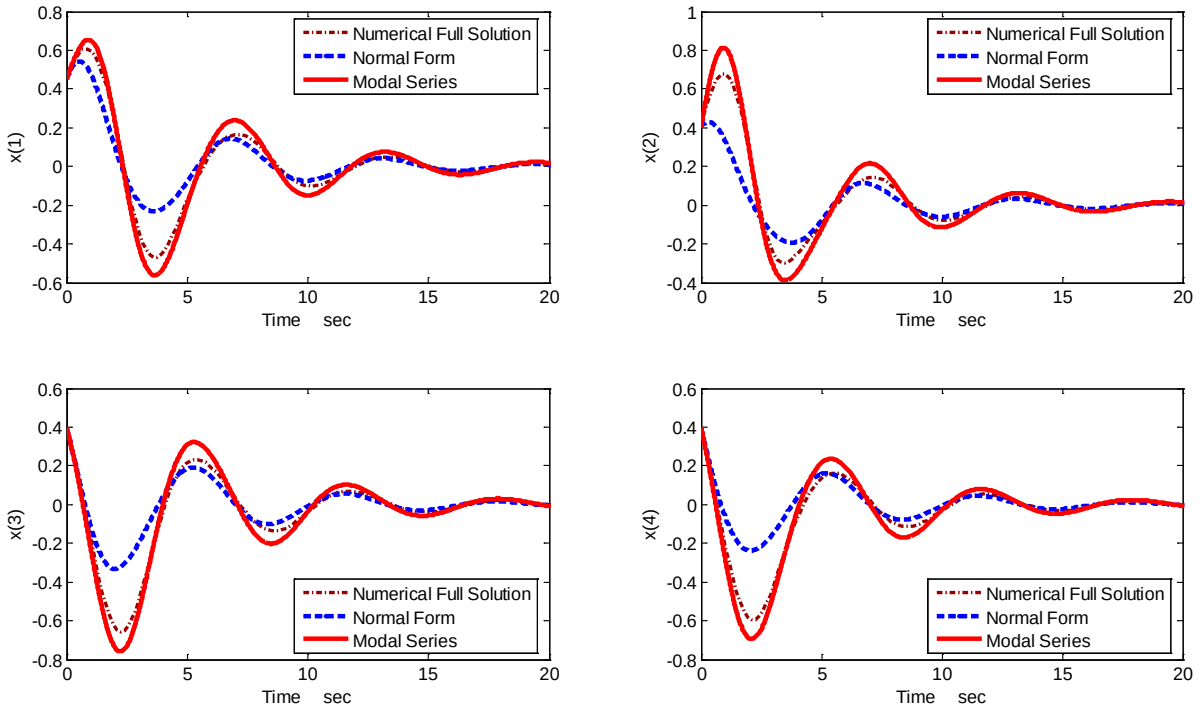

Figure 2.14. State variables for the case of parameters $\varepsilon = 4.5,\ \mu = 0.65$ in the fourth order nonlinear benchmark system

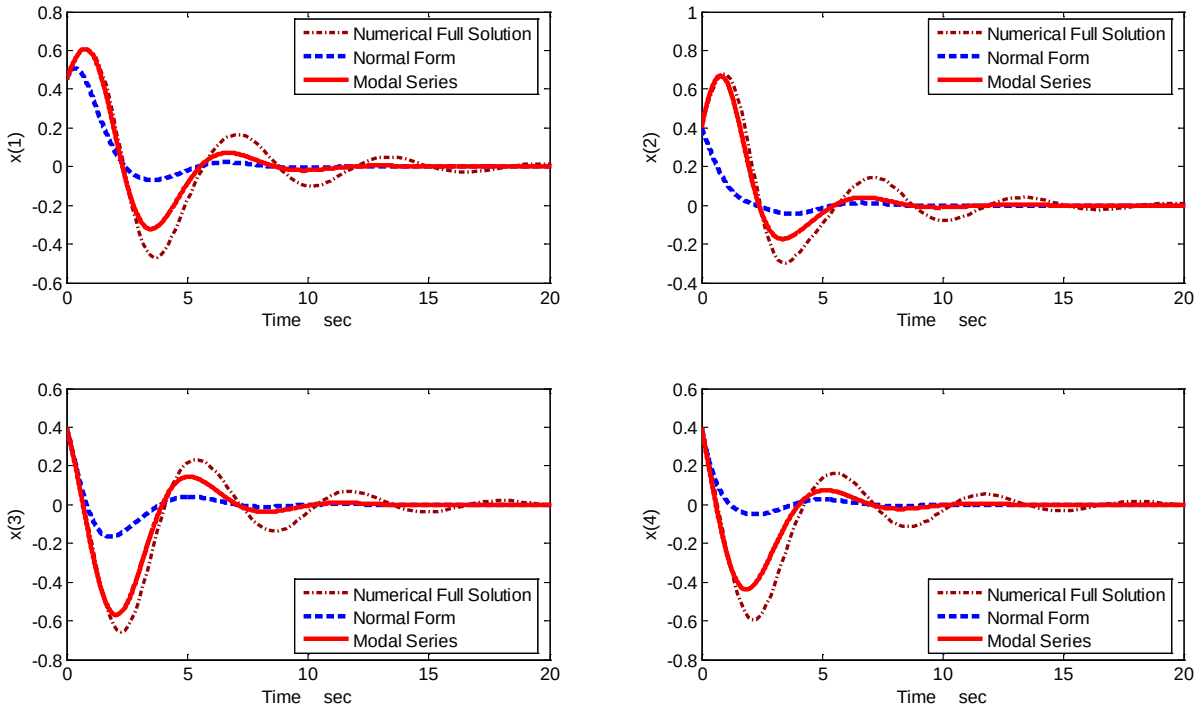

Figure 2.15. State variables for the case of parameters $\varepsilon = 4.5,\ \mu = 0.3250$ in the fourth order nonlinear benchmark system

- Figure 2.16 shows the state variables for $\varepsilon = 4.5$, higher than the initial value, with μ reduced to $\mu = 0.065$. The Modal Series and the Normal Forms approximation, do not closely follow the time evolution of the direct numerical approximation. A similar situation is presented for the case denoted by Figure 2.17 where, although ε is even more larger ($\varepsilon = 6.5$), neither the Modal Series method nor Normal Forms method can closely follow the trajectory of the direct numerical approximation for the assumed range of study.
- Finally, a substantial increase on ε to $\varepsilon = 8.5$ combined with a remarkable reduction on μ to $\mu = 0.0065$, significantly improves the agreement of Modal Series to direct numerical approximation, being the Normal Forms approximation the worse alternative for this case. The experiment is shown in Figure 2.18.
- It can be observed, that under the same selected conditions for the application of the three methods, over the range of changes on nonlinear system parameters analyzed through Figures 2.14 to 2.18, the Normal Forms method gave the worse approximation for all the cases here described, when the parameters ε and μ are varied as: $\varepsilon = 4.5,\ \mu = 0.065$ (Figure 2.16); $\varepsilon = 6.5,\ \mu = 0.065$ (Figure 2.17); $\varepsilon = 8.5,\ \mu = 0.0065$ (Figure 2.18).

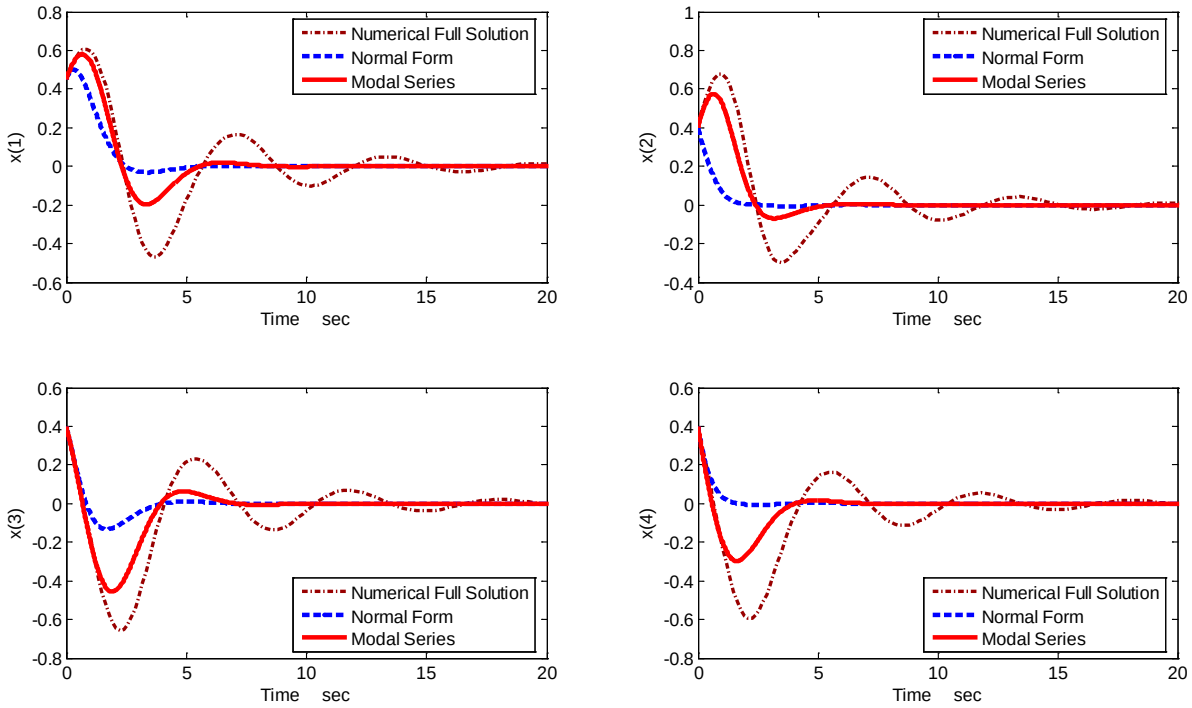

Figure 2.16. State variables for the case of parameters $\varepsilon = 4.5,\ \mu = 0.065$ in the fourth order nonlinear benchmark system

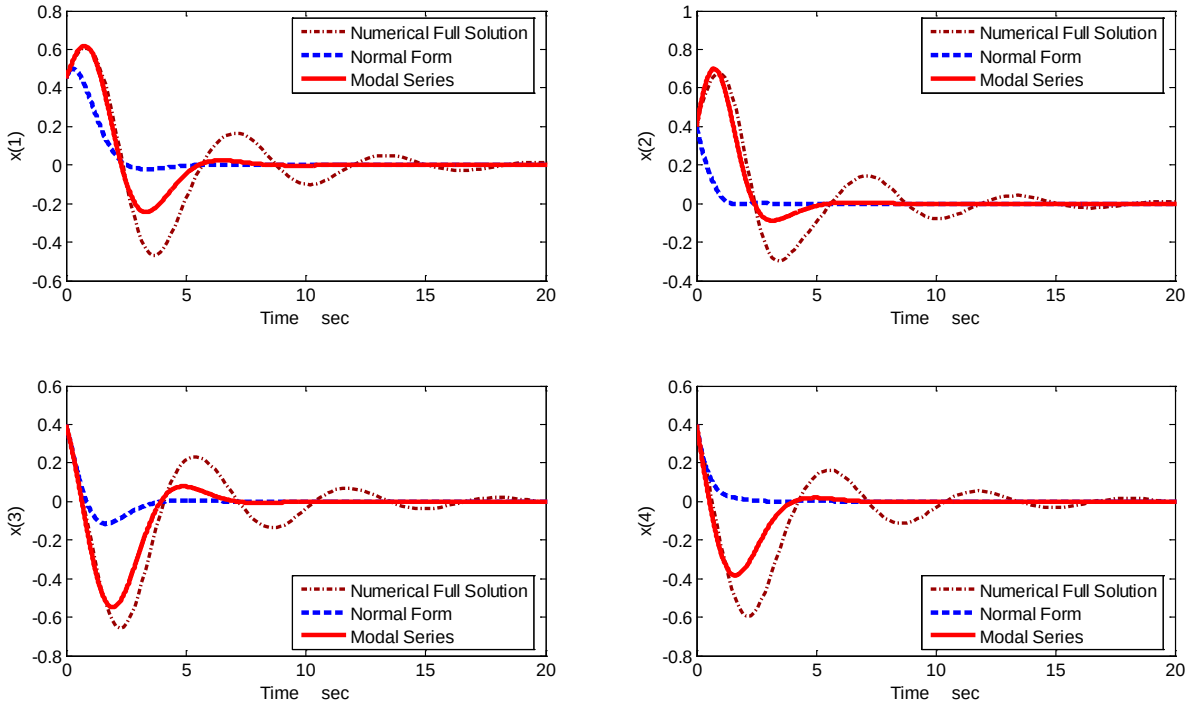

Figure 2.17. State variables for the case of parameters $\varepsilon = 6.5,\ \mu = 0.065$ in the fourth order nonlinear benchmark system

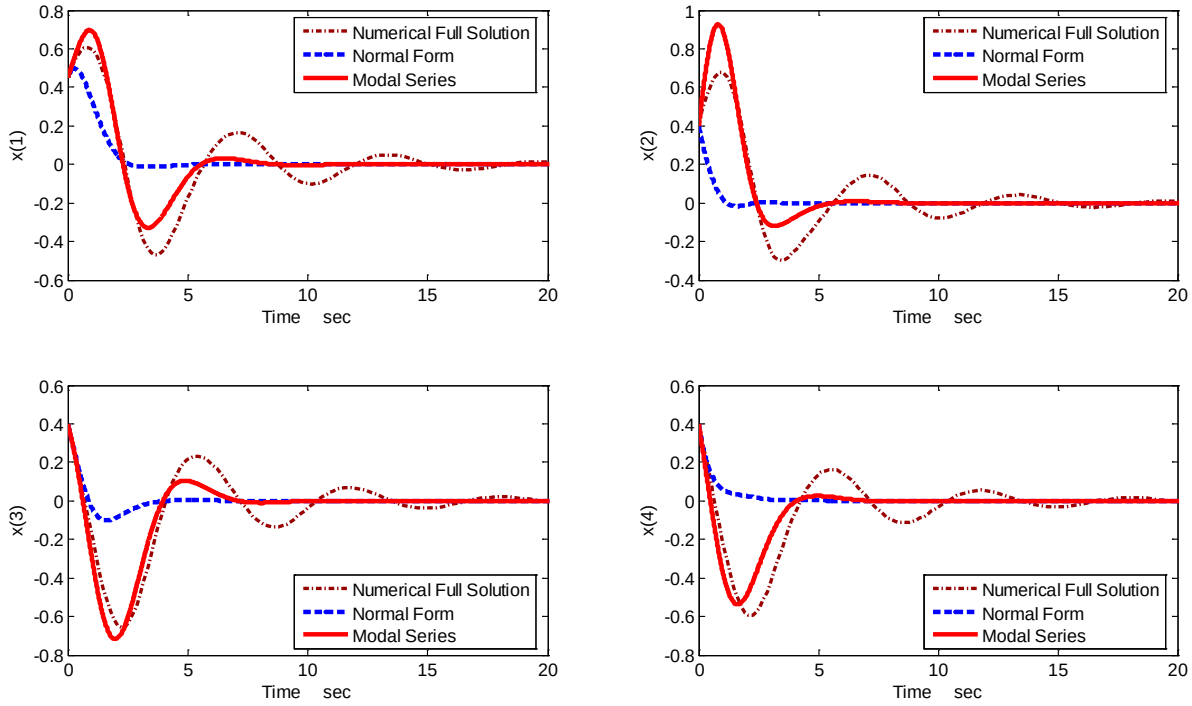

Figure 2.18. State variables for the case of parameters $\varepsilon = 8.5,\ \mu = 0.0065$ in the fourth order nonlinear benchmark system

2.8 DISCUSSION

A comparison study of the Normal Forms and Modal Series methods has been studied in this Chapter. The main mathematical fundaments and analytical characteristics have been described. It can be inferred that both methods in their own fundations have some similarities but each of them keep their own characteristics, basically on the linear and nonlinear transformations needed. Normal Forms must perform a nonlinear transformation, while Modal Series only needs a linear transformation. Even when the Normal Forms method has been successfully used for a wide range of applications in power systems, the method of Modal Series may present an important advantage also guided by the absence of numerical solution determination of its initial conditions, being this fact a big disadvantage of the Normal Forms method. The numerical solution of nonlinear algebraic systems is cumbersome and can present convergence problems.

The application of both methods to the solution of a nonlinear fourth order benchmark system has shown remarkable differences along the study, when the initial conditions of both methods were changed; also, parameter variations may result in some notorious differences with respect to the validation solution obtained by the direct numerical simulation of the nonlinear set of differential equations.

THIS PAGE IS INTENTIONALLY LEFT BLANK

3

THE MODAL SERIES METHOD BASED ON THE MULTIDIMENSIONAL LAPLACE TRANSFORM

The method of modal series described in the previous Chapter is revisited here. Some important additions on its analytical basis, mainly described by the re-formulation applying the multidimensional Laplace Transform and association of variables approach are described in detail. The extension to include higher order terms in a systematical way is proposed. Advantages and disadvantages observed in the modal series method are pointed out. A detailed application of the methodology to a simple synchronous machine-infinite busbar power system is performed.

3.1 INTRODUCTION

The identification of the nonlinear system behavior is an increasingly important area of research, with applications in many areas of power system analysis and control. Various methods based on modal expansion procedures and perturbation theory have been explored to represent the power system nonlinear dynamics following small perturbations. Normal form theory and modal series analysis methods have been developed and applied to investigate various aspects of the system dynamic response. These methods allow the definition of nonlinear modal coupling indices in terms of the structural parameters and can be used to express the system response as a superposition of modal responses. A proper estimate of nonlinear modal interaction is essential to accurately predict dominant modes and the location and design of system controllers.

In [Pariz *et al.* 2003] and [Schanechi *et al.* 2003], a technique based on modal analysis of the perturbation model of the power system was used to investigate nonlinear effects in power system dynamics. The main advantage of this method is its simplicity, while some drawbacks arise from the need to generalize the method to more complex system representations.

In this chapter, some aspects behind the underlying theory of modal series methods are critically examined. Using an extended modal analysis method and concepts from Volterra series theory, a

systematic technique to derive closed-form approximate solutions of a perturbation model of the power system is developed. Then, a general procedure based on the multi-dimensional Laplace transform is proposed to derive closed form modal series.

3.2 BACKGROUND OF THE MODAL SERIES METHOD

Nonlinear modal analysis has been extensively used to study the system dynamic behavior in a variety of nonlinear system events. In this section, we summarize the modal series analysis method and the main results obtained from modal analysis.

Considering an *n*-dimensional dynamical system model described by *n* first-order nonlinear differential equations of the form,

$$\dot{\mathbf{x}} = \mathbf{f}(\mathbf{x}, \mathbf{u}) \tag{3.1}$$

where **x** is an *n*-dimensional vector of system states, and $\mathbf{f} : R^n \to R^n$ is a smooth vector field; $\mathbf{u} \in \Re^m$ is the control vector. The vector function $\mathbf{f}(\mathbf{x}, \mathbf{u})$ and its partial derivatives with respect to **x** and **u** are assumed to be continuously differentiable functions of **x** and **u**.

Expanding $\mathbf{f}(\mathbf{x}, \mathbf{u})$ in Taylor series (as it was described in Section 2.2) about the initial equilibrium point, X_{sep} yields,

$$\dot{\mathbf{x}} = \mathbf{A}\mathbf{x} + \mathbf{F}_2(\mathbf{x}) + ... + \mathbf{F}_{r-1}(\mathbf{x}) + O(|\mathbf{x}|^r) + \mathbf{B}\mathbf{u} \tag{3.2}$$

where **A** contains the linear part of the vector field, and the terms $\mathbf{F}_k$, $k \geq 2$ contain nonlinear terms; *r* is the order of the approximation.

Equation (3.2) can be rewritten as

$$\dot{x}_i = A_i x + \frac{1}{2}\sum_{k=1}^{n}\sum_{l=1}^{n} F_{2kl}^{i} x_k x_l + \frac{1}{6}\sum_{p=1}^{n}\sum_{q=1}^{n}\sum_{r=1}^{n} F_{3pqr}^{i} x_p x_q x_r + \ldots + b_i u_i \tag{3.3}$$

where ,

A_i is the i^{th} row of the Jacobian matrix, $A_i = \left(\frac{\partial f_i}{\partial x}\right)\Big|_{x_{sep}}$ of $f(x)$

F_{2kl}^{i} is the kl^{th} second-order term associated with the i^{th} state, $F_{2kl}{}^{i} = \left(\frac{\partial^2 f_i}{\partial x_k \partial x_l}\right)\Big|_{x_{sep}}$ or Hessian of $f(x)$

F_{3pqr}^{i} is the pqr^{th} third-order term associated with the *i*th state, $F_{3pqr}^{i} = \left(\frac{\partial^3 f_i}{\partial x_p \partial x_q \partial x_r}\right)\Big|_{x_{sep}}$

and so on.

The above modal expansion procedure has been used by several authors to carry-out modal analysis of complex power system models [Vittal *et al.* 1991]. At the core of this framework is the identification of the nonlinear modal interaction arising from a stressed power system behavior and the computation of closed-form analytical expressions assuming the modal series as the analysis platform.

Let the state matrix $\mathbf{A} = Df(x_{sep})$ have an eigenvalue set $\{\lambda_1 \quad \lambda_2 \quad \cdots \quad \lambda_n\}$ with associated eigenvectors **U** and reciprocal eigenvectors $\mathbf{V} = \mathbf{U}^{-1}$. Then, the linear change of coordinates $\mathbf{x} = \mathbf{U}\mathbf{y}$ (known as a Jordan canonical form transformation) linearly transforms the system in Equation (3.3) into its decoupled form,

$$\dot{y}_j = \lambda_j y_j + \sum_{k=1}^{n}\sum_{l=1}^{n} C_{kl}^{j} y_k y_l + \sum_{p=1}^{n}\sum_{q=1}^{n}\sum_{r=1}^{n} D_{pqr}^{j} y_p y_q y_r + \ldots + \hat{b}_i u_i \tag{3.4}$$

with $j = 1,...,n$

with initial conditions, $y_j^o = y_{jo}$, where terms above third-order are assumed to be negligible, and

$$C_{kl}^{j} = \frac{1}{2}\sum_{p=1}^{n} V_{jp}^{T}\left[U^T H_2{}^P U\right] \tag{3.5}$$

$$D_{pqr}^{j} = \frac{1}{6}\sum_{p=1}^{n}\sum_{q=1}^{n}\sum_{r=1}^{n} H_3^j V_p^P V_q^Q V_r^R \tag{3.6}$$

$\vdots$

By analogy to the second order coefficients definition, the D_{pqr}^{j} represent the contribution of modes *p*, *q* and *r* to the mode *j* in the dynamic behavior of the Jordan coordinates system represented by (3.4) [Barocio 2003].

In situations where truncation is sufficient to approximate the system behavior, low-dimensional representations can be used. Efforts to extend this approach to the higher-dimensional case have been limited and have concentrated on normal form analysis [Martínez 2006] [Martinez *et al.* 2004*a*] and bilinear analysis techniques [Arroyo 2007].

3.3 THE MODAL SERIES REVISITED: MATHEMATICAL MODEL

The modal series method revisited in this section incorporates the multidimensional Laplace transform as a versatile way of solution for the still coupled dynamic system given by (3.4). Indeed, this system is solved not only for the already uncoupled linear part of (3.4), but in addition the second, third, etc. order terms have to be determined. Laplace transform means a very practical way to solve this system; besides, it is possible to obtain transfer functions of these terms as it will treated in the next Chapter.

Hence, referring to the basis of modal series from [Pariz *et al.* 2003] and [Schanechi *et al.* 2003] a systematic determination of modal response, including the assessment of the extent to which specific modes contribute to the system response is developed [Rodríguez and Medina 2010].

3.3.1 The Modal Series Free System Response

Assuming the natural response of the nonlinear system, that is, $u = 0$, the system response can be expressed in the general form following the definition from Volterra series, which expressed the output of a nonlinear system [Rugh 1981] in the form,

$$y(t) = \sum_{n=1}^{\infty} \varepsilon^n y_n(t) \tag{3.7}$$

and its derivate terms,

$$\dot{y}(t) = \sum_{n=1}^{\infty} \varepsilon^n \dot{y}_n(t) \tag{3.8}$$

Substituting Equations (3.7) and (3.8) in Equation (3.4) and equating the coefficients of ε (variational approach) [Rugh 1981], results in

$$\begin{aligned}
&\varepsilon\, \dot{y}_j^1(t) + \varepsilon^2 \dot{y}_j^2(t) + \varepsilon^3 \dot{y}_j^3(t) + \ldots = \\
&\lambda_j \left(\varepsilon\, y_j^1(t) + \varepsilon^2 y_j^2(t) + \varepsilon^3 y_j^3(t) + \ldots \right) + \\
&\sum_{k=1}^{n} \sum_{l=1}^{n} C_{kl}^j \left[\varepsilon^2 y_k(t) y_l(t) + \varepsilon^3 y_k^2(t) y_l(t) + \varepsilon^3 y_k(t) y_l^2(t) + \right. \\
&\qquad \left. \varepsilon^4 y_k(t) y_l^3(t) + \varepsilon^4 y_k^2(t) y_l^2(t) + \varepsilon^4 y_k^3(t) y_l(t) + \ldots \right]
\end{aligned} \tag{3.9}$$

Carrying out the indicated operations yields

$$\dot{y}_j(t) = \lambda_j y_j(t) \tag{3.10}$$

$$\dot{y}_j^2(t) = \lambda_j y_j^2(t) + \sum_{k=1}^{n} \sum_{l=1}^{n} C_{kl}^j y_k(t) y_l(t) \tag{3.11}$$

$$\dot{y}_j^3(t) = \lambda_j y_j^3(t) + \sum_{k=1}^{n} \sum_{l=1}^{n} C_{kl}^j \left[y_k^2(t) y_l(t) + y_k(t) y_l^2(t) \right] + \sum_{p=1}^{n} \sum_{q=1}^{n} \sum_{r=1}^{n} D_{pqr}^j y_p^1(t) y_q^1(t) y_r^1(t) \tag{3.12}$$

$\vdots$

Transforming the equations (3.10)-(3.12) using Laplace transform, a system defined in terms of Laplace domain is obtained. In this step, the higher order terms may be either included or neglected, depending on the accuracy required for the dynamic analysis. Hence, the transformed system has the form,

$$s_1 Y_j^1(s) - Y_j^1(0) = \lambda_j Y_j^1(s) \tag{3.13}$$

$$(s_1 + s_2) Y_j^2(s_1, s_2) = \lambda_j Y_j^2(s_1, s_2) + \sum_{k=1}^{n} \sum_{l=1}^{n} C_{kl}^j Y_k^1(s_1) Y_l^1(s_2) \tag{3.14}$$

$$\begin{aligned}(s_1+s_2+s_3)Y_j^3(s_1,s_2,s_3)=\lambda_j Y_j^3(s_1,s_2,s_3)+\sum_{k=1}^{n}\sum_{l=1}^{n}C_{kl}^{j}\left[Y_k^2(s_1,s_2)Y_l^1(s_3)+Y_k^1(s_1)Y_l^2(s_2,s_3)\right]\\ +\sum_{p=1}^{n}\sum_{q=1}^{n}\sum_{r=1}^{n}D_{pqr}^{j}\left[Y_p^1(s_1)Y_q^1(s_2)Y_r^1(s_3)\right]\end{aligned} \tag{3.15}$$

$\vdots$

Please observe that the transformed system is given in the multidimensional Laplace domain, being $s_1, s_2, s_3, \ldots$ the first, second, third, etc. order terms associated to the same order coupled terms. The generalization to the multidimensional case is rather cumbersome and difficult to apply. To circumvent these limitations, an efficient approach based on the application of multidimensional Laplace transform is suggested.

3.3.2 Multidimensional Laplace Transform

For an assumed multivariate function or kernel $f(t_1,t_2,...,t_n)$ of *n* variables $t_1,t_2,...,t_n$, the direct Laplace transform of *f* is defined by [Shmaliy 2007],

$$F(s_1,s_2,\ldots,s_n)=Lf(t_1,t_2,\ldots,t_n)$$

$$F(s_1,s_2,\ldots,s_n)=\int_{-\infty}^{\infty}\ldots\int_{-\infty}^{\infty}f(t_1,t_2,\ldots,t_n)e^{-s_1t_1}dt_1\ldots dt_n \tag{3.16}$$

Now, being $F(s_1,s_2,\ldots,s_n)$ a Laplace Transform of $f(t_1,t_2,...,t_n)$, the inverse of the multi-dimensional Laplace transform can be written as [Debnath 1989],

$$f(t_1,t_2,\ldots,t_n)=L_n^{-1}\left[F(s_1,s_2,\ldots,s_n);t_1,t_2,\ldots,t_n\right] \tag{3.17}$$

or,

$$f(t_1,t_2,\ldots,t_n)=\frac{1}{(2\pi i)^n}\int_{\alpha_1-i\infty}^{\alpha_1+i\infty}\ldots\int_{\alpha_n-i\infty}^{\alpha_n+i\infty}e^{\left(\sum_{j=1}^{n}s_jt_j\right)}F(s_1,s_2,\ldots,s_n)ds_1\,ds_2\ldots ds_n \tag{3.18}$$

where $f(t_1,t_2,...,t_n)$ are real-valued functions of t_1 and t_2 and the transform is a function of *n* variables.

If there two or more multivariate functions of the same class with different number of variables are presented, there are some useful properties of the Laplace transform that can be applied [Shmaliy 2007].

Distributivity

Given f_i the distributivity property is expressed as,

$$L\sum_{i=1}^{n}f_i(t_1,t_2,\ldots,t_n)=\sum_{i=1}^{n}Lf_i(t_1,t_2,\ldots,t_n) \tag{3.19}$$

Product Transform

Assuming a function $f(t_1,t_2,...,t_n)$ that is represented by the product of two subfunctions $f(t_1,t_2,...,t_n)=f_1(t_1,t_2,...,t_k)\,f_2(t_{k+1},t_{k+2},...,t_n)$. If subfunctions are given by different variables non-overlaped in time, the transform of *f* is given by,

$$F(s_1,s_2,\ldots,s_n)=F_1(s_1,s_2,\ldots,s_k)\,F_2(s_{k+1},s_{k+2},\ldots,s_n) \tag{3.20}$$

In case of the same variables

$$f(t_1,t_2,...,t_n)=f_1(t_1,t_2,...,t_n)\,f_2(t_1,t_2,...,t_n)$$

The transform is represented by the convolution

$$F(s_1,s_2,\ldots,s_n)=\frac{1}{(2\pi j)^n}\int_{\sigma-j\infty}^{\sigma+j\infty}F_1(s_1-v_1,s_2-v_2,\ldots,s_n-v_n)\,F_2(v_1,v_2,\ldots,v_n)\,dv_1dv_2\ldots dv_n \tag{3.21}$$

Convolution Transform

If a function *f* is represented by the convolution, two special cases are presented. When $f(t_1,t_2,...,t_n)=f_1(t_1)*f_2(t_1,t_2,...,t_n)$ the transform produces,

$$F(s_1,s_2,\ldots,s_n)=F_1(s_1+s_2+\ldots+s_n)\,F_2(s_1,s_2,\ldots,s_n) \tag{3.22}$$

For the case of n-fold convolution, $f(t_1,t_2,...,t_n)=f_1(t_1,t_2,...,t_n)*f_2(t_1,t_2,...,t_n)$, the transform is similar to the single variable case, that is,

$$F(s_1,s_2,\ldots,s_n)=F_1(s_1,s_2,\ldots,s_n)\,F_2(s_1,s_2,\ldots,s_n) \tag{3.23}$$

3.3.3 Association of variables

In practice, however, it is desirable to find the inverse of the *n*-dimensional Laplace transform by specifying the inverse image at a single variable. That is,

$$g(t)=f(t_1,t_2,\ldots,t_n)\big|_{t=t_1=t_2=\ldots=t_n=t} \tag{3.24}$$

Among the classical treatments, a method based on the idea of computing the Laplace Transform of the function $Y(s)$ directly from $F(s_1,s_2,\ldots,s_n)$ is adopted, where a single variable inverse Laplace transform is only required to find *y*(*t*); this enables the evaluation of complicated integrals in a straightforward manner.

In this approach, a *n*-dimension transformed function is first evaluated at a single transformed variable and then a single dimensional inverse Laplace transform is taken. The procedure to find $Y(s)$ from $F(s_1,s_2,\ldots,s_n)$ is known as the *association of variables* [Rugh 1981].

The following sections introduce several theorems that will be especially important in the analysis of complex systems, which allows the direct determination of the function $Y(s)$ without solving integral equations, rather than working in a direct way an algebraic system.

Very useful theorems developed to the treatment of multidimensional Laplace kernels may be taken in order to solve some of the characteristic kernels derived from the modal series deduction. These theorems are detailed in Appendix A.

3.4 MODAL SERIES CLOSED FORM SOLUTION

We can now conveniently apply Theorem 1 to derive the two-dimensional Laplace transform of the system (3.13)-(3.15) as follows.

$$Y_j(s_1)(s_1-\lambda_j)=Y_j(0)$$

$$Y_j(s_1)=\frac{Y_j(0)}{(s_1-\lambda_j)} \tag{3.25}$$

Therefore,

$$y_j(t)=y_j(0)e^{\lambda_j t} \tag{3.26}$$

Then, from (3.14), solving for $Y_j^2(s_1,s_2)$ we have,

$$(s_1+s_2-\lambda_j)Y_j^2(s_1,s_2)=\sum_{k=1}^{n}\sum_{l=1}^{n}C_{kl}^{j}Y_k^1(s_1)Y_l^1(s_2)$$

$$Y_j^2(s_1,s_2)=\sum_{k=1}^{n}\sum_{l=1}^{n}\frac{1}{(s_1+s_2-\lambda_j)}C_{kl}^{j}Y_k^1(s_1)Y_l^1(s_2) \tag{3.27}$$

Applying association of variables to the second order terms a single variable Laplace transform is obtained, which is easily solved through the direct application of common inverse Laplace transform transformations. A detailed description, step by step, of the procedure followed to carry out the closed form solution of modal series second order terms is described in Appendix B. Hence, performing the inversion with respect to *x*, the closed-form solutions are obtained

$$y_j^2(t)=\sum_{k=1}^{n}\sum_{l=1}^{n}C_{kl}^{j}y_k^1(0)y_l^1(0)\frac{1}{(\lambda_k+\lambda_l-\lambda_j)}\left[e^{(\lambda_k+\lambda_l)t}-e^{\lambda_j t}\right] \tag{3.28}$$

Upon rearranging terms, one has

$$y_j(t)=\left(y_j^1(0)-\sum_{k=1}^{N}\sum_{l=1}^{N}h_{2kl}^{j}y_k^1(0)y_l^1(0)\right)e^{\lambda_j t}+\sum_{k=1}^{N}\sum_{l=1}^{N}h_{2kl}^{j}y_k^1(0)y_l^1(0)e^{(\lambda_k+\lambda_l)t} \tag{3.29}$$

and

$$x_i(t)=\sum_{j=1}^{N}\left(u_{ij}y_j^1(0)-\sum_{k=1}^{N}\sum_{l=1}^{N}u_{ij}h_{2kl}^j y_k^1(0)y_l^1(0)\right)e^{\lambda_j t}+\sum_{j=1}^{N}\sum_{k=1}^{N}\sum_{l=1}^{N}u_{ij}h_{2kl}^j y_k^1(0)y_l^1(0)e^{(\lambda_k+\lambda_l)t} \tag{3.30}$$

where $i=1,...,n$

$$h_{2kl}^{j}=\frac{C_{kl}^j}{\lambda_k+\lambda_l-\lambda_j} \tag{3.31}$$

which, for the case when $u=0$, reduces to (3.30). This agrees with the results obtained in [Schanechi *et al.* 2003].

A useful variant of the modal series solution for the conveyed system in its physical variables is based on writing the final result in the Laplace domain. Some characteristics of the transfer functions may be accommodated in order to analyze the oscillations in dynamic systems with respect to a sample frequency range. According to Equation (3.2) and using the linearity properties of the Laplace transform, the complete solution for the nonlinear system can be written as,

$$Y_j(s)=F_j^1(s)+F_j^2(s)+F_j^3(s)+\ldots \tag{3.32}$$

Also, assuming the relationship,

$$X(s)=\mathbf{U}Y(s)$$

where **U** is the right eigenvectors matrix, then,

$$X_j(s)=\mathbf{U}\left[F_j^1(s)+F_j^2(s)+F_j^3(s)+\ldots\right] \tag{3.33}$$

where $F_j^1(s)$, $F_j^2(s)$, $F_j^3(s)$, … are the first, second, third, etc. order functions expressed in the single Laplace domain.

Substituting the first and second order terms (Equations (3.25) and (3.27)) obtained for the modal series analysis, it yields,

$$X_i(s)=\sum_{j=1}^{n}\left\{u_{ij}\frac{Y_j(0)}{(s-\lambda_j)}+\sum_{k=1}^{n}\sum_{l=1}^{n}\left[u_{ij}C_{kl}^jY_k^1(0)Y_l^1(0)\frac{1}{(\lambda_k+\lambda_l-\lambda_j)}\cdot\left(\frac{1}{(s-\lambda_k-\lambda_l)}-\frac{1}{(s-\lambda_j)}\right)\right]\right\}$$

$$X_i(s)=\sum_{j=1}^{n}\left\{u_{ij}\frac{Y_j(0)}{(s-\lambda_j)}+\sum_{k=1}^{n}\sum_{l=1}^{n}\left[u_{ij}C_{kl}^jY_k^1(0)Y_l^1(0)\frac{1}{(\lambda_k+\lambda_l-\lambda_j)}\cdot F_i(s)\right]\right\} \tag{3.34}$$

where,

$$F_i(s)=\left[\frac{1}{(s-\lambda_k-\lambda_l)}-\frac{1}{(s-\lambda_j)}\right]$$

These equations can be conveniently analyzed using the proposed framework. Straightforward application of the Laplace transforms means a systematic procedure, which allows the analytical solution of the nonlinear system, assuming uncoupled each term (linear and nonlinear terms).

3.5 MODAL SERIES CLOSED FORM SOLUTION UNDER RESONANCE CONDITION

Recalling the nonlinear coefficients h_2 defined by Equation (3.31), the resonance condition is established as,

$$\lambda_k + \lambda_l - \lambda_j = 0 \tag{3.35}$$

or,

$$\lambda_k + \lambda_l = \lambda_j$$

Thus, the Laplace transform kernels considering the resonance assumption are obtained as,

$$Y_j^1(s_1) = \frac{Y_j^1(0)}{(s_1 - \lambda_j)}$$

$$Y_j^2(s_1, s_2) = \sum_{k=1}^{n}\sum_{l=1}^{n} \frac{1}{(s_1 + s_2 - \lambda_j)} C_{kl}^j Y_k^1(s_1) Y_l^1(s_2)$$

$$Y_j^2(s_1, s_2) = \sum_{k=1}^{n}\sum_{l=1}^{n} C_{kl}^j Y_k^1(0) Y_l^1(0) \frac{1}{(s_1 + s_2 - \lambda_j)(s_1 - \lambda_k)(s_2 - \lambda_l)}$$

According to the resonance condition constraint, the kernel is defined as,

$$Y_j^2(s_1, s_2) = \sum_{k=1}^{n}\sum_{l=1}^{n} C_{kl}^j Y_k^1(0) Y_l^1(0) \frac{1}{(s_1 + s_2 - \lambda_k - \lambda_l)(s_1 - \lambda_k)(s_2 - \lambda_l)} \tag{3.36}$$

which is associated in terms of Laplace domain as,

$$Y_j^1(s) = \frac{Y_j^1(0)}{(s_1 - \lambda_k - \lambda_l)}$$

Obtaining a time domain solution through inverse Laplace leads to,

$$y_j^1(t) = y_j^1(0) e^{(\lambda_k + \lambda_l)t} \tag{3.37}$$

or

$$y_j^1(t) = y_j^1(0) e^{\lambda_j t}$$

The second order kernel,

$$H_2(s_1, s_2) = \frac{1}{(s_1 + s_2 - \lambda_k - \lambda_l)(s_1 - \lambda_k)(s_2 - \lambda_l)}$$

is associated following the rule of association of variables detailed in Appendix A as,

$$H_2(s) = \frac{1}{(s-\lambda_k-\lambda_l)(s-\lambda_k-\lambda_l)} = \frac{1}{(s-\lambda_k-\lambda_l)^2}$$

$$H_2(s) = \frac{1}{(s-\lambda_j)^2} \tag{3.38}$$

from which the time domain solution solving the inverse Laplace is,

$$h_2(t) = t e^{\lambda_j t}$$

Thus, the complete closed form solution when a modal resonance condition is presented is,

$$y_j(t) = y_j(0)e^{\lambda_j t} + \sum_{k=1}^{n}\sum_{l=1}^{n} C_{kl}^{j} y_k(0) y_l(0) t e^{\lambda_j t} \tag{3.39}$$

$$x_i(t) = u_{i,j} y_j(0)e^{\lambda_j t} + \sum_{k=1}^{n}\sum_{l=1}^{n} u_{i,j} C_{kl}^{j} y_k(0) y_l(0) t e^{\lambda_j t} \tag{3.40}$$

3.6 HIGHER ORDER APPROXIMATIONS OF THE MODAL SERIES METHOD

It is possible to extend the modal series method in order to incorporate higher order terms in the expansion of Taylor series from the original nonlinear system. Consider again the Taylor series expansion about a fixed stable equilibrium point x_{sep}, that is,

$$\begin{aligned} f_i(\mathbf{x}) = f_i(\mathbf{x}_{sep}) + \left[\frac{\partial f_i(\mathbf{x}_{sep})}{\partial \mathbf{x}_{sep}}\right](\mathbf{x}-\mathbf{x}_{sep}) + \frac{1}{2}(\mathbf{x}-\mathbf{x}_{sep})^T \left[\frac{\partial}{\partial \mathbf{x}_{sep}}\left(\frac{\partial f_i(\mathbf{x}_{sep})}{\partial \mathbf{x}_{sep}}\right)\right]^T (\mathbf{x}-\mathbf{x}_{sep}) + \\ \frac{1}{6}(\mathbf{x}-\mathbf{x}_{sep})^T \left\{(\mathbf{x}-\mathbf{x}_{sep})^T \frac{\partial}{\partial \mathbf{x}_{sep}}\left(\frac{\partial}{\partial \mathbf{x}_{sep}}\left[\frac{\partial f_i(\mathbf{x}_{sep})}{\partial \mathbf{x}_{sep}}\right]\right)^T\right\}(\mathbf{x}-\mathbf{x}_{sep}) + \dots \end{aligned} \tag{3.41}$$

for $i = 1, 2, \dots, n$

Rewriting the Taylor series expansion, it yields,

$$\dot{\mathbf{x}} = f_1(\mathbf{x}) + f_2(\mathbf{x}) + f_3(\mathbf{x}) + f_4(\mathbf{x}) + \dots \tag{3.42}$$

where:

$$f_1(\mathbf{x}) = \mathbf{A}\mathbf{x}, \text{ and,} \qquad \mathbf{A} = D\mathbf{f}(0) = \left[\begin{array}{cccc} \frac{\partial f_1}{\partial x_1} & \frac{\partial f_1}{\partial x_2} & \dots & \frac{\partial f_1}{\partial x_n} \\ \frac{\partial f_2}{\partial x_1} & \frac{\partial f_2}{\partial x_2} & \dots & \frac{\partial f_2}{\partial x_n} \\ \vdots & \vdots & \ddots & \vdots \\ \frac{\partial f_n}{\partial x_1} & \frac{\partial f_n}{\partial x_2} & \dots & \frac{\partial f_n}{\partial x_n} \end{array}\right]_{x=x_{SEP}} \tag{3.43}$$

$$f_2(\mathbf{x}) = \frac{1}{2!}\begin{bmatrix} \mathbf{x}^T\mathbf{H}^1\mathbf{x} \\ \mathbf{x}^T\mathbf{H}^2\mathbf{x} \\ \vdots \\ \mathbf{x}^T\mathbf{H}^n\mathbf{x} \end{bmatrix} \qquad \text{with} \qquad \mathbf{H}^j = \begin{bmatrix} \frac{\partial^2 f_j}{\partial x_1 \partial x_1} & \frac{\partial^2 f_j}{\partial x_1 \partial x_2} & \cdots & \frac{\partial^2 f_j}{\partial x_1 \partial x_n} \\ \frac{\partial^2 f_j}{\partial x_1 \partial x_2} & \frac{\partial^2 f_j}{\partial x_2 \partial x_2} & \cdots & \frac{\partial^2 f_j}{\partial x_2 \partial x_n} \\ \vdots & \vdots & \ddots & \vdots \\ \frac{\partial^2 f_j}{\partial x_1 \partial x_n} & \frac{\partial^2 f_j}{\partial x_2 \partial x_n} & \cdots & \frac{\partial^2 f_j}{\partial x_n \partial x_n} \end{bmatrix}_{x=x_{SEP}} \tag{3.44}$$

$$f_3(\mathbf{x}) = \frac{1}{6}\begin{bmatrix} \mathbf{x}^T\mathbf{H}_3^1\begin{bmatrix} \mathbf{x} & \mathbf{0} & \mathbf{0} \\ \mathbf{0} & \mathbf{x} & \mathbf{0} \\ \mathbf{0} & \mathbf{0} & \mathbf{x} \end{bmatrix}\mathbf{x} \\ \mathbf{x}^T\mathbf{H}_3^2\begin{bmatrix} \mathbf{x} & \mathbf{0} & \mathbf{0} \\ \mathbf{0} & \mathbf{x} & \mathbf{0} \\ \mathbf{0} & \mathbf{0} & \mathbf{x} \end{bmatrix}\mathbf{x} \\ \vdots \\ \mathbf{x}^T\mathbf{H}_3^n\begin{bmatrix} \mathbf{x} & \mathbf{0} & \mathbf{0} \\ \mathbf{0} & \mathbf{x} & \mathbf{0} \\ \mathbf{0} & \mathbf{0} & \mathbf{x} \end{bmatrix}\mathbf{x} \end{bmatrix} \quad \text{with} \quad \mathbf{H}_3^j = \begin{bmatrix} \frac{\partial^3 f_j}{\partial x_1 \partial x_1 \partial x_1} & \frac{\partial^3 f_j}{\partial x_1 \partial x_1 \partial x_2} & \cdots & \frac{\partial^3 f_j}{\partial x_1 \partial x_1 \partial x_n} \\ \frac{\partial^3 f_j}{\partial x_1 \partial x_2 \partial x_2} & \frac{\partial^3 f_j}{\partial x_2 \partial x_2 \partial x_2} & \cdots & \frac{\partial^3 f_j}{\partial x_2 \partial x_2 \partial x_n} \\ \vdots & \vdots & \ddots & \vdots \\ \frac{\partial^3 f_j}{\partial x_1 \partial x_n \partial x_n} & \frac{\partial^3 f_j}{\partial x_2 \partial x_n \partial x_n} & \cdots & \frac{\partial^3 f_j}{\partial x_n \partial x_n \partial x_n} \end{bmatrix}_{x=x_{SEP}} \tag{3.45}$$

$$f_4(\mathbf{x}) = \frac{1}{4!}\begin{bmatrix} \mathbf{x}^T\mathbf{H}_4^1\begin{bmatrix} \begin{bmatrix} \mathbf{x} & \mathbf{0} \\ \mathbf{0} & \mathbf{x} \end{bmatrix}\mathbf{x} & \begin{bmatrix} \mathbf{0} \\ \mathbf{0} \end{bmatrix} \\ \begin{bmatrix} \mathbf{0} \\ \mathbf{0} \end{bmatrix} & \begin{bmatrix} \mathbf{x} & \mathbf{0} \\ \mathbf{0} & \mathbf{x} \end{bmatrix}\mathbf{x} \end{bmatrix}\mathbf{x} \\ \mathbf{x}^T\mathbf{H}_4^2\begin{bmatrix} \begin{bmatrix} \mathbf{x} & \mathbf{0} \\ \mathbf{0} & \mathbf{x} \end{bmatrix}\mathbf{x} & \begin{bmatrix} \mathbf{0} \\ \mathbf{0} \end{bmatrix} \\ \begin{bmatrix} \mathbf{0} \\ \mathbf{0} \end{bmatrix} & \begin{bmatrix} \mathbf{x} & \mathbf{0} \\ \mathbf{0} & \mathbf{x} \end{bmatrix}\mathbf{x} \end{bmatrix}\mathbf{x} \\ \vdots \\ \mathbf{x}^T\mathbf{H}_4^n\begin{bmatrix} \begin{bmatrix} \mathbf{x} & \mathbf{0} \\ \mathbf{0} & \mathbf{x} \end{bmatrix}\mathbf{x} & \begin{bmatrix} \mathbf{0} \\ \mathbf{0} \end{bmatrix} \\ \begin{bmatrix} \mathbf{0} \\ \mathbf{0} \end{bmatrix} & \begin{bmatrix} \mathbf{x} & \mathbf{0} \\ \mathbf{0} & \mathbf{x} \end{bmatrix}\mathbf{x} \end{bmatrix}\mathbf{x} \end{bmatrix} \quad \text{with} \quad \mathbf{H}_4^j = \begin{bmatrix} \frac{\partial^4 f_j}{\partial x_1^4} & \frac{\partial^4 f_j}{\partial x_1^3 \partial x_2} & \cdots & \frac{\partial^4 f_j}{\partial x_1^3 \partial x_n} \\ \frac{\partial^4 f_j}{\partial x_1 \partial x_2^3} & \frac{\partial^4 f_j}{\partial x_2^4} & \cdots & \frac{\partial^4 f_j}{\partial x_2^3 \partial x_n} \\ \vdots & \vdots & \ddots & \vdots \\ \frac{\partial^4 f_j}{\partial x_1 \partial x_n^3} & \frac{\partial^4 f_j}{\partial x_2 \partial x_n^3} & \cdots & \frac{\partial^4 f_j}{\partial x_n^4} \end{bmatrix}_{x=x_{SEP}} \tag{3.46}$$

$$\vdots$$

Taking into account the result obtained in Section 3.2 through the variational approach, that is,

$$\dot{y}_j = \lambda_j y_j \tag{3.47}$$

$$\dot{y}_j^2 = \lambda_j y_j^2 + \sum_{k=1}^{n}\sum_{l=1}^{n} C_{kl}^j y_k^1 y_l^1 \tag{3.48}$$

$$\dot{y}_j^3 = \lambda_j y_j^3(t) + \sum_{k=1}^{n}\sum_{l=1}^{n} C_{kl}^j \left[y_k^2 y_l^1 + y_k^1 y_l^2 \right] + \sum_{p=1}^{n}\sum_{q=1}^{n}\sum_{r=1}^{n} D_{pqr}^j y_p^1 y_q^1 y_r^1 \tag{3.49}$$

$$\begin{aligned}\dot{y}_j^4 = \lambda_j y_j^4 &+ \sum_{k=1}^{n}\sum_{l=1}^{n} C_{kl}^j \left[y_k^1 y_l^3 + y_k^2 y_l^2 + y_k^3 y_l^1 \right] + \sum_{k=1}^{n}\sum_{l=1}^{n}\sum_{m=1}^{n} D_{klm}^j \left[y_k^1 y_l^1 y_m^2 + y_k^1 y_l^2 y_m^1 + y_k^2 y_l^1 y_m^1 \right] \\ &+ \sum_{m=1}^{n}\sum_{p=1}^{n}\sum_{q=1}^{n}\sum_{r=1}^{n} E_{mpqr}^j \left[y_m^1 y_p^1 y_q^1 y_r^1 \right]\end{aligned} \tag{3.50}$$

$\vdots$

From the first order term, it is possible to determine the second and higher order terms. Being,

$$Y_j^1(s_1) = \frac{Y_j(0)}{(s_1 - \lambda_j)} \tag{3.51}$$

and the second order terms obtained in Section 3.4, given by Equation (3.27),

$$Y_j^2(s_1, s_2) = \sum_{k=1}^{n}\sum_{l=1}^{n} C_{kl}^j Y_k(0) Y_l(0) \frac{1}{(s_1 + s_2 - \lambda_j)(s_1 - \lambda_k)(s_2 - \lambda_l)} \tag{3.52}$$

the third order terms are obtained from the substitution of (3.51) and (3.52) in (3.15), that is,

$$\begin{aligned}&Y_j^3(s_1, s_2, s_3) = \\ &\sum_{k=1}^{n}\sum_{l=1}^{n}\sum_{p=1}^{n}\sum_{q=1}^{n} C_{kl}^j C_{pq}^k y_p(0) y_q(0) y_l(0) \frac{1}{(s_1 + s_2 + s_3 - \lambda_j)(s_1 + s_2 - \lambda_k)(s_1 - \lambda_p)(s_2 - \lambda_q)(s_3 - \lambda_l)} \\ &+ \sum_{k=1}^{n}\sum_{l=1}^{n}\sum_{p=1}^{n}\sum_{q=1}^{n} C_{kl}^j C_p^l \, y_p(0) y_q(0) y_k(0) \frac{1}{(s_1 + s_2 + s_3 - \lambda_j)(s_2 + s_3 - \lambda_l)(s_1 - \lambda_l)(s_2 - \lambda_p)(s_3 - \lambda_q)} \\ &+ \sum_{p=1}^{n}\sum_{q=1}^{n}\sum_{r=1}^{n} D_{pqr}^j \frac{1}{(s_1 + s_2 + s_3 - \lambda_j)(s_1 - \lambda_p)(s_2 - \lambda_q)(s_3 - \lambda_r)}\end{aligned} \tag{3.53}$$

Step by step deduction procedure of expressions in Equation (3.53) is described in Appendix B. The inverse of the multidimensional Laplace transform in (3.52) and (3.53) can be obtained by the method of association of variables as discussed above, i.e.

$$
\begin{aligned}
Y_j^3(s) = & \\
& C_{kl}^j C_{pq}^k Y_p^1(0) Y_q^1(0) Y_l^1(0) \cdot \\
& \sum_{k=1}^{n}\sum_{l=1}^{n}\sum_{p=1}^{n}\sum_{q=1}^{n} \frac{1}{\left(\lambda_j - \lambda_p - \lambda_q - \lambda_l\right)}\left[\frac{1}{\left(\lambda_j - \lambda_l - \lambda_k\right)}\frac{1}{\left(s - \lambda_j\right)} - \frac{1}{\left(\lambda_p + \lambda_q - \lambda_k\right)}\frac{1}{\left(s - \lambda_p - \lambda_q - \lambda_l\right)}\right] + \\
& C_{kl}^j C_{pq}^l Y_k^1(0) Y_p^1(0) Y_q^1(0) \cdot \\
& \sum_{k=1}^{n}\sum_{l=1}^{n}\sum_{p=1}^{n}\sum_{q=1}^{n} \frac{1}{\left(\lambda_j - \lambda_p - \lambda_q - \lambda_k\right)}\frac{1}{\left(\lambda_p + \lambda_q - \lambda_l\right)}\left[\frac{1}{\left(s - \lambda_j\right)} - \frac{1}{\left(s_1 - \lambda_p - \lambda_q - \lambda_k\right)}\right] + \\
& \sum_{p=1}^{n}\sum_{q=1}^{n}\sum_{r=1}^{n} D_{pqr}^j Y_p^1(0) Y_q^1(0) Y_r^1(0) \frac{1}{\left(\lambda_j - \lambda_p - \lambda_q - \lambda_r\right)}\left[\frac{1}{\left(s - \lambda_j\right)} - \frac{1}{\left(s - \lambda_p - \lambda_q - \lambda_r\right)}\right]
\end{aligned}
\tag{3.54}
$$

Higher order terms are obtained in identical manner. The key point to be emphasized is that closed-form solutions can be obtained by inverse Laplace transformation of (3.54).

Performing the inversion with respect to *s*, the closed-form solutions are obtained as,

$$
\begin{aligned}
y_j^3(t) = & \\
& C_{kl}^j C_{pq}^k Y_p^1(0) Y_q^1(0) Y_l^1(0) \cdot \\
& \sum_{k=1}^{n}\sum_{l=1}^{n}\sum_{p=1}^{n}\sum_{q=1}^{n} \frac{1}{\left(\lambda_j - \lambda_p - \lambda_q - \lambda_l\right)}\left[\frac{1}{\left(\lambda_j - \lambda_l - \lambda_k\right)} e^{\lambda_j t} - \frac{1}{\left(\lambda_p + \lambda_q - \lambda_k\right)} e^{\left(\lambda_p + \lambda_q + \lambda_l\right)t}\right] + \\
& C_{kl}^j C_{pq}^l Y_k^1(0) Y_p^1(0) Y_q^1(0) \cdot \\
& \sum_{k=1}^{n}\sum_{l=1}^{n}\sum_{p=1}^{n}\sum_{q=1}^{n} \frac{1}{\left(\lambda_j - \lambda_p - \lambda_q - \lambda_k\right)}\frac{1}{\left(\lambda_p + \lambda_q - \lambda_l\right)}\left[e^{\lambda_j t} - e^{\left(\lambda_p + \lambda_q + \lambda_k\right)t}\right] + \\
& \sum_{p=1}^{n}\sum_{q=1}^{n}\sum_{r=1}^{n} D_{pqr}^j Y_p^1(0) Y_q^1(0) Y_r^1(0) \frac{1}{\left(\lambda_j - \lambda_p - \lambda_q - \lambda_r\right)}\left[e^{\left(\lambda_j\right)t} - e^{\left(\lambda_p + \lambda_q + \lambda_r\right)t}\right]
\end{aligned}
\tag{3.55}
$$

which after some manipulations gives,

$$
\begin{aligned}
y_j^3(t) = & \sum_{p=1}^{n}\sum_{q=1}^{n}\sum_{r=1}^{n} h_{3\,pqr}^j y_p^1(0) y_q^1(0) y_r^1(0)\left[e^{\left(\lambda_j\right)t} - e^{\left(\lambda_p + \lambda_q + \lambda_r\right)t}\right] + \\
& \sum_{k=1}^{n}\sum_{l=1}^{n}\sum_{p=1}^{n}\sum_{q=1}^{n} \frac{y_p^1(0) y_q^1(0) y_l^1(0)}{\left(\lambda_j - \lambda_p - \lambda_q - \lambda_l\right)}\left[h_{2\,kl}^j e^{\lambda_j t} - h_{2\,pq}^l e^{\left(\lambda_p + \lambda_q + \lambda_l\right)t}\right] + \\
& \sum_{k=1}^{n}\sum_{l=1}^{n}\sum_{p=1}^{n}\sum_{q=1}^{n} h_{2\,pq}^l C_{kl}^j \frac{y_k^1(0) y_p^1(0) y_q^1(0)}{\left(\lambda_j - \lambda_p - \lambda_q - \lambda_k\right)}\left[e^{\lambda_j t} - e^{\left(\lambda_p + \lambda_q + \lambda_k\right)t}\right]
\end{aligned}
$$

and

$$x_i^3(t)=\sum_{p=1}^{n}\sum_{q=1}^{n}\sum_{r=1}^{n}u_{ij}h_{3pqr}^{j}y_p^1(0)y_q^1(0)y_r^1(0)\left[e^{(\lambda_j)t}-e^{(\lambda_p+\lambda_q+\lambda_r)t}\right]+$$

$$\sum_{k=1}^{n}\sum_{l=1}^{n}\sum_{p=1}^{n}\sum_{q=1}^{n}u_{ij}\frac{y_p^1(0)y_q^1(0)y_l^1(0)}{\left(\lambda_j-\lambda_p-\lambda_q-\lambda_l\right)}\left[h_{2kl}^{j}e^{\lambda_j t}-h_{2pq}^{l}e^{(\lambda_p+\lambda_q+\lambda_l)t}\right]+ \qquad i=1,2,\ldots,n \qquad (3.56)$$

$$\sum_{k=1}^{n}\sum_{l=1}^{n}\sum_{p=1}^{n}\sum_{q=1}^{n}u_{ij}h_{2pq}^{l}C_{kl}^{j}\frac{y_k^1(0)y_p^1(0)y_q^1(0)}{\left(\lambda_j-\lambda_p-\lambda_q-\lambda_k\right)}\left[e^{\lambda_j t}-e^{(\lambda_p+\lambda_q+\lambda_k)t}\right]$$

In the above, the second and third-order nonlinear coefficients $h3_{pqr}^{j}$ are defined by

$$h_{2pq}^{l}=\frac{C_{pq}^{k}}{\left(\lambda_p+\lambda_q-\lambda_k\right)} \qquad (3.57)$$

$$h_{2kl}^{j}=\frac{C_{kl}^{j}}{\left(\lambda_j-\lambda_l-\lambda_k\right)} \qquad (3.58)$$

$$h_{3pqr}^{j}=\frac{D_{pqr}^{j}}{\left(\lambda_j-\lambda_p-\lambda_q-\lambda_r\right)} \qquad (3.59)$$

The procedure can be indefinitely continued to determine higher-order nonlinear expressions in terms of the lower-order modal expansions. For the sake of simplicity only terms up to third are obtained.

3.7 POWER SYSTEM MODELING BY HIGHER ORDER MODAL SERIES

The application of the modal series method including higher order terms is demonstrated through the application to the synchronous machine-infinite busbar power system as illustrated in Figure 3.1

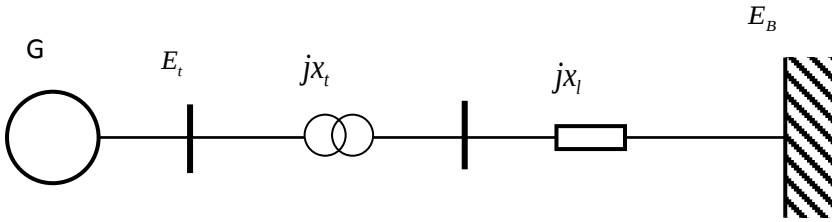

Figure 3.1. Synchronous machine-infinite busbar power system

Two different cases are conducted in order to remark the main advantages of utilizing the modal series method. As a first case, the power system of Figure 3.1 is modeled with the classical model of the synchronous machine; as a second one, the model is switched to the one flux modeling, which includes the dynamics of a simplified stator equivalence included in the *q* axis winding. Both cases of study are modeled using higher order modal series, taking into account up to third order terms. Higher order terms have not been considered yet by the author, leaving their development for future contributions.

3.7.1 Case 1: Classical Model

The set of differential equations that represent the model of the synchronous machine connected to the infinite busbar are given by [Kundur 1994],

$$\frac{d\delta}{dt} = \omega, \qquad \frac{d\omega}{dt} = \frac{1}{2H}\left(P_m - P_{\max}\sin\delta - D_m\omega\right) \tag{3.60}$$

with, $$P_{\max} = \frac{E_t E_B}{x'_d + x_t + x_\ell}$$

where δ represents the rotor angular position in electric radians with reference to the infinite busbar, ω is the rotor angular velocity in rad/s, P_m is the mechanical power input which comprises the primotor mechanical system in p.u., D_m is referred as the damping coefficient of the generator in torque p.u./speed p.u., and H is the inertia constant in MWs/MVA. Simulation data used during the experiment are taken and adapted to our study case from [Kundur 1994],

$$H = 3.5\,MW/MVA,\ D = 10\ p.u.,\ x'_d = 0.3\ p.u.,\ x_t = 0.15\ p.u.,\ x_l = 0.8\ p.u.$$

The nonlinear system is described by,

$$\mathbf{x} = \begin{bmatrix} x_1 & x_2 \end{bmatrix}^T = \begin{bmatrix} \delta & \omega \end{bmatrix}^T \tag{3.61}$$

The movement equation is described by the nonlinear system [Martínez *et al.* 2004],

$$\dot{\mathbf{x}} = \mathbf{f}\left(\mathbf{x}\right) = \begin{bmatrix} f_1\left(x_1, x_2\right) \\ f_2\left(x_1, x_2\right) \end{bmatrix} = \begin{bmatrix} \omega \\ \dfrac{1}{2H}\left(P_m - P_{\max}\sin\delta - D_m\omega\right) \end{bmatrix} \tag{3.62}$$

with equilibrium point is defined as,

$$x_0 = \begin{bmatrix} \delta_0 & \omega_0 \end{bmatrix}^T = \begin{bmatrix} \sin^{-1}\left(\dfrac{P_m}{P_{\max}}\right) & 0 \end{bmatrix}^T \tag{3.63}$$

Expanding the system (3.62) in Taylor series, a perturbed system is deduced, that is,

$$\dot{\mathbf{x}} = \begin{bmatrix} \Delta\delta \\ \Delta\omega \end{bmatrix} = \begin{bmatrix} \Delta\omega \\ -\dfrac{P_{\max}}{2H}\cos\delta_0\Delta\delta - \dfrac{D_m}{2H}\Delta\omega \end{bmatrix} + \frac{1}{2!}\begin{bmatrix} 0 \\ \dfrac{P_{\max}}{2H}\sin\delta_0\Delta\delta^2 \end{bmatrix} + \frac{1}{3!}\begin{bmatrix} 0 \\ \dfrac{P_{\max}}{2H}\cos\delta_0\Delta\delta^3 \end{bmatrix} + O\left(4\right) \tag{3.64}$$

where $O(4)$ represents the terms of fourth order and higher order which are truncated during the linearization process. Applying the definitions associated to vector fields, which specify that a system can be described by a decomposition of first-second-… etc. order terms, the linearized system can be described as,

$$\dot{\mathbf{x}} \approx \mathbf{f_1}\left(\mathbf{x}\right) + \mathbf{f_2}\left(\mathbf{x}\right) + \mathbf{f_3}\left(\mathbf{x}\right) \tag{3.65}$$

where each function is defined follows,

- First order terms:

$$\mathbf{f}_1(\mathbf{x}) = \mathbf{A}\mathbf{x}$$

$$\mathbf{A} = D\mathbf{f}(\mathbf{x}_0) = \left[\begin{array}{cc} \frac{\partial f_1(\delta,\omega)}{\partial\delta} & \frac{\partial f_1(\delta,\omega)}{\partial\omega} \\ \frac{\partial f_2(\delta,\omega)}{\partial\delta} & \frac{\partial f_2(\delta,\omega)}{\partial\omega} \end{array}\right]_{\mathbf{x}=\mathbf{x}_{sep}} = \left[\begin{array}{cc} 0 & 1 \\ -\frac{P_{\max}}{2H}\cos\delta_0 & -\frac{D_m}{2H} \end{array}\right]_{\mathbf{x}=\mathbf{x}_{sep}} \tag{3.66}$$

- Second order terms:

$$\mathbf{f}_2(\mathbf{x}) = \frac{1}{2!}\left[\begin{array}{c} \mathbf{x}^{\mathbf{T}}\mathbf{H}_2^1\mathbf{x} \\ \mathbf{x}^{\mathbf{T}}\mathbf{H}_2^2\mathbf{x} \end{array}\right] = \frac{1}{2}\left[\begin{array}{c} 0 \\ \frac{P_{\max}}{2H}\sin\delta_0 \end{array}\right] \tag{3.67}$$

$$\mathbf{H}_2^1 = \left[\begin{array}{cc} \frac{\partial^2 f_1(\delta,\omega)}{\partial\delta^2} & \frac{\partial^2 f_1(\delta,\omega)}{\partial\delta\partial\omega} \\ \frac{\partial^2 f_1(\delta,\omega)}{\partial\omega\partial\delta} & \frac{\partial^2 f_1(\delta,\omega)}{\partial\omega^2} \end{array}\right]_{\mathbf{x}=\mathbf{x}_{sep}} = \left[\begin{array}{cc} 0 & 0 \\ 0 & 0 \end{array}\right]$$

$$\mathbf{H}_2^2 = \left[\begin{array}{cc} \frac{\partial^2 f_2(\delta,\omega)}{\partial\delta^2} & \frac{\partial^2 f_2(\delta,\omega)}{\partial\delta\partial\omega} \\ \frac{\partial^2 f_2(\delta,\omega)}{\partial\omega\partial\delta} & \frac{\partial^2 f_2(\delta,\omega)}{\partial\omega^2} \end{array}\right]_{\mathbf{x}=\mathbf{x}_{sep}} = \left[\begin{array}{cc} 0 & \frac{P_{\max}}{2H}\sin\delta_0 \\ 0 & 0 \end{array}\right]$$

- Third order terms:

$$\mathbf{f}_3(\mathbf{x}) = \frac{1}{6}\left[\begin{array}{c} \mathbf{x}^T\mathbf{H}_3^1\begin{bmatrix}\mathbf{x}&\mathbf{0}&\mathbf{0}\\\mathbf{0}&\mathbf{x}&\mathbf{0}\\\mathbf{0}&\mathbf{0}&\mathbf{x}\end{bmatrix}\mathbf{x} \\ \mathbf{x}^T\mathbf{H}_3^2\begin{bmatrix}\mathbf{x}&\mathbf{0}&\mathbf{0}\\\mathbf{0}&\mathbf{x}&\mathbf{0}\\\mathbf{0}&\mathbf{0}&\mathbf{x}\end{bmatrix}\mathbf{x} \end{array}\right]$$

$$\mathbf{H}_3^1 = \left[\begin{array}{cccc} \frac{\partial^3 f_1}{\partial\delta^3} & \frac{\partial^3 f_1}{\partial\delta^2\partial\omega} & \frac{\partial^3 f_1}{\partial\delta\partial\omega\partial\delta} & \frac{\partial^3 f_1}{\partial\delta\partial\omega^2} \\ \frac{\partial^3 f_1}{\partial\omega\partial\delta^2} & \frac{\partial^3 f_1}{\partial\omega\partial\delta\partial\omega} & \frac{\partial^3 f_1}{\partial\omega^2\partial\delta} & \frac{\partial^3 f_1}{\partial\omega^3} \end{array}\right]_{x=x_{SEP}} = \left[\begin{array}{cccc} 0 & 0 & 0 & 0 \\ 0 & 0 & 0 & 0 \end{array}\right]$$

$$\mathbf{H}_3^2 = \left[\begin{array}{cccc} \frac{\partial^3 f_2}{\partial\delta^3} & \frac{\partial^3 f_2}{\partial\delta^2\partial\omega} & \frac{\partial^3 f_2}{\partial\delta\partial\omega\partial\delta} & \frac{\partial^3 f_2}{\partial\delta\partial\omega^2} \\ \frac{\partial^3 f_2}{\partial\omega\partial\delta^2} & \frac{\partial^3 f_2}{\partial\omega\partial\delta\partial\omega} & \frac{\partial^3 f_2}{\partial\omega^2\partial\delta} & \frac{\partial^3 f_2}{\partial\omega^3} \end{array}\right]_{x=x_{SEP}} = \left[\begin{array}{cccc} 0 & 0 & \frac{P_{\max}}{2H}\cos\delta_0 & 0 \\ 0 & 0 & 0 & 0 \end{array}\right]_{x=x_{SEP}}$$

The system eigenvalues are obtained from the state matrix **A**, being for this case given by,

$$\lambda^2 + \frac{D}{2H}\lambda + \frac{P_{\max}\cos\delta_0}{2H} = 0 \tag{3.68}$$

$$\lambda_{1,2} = -\frac{D_m}{4H} \pm \frac{1}{2}\sqrt{\left(\frac{D_m}{2H}\right)^2 - 4\left(\frac{P_{\max}\cos\delta_0}{2H}\right)} \tag{3.69}$$

Hence the eigenvalues are calculated; it is possible to determine the right and left eigenvectors and therefore, the coefficients C_{kl}^{j}, h_{2kl}^{j}, h_{3klm}^{j} using (3.5) and (3.31).

3.7.1.1 Linear approximation

From the linearized system and considering only the linear part of Equation (3.64), an approximate solution is obtained based on the modal analysis of the original system. Recalling the right and left eigenvectors,

$$\mathbf{U} = \begin{bmatrix} u_{11} & u_{12} \\ u_{21} & u_{22} \end{bmatrix} \qquad \text{and} \qquad \mathbf{V} = \mathbf{U}^{-1} = \begin{bmatrix} v_{11} & v_{12} \\ v_{21} & v_{22} \end{bmatrix}$$

The time domain solution based on the linear part of the nonlinear system is given by,

$$\begin{bmatrix} \Delta\delta(t) \\ \Delta\omega(t) \end{bmatrix} = \begin{bmatrix} u_{11} & u_{12} \\ u_{21} & u_{22} \end{bmatrix} \begin{bmatrix} c_1 e^{\lambda_1 t} \\ c_2 e^{\lambda_2 t} \end{bmatrix} \tag{3.70}$$

where

$$\begin{bmatrix} c_1 \\ c_2 \end{bmatrix} = \begin{bmatrix} v_{11} & v_{12} \\ v_{21} & v_{22} \end{bmatrix} \begin{bmatrix} \Delta\delta(0) \\ \Delta\omega(0) \end{bmatrix}$$

3.7.1.2 Simulation Results

The experiment is conducted considering a perturbation on the rotor angle of $\Delta\delta = 30^{\circ}$. For this study case the solution obtained with the modal series technique is compared against the linear approximation and the numerical full solution obtained by solving the nonlinear differential equations that represent the dynamic system.

Figures 3.2 through 3.5 show the comparison of the oscillations presented after the perturbation on the rotor angle obtained by the three different forms of solution described above, *i.e.* the full solution, the linear approximations and the modal series solution. The waveforms in Figure 3.2 are the rotor angle and speed deviations respectively; assuming a mechanical power input $P_m = 0.9$ *p.u.* Throughout the simulation an agreement between trajectories on the obtained waveforms is observed with a lighter difference on the waveform obtained with the linear approximation method.

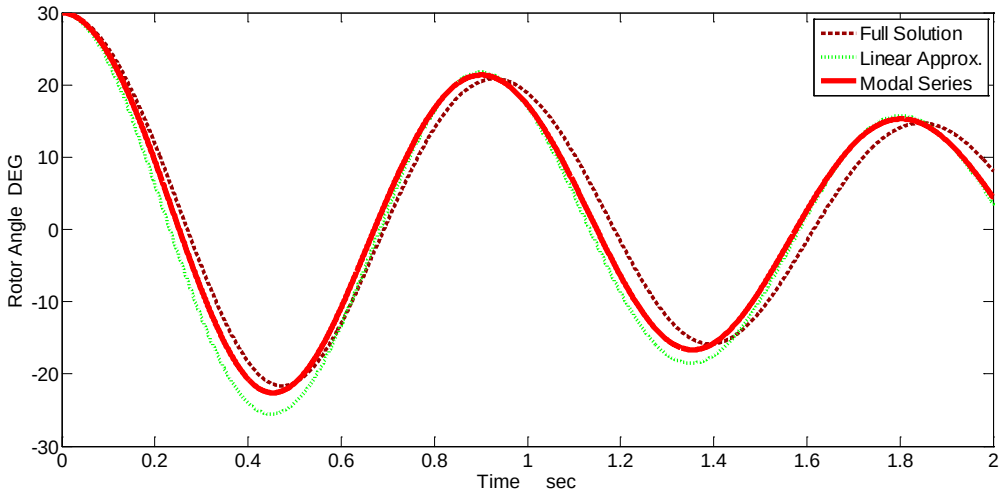

a) Rotor angle δ

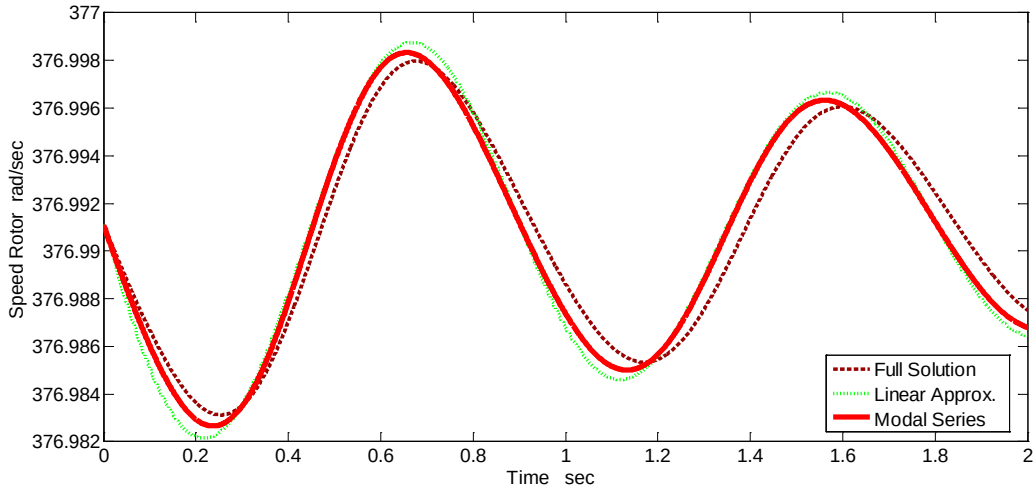

b) Rotor speed ω

Figure 3.2. Rotor angle and speed deviations comparison for a load condition of P_m=0.9 p.u. y $\Delta\delta$=30°

Figure 3.3 shows the phase plane of δ *vs* ω for this stable case study. It can be observed that the oscillations in the state variables eventually reach a stable equilibrium point before a low frequency transient period. Also it is of importance the agreement between the full numerical solution and modal series approximation thus demonstrating the applicability of the method under low stress conditions.

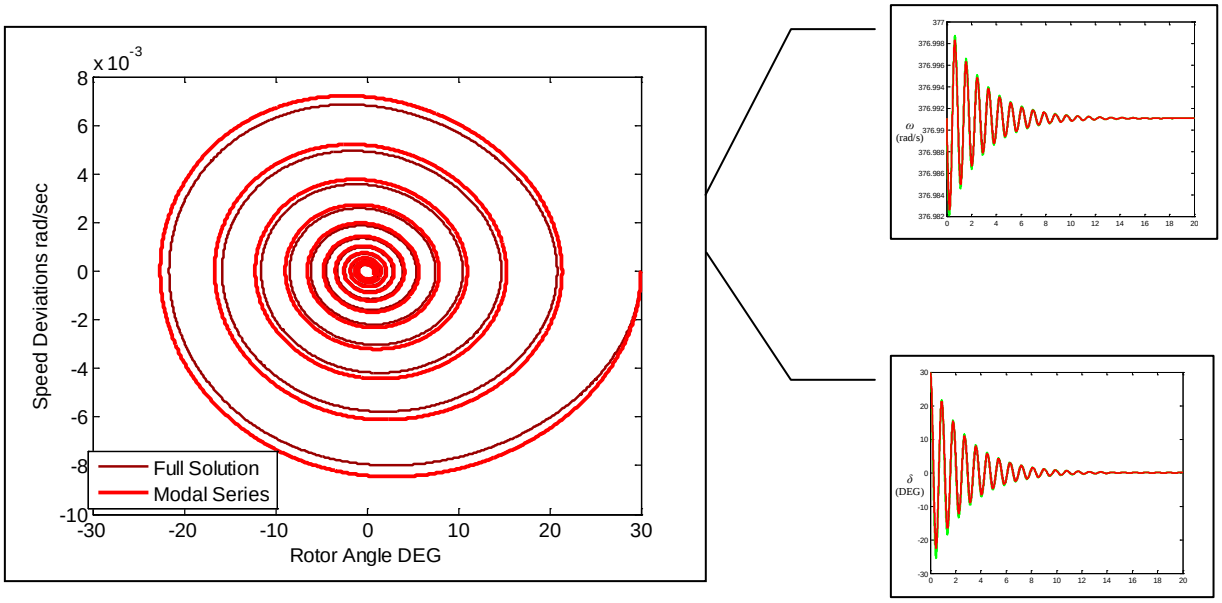

Figure 3.3. Rotor angle and speed deviations phase plane comparison for a load condition of P_m=0.9 p.u. y $\Delta\delta$=30°

The next step of the experiment considers an increase on the input mechanical power, which emulates an overload of the generator (stress condition). Under this load condition the system can eventually become unstable. This point of loss of stability is reached when the electric power generated is less than the mechanical power demanded to the generator, causing a lack of damping torque.

The Figure 3.4 shows the new condition mentioned above when an increase on the mechanical power is presented; *e.g.* to $P_m = 1.12$ *p.u.* That means a stress condition of operation for the generator. It is important to point-out that under this condition the modal series method shows a significant difference with respect to the full numerical solution.

The reason of this effect is that when the system is operated under strong stress conditions, intermodulation frequencies of second and higher order are presented [Martinez *et al.* 2004]. This phenomenon can be easily verified using Fourier analysis. Also, the inclusion of higher order terms in the modal series solution is very useful to get insight into the nature of the nonlinear oscillations presented, due to nonlinearities in the dynamic systems operating under such stress conditions.

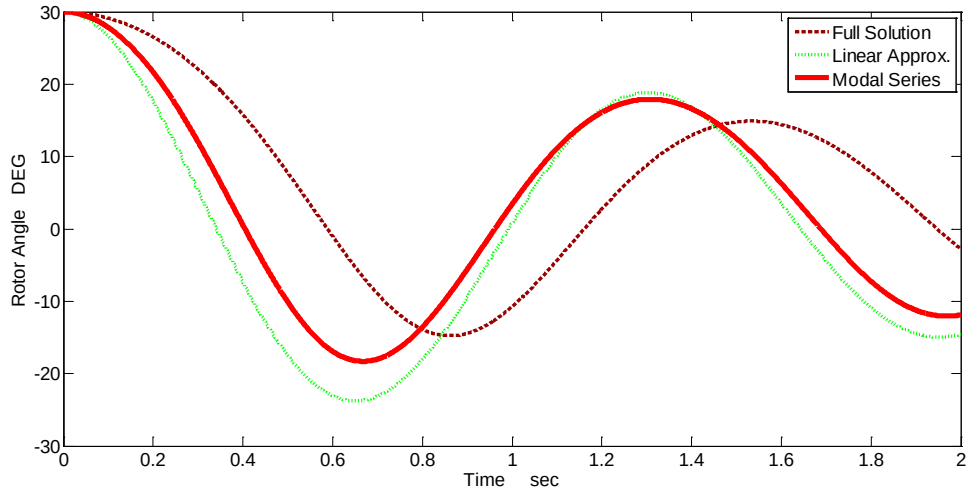

a) Rotor angle δ

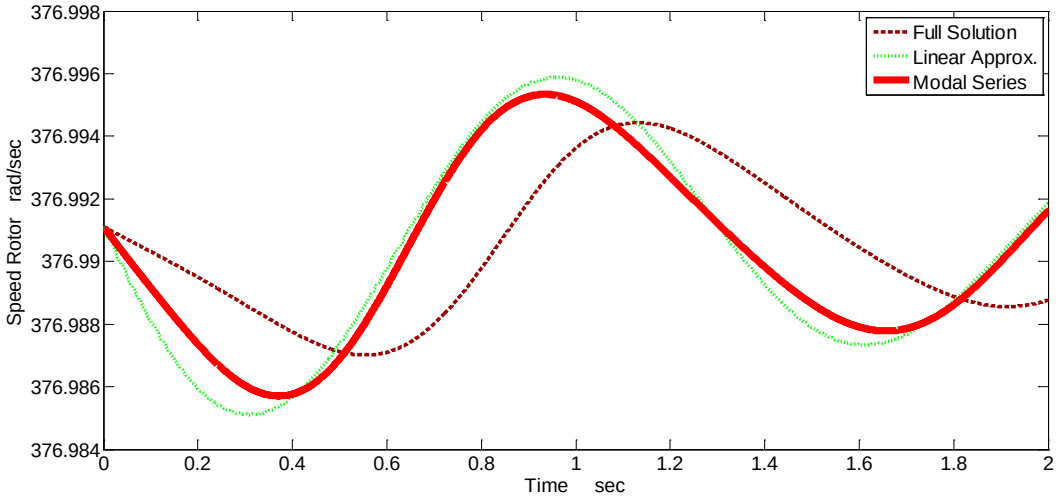

b) Rotor speed ω

Figure 3.4. Rotor angle and speed deviations comparison for a load condition of P_m=1.12 p.u. and $\Delta\delta$=30°

As an intent to show in a different way the behavior of the state variables, a three dimensional graphic is depicted in Figure 3.5, showing the transient of state variables but noting the differences in the trajectory for this case of increasing stress conditions. Even though the solution is stable, during the transient, there are differences observed in the trajectories followed by full numerical solution and modal series approximation due to the reasons pointed out above.

The experiment has demonstrated that the exactitude of the modal series technique depends on the magnitude of the initial perturbation and the stress level of the system operation, such as it has been observed in Figures 3.2 to 3.5. Perhaps it can be said for further applications, that one of the main handicaps of methods based on linearization through Taylor series expansion, is that the approximated solution is not valid at all when strong perturbations are presented (high stresses constraints).

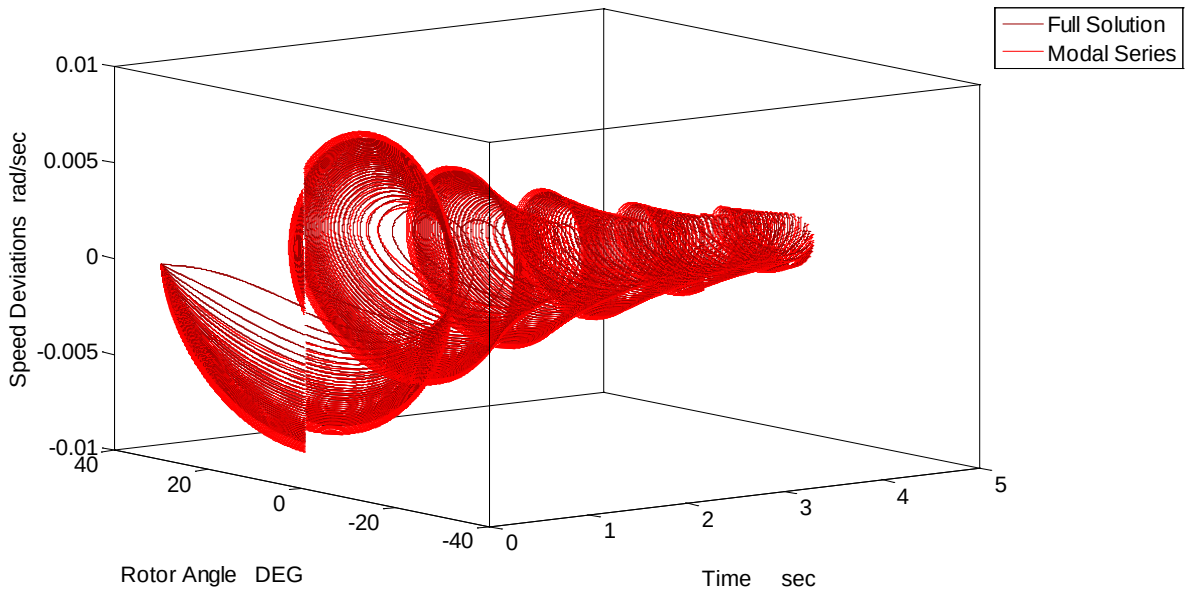

Figure 3.5. Rotor angle and speed deviations comparison for a load condition of P_m=1.12 p.u. and $\Delta\delta$=30° in a three dimensional view that shown the differences between full solution and modal series trajectories.

Hence for the cases near to transient stability approximations based on modal analysis and their modal combinations, the dynamics could not be followed due to the farawayness with respect to the equilibrium point, a condition that has to be previously met as a part of the linearization approach.

3.7.2 Case 2: Flux Decay Model

A third order generator model is assumed, which incorporates the dynamic of the electromechanical system. This system is interesting and adds to the previous case of classical model the inclusion of algebraic equations, thus commuting the model into a combination of differential-algebraic modeling. The differential equations are [Sauer and Pai 1998],

$$\begin{aligned}
\frac{dE'_q}{dt} &= -\left(\frac{1}{T'_{d0}}\right)\left[E'_q + \left(x_d - x'_d\right)I_d - E_{fd}\right] = f_1 \\
\frac{d\delta}{dt} &= \omega - \omega_0 = f_2 \\
\frac{d\omega}{dt} &= \left(\frac{\omega_0}{2H}\right)\left[T_M - \left\{E'_q I_q + \left(x_q - x'_d\right)I_d I_q - D\left(\omega - \omega_0\right)\right\}\right] = f_3
\end{aligned} \tag{3.71}$$

Furthermore, eliminating the stator resistance effects, the algebraic equations are,

$$-\left(x_q + x_t + x_l\right)I_q + V_b \sin\delta = 0 \tag{3.72}$$

$$\left(x'_d + x_t + x_l\right)I_d - E'_q + V_b \cos\delta = 0 \tag{3.73}$$

Linearizing the system at a stable equilibrium point, it has the form,

$$\dot{\mathbf{x}} = f_1(\mathbf{x}) + f_2(\mathbf{x}) + f_3(\mathbf{x}) + \ldots \tag{3.74}$$

with

$$\mathbf{x} = \begin{bmatrix} x_1 & x_2 & x_3 \end{bmatrix}^T = \begin{bmatrix} E'_q & \delta & \omega \end{bmatrix}^T$$

where each term is defined as,

$$\dot{\mathbf{x}} = \mathbf{f}(\mathbf{x}) = \begin{bmatrix} f_1(x_1, x_2, x_3) \\ f_2(x_1, x_2, x_3) \\ f_3(x_1, x_2, x_3) \end{bmatrix} = \begin{bmatrix} -\left(\frac{1}{T'_{d0}}\right)\left[E'_q + (x_d - x'_d) I_d - E_{fd}\right] \\ \omega - \omega_0 \\ \left(\frac{\omega_0}{2H}\right)\left[T_M - \left\{E'_q I_q + (x_q - x'_d) I_d I_q - D(\omega - \omega_0)\right\}\right] \end{bmatrix} \tag{3.75}$$

This dynamic system has the equilibrium point,

$$\begin{aligned} x_0 &= \begin{bmatrix} E'_{q0} & \delta_0 & \omega_0 \end{bmatrix}^T \\ x_0 &= \begin{bmatrix} V_b \cos(\delta_0 - \theta_{vs}) + (x_t + x_l + x'_d) I_d & angle\left(V_b e^{j\theta_{vs}} + j(x_q + x_t + x_l) I_G e^{j\gamma}\right) & \omega_0 \end{bmatrix}^T \end{aligned} \tag{3.76}$$

The linear and nonlinear functions defined by (3.74) for which it is necessary to determine their closed form solutions are obtained next, that is:

- First order terms,

$$f_1(\mathbf{x}) = \mathbf{A}\mathbf{x}, \text{ with,} \qquad \mathbf{A} = \begin{bmatrix} \frac{\partial f_1}{\partial E'_q} & \frac{\partial f_1}{\partial \delta} & \frac{\partial f_1}{\partial \omega} \\ \frac{\partial f_2}{\partial E'_q} & \frac{\partial f_2}{\partial \delta} & \frac{\partial f_2}{\partial \omega} \\ \frac{\partial f_3}{\partial E'_q} & \frac{\partial f_3}{\partial \delta} & \frac{\partial f_3}{\partial \omega} \end{bmatrix}_{x = x_{SEP}} \tag{3.77}$$

Applied to the case of the third order power system under study, the state matrix has the form,

$$\mathbf{A} = \begin{bmatrix} \frac{1}{T'_{d0}}[K_1 - 1] & \frac{1}{T'_{d0}}[K_1 V_b \sin\delta] & 0 \\ 0 & 0 & 1 \\ \frac{\omega_0}{2H}[K_2 V_b \sin\delta + K_3 V_b \sin\delta] & \frac{\omega_0}{2H}\begin{bmatrix} K_2 E'_q V_b \cos\delta + K_3 V_b^2 \sin^2\delta + \\ K_3 (E'_q - V_b \cos\delta) V_b \cos\delta \end{bmatrix} & -\frac{\omega_0}{2H} D \end{bmatrix}_{x = x_{SEP}}$$

where,

$$K_1 = -\frac{x_d - x'_d}{x'_d + x_{ep}}$$

$$K_2 = -\frac{1}{x_q + x_{ep}}$$

$$K_3 = -\frac{x_q - x'_d}{\left(x'_d + x_{ep}\right)\left(x_q + x_{ep}\right)}$$

$$x_{ep} = x_t + x_l$$

- The second order terms are,

$$f_2(\mathbf{x}) = \frac{1}{2}\begin{bmatrix} \mathbf{x}^T\mathbf{H}^1\mathbf{x} \\ \mathbf{x}^T\mathbf{H}^2\mathbf{x} \\ \mathbf{x}^T\mathbf{H}^3\mathbf{x} \end{bmatrix} = \frac{1}{2}\begin{bmatrix} \sum_{k=1}^{n}\sum_{l=1}^{n} H_{kl}^1 x_k x_l \\ \sum_{k=1}^{n}\sum_{l=1}^{n} H_{kl}^2 x_k x_l \\ \sum_{k=1}^{n}\sum_{l=1}^{n} H_{kl}^3 x_k x_l \end{bmatrix} \tag{3.78}$$

With, $H^j = \begin{bmatrix} \frac{\partial^2 f_j}{\partial E'_q \partial E'_q} & \frac{\partial^2 f_j}{\partial E'_q \partial \delta} & \frac{\partial^2 f_j}{\partial E'_q \partial \omega} \\ \frac{\partial^2 f_j}{\partial \delta \partial E'_q} & \frac{\partial^2 f_j}{\partial \delta \partial \delta} & \frac{\partial^2 f_j}{\partial \delta \partial \omega} \\ \frac{\partial^2 f_j}{\partial \omega \partial E'_q} & \frac{\partial^2 f_j}{\partial \omega \partial \delta} & \frac{\partial^2 f_j}{\partial \omega \partial \omega} \end{bmatrix}_{x=x_{SEP}}$ which has the form,

$$H = \left[\begin{array}{ccc|ccc|cc} 0 & 0 & 0 & 0 & 0 & 0 & 0 & H_{(1,8)} & 0 \\ 0 & H_{(2,2)} & 0 & 0 & 0 & 0 & H_{(2,7)} & H_{(2,8)} & 0 \\ 0 & 0 & 0 & 0 & 0 & 0 & 0 & 0 & 0 \end{array}\right]$$

$$H_{(1,8)} = \frac{\omega_r}{2H}\left(-K_2 V_b \cos\delta + K_3 V_b \cos\delta\right)$$

$$H_{(2,2)} = -\frac{1}{T'_{d0}} K_1 V_b \cos\delta\,; \qquad H_{(2,7)} = \frac{\omega_r}{2H}\left(K_2 V_b \cos\delta + K_3 V_b \cos\delta\right)$$

$$H_{(2,8)} = \frac{\omega_r}{2H}\left\{-K_2 E'_q V_b \sin\delta + 3K_3 V_b^2 \sin\delta\cos\delta + K_4\left(E'_q - V_b\cos\delta\right)V_b \sin\delta\right\}$$

$$K_4 = \frac{x_q - x'_d}{\left(x'_d - x_{ep}\right)\left(x_q + x_{ep}\right)}$$

- The third order terms of the linearization are,

$$f_3(\mathbf{x}) = \frac{1}{6}\begin{bmatrix} \mathbf{x}^T\mathbf{H}_3^1\begin{bmatrix}\mathbf{x}&\mathbf{0}&\mathbf{0}\\\mathbf{0}&\mathbf{x}&\mathbf{0}\\\mathbf{0}&\mathbf{0}&\mathbf{x}\end{bmatrix}\mathbf{x} \\ \mathbf{x}^T\mathbf{H}_3^2\begin{bmatrix}\mathbf{x}&\mathbf{0}&\mathbf{0}\\\mathbf{0}&\mathbf{x}&\mathbf{0}\\\mathbf{0}&\mathbf{0}&\mathbf{x}\end{bmatrix}\mathbf{x} \\ \mathbf{x}^T\mathbf{H}_3^3\begin{bmatrix}\mathbf{x}&\mathbf{0}&\mathbf{0}\\\mathbf{0}&\mathbf{x}&\mathbf{0}\\\mathbf{0}&\mathbf{0}&\mathbf{x}\end{bmatrix}\mathbf{x} \end{bmatrix} = \frac{1}{6}\begin{bmatrix} \sum_{k=1}^{n}\sum_{l=1}^{n}\sum_{m=1}^{n} H_{3klm}^1 x_k x_l x_m \\ \sum_{k=1}^{n}\sum_{l=1}^{n}\sum_{m=1}^{n} H_{3klm}^2 x_k x_l x_m \\ \sum_{k=1}^{n}\sum_{l=1}^{n}\sum_{m=1}^{n} H_{3klm}^3 x_k x_l x_m \end{bmatrix} \tag{3.79}$$

where the third order matrix is defined by

$$\mathbf{H}_3^j = \begin{bmatrix} \frac{\partial^3 f_j}{\partial E_q'^3} & \frac{\partial^3 f_j}{\partial E_q'^2\partial\delta} & \frac{\partial^3 f_j}{\partial E_q'^2\partial\omega} & \frac{\partial^3 f_j}{\partial E_q'\partial\delta\partial E_q'} & \frac{\partial^3 f_j}{\partial E_q'\partial\delta^2} & \frac{\partial^3 f_j}{\partial E_q'\partial\delta\partial\omega} & \frac{\partial^3 f_j}{\partial E_q'\partial\omega\partial E_q'} & \frac{\partial^3 f_j}{\partial E_q'\partial\omega\partial\delta} & \frac{\partial^3 f_j}{\partial E_q'\partial\omega^2} \\ \frac{\partial^3 f_j}{\partial\delta\partial E_q'^2} & \frac{\partial^3 f_j}{\partial\delta\partial E_q'\partial\delta} & \frac{\partial^3 f_j}{\partial\delta\partial E_q'\partial\omega} & \frac{\partial^3 f_j}{\partial\delta^2\partial E_q'} & \frac{\partial^3 f_j}{\partial\delta^3} & \frac{\partial^3 f_j}{\partial\delta^2\partial\omega} & \frac{\partial^3 f_j}{\partial\delta\partial\omega\partial E_q'} & \frac{\partial^3 f_j}{\partial\delta\partial\omega\partial\delta} & \frac{\partial^3 f_j}{\partial\delta\partial\omega^2} \\ \frac{\partial^3 f_j}{\partial\omega\partial E_q'^2} & \frac{\partial^3 f_j}{\partial\omega\partial E_q'\partial\delta} & \frac{\partial^3 f_j}{\partial\omega\partial E_q'\partial\omega} & \frac{\partial^3 f_j}{\partial\omega\partial\delta\partial E_q'} & \frac{\partial^3 f_j}{\partial\omega\partial\delta^2} & \frac{\partial^3 f_j}{\partial\omega\partial\delta\partial\omega} & \frac{\partial^3 f_j}{\partial\omega^2\partial E_q'} & \frac{\partial^3 f_j}{\partial\omega^2\partial\delta} & \frac{\partial^3 f_j}{\partial\omega^3} \end{bmatrix}_{x=x_{SEP}} \tag{3.80}$$

Fitting to this case study, $\mathbf{H}_3^j$ has the next elements,

$$\mathbf{H}_3^1 = \left[\begin{array}{ccc|ccc|ccc} 0&0&0&0&0&0&0&0&0\\0&0&0&0&H_{(2,5)}^1&0&0&0&0\\0&0&0&0&0&0&0&0&0 \end{array}\right]_{x=x_{SEP}}$$

$$\mathbf{H}_3^2 = zeros(3\times 9) \tag{3.81}$$

$$\mathbf{H}_3^3 = \left[\begin{array}{ccc|ccc|ccc} 0&0&0&0&H_{(1,5)}^3&0&0&0&0\\0&H_{(2,2)}^3&0&H_{(2,4)}^3&H_{(2,5)}^3&0&0&0&0\\0&0&0&0&0&0&0&0&0 \end{array}\right]_{x=x_{SEP}}$$

$$H_{(2,5)}^1 = -\frac{1}{T_{d0}'}K_1 V_b \sin\delta$$

$$H_{(2,2)}^3 = \frac{\omega_r}{2H}\left(-K_2 V_b \sin\delta - K_3 V_b \sin\delta\right)$$

$$H_{(2,4)}^3 = \frac{\omega_r}{2H}\left(-K_2 V_b \sin\delta - K_3 V_b \sin\delta\right) \tag{3.82}$$

$$H_{(1,5)}^3 = \frac{\omega_r}{2H}\left(-K_2 V_b \sin\delta - K_3 V_b \sin\delta\right)$$

$$H_{(2,5)}^3 = -\frac{\omega_r}{2H}\left\{K_2 V_b \cos\delta + 3K_4 V_b^2 \cos^2\delta + 4K_3 V_b^2 \sin^2\delta + K_3\left(E_q' - V_b\cos\delta\right)V_b\ \cos\ \delta\right\}$$

Based on equation which links the relationship between the transformed variables with Jordan canonical form, the system (3.74) is then transformed, resulting in,

$$\dot{\mathbf{y}} = \mathbf{A}\mathbf{y} + \mathbf{f}_2(\mathbf{y}) + \mathbf{f}_3(\mathbf{y}) \tag{3.83}$$

where,

$$\mathbf{f}_2(\mathbf{y}) = \frac{1}{2}\mathbf{U}^{-1}\begin{bmatrix} (\mathbf{U}\mathbf{y})^{\mathrm{T}}\mathbf{H}_2^1\mathbf{U}\mathbf{y} \\ (\mathbf{U}\mathbf{y})^{\mathrm{T}}\mathbf{H}_2^2\mathbf{U}\mathbf{y} \\ (\mathbf{U}\mathbf{y})^{\mathrm{T}}\mathbf{H}_2^3\mathbf{U}\mathbf{y} \end{bmatrix} \tag{3.84}$$

$$\mathbf{f}_2(\mathbf{y}) = \frac{1}{2}\begin{bmatrix} \sum_{k=1}^{N}\sum_{l=1}^{N} C_{kl}^1 y_k y_l \\ \sum_{k=1}^{N}\sum_{l=1}^{N} C_{kl}^2 y_k y_l \\ \sum_{k=1}^{N}\sum_{l=1}^{N} C_{kl}^3 y_k y_l \end{bmatrix} \tag{3.85}$$

and,

$$\mathbf{f}_3(\mathbf{x}) = \frac{1}{6}\mathbf{U}^{-1}\begin{bmatrix} (\mathbf{U}\mathbf{y})^{T}\mathbf{H}_3^1\begin{bmatrix} \mathbf{U}\mathbf{y} & \mathbf{0} & \mathbf{0} \\ \mathbf{0} & \mathbf{U}\mathbf{y} & \mathbf{0} \\ \mathbf{0} & \mathbf{0} & \mathbf{U}\mathbf{y} \end{bmatrix}\mathbf{U}\mathbf{y} \\ (\mathbf{U}\mathbf{y})^{T}\mathbf{H}_3^2\begin{bmatrix} \mathbf{U}\mathbf{y} & \mathbf{0} & \mathbf{0} \\ \mathbf{0} & \mathbf{U}\mathbf{y} & \mathbf{0} \\ \mathbf{0} & \mathbf{0} & \mathbf{U}\mathbf{y} \end{bmatrix}\mathbf{U}\mathbf{y} \\ (\mathbf{U}\mathbf{y})^{T}\mathbf{H}_3^3\begin{bmatrix} \mathbf{U}\mathbf{y} & \mathbf{0} & \mathbf{0} \\ \mathbf{0} & \mathbf{U}\mathbf{y} & \mathbf{0} \\ \mathbf{0} & \mathbf{0} & \mathbf{U}\mathbf{y} \end{bmatrix}\mathbf{U}\mathbf{y} \end{bmatrix} \tag{3.86}$$

$$\mathbf{f}_3(\mathbf{y}) = \frac{1}{6}\begin{bmatrix} \sum_{k=1}^{n}\sum_{l=1}^{n}\sum_{m=1}^{n} C_{3klm}^1 y_k y_l y_m \\ \sum_{k=1}^{n}\sum_{l=1}^{n}\sum_{m=1}^{n} C_{3klm}^2 y_k y_l y_m \\ \sum_{k=1}^{n}\sum_{l=1}^{n}\sum_{m=1}^{n} C_{3klm}^3 y_k y_l y_m \end{bmatrix} \tag{3.87}$$

where C_{kl}^j and C_{3klm}^j are defined in (3.57) to (3.59).

Once the nonlinear dynamic system has been transformed to the Jordan canonical form, the Laplace transformation has to be carried-out. The system expressed in the Laplace domain represents the contributions of linear and nonlinear higher order terms, which have to be solved by association of variables theorems such as described above.

Finally, after the inverse Laplace transform has been applied, the time domain solution is expressed as,

$$y_j(t) \approx f_j^1(t) + f_j^2(t) + f_j^3(t) \tag{3.88}$$

The full solution obtained for the nonlinear system is given by,

$$\begin{bmatrix} y_1(t) \\ y_2(t) \\ y_3(t) \end{bmatrix} = \begin{bmatrix} f_1^1(t) \\ f_2^1(t) \\ f_3^1(t) \end{bmatrix} + \begin{bmatrix} f_1^2(t) \\ f_2^2(t) \\ f_3^2(t) \end{bmatrix} + \begin{bmatrix} f_1^3(t) \\ f_2^3(t) \\ f_3^3(t) \end{bmatrix} \tag{3.89}$$

where this time domain solution is presented as a function of the Jordan variables; that is,

$$\begin{bmatrix} y_1(t) \\ y_2(t) \\ y_3(t) \end{bmatrix} = \begin{bmatrix} y_1^0 e^{\lambda_1 t} \\ y_2^0 e^{\lambda_2 t} \\ y_3^0 e^{\lambda_3 t} \end{bmatrix} - \begin{bmatrix} \sum_{k=1}^{N}\sum_{l=1}^{N} h_{2kl}^1 y_k^0 y_l^0 e^{\lambda_1 t} \\ \sum_{k=1}^{N}\sum_{l=1}^{N} h_{2kl}^2 y_k^0 y_l^0 e^{\lambda_2 t} \\ \sum_{k=1}^{N}\sum_{l=1}^{N} h_{2kl}^3 y_k^0 y_l^0 e^{\lambda_3 t} \end{bmatrix} + \begin{bmatrix} \sum_{k=1}^{N}\sum_{l=1}^{N} h_{2kl}^1 y_k^0 y_l^0 e^{(\lambda_k+\lambda_l)t} \\ \sum_{k=1}^{N}\sum_{l=1}^{N} h_{2kl}^2 y_k^0 y_l^0 e^{(\lambda_k+\lambda_l)t} \\ \sum_{k=1}^{N}\sum_{l=1}^{N} h_{2kl}^3 y_k^0 y_l^0 e^{(\lambda_k+\lambda_l)t} \end{bmatrix} \tag{3.90}$$

Transforming to the original state variables, the time domain final solution has the form,

$$\begin{bmatrix} x_1(t) \\ x_2(t) \\ x_3(t) \end{bmatrix} = \begin{bmatrix} \Delta E_q'(t) \\ \Delta\delta(t) \\ \Delta\omega(t) \end{bmatrix} = \begin{bmatrix} u_{11} & u_{12} & u_{13} \\ u_{21} & u_{22} & u_{23} \\ u_{31} & u_{32} & u_{33} \end{bmatrix} \begin{bmatrix} y_1(t) \\ y_2(t) \\ y_3(t) \end{bmatrix} \tag{3.91}$$

Equation (3.91) provides closed form solutions to the state in terms of the initial conditions in the Jordan state variables. Also, the dynamic information given by the modal analysis is maintained at this part of the final solution. In a identical manner to the study case with the machine classical model, the linear approximation is obtained according to (3.70), extended for this case to three state variables and the algebraic equations.

3.7.2.1 Simulation Results

The experiment is conducted assuming a perturbation in the rotor angle. The solution obtained with the modal series technique is compared against the linear approximation and the numerical full solution obtained from the nonlinear differential equations that represent the dynamic system. The model of the system consists on stator dynamics represented by the state variable of voltage along the *q* axis, neglecting *d* axis effects (one axis flux decay model ((3.71))). The perturbation is initially applied assuming an increment in input torque (mechanical power in the generator); afterwards, a larger increment in the same power joint with another increase in the rotor angle perturbation is reflected as a stress condition.

The modal analysis is resumed in Table 3.1. Two oscillatory modes are present, due to the electromechanical oscillations and a real mode, mainly due to the stator variable E_q'. The experiment is

performed to compare the solution obtained by modal series against the linear approximation and the direct solution of the nonlinear set of differential equations basically described by ((3.71)).

Table 3.1 Modal analysis of SMIB with one flux model

Eigenvalue	Frequency (Hz)	Damping Ratio
$\lambda_1 = -0.032786337262722$	-	-
$\lambda_{2,3} = -0.478749 \pm 5.137238i$	0.817616863444186	0.092789977022137

Figure 3.6 through 3.9 show the oscillations of the state variables δ, ω and E'_q when a rotor angle perturbation conditions are applied. Figure 3.6 is showing the oscillations followed to a perturbation in the rotor angle of $\Delta\delta = 10^\circ$ followed by an increase on the power demand to $P_m = 1.12\, p.u.$. The full transient followed by state variables can be observed. Qualitative differences are noticed between modal series approximation with respect to the linear approximation in the waveform of the voltage E'_q, that presents an offset. Eventually since the system is stable, even in the presence of perturbation conditions, it eventually reaches a steady state point after a transient period, being larger for the case of voltage E'_q. Also, Figure 3.6 shows the transient behavior of selected state variables.

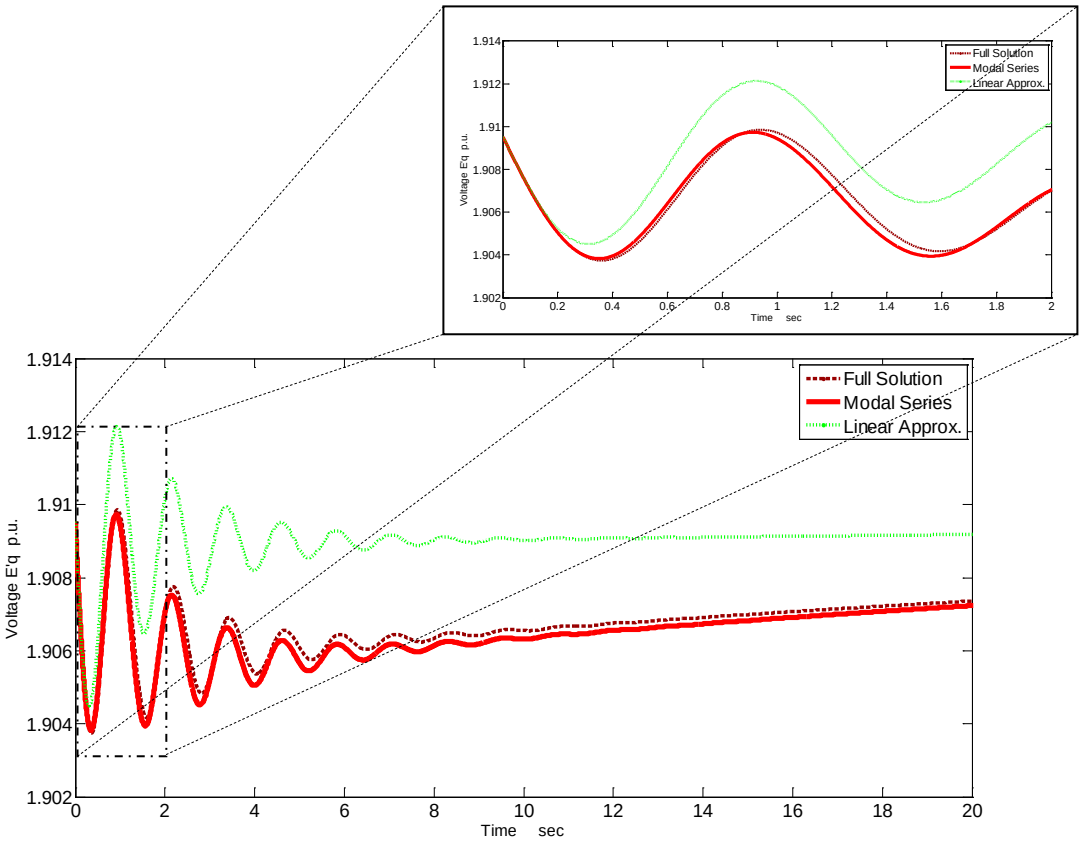

a) Voltage E'_q

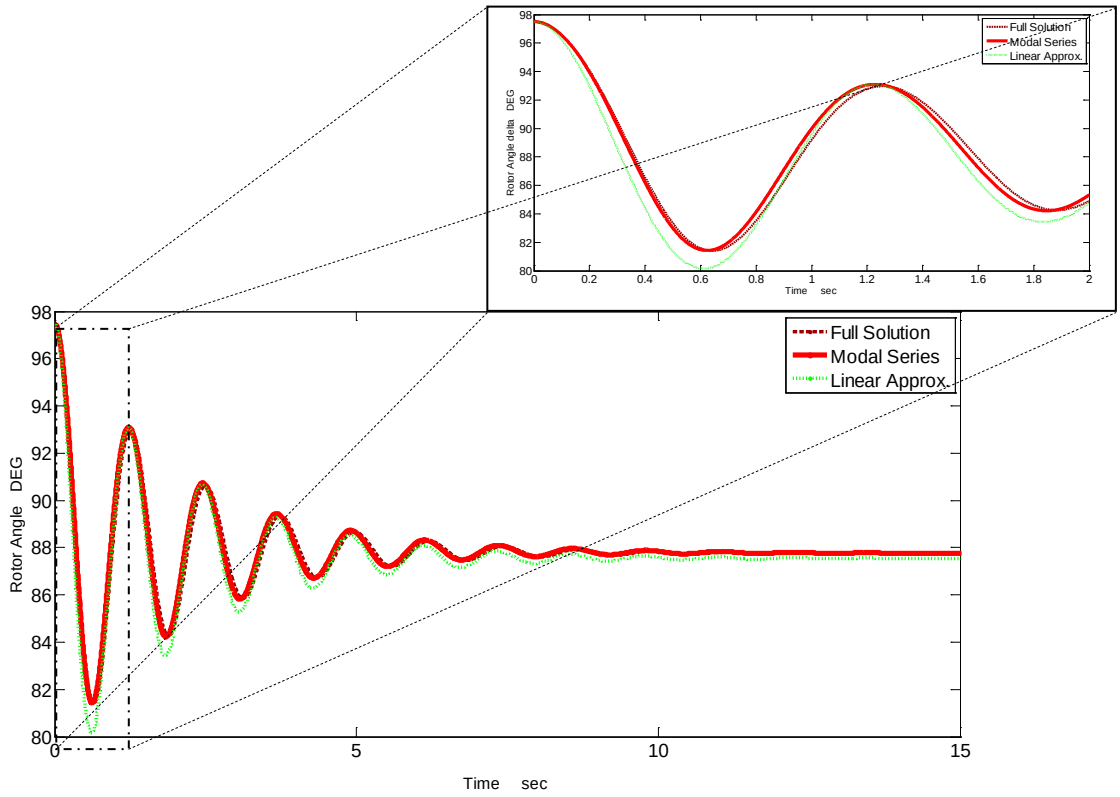

b) Rotor angle δ

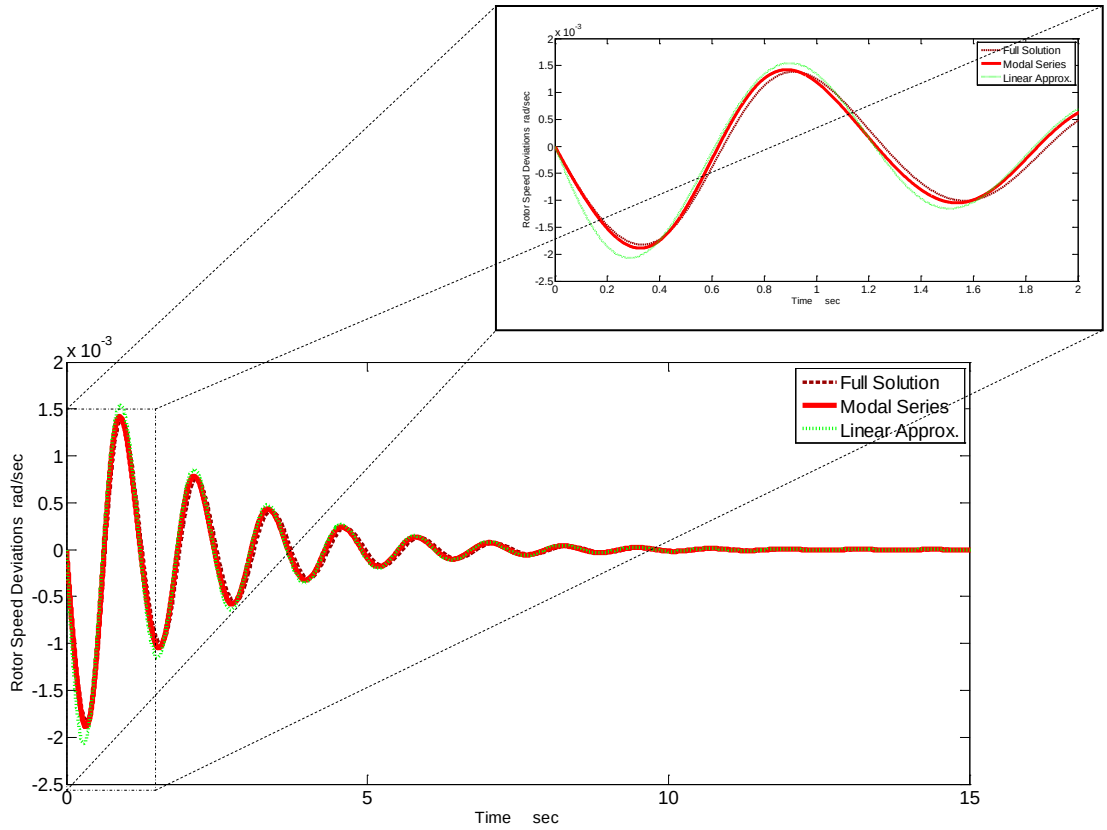

c) Speed Rotor ω

Figure 3.6. Rotor angle and speed deviations comparison for a load condition of P_m=1.12 p.u. and $\Delta\delta$=10°

The Figure has been conveniently zoomed to illustrate the differences between solutions in more detail.

The phase planes shown in Figures 3.7 demonstrate that the system is stable after the oscillations followed due to the disturbance conditions. Both the rotor angle and speed rotor approaches to a stable equilibrium point, which is clearly observable in the phase plane of Figure 3.7 a).

Figure 3.7 b) denotes a tridimensional phase plane that involves the three state variables where the final solution goes to a fixed steady state operating point in the same form as in the two dimensional phase plane. It is important to point out that the solution obtained by modal series is in close agreement to the solution obtained directly from numerical full approximation.

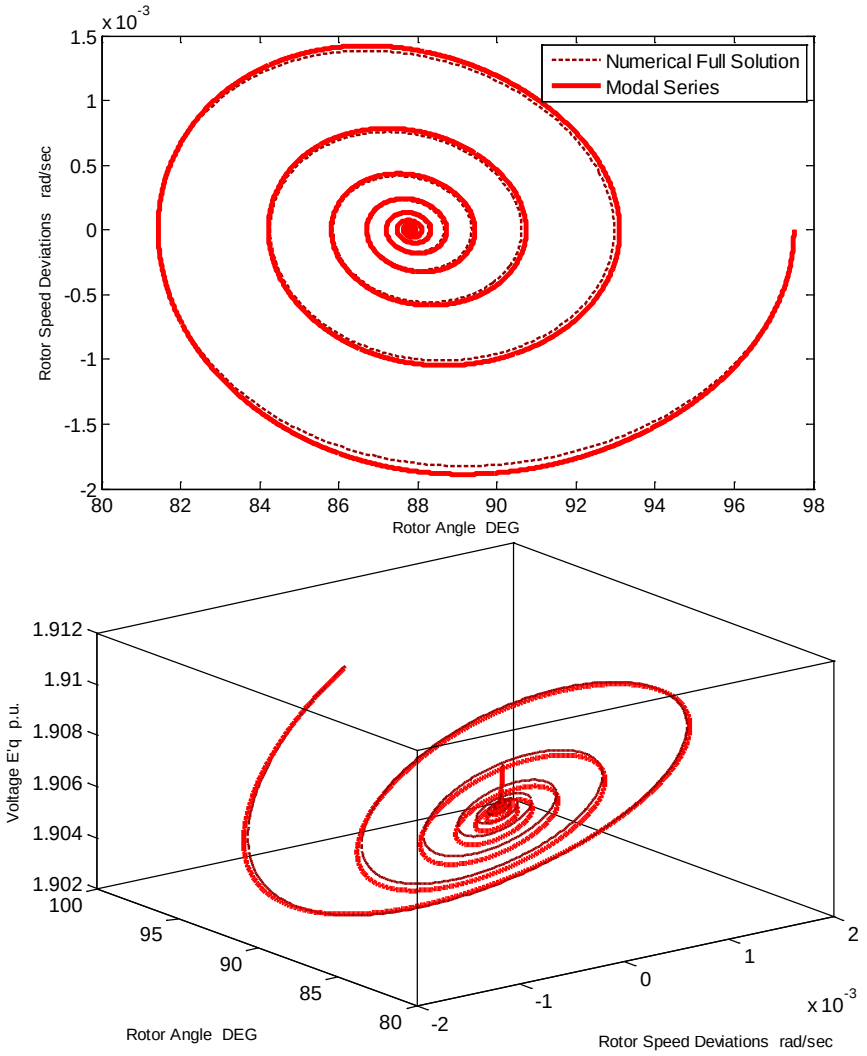

Figure 3.7. Rotor angle and speed deviations comparison for a load condition of P_m=1.15 p.u. and $\Delta\delta$=10°

The oscillatory behavior in the generator after the change in the initial angle conditions. There is a deceleration in the synchronous machine, so noted by the decrement in the rotor speed which is

accompanied by a decrement in the rotor angle and the magnitude on the voltage E'_q. The system keeps oscillating until it reaches the new equilibrium point, which is different in comparison with the initial operation conditions.

Hence, it can be said that the method of modal series has a good accuracy in presence of low perturbation or low stress conditions, since the operation point is near to the initial equilibrium point defined for the linearization of the nonlinear system.

Now the experiment is continued selecting different conditions of perturbation. The system is stressed by a step change of the demanded power of the synchronous machine moving it to $P_m = 1.15\,p.u.$ together with a perturbation increment of $\Delta\delta = 30^\circ$. Figure 3.8 shows the oscillation due to this constraint where it can be observed a clear difference between the three methods utilized (full solution, modal series and linear approximation). With respect to the voltage E'_q (Figure 7.8a) the offset is clearly observable from the linear approximation; there is an appreciable difference between the modal series and full solution waveform; such differences are remarkable in amplitude and phase angle. The same result is noted in Figures 3.8(b) and 3.8(c) for the rotor angle and rotor speed. Again, the waveforms have been conveniently zoomed to detail the initial oscillatory periods following the transient until reach the new steady state condition.

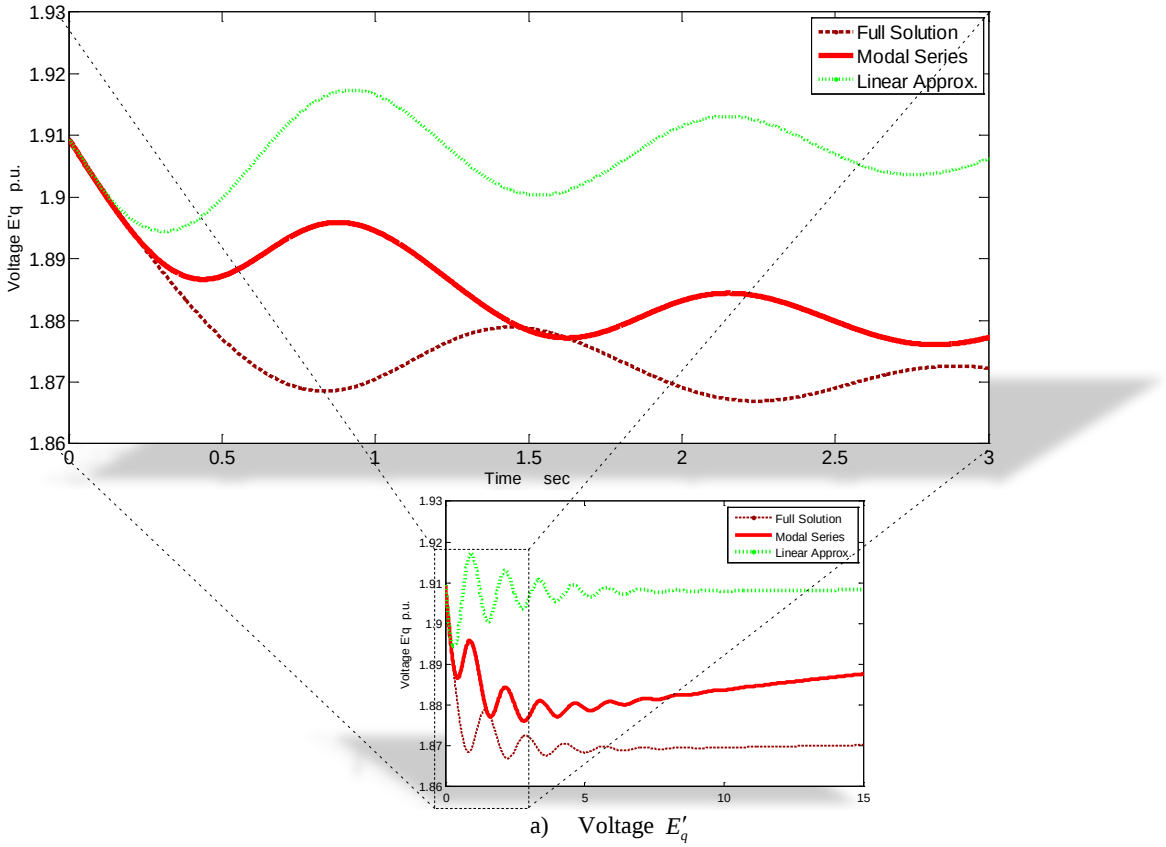

a) Voltage E'_q

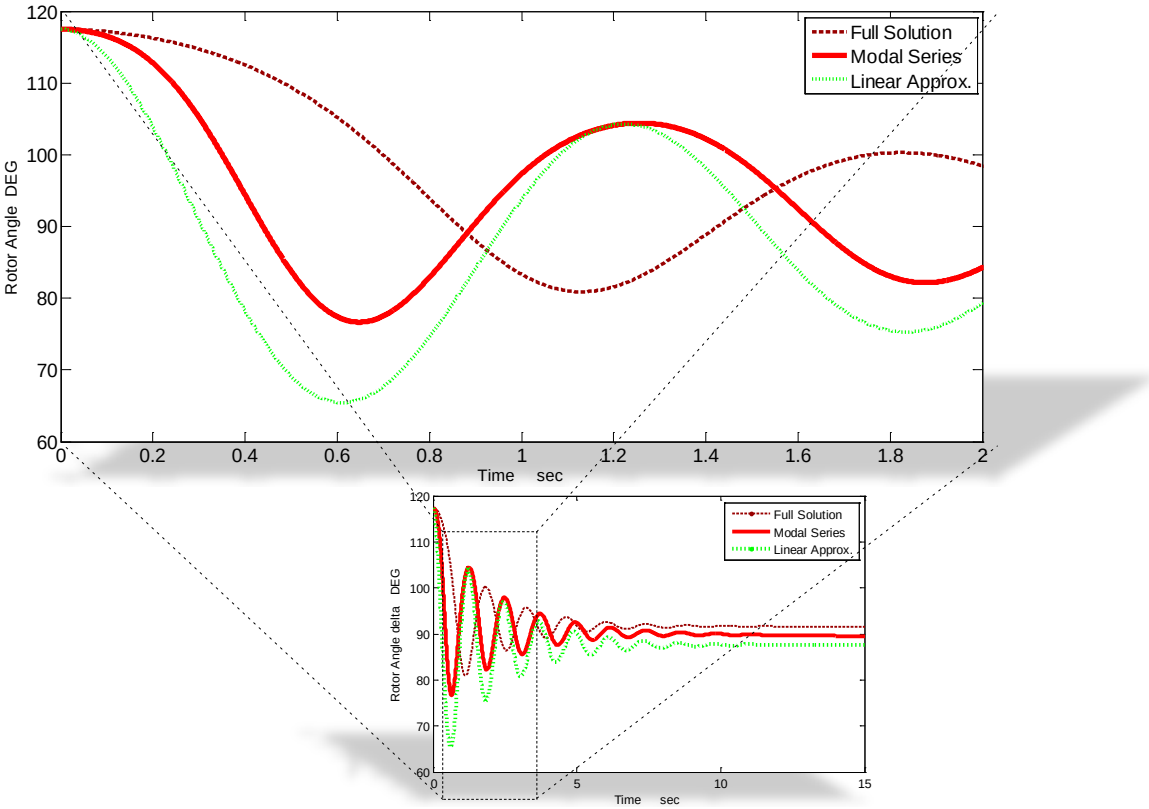

b) Rotor angle δ

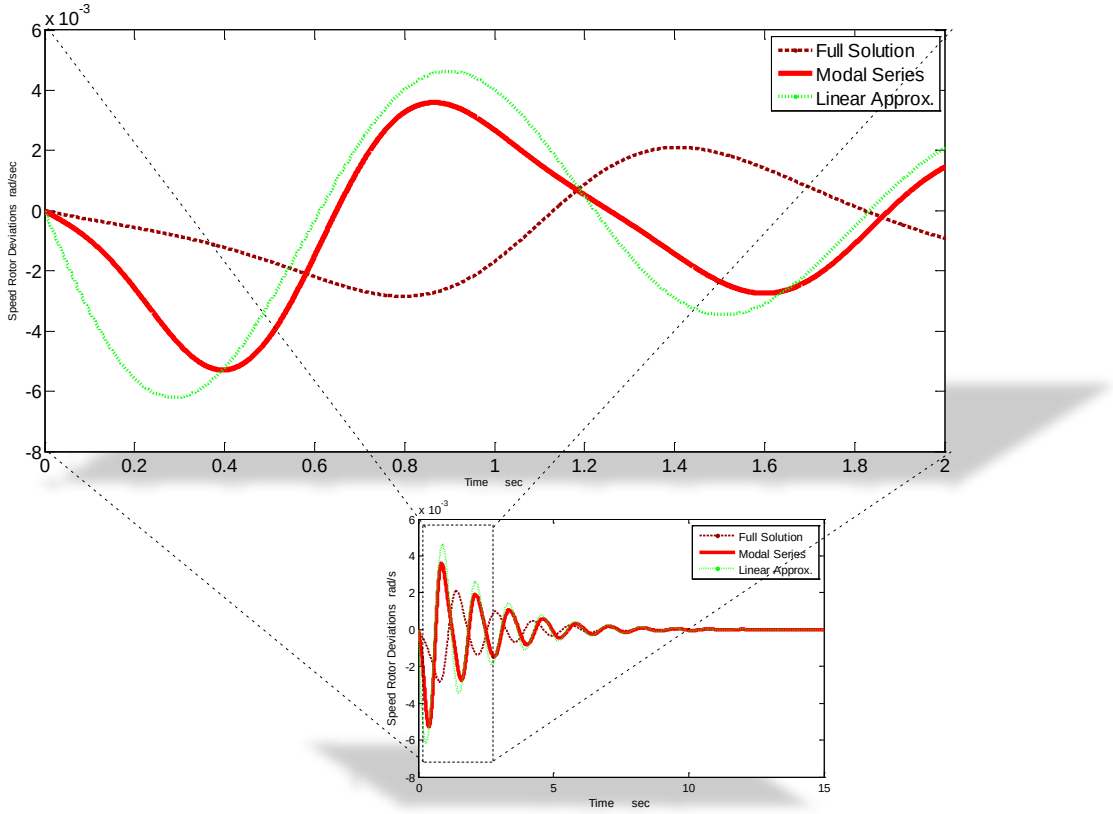

c) Speed Rotor ω

Figure 3.8. Rotor angle and speed deviations comparison for a load condition of P_m=1.15 p.u. and $\Delta\delta$=30°

From this oscillatory condition, it is clear that the system is still stable despite the stress conditions previously established for the analysis (see zoomed Figures 3.8(b) and 3.8(c)). This situation can be denoted in the phase planes of Figures 3.9. The two dimensional phase plane of Figure 3.9(a) is showing the behavior of rotor angle versus speed rotor, where a different trajectory is followed by the modal series solution and the full numerical solution, although at the end both solutions find the same steady state point.

Figure 3.9b shows a three dimensional trajectory followed by the two compared methods, where a different body of solution can be noticed, but similarly to the two dimensional phase plane case, both solutions eventually find the same final operating point.

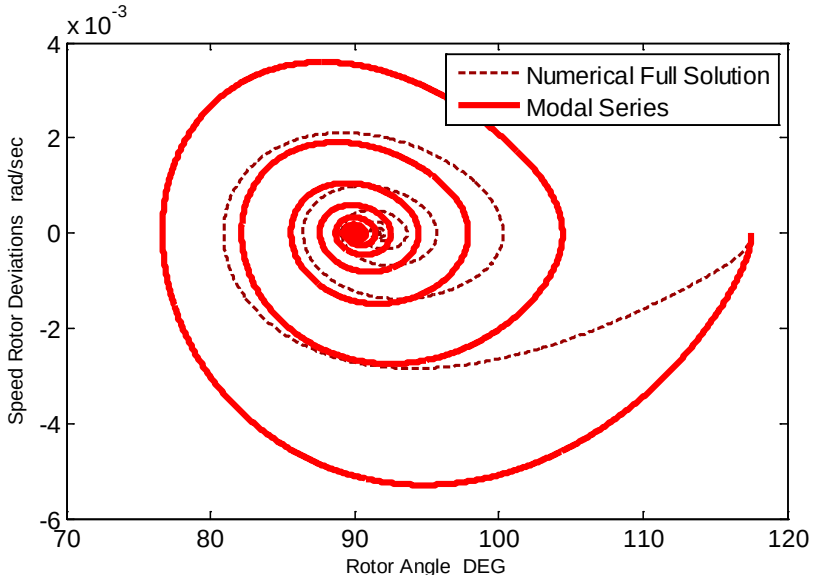

a) Two dimensional phase plane $\delta vs\,\omega$

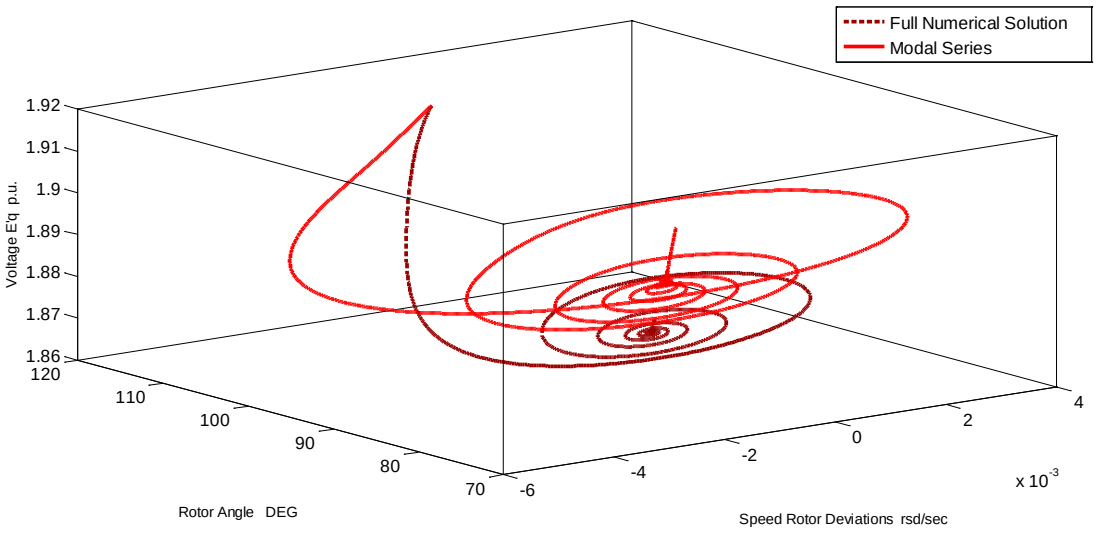

b) Three dimensional phase plane $\delta vs\,\omega vs\,E'_q$

Figure 3.9. Phase plane comparison for a load condition of P_m=1.5 p.u. and $\Delta\delta$=30°

Thus, this experiment demonstrates that the modal series method approximation could fail when the stress conditions are increased in such a way that the operating point is moved away from the steady state conditions. It can be concluded that a stressed power system tends to change the apparent linear behavior, moving the system to oscillate near the edge of unstable conditions

3.8 DISCUSSION

Compared to other approaches, the main theoretical advantage of the revisited modal series lies in its ability to derive higher-order modal solutions, associated modal quantities and the computation of second and higher-order terms, which can be extended as it will be demonstrated in the Chapter 5 to obtain nonlinear transfer functions.

Some limitations arise, however, associated with modeling assumptions as discussed below. The inclusion of detailed machine and control models is under development and will be discussed in future developments. The core of the experiments performed along this Chapter tried to demonstrate the advantages and limitations that can be found when the method of modal series is used to analyze a stressed system, in addition to the conclusions given early in the same tone, in the Chapter 2 (when the method was compared with Normal Forms method).

Furthermore, a comparison of the modal series method with other methods including the previouly proposed modal series [Schanechi, *et al.* 2003] is detailed in Table 3.2. The comparison is focused on the modeling detail, analysis capacity and future developments so related with the other approaches.

Table 3.2 Comparison between the modeling capacities of the proposed approach with other formulations

Modeling Detail and Analysis Capability	**NF Method**	**Conventional Modal Series Methods**	**Proposed Modal Series Technique**
Higher order transfer function computation	X	Currently limited to second order	Available
Detailed system modeling/FACTS controllers	Available	Not reported	Under development
Sparsity representation	Available	Not reported	X
Higher order nonlinear solutions	Available (third-order)*	Second-order approximation	Higher-order approximation*
Bifurcation analysis	Available	X	Under Development

* Theoretically possible up to arbitrary order

On the other side, modal series analysis methods are based on the first steps of the normal forms formulation and use similar interaction coefficients and nonlinearity indexes. In the former method,

however, the computation of higher-order initial conditions in the normal form space needs to solve the nonlinear algebraic homological equations while the modal series method does not need any numerical algorithm. Thus, the nonlinear indexes are computed in a more straightforward manner.

Modal analysis methods are still evolving to address theoretical and numerical problems and need further evaluation, particularly in regard to the study of various dynamic issues.

The application of these methods to the study of power system separation mechanisms, stability boundaries, and the analysis and design of system controllers warrant further investigation.

Finally, the flow chart diagram of Figure 3.10 illustrates the steps followed by the modal series method compared with the Normal Forms method and linear approximation. It is important to remark the accuracy of application based on multidimensional Laplace transform, which makes possible to obtain a closed form analytical solution. The Chapter 5 details its extension to the inclusion of a forced input response.

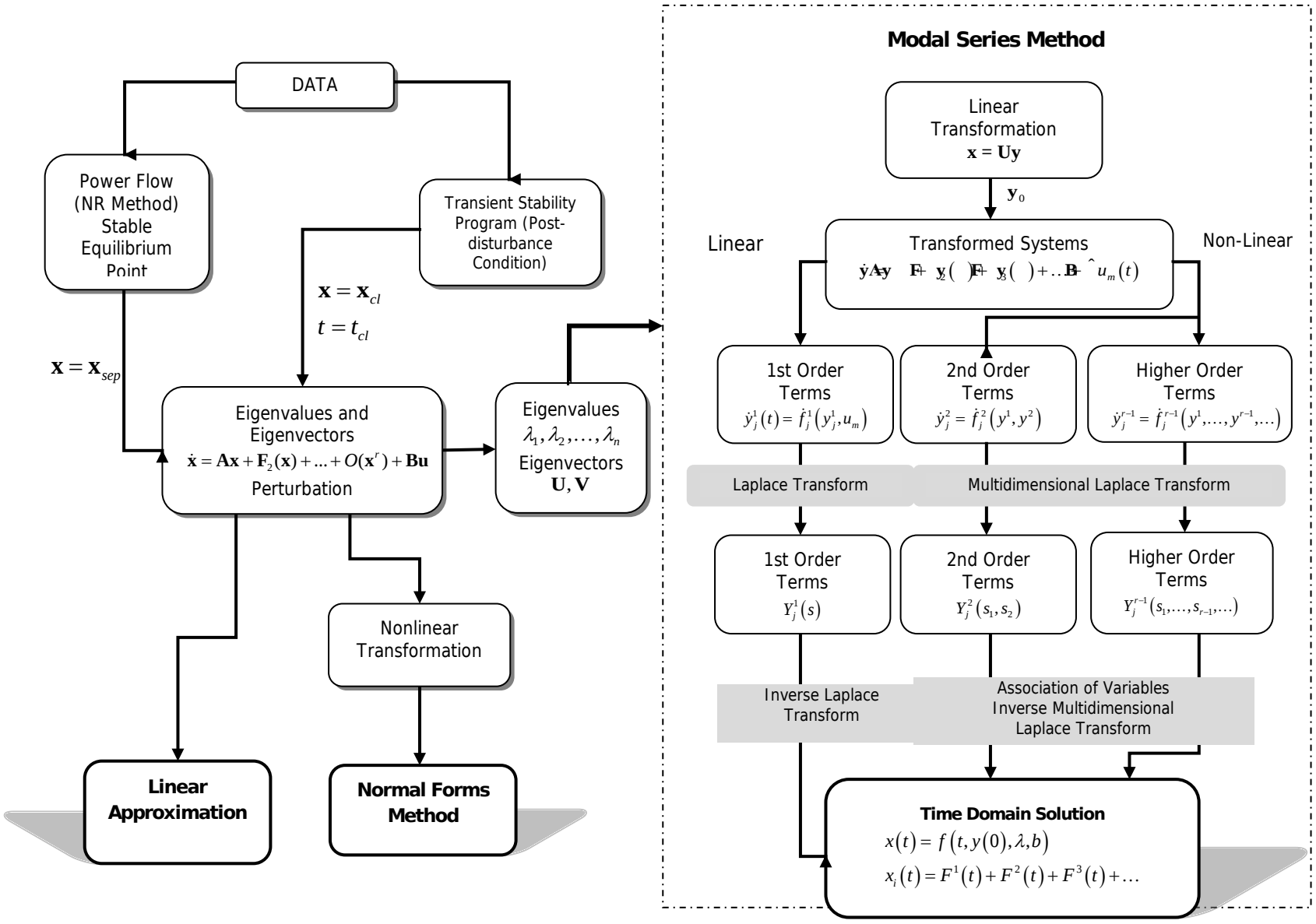

Figure. 3.10. Flow chart of the proposed method and its relationship with other approaches

THIS PAGE IS INTENTIONALLY LEFT BLANK

4

MULTIMACHINE POWER SYSTEMS MODELLING FOR NONLINEAR OSCILLATIONS STUDIES

A power system having ng generators interacting with the rest of the system is analyzed. The core the modeling of multimachine power system here described is based on the combination of the synchronous machine reference framework with the rest of the network. The load modeling considered in this research is based on static constant impedances; however, it is possible to extend the analysis to incorporate dynamic nonlinear loads, since the modeling platforms allow the inclusion of dynamic and time varying devices. In the sections to follow, the multimachine power system modeling used for the experiments that will be analyzed in the studies case exemplified in Chapters 5 and 6 is described in detail.

4.1. SYNCHRONOUS MACHINE GENERATORS MODELLING

Synchronous generators in power systems are modeled according to two axis theory [Sauer and Pai 1998] [Anderson and Fouad 2003]. Magnetic saturation effects and saliency are not considered. A simple automatic voltage regulator is included to control the synchronous machine field excitation.

The equations that describe the generator model taken from [Sauer and Pai 1998] are,

$$\frac{dE'_{q_k}}{dt} = \frac{1}{T'_{d0_k}}\left(E_{fd_k} - \left(x_{d_k} - x'_{d_k}\right)I_{d_k} - E'_{q_k}\right) \tag{4.1}$$

$$\frac{dE'_{d_k}}{dt} = \frac{1}{T'_{q0_k}}\left(-E'_{d_k} + \left(x_{q_k} - x'_{q_k}\right)I_{q_k}\right) \tag{4.2}$$

$$\frac{d\delta_k}{dt} = \omega - \omega_0 \tag{4.3}$$

$$\frac{d\omega_k}{dt} = \frac{1}{M_k}\left(P_{mk} - \left(E'_{d_k}I_{d_k} + E'_{q_k}I_{q_k}\right) - D_k\omega_k\right) \tag{4.4}$$

- Excitation system

$$\frac{dE_{fd_k}}{dt} = \frac{1}{T_{exc_k}}\left(-E_{fd_k} + K_{exc_k}\left(V_{ref_k} - V_{t\,exc_k}\right)\right) \tag{4.5}$$

$$V_{texc\,k} = \sqrt{\left(E'_{dk} + x'_k I_{qk}\right)^2 + \left(E'_{qk} - x'_k I_{dk}\right)^2} \qquad (4.6)$$

4.2. TRANSMISSION NETWORK MODELING

The transmission network is represented by nodal admittance equations, modified in order to incorporate internal generators buses; that is, the system is referenced to the internal generator nodes. Each synchronous machine is represented as an *emf* behind its reactance. Figure 4.1 shows the schematic of power system representation.

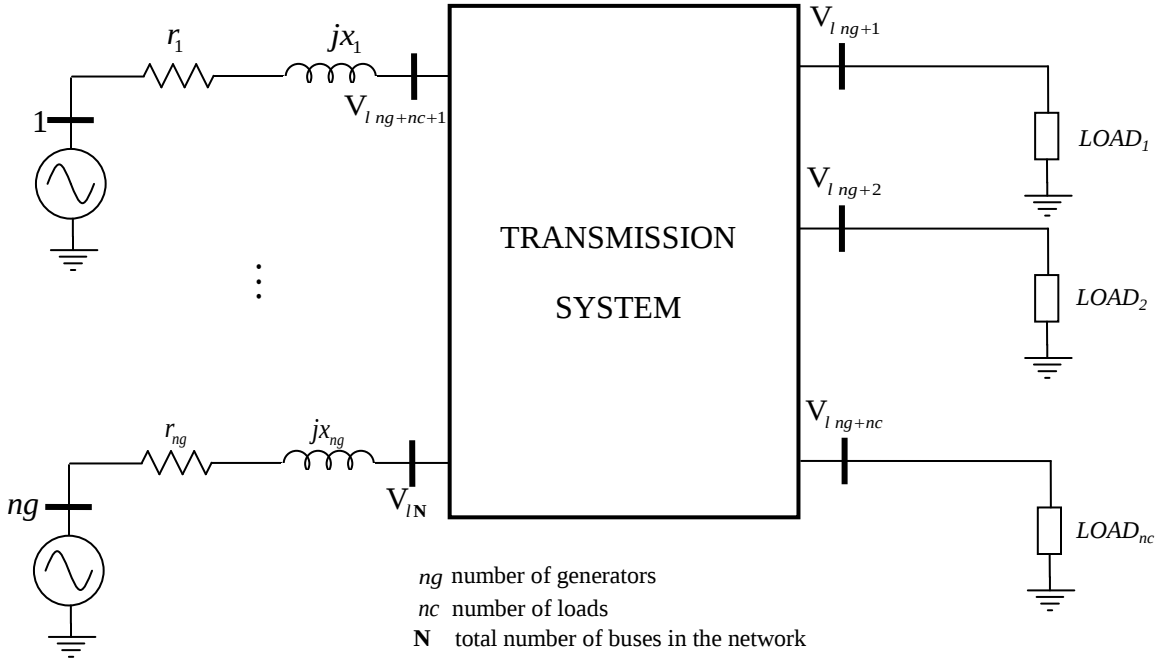

Figure 4.1 Schematic diagram of power system modeling

The equation that represents the network is given by,

$$\begin{bmatrix} \mathbf{I}_g \\ 0 \end{bmatrix} = \begin{bmatrix} \mathbf{Y}_{gg} & \mathbf{Y}_{gl} \\ \mathbf{Y}_{lg} & \mathbf{Y}_{ll} \end{bmatrix} \begin{bmatrix} \mathbf{V}_g \\ \mathbf{V}_l \end{bmatrix} \qquad (4.7)$$

where, $\mathbf{Y}_{gg}$, $\mathbf{Y}_{gl}$, $\mathbf{Y}_{lg}$ and $\mathbf{Y}_{ll}$ are reduced admittance submatrices. Moreover,

$$\mathbf{I}_g = \begin{bmatrix} I_{D1} + jI_{Q1} & I_{D2} + jI_{Q2} & \dots & I_{Dng} + jI_{Qng} \end{bmatrix}^T \qquad (4.8)$$

$$\mathbf{V}_g = \begin{bmatrix} E'_{D1} + jE'_{Q1} & E'_{D2} + jE'_{Q2} & \dots & E'_{Dng} + jE'_{Qng} \end{bmatrix}^T \qquad (4.9)$$

$$\mathbf{V}_l = \begin{bmatrix} V_{Dng+1} + jI_{Qng+1} & V_{Dng+2} + jV_{Qng+2} & \dots & V_{Dng+nc} + jV_{Qng+nc} \end{bmatrix}^T \qquad (4.10)$$

The power system shown in Figure 4.1 is reduced to the network shown in Figure 4.2. Referring to this network, nodal currents and voltages, such as described in Equations (4.8)-(4.10) are expressed using phasor notation as,

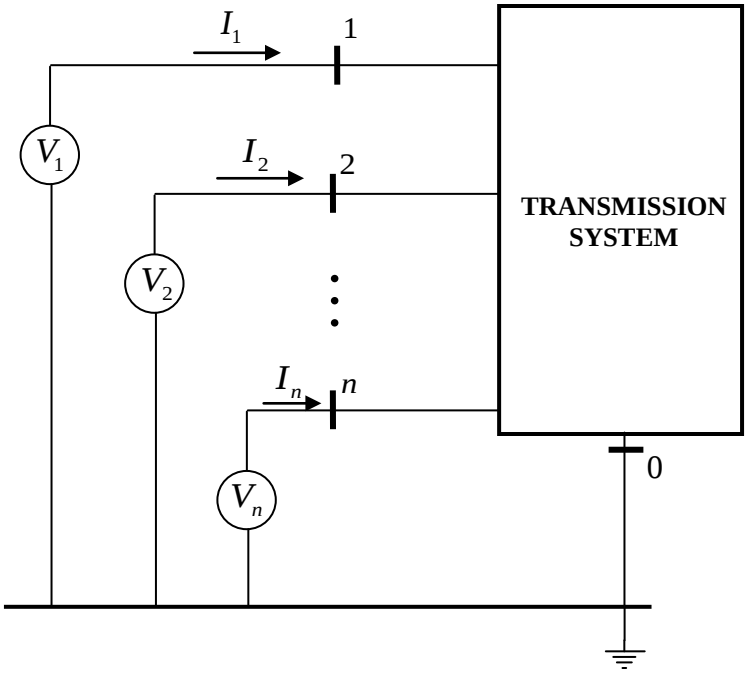

Figure 4.2 Transmission system reduced to the internal generator nodes

Indeed, the network is described by,

$$\mathbf{I} = \mathbf{YV} \tag{4.11}$$

where

Y Admittance matrix reduced to internal generators

I Nodal current injections vector

V Nodal voltages vector

The reduction approach of admittances matrix is described according to the following steps [Sauer and Pai 1994]:

- Obtain $\mathbf{Y}_{BUS}$ matrix by inspection, not considering the matrices associated to generators and loads
- Add the nodes corresponding to the generators.
- Conform the augmented admittance matrix, according to:

$$\mathbf{Y}_{AUG} = \left[\begin{array}{c|c} \mathbf{Y}_A & \mathbf{Y}_B \\ \hline \mathbf{Y}_C & \mathbf{Y}_D \end{array}\right] \tag{4.12}$$

That is,

$$\mathbf{Y}_{AUG}=\left[\begin{array}{c|c} \left[\mathbf{Y}_I\right]_{ng\times ng} & \left[-\left[\mathbf{Y}_I\right]_{ng\times ng} \mid \left[0\right]_{ng\times(n-ng)}\right]_{ng\times n} \\ \hline \left[\begin{array}{c} -\left[\mathbf{Y}_I\right]_{ng\times ng} \\ \hline \left[0\right]_{(n-ng)\times ng} \end{array}\right]_{n\times ng} & \left[\left[\mathbf{Y}_{BUS}\right]+\left[\mathbf{Y}_{LOAD}\right]+\left[\mathbf{Y}_I\right]\right]_{n\times n} \end{array}\right]_{(n+ng)\times(n+ng)} \tag{4.13}$$

where

$\mathbf{Y}_I = diag\left[Y_{gi}\right]$; Y_{gi} generator admittance *i*

$\mathbf{Y}_{LOAD}$ load admittance matrix corresponding to the bus where the load is connected

Finally, the admittance matrix is reduced as,

$$\mathbf{Y}_{RED}=\mathbf{Y}_A-\mathbf{Y}_B\mathbf{Y}_D^{-1}\mathbf{Y}_C \tag{4.14}$$

where

$$\mathbf{Y}_A=\left[\mathbf{Y}_I\right]_{ng\times ng} \qquad \mathbf{Y}_B=\left[-\left[\mathbf{Y}_I\right]_{ng\times ng} \mid \left[0\right]_{ng\times(n-ng)}\right]$$

$$\mathbf{Y}_C=\left[-\left[\mathbf{Y}_I\right]_{ng\times ng} \mid \left[0\right]_{ng\times(n-ng)}\right]^T \qquad \mathbf{Y}_D=\left[\mathbf{Y}_{BUS}+\mathbf{Y}_{LOAD}+\mathbf{Y}_I\right]_{n\times n}$$

4.3. COORDINATE TRANSFORMATION TO A COMMON REFERENCE FRAMEWORK

The formulated power network has been expressed in the coordinate system $DQ0$, in such a way that it is necessary to transform the transmission system to a common coordinate reference framework or simply a common reference. The conversion process is graphically illustrated by Figure 4.3. This figure represents the $dq0$ and $DQ0$ axes framework. It is important to point out that the angle δ_i relates the angular difference between both frameworks (that is, network reference and synchronous rotating reference frame).

From Figure, it is possible to obtain the expressions that relate both frames dq and DQ. Hence,

$$I_{Di}=I_{di}\sin\delta_i+I_{qi}\cos\delta_i \tag{4.15}$$

$$I_{Qi}=-I_{di}\cos\delta_i+I_{qi}\sin\delta_i \tag{4.16}$$

Conveying all network currents in matrix form, it yields,

$$\begin{bmatrix} I_{D1}+jI_{Q1} \\ I_{D2}+jI_{Q2} \\ \vdots \\ I_{Dn}+jI_{Qn} \end{bmatrix}=\begin{bmatrix} \cos\delta_1+j\sin\delta_1 & & & \\ & \cos\delta_2+j\sin\delta_2 & & \\ & & \ddots & \\ & & & \cos\delta_n+j\sin\delta_n \end{bmatrix}\begin{bmatrix} I_{d1}+jI_{q1} \\ I_{d2}+jI_{q2} \\ \vdots \\ I_{dn}+jI_{qn} \end{bmatrix} \tag{4.17}$$

In compact form

$$\mathbf{I}_{DQ} = \mathbf{T}\mathbf{I}_{dq} \tag{4.18}$$

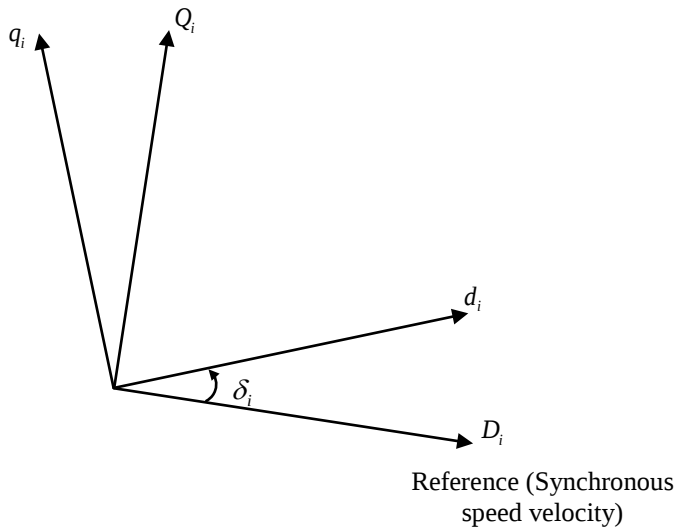

Figure 4.3 Reference relationship between *dq* and *DQ* variables

where the transformation matrix **T** is defined as,

$$\mathbf{T} = diag\left(\begin{bmatrix} e^{j\delta_1} & e^{j\delta_2} & \dots & e^{j\delta_n} \end{bmatrix}\right) \tag{4.19}$$

with

$$\mathbf{I}_{DQ} = \begin{bmatrix} I_{D1} + jI_{Q1} \\ I_{D2} + jI_{Q2} \\ \vdots \\ I_{Dn} + jI_{Qn} \end{bmatrix} \qquad \mathbf{I}_{dq} = \begin{bmatrix} I_{d1} + jI_{q1} \\ I_{d2} + jI_{q2} \\ \vdots \\ I_{dn} + jI_{qn} \end{bmatrix}$$

Same definitions may be applied to voltage transformation, that is,

$$\hat{\mathbf{V}} = \mathbf{T}\mathbf{V} \tag{4.20}$$

where,

$$\hat{\mathbf{V}} = \begin{bmatrix} V_{D1} + jV_{Q1} \\ V_{D2} + jV_{Q2} \\ \vdots \\ V_{Dn} + jV_{Qn} \end{bmatrix} \qquad \mathbf{V} = \begin{bmatrix} V_{d1} + jV_{q1} \\ V_{d2} + jV_{q2} \\ \vdots \\ V_{dn} + jV_{qn} \end{bmatrix}$$

The transformation matrix described by Equation (4.19) is a kind of orthogonal matrix, which satisfies with,

$$\mathbf{T}^{-1} = \mathbf{T}^{*} \tag{4.21}$$

Therefore, applying the transformation matrix (4.19) to the network of Figure 4.2, results in,

$$\mathbf{I}_g = \mathbf{I}_{DQ} = \mathbf{T}\mathbf{I}_{dq} \tag{4.22}$$

$$\mathbf{V}_g = \mathbf{V}_{DQ} = \mathbf{T}\,\mathbf{V}_{dq} \tag{4.23}$$

Substituting $\mathbf{I}_g$ and $\mathbf{V}_g$ in Equation (4.7) yields,

$$\begin{aligned} \mathbf{I}_g &= \mathbf{Y}_{gg}\mathbf{V}_g + \mathbf{Y}_{gl}\mathbf{V}_l \\ 0 &= \mathbf{Y}_{lg}\mathbf{V}_g + \mathbf{Y}_{ll}\mathbf{V}_l \end{aligned} \tag{4.24}$$

$$\begin{aligned} \mathbf{T}\mathbf{I}_{dq} &= \mathbf{Y}_{gg}\mathbf{T}\mathbf{E}_{dq} + \mathbf{Y}_{gl}\mathbf{V}_l \\ 0 &= \mathbf{Y}_{lg}\mathbf{T}\mathbf{E}_{dq} + \mathbf{Y}_{ll}\mathbf{V}_l \end{aligned} \tag{4.25}$$

Doing over some simplifications, a final definition is obtained as,

$$\mathbf{I}_{dq} = \mathbf{T}^{-1}\mathbf{Y}_{net}\mathbf{T}\mathbf{E}_{dq} \tag{4.26}$$

where,

$$\mathbf{Y}_{net} = \mathbf{Y}_{gg} - \mathbf{Y}_{gl}\mathbf{Y}_{ll}^{-1}\mathbf{Y}_{lg} \tag{4.27}$$

which in turn has the form,

$$Y_{net} = \begin{bmatrix} Y_{11}e^{j\theta_{11}} & Y_{12}e^{j\theta_{12}} & \cdots & Y_{1,ng}e^{j\theta_{1,ng}} \\ Y_{21}e^{j\theta_{21}} & Y_{22}e^{j\theta_{22}} & \cdots & Y_{2,ng}e^{j\theta_{2,ng}} \\ \vdots & \vdots & \ddots & \vdots \\ Y_{ng,1}e^{j\theta_{ng,1}} & Y_{ng,2}e^{j\theta_{ng,2}} & \cdots & Y_{ng,ng}e^{j\theta_{ng,ng}} \end{bmatrix} \tag{4.28}$$

It is possible to obtain an explicit solution for $\mathbf{I}_{dq}$, which represents the injection current in the same $dq0$ frame of reference. That means that both, transmission network and generators, are represented in the same framework just shifted by angle δ_i. According to Equations (4.19) and (4.28), the product $\mathbf{T}^{-1}\mathbf{Y}_{net}\mathbf{T}$ is given by,

$$\mathbf{T}^{-1}\mathbf{Y}_{net}\mathbf{T} = \begin{bmatrix} Y_{11}e^{j(\theta_{11})} & Y_{12}e^{j(\theta_{12}-\delta_{12})} & \cdots & Y_{1,ng}e^{j(\theta_{1,ng}-\delta_{1,ng})} \\ Y_{21}e^{j(\theta_{21}-\delta_{21})} & Y_{22}e^{j(\theta_{22})} & \cdots & Y_{2,ng}e^{j(\theta_{2,ng}-\delta_{2,ng})} \\ \vdots & \vdots & \ddots & \vdots \\ Y_{ng,1}e^{j(\theta_{ng,1}-\delta_{ng,1})} & Y_{ng,2}e^{j(\theta_{ng,2}-\delta_{ng,2})} & \cdots & Y_{ng,ng}e^{j(\theta_{ng,ng})} \end{bmatrix} \tag{4.29}$$

Simplifying and defining,

$$Y_{km}e^{j(\theta_{km}-\delta_{km})} = \left(G_{km}\cos\delta_{km} + B_{km}\sin\delta_{km}\right) + j\left(B_{km}\cos\delta_{km} - G_{km}\sin\delta_{km}\right) \tag{4.30}$$

as well as,

$$F_{G+B}\left(\delta_{km}\right) = G_{km}\cos\delta_{km} + B_{km}\sin\delta_{km} \tag{4.31}$$

$$F_{B-G}\left(\delta_{km}\right) = B_{km}\cos\delta_{km} - G_{km}\sin\delta_{km} \tag{4.32}$$

Consequently,

$$I_{dk} + jI_{qk} = \sum_{m=1}^{ng} Y_{km}\left(E'_{dm} + jE'_{qm}\right) \tag{4.33}$$

$$I_{dk} + jI_{qk} = \sum_{m=1}^{ng}\left(F_{G+B}\left(\delta_{km}\right)\right)E'_{dm} + j\left(F_{G+B}\left(\delta_{km}\right)\right)E'_{qm} + j\left(F_{B-G}\left(\delta_{km}\right)\right)E'_{qm} - \left(F_{B-G}\left(\delta_{km}\right)\right)E'_{qm} \tag{4.34}$$

$$I_{dk} = \sum_{m=1}^{ng}\left(F_{G+B}\left(\delta_{km}\right)\right)E'_{dm} - \left(F_{B-G}\left(\delta_{km}\right)\right)E'_{qm} \tag{4.35}$$

$$I_{qk} = \sum_{m=1}^{ng}\left(F_{G+B}\left(\delta_{km}\right)\right)E'_{qm} + \left(F_{B-G}\left(\delta_{km}\right)\right)E'_{dm} \tag{4.36}$$

The *dq0* currents expressed in matrix form, are obtained as,

$$\begin{bmatrix} I_{d1} \\ I_{d2} \\ \vdots \\ I_{d,ng} \end{bmatrix} = \begin{bmatrix} G_{11} & F_{G+B}\left(\delta_{12}\right) & \cdots & F_{G+B}\left(\delta_{1,ng}\right) \\ F_{G+B}\left(\delta_{21}\right) & G_{22} & \cdots & F_{G+B}\left(\delta_{2,ng}\right) \\ \vdots & \vdots & \ddots & \vdots \\ F_{G+B}\left(\delta_{ng,1}\right) & F_{G+B}\left(\delta_{ng,2}\right) & \cdots & G_{ng,ng} \end{bmatrix}\begin{bmatrix} E'_{d1} \\ E'_{d2} \\ \vdots \\ E'_{d\,ng} \end{bmatrix} - \begin{bmatrix} B_{11} & F_{B-G}\left(\delta_{12}\right) & \cdots & F_{B-G}\left(\delta_{1,ng}\right) \\ F_{B-G}\left(\delta_{21}\right) & B_{22} & \cdots & F_{B-G}\left(\delta_{2,ng}\right) \\ \vdots & \vdots & \ddots & \vdots \\ F_{B-G}\left(\delta_{ng,1}\right) & F_{B-G}\left(\delta_{ng,2}\right) & \cdots & B_{ng,ng} \end{bmatrix}\begin{bmatrix} E'_{q1} \\ E'_{q2} \\ \vdots \\ E'_{q\,ng} \end{bmatrix} \tag{4.37}$$

$$\begin{bmatrix} I_{q1} \\ I_{q2} \\ \vdots \\ I_{q,ng} \end{bmatrix} = \begin{bmatrix} G_{11} & F_{G+B}\left(\delta_{12}\right) & \cdots & F_{G+B}\left(\delta_{1,ng}\right) \\ F_{G+B}\left(\delta_{21}\right) & G_{22} & \cdots & F_{G+B}\left(\delta_{2,ng}\right) \\ \vdots & \vdots & \ddots & \vdots \\ F_{G+B}\left(\delta_{ng,1}\right) & F_{G+B}\left(\delta_{ng,2}\right) & \cdots & G_{ng,ng} \end{bmatrix}\begin{bmatrix} E'_{q1} \\ E'_{q2} \\ \vdots \\ E'_{q\,ng} \end{bmatrix} + \begin{bmatrix} B_{11} & F_{B-G}\left(\delta_{12}\right) & \cdots & F_{B-G}\left(\delta_{1,ng}\right) \\ F_{B-G}\left(\delta_{21}\right) & B_{22} & \cdots & F_{B-G}\left(\delta_{2,ng}\right) \\ \vdots & \vdots & \ddots & \vdots \\ F_{B-G}\left(\delta_{ng,1}\right) & F_{B-G}\left(\delta_{ng,2}\right) & \cdots & B_{ng,ng} \end{bmatrix}\begin{bmatrix} E'_{d1} \\ E'_{d2} \\ \vdots \\ E'_{d\,ng} \end{bmatrix} \tag{4.38}$$

4.4. INITIAL CONDITIONS CALCULATION FOR DYNAMIC ANALYSIS OF MULTIMACHINE SYSTEMS

Before proceeding with the dynamic analysis, the initial conditions for the state and algebraic variables are obtained carrying out the procedure proposed by [Sauer and Pai 1998]. The process is

based, at a first stage, on performing a power flow solution followed by an algebraic substitution procedure of differential equations valuated under steady state conditions (zero dynamics constraint).

Through this simple procedure, it is possible to determine the equilibrium point of the nonlinear power system dynamics, in such a way that it allows the evaluation of the linearized system of the nonlinear system. In power system dynamic analysis, the fixed points and initial conditions are normally obtained from a base case load flow solution. The values are computed for each generator state variables of the whole system.

The power flow equations are given by,

$$P_1 + jQ_1 = \sum_{k=1}^{n} V_1 V_k Y_{1k} e^{j(\theta_1 - \theta_k - \alpha_{1k})}$$

$$Q_i = \sum_{k=1}^{n} V_i V_k Y_{ik} \sin(\theta_i - \theta_k - \alpha_{ik}) \qquad \text{SLACK BUS} \qquad (4.39)$$

$$P_i = \sum_{k=1}^{n} V_i V_k Y_{ik} \cos(\theta_i - \theta_k - \alpha_{ik}) \qquad \text{PV BUSES} \qquad (4.40)$$

$$0 = -P_{Li} + \sum_{k=1}^{n} V_i V_k Y_{ik} \cos(\theta_i - \theta_k - \alpha_{ik})$$

$$0 = -Q_{Li} + \sum_{k=1}^{n} V_i V_k Y_{ik} \sin(\theta_i - \theta_k - \alpha_{ik}) \qquad \text{PQ BUSES} \qquad (4.41)$$

Remembering that the power system equilibrium values are obtained by numerically computing the nonlinear algebraic system, the magnitudes and angles of voltages for each busbar of the power system are determined. Thus, a step by step approach is followed for the calculation of the rest of variables of the power system dynamic model. The procedure is as follows,

- *Step 1*

Considering that $P_{Gi} = P_i - P_{Li}$ y $Q_{Gi} = Q_i - Q_{Li}$

$$I_{Gi} e^{j\gamma_i} = (P_i - P_{Li}) - j(Q_i - Q_{Li}) / V_i e^{-j\theta_i}$$

$$I_{Gi} e^{j\gamma_i} = (P_{Gi} - P_{Li}) / V_i^* \qquad (4.42)$$

Generator currents are set over the same network. They have the form,

$$I_{Gi} e^{j\gamma_i} = (I_{di} + jI_{qi}) e^{j(\delta - \pi/2)} \qquad (4.43)$$

Under steady state condition, all derivatives are zero valued. Therefore, it is possible to obtain an equivalent that represents both the state variables and network variables over the same equivalent circuit. This is based on,

$$T'_{q0i}\frac{dE'_{di}}{dt} = -E'_{di} + \left(x_{qi} - x'_{qi}\right) I_{qi} = 0 \tag{4.44}$$

Indeed,

$$E'_{di} = \left(x_{qi} - x'_{qi}\right) I_{qi} \tag{4.45}$$

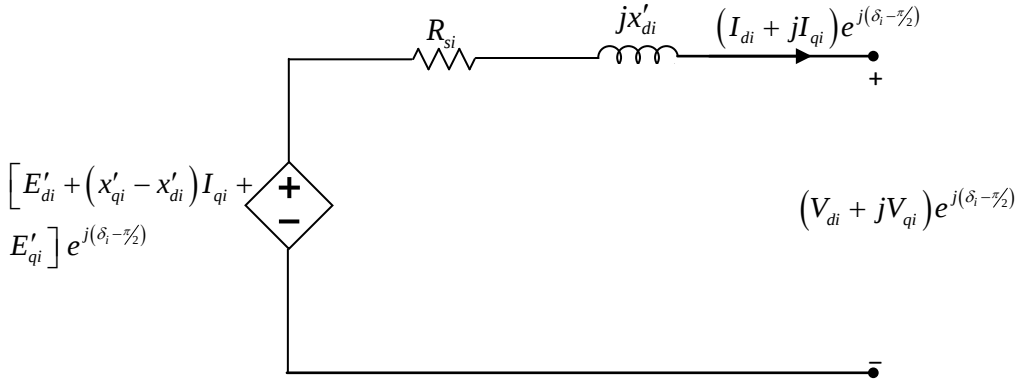

Figure 4.4 Generator Equivalent Circuit

Analyzing the equivalent circuit shown by Figure 4.4, an explicit equation for calculating voltage angle δ_i is found. Applying KVL,

$$0 = V_i e^{j\theta_i} + \left(R_{si} + jx'_{di}\right)\left(I_{di} + jI_{qi}\right)e^{j(\delta_i - \pi/2)} - \left[E'_{di} + \left(x'_{qi} - x'_{di}\right)I_{qi} + jE'_{qi}\right]e^{j(\delta_i - \pi/2)} \tag{4.46}$$

Substituting E'_{di} in Equation (4.46), results in,

$$0 = V_i e^{j\theta_i} + \left(R_{si} + jx'_{di}\right)\left(I_{di} + jI_{qi}\right)e^{j(\delta_i - \pi/2)} - \left[\left(x_{qi} - x'_{qi}\right)I_{qi} + \left(x'_{qi} - x'_{di}\right)I_{qi} + jE'_{qi}\right]e^{j(\delta_i - \pi/2)}$$

Rearranging some terms and additionally considering that $I_{Gi}\, e^{j\gamma_i} = \left(I_{di} + jI_{qi}\right) e^{j(\delta - \pi/2)}$, it yields

$$V_i\, e^{j\theta_i} + \left(R_{si} + jx_{qi}\right) I_{Gi}\, e^{j\gamma_i} = \left[\left(x_{qi} - x'_{di}\right) I_{di} + E'_{qi}\right] e^{j\delta_i} \tag{4.47}$$

with $i = 1, 2, \ldots, m$

The right hand side of Equation (4.47) represents the voltage behind the impedance $\left(R_{si} + jx_{qi}\right)$ and it has an angle δ_i. The voltage has a magnitude $\left[\left(x_{qi} - x'_{di}\right) I_{di} + E'_{qi}\right]$ and angle $\delta_i = angle\left[V_i\, e^{j\theta_i} + \left(R_{si} + jx_{qi}\right) I_{Gi}\, e^{j\gamma_i}\right]$ [Sauer and Pai 1998].

- *Step 2*

  Calculate δ_i from,

$$\delta_i = angle\left[V_i\, e^{j\theta_i} + \left(R_{si} + jx_{qi}\right) I_{Gi}\, e^{j\gamma_i}\right] \tag{4.48}$$

- *Step 3*

  Calculate $I_{di}, I_{qi}, V_{di}, V_{qi}$

$$\left(I_{di} + jI_{qi}\right) = I_{Gi} e^{j(\gamma_i - \delta_i + \pi/2)} \tag{4.49}$$

$$\left(V_{di} + jV_{qi}\right) = V_i e^{j(\theta_i - \delta_i + \pi/2)} \tag{4.50}$$

- *Step 4*

  Determine E'_{di} from,

$$E'_{di} = V_{di} + R_{si} I_{di} - x'_{qi} I_{qi} \tag{4.51}$$

  Also,

$$E'_{di} = \left(x_{qi} - x'_{qi}\right) I_{qi} \tag{4.52}$$

- *Step 5*

  Calculate E'_{qi}

$$E'_{qi} = V_{qi} + R_{si} I_{qi} + x'_{di} I_{di} \tag{4.53}$$

- *Step 6*

  Also, calculate E'_{fdi} from,

$$\frac{dE'_{qi}}{dt} = \frac{1}{T'_{d0i}}\left(E_{fdi} - \left(x_{di} - x'_{di}\right) I_{di} - E'_{qi}\right) = 0 \tag{4.54}$$

$$E_{fdi} = \left(x_{di} - x'_{di}\right) I_{di} + E'_{qi} \tag{4.55}$$

- *Step 7*

  With E'_{fdi} earlier known, obtain $V_{ref\,i}$ from (4.5),

$$\frac{dE_{fdi}}{dt} = \frac{1}{T_{exci}}\left(-E_{fdi} + K_{exci}\left(V_{ref\,i} - V_{texci}\right)\right) = 0 \tag{4.56}$$

$$E_{fd\,i} = K_{exci}\left(V_{ref\,i} - V_{texci}\right) \tag{4.57}$$

  Hence,

$$V_{ref\,i} = V_{texci} + \frac{E_{fdi}}{K_{exci}} \tag{4.58}$$

  Finally, from the swing equation,

$$\frac{d\delta_i}{dt} = \omega - \omega_0 = 0 \tag{4.59}$$

$$\frac{d\omega_i}{dt} = \frac{1}{M_i}\left(P_{mi} - \left(E'_{di} I_{di} + E'_{qi} I_{qi}\right) - D_i \omega_i\right) = 0 \tag{4.60}$$

And, with this, it is obtained,

$$\omega = \omega_0 \qquad \text{(Depends on system reference)} \tag{4.61}$$

$$P_{mi} = \left(E'_{di} I_{di} + E'_{qi} I_{qi} \right) + D_i \omega_i \tag{4.62}$$

4.5. APPLICATION EXAMPLE. 9 BUSES, 3 GENERATORS TEST POWER SYSTEM

The procedure described along this Chapter is carried out to exemplify its application to the test power system of 3 synchronous machine, 9 buses [Anderson and Fouad 2003] which it will be experimented in the cases studies of Chapters 5 and 6. The parameters of this system are shown in Appendix C.

The example tried to follow numerically almost every calculation needed before executing the dynamic process of the multimachine power system, that are the initial conditions of the nonlinear system.

The numerical calculations are detailed in Appendix D following the procedure previously described along this Chapter.

4.6. DISCUSSION

This Chapter has described in detail the modeling of the multimachine power systems, to be applied in nonlinear oscillation studies. Although there are other different forms of modeling the same system, the approach followed here represents an alternative of wide application even when some other components of the power system (such as time variant loads, FACTS devices, etc.) are included in the model.

It is important to mention that the requirements of detailed modeling in some cases have to be extended, thus resulting necessary to incorporate the model of global elements around the generators (PSS, AVR, turbine-governors models, etc.) or some other components (transformers, transmission lines, etc.) resulting in an increment on complexity of the power system modeling that allows a more rigorous study.

In the same form, the approach before described is centered on the dynamic analysis of the synchronous machine and power network considering their nonlinear characteristics. Thus, the main goal is to apply the modal series approach to the multimachine modeling, resulting necessary the linearization of the power system model in order to take the properties of the linear and nonlinear contributions to the system behavior.

Also important to mention to the reader is the reason for the inclusion of this chapter. Even when the procedure followed before the application of a dynamic study is based on systematic and somehow trivial procedure, it is sometimes critical the time spent for these calculations. Hence, the chapter tries to clarify each step followed before starting the transient or dynamic study; the numerical tables can be easily reproduced by other author.

5

FORCED OSCILLATIONS FROM THE MODAL SERIES METHOD

A systematic procedure to consider higher order terms of the linearized dynamic system applying the modal series method is described. This addition represents one of the main contributions of this thesis. Also, an extension that incorporates the concept of nonlinear transfer function is described representing the basis of future research work to be developed in further contributions.

5.1 INTRODUCTION

The modal series method detailed in chapters 2 and 3 is based on the closed form solution of a homogeneous nonlinear dynamic system; the forced contribution is not considered so far. Nevertheless, it is possible to assume an arbitrary input signal to the dynamic system following the same systematic procedure, thus obtaining a closed form solution that incorporates control variables.

Why is it important to consider the control variables in the dynamic behavior of a nonlinear system? This is a question that can be answered mainly over the extensive work developed to analyze controlled systems in many areas, including power systems. However, with respect to the nonlinear power system modeling, it has been detected a lack of work in this field, focused only in the analysis of linear contributions. This chapter will try to introduce an application of the multidimensional Laplace transform described above, which expresses the contribution of both linear and nonlinear terms through Laplace domain kernels, thus leading in a direct way to the inclusion of higher order terms, following the same rules of a linear transfer functions. Also, taking advantage of the residue theorems, multidimensional Laplace kernels are expressed in the form of a partial fraction expansions, where their residues are directly available. This affirmation will be extended along this chapter.

5.2 MODAL SERIES BACKGROUNG

The equations of motion are assumed to be of the form

$$\dot{x} = f\left(x,u\right) \tag{5.1}$$

where $x \in \Re^n$ is the state vector and $u \in \Re^m$ is the control vector. The vector function $f(x,u)$ and its partial derivatives with respect to *x* and *u* are assumed to be continuously differentiable functions of *x* and *u*.

To solve this model approximately, we expand (5.1) into a finite Taylor series as

$$\dot{\mathbf{x}} = \mathbf{A}\mathbf{x} + \frac{1}{2}\mathbf{x}^{\mathbf{T}}\mathbf{H}^{\mathbf{i}}\mathbf{x} + O\left(|\mathbf{x}|^{\mathbf{3}}\right) + \mathbf{B}\mathbf{u} \tag{5.2}$$

where, **A** and **H** are defined as in (3.3) and $\mathbf{B} = \left(\partial G / \partial u\right)$

Equation (5.2) in its Jordan canonical form and considering the third order terms as well, can be written as

$$\dot{y}_j = \lambda_j y_j + \sum_{k=1}^{n}\sum_{l=1}^{n} C_{kl} y_k y_l + \sum_{p=1}^{n}\sum_{q=1}^{n}\sum_{r=1}^{n} D^j_{pqr} y_p y_q y_r + \ldots + \sum_{i=1}^{r} \hat{b}_{ji} u_i \qquad j = 1, \ldots, n \tag{5.3}$$

The last term of Equation (5.3) associated to r represents the control variables. This term is reduced to $\hat{b}_{ji} u_i$ when a single input-single output (SISO) system is under study; on the other side, the term is the summatory assuming a multiple input-multiple output (MIMO) system of number r. Thus, (5.3) is written for the general case.

The case of forced system response is represented manipulating and solving Equation (5.3) in the same form as the unforced case obtained in Chapter 3.

5.3 FORCED OSCILLATIONS

The above approach can be easily generalized to the case of forced oscillations resulting from arbitrary excitations. Agreeing with the procedure detailed in Section 3.3, considering the system (3.10)-(3.12), assuming a single input-single output system, and following a line of reasoning similar to the unforced case, we have

$$\dot{y}_j = \lambda_j y_j + \hat{b}_j u_j \tag{5.4}$$

$$\dot{y}^2_j = \lambda_j y^2_j + \sum_{k=1}^{n}\sum_{l=1}^{n} C^j_{kl} y^1_k y^1_l \tag{5.5}$$

$$\dot{y}^3_j = \lambda_j y^3_j + \sum_{k=1}^{n}\sum_{l=1}^{n} C^j_{kl}\left[y^2_k y_l + y_k y^2_l\right] + \sum_{p=1}^{n}\sum_{q=1}^{n}\sum_{r=1}^{n} D^j_{pqr} y^1_p y^1_q y^1_r \tag{5.6}$$

$$\vdots$$

from which it follows that

$$Y_j(s) = \frac{\hat{b}_j}{s - \lambda_j} U(s) - \frac{Y_j(0)}{s - \lambda_j} \tag{5.7}$$

$$Y_j^2(s_1,s_2)=\sum_{k=1}^{n}\sum_{l=1}^{n}\frac{1}{(s_1+s_2-\lambda_j)}C_{kl}^{j}Y_k^1(s_1)Y_l^1(s_2) \tag{5.8}$$

where

$$Y_k^1(s_1)=\frac{\hat{b}_k}{s_1-\lambda_k}U(s_1)-\frac{Y_k^1(0)}{s_1-\lambda_k} \tag{5.9}$$

$$Y_l^1(s_2)=\frac{\hat{b}_l}{s_2-\lambda_l}U(s_2)-\frac{Y_l^1(0)}{s_2-\lambda_l} \tag{5.10}$$

To illustrate the proposed method, consider the case of an impulse function. If $u_j(t)$ is an impulse function, then,

$$u_j(t)=\delta(t) \tag{5.11}$$

$$U_j(s)=1 \tag{5.12}$$

Transforming to Laplace domain the Jordan system including the input function, it is obtained,

$$sY_j(s)=\lambda_j Y_j(s)+\hat{b}_j U(s)-Y_j(0)$$

$$Y_j(s)(s-\lambda_j)=\hat{b}_j U(s)-Y_j(0)$$

$$Y_j(s)=\frac{\hat{b}_j}{(s-\lambda_j)}U(s)-\frac{Y_j(0)}{(s-\lambda_j)} \tag{5.13}$$

Since $U(s)$ is an impulse function,

$$Y_j(s)=\frac{\hat{b}_j}{(s-\lambda_j)}-\frac{Y_j(0)}{(s-\lambda_j)} \tag{5.14}$$

Applying inverse Laplace Transform, it yields,

$$y_j(t)=\left(\hat{b}_j-y_j(0)\right)e^{\lambda_j t} \tag{5.15}$$

which represents the time domain solution of the first order terms in the Jordan system.

In a similar manner, the second-order terms are given by

$$Y_j^2(s_1,s_2)=\sum_{k=1}^{n}\sum_{l=1}^{n}\frac{1}{(s_1+s_2-\lambda_j)}C_{kl}^{j}Y_k^1(s_1)Y_l^1(s_2)$$

with,

$$Y_k^1(s_1)=\frac{\hat{b}_k}{(s_1-\lambda_k)}-\frac{Y_k^1(0)}{(s_1-\lambda_k)} \tag{5.16}$$

$$Y_l^1(s_2)=\frac{\hat{b}_l}{(s_2-\lambda_l)}-\frac{Y_l^1(0)}{(s_2-\lambda_l)} \tag{5.17}$$

Rearranging some terms,

$$Y_j^2(s_1,s_2)=\sum_{k=1}^{n}\sum_{l=1}^{n}C_{kl}^j\left\{\frac{1}{(s_1+s_2-\lambda_j)}\frac{1}{(s_1-\lambda_k)(s_2-\lambda_l)}\left[\hat{b}_k\hat{b}_l-\hat{b}_kY_l^1(0)-\hat{b}_lY_k^1(0)-Y_k^1(0)Y_l^1(0)\right]\right\} \tag{5.18}$$

Considering,

$$N_2(s_1,s_2)=\frac{1}{(s_1+s_2-\lambda_j)}\frac{1}{(s_1-\lambda_k)(s_2-\lambda_l)} \tag{5.19}$$

and using Theorem 1 from Appendix A to convert $N_2(s_1,s_2)$ into $N_2(s)$ it yields,

$$N_2(s)=\frac{(s_1-\lambda_k)(s_2-\lambda_l)N_2(s_1,s_2)\big|_{\substack{s_1=\lambda_k\\s_2=\lambda_l}}}{(s-\lambda_k-\lambda_l)}+\frac{(s_1+s_2-\lambda_j)(s_2-\lambda_l)N_2(s_1,s_2)\big|_{\substack{s_1=-\lambda_l+\lambda_j\\s_2=\lambda_l}}}{(s-\lambda_j)} \tag{5.20}$$

Therefore,

$$N_2(s)=\frac{1}{(\lambda_k+\lambda_l-\lambda_j)}\left[\frac{1}{(s-\lambda_k-\lambda_l)}-\frac{1}{(s-\lambda_j)}\right] \tag{5.21}$$

Having obtained the coefficients, the second order terms can be written in the form

$$\begin{aligned}Y_j^2(s_1,s_2)=\sum_{k=1}^{n}\sum_{l=1}^{n}\Bigg\{&C_{kl}^j\frac{1}{(\lambda_k+\lambda_l-\lambda_j)}\left[\hat{b}_k\hat{b}_l-\hat{b}_kY_l^1(0)-\hat{b}_lY_k^1(0)-Y_k^1(0)Y_l^1(0)\right]\\&\left[\frac{1}{(s-\lambda_k-\lambda_l)}-\frac{1}{(s-\lambda_j)}\right]\Bigg\}\end{aligned} \tag{5.22}$$

The time domain solution obtained by inverse Laplace Transform applied to the second order terms is,

$$\begin{aligned}y_j^2(t)=\sum_{k=1}^{n}\sum_{l=1}^{n}\Bigg\{&C_{kl}^j\frac{1}{(\lambda_k+\lambda_l-\lambda_j)}\left[\hat{b}_k\hat{b}_l-\hat{b}_kY_l^1(0)-\hat{b}_lY_k^1(0)-Y_k^1(0)Y_l^1(0)\right]\\&\left[e^{(\lambda_k+\lambda_l)t}-e^{(\lambda_j)t}\right]\Bigg\}\end{aligned} \tag{5.23}$$

It can be observed that Equation (5.23) expresses the closed form time domain solution of the second order nonlinear term, when an impulse function is applied to the dynamic system. In the following sections, the dependence of modal combination in this solution will be detailed. Thinking in a short analysis of the given solution, it is evident its dependence to the resonant condition, mostly due to the eigenvalues combination; also, there is a combination of modal solution and a dependence on the initial conditions. Finally, the solution of (5.1) for the case of an impulse function can be expressed as,

$$y_j(t) = \left[\hat{b}_j - y_j(0)\right] e^{\lambda_j t} + \sum_{k=1}^{n}\sum_{l=1}^{n}\left\{ C_{kl}^{j} \frac{1}{\left(\lambda_k + \lambda_l - \lambda_j\right)} \left[\hat{b}_k\hat{b}_l - \hat{b}_k Y_l^1(0) - \hat{b}_l Y_k^1(0) - Y_k^1(0) Y_l^1(0)\right] \left[e^{(\lambda_k+\lambda_l)t} - e^{(\lambda_j)t}\right]\right\} \tag{5.24}$$

and

$$x_i(t) = \sum_{j=1}^{n}\left(u_{ij}\left[b_j - y_j^1(0)\right] - \sum_{k=1}^{n}\sum_{l=1}^{n} u_{ij} h_{2kl}^{j} \left[\hat{b}_k\hat{b}_l - \hat{b}_k Y_l^1(0) - \hat{b}_l Y_k^1(0) - Y_k^1(0) Y_l^1(0)\right]\right) e^{\lambda_j t} + \sum_{j=1}^{n}\sum_{k=1}^{n}\sum_{l=1}^{n}\left(u_{ij} h_{2kl}^{j} \left[\hat{b}_k\hat{b}_l - \hat{b}_k Y_l^1(0) - \hat{b}_l Y_k^1(0) - Y_k^1(0) Y_l^1(0)\right] e^{(\lambda_k+\lambda_l)t}\right) \tag{5.25}$$

with $i = 1, \ldots, n$

5.4 SYNTHETIC EXAMPLE

To illustrate the application of the method, let us assume a synthetic example taken from [Zhu *et al.* 1995]. A first order nonlinear differential equation of the form,

$$\tau\dot{y} + y + \beta y^3 = u(t) \tag{5.26}$$

is solved when the input function $u(t)$ is an impulse function, as a first step, and afterwards, a step function is also studied; both using the modal series method.

The differential equation has first and third order elements, which are considered in the final solution. Thus, assuming an impulse function, the equation takes the form,

$$\dot{y} = -\frac{1}{\tau}y - \frac{\beta}{\tau}y^3 + \frac{1}{\tau}F \tag{5.27}$$

Being,

$$\lambda = -\frac{1}{\tau} \text{ (eigenvalue)}$$

$$C = 0$$

$$D = \frac{\beta}{\tau}$$

$$u(t) = \frac{1}{\tau}F\delta(t)$$

with,

$$b = \frac{F}{\tau}$$

The first order term is calculated as,

$$y^1(s) = \frac{b}{s-\lambda}U(s) - \frac{y(0)}{s-\lambda} \tag{5.28}$$

with $y(0)=0$

$$y^1(s)=\frac{F}{\tau}\frac{1}{(s-\lambda)} \tag{5.29}$$

Applying inverse Laplace transform,

$$y(t)=\frac{F}{\tau}e^{-t/\tau} \tag{5.30}$$

This system does not particularly have second order terms. Hence, the third order terms are expressed by,

$$y^3(s_1,s_2,s_3)=\frac{1}{(s_1+s_2+s_3-\lambda)}\left[D\left(y^1(s_1)y^1(s_2)y^1(s_3)\right)\right] \tag{5.31}$$

where,

$$y^1(s_j)=\frac{b}{s_j-\lambda} \qquad\qquad j=1,2,3 \tag{5.32}$$

Substituting the first order terms into the third order expression (5.31), yields,

$$y^3(s_1,s_2,s_3)=\frac{1}{(s_1+s_2+s_3-\lambda)}\left[Db^3\frac{1}{(s_1-\lambda)}\frac{1}{(s_2-\lambda)}\frac{1}{(s_3-\lambda)}\right] \tag{5.33}$$

Applying the Theorem 2 given in Appendix A, the equation (5.33) is associated to the single variable equation with the form,

$$y^3(s)=-\frac{1}{2\lambda}\frac{1}{(s-\lambda)}+\frac{1}{2\lambda}\frac{1}{(s-3\lambda)} \tag{5.34}$$

The full solution to the differential equation (5.26) for an input impulse function has the form,

$$y(t)=\frac{F}{\tau}e^{-t/\tau}-\frac{\beta F^3}{2\tau^3}\left(e^{-t/\tau}-e^{-3t/\tau}\right)+\ldots \tag{5.35}$$

The time domain solution expressed in the Equation (5.35) is similar to that described in [Zhu *et al*. 1995] for the same conditions. This sample has demonstrated the viability of the extension of the modal series method to the inclusion of a forced input signal.

Similarly to the previous case, a step input function is analyzed now for the same nonlinear differential equation. This differential equation takes a similar form to (5.26); however, the first order terms, which include the step function have the form,

$$y^1(s_1)=\frac{F}{\tau}\frac{1}{(s_1-\lambda)}\frac{1}{s_1} \tag{5.36}$$

with $y(0)=0$

Therefore,

$$y^1(s) = -F\frac{1}{(s-\lambda)} + F\frac{1}{s} \tag{5.37}$$

Executing the inverse Laplace transform,

$$y^1(t) = F\left(1 - e^{-t/\tau}\right) \tag{5.38}$$

The third order terms are those of (5.31), but for the step function take the form,

$$y^3(s_1, s_2, s_3) = \frac{1}{(s_1 + s_2 + s_3 - \lambda)}\left[Db^3 \frac{1}{(s_1 - \lambda)s_1(s_2 - \lambda)s_2(s_3 - \lambda)s_3} \right] \tag{5.39}$$

This equation may be solved using the theorems of association of variables on multidimensional Laplace transform, described in [Chen and Chiu 1973]

- *Real Convolution Theorem*

If a given function $F(s_1, s_2, \ldots, s_n)$ has the following structure:

$$F(s_1, s_2, \ldots, s_n) = H(s_1 + s_2 + \ldots + s_n)F(s_1, s_2, \ldots, s_n)$$

and

$$F_1(s_1, s_2, \ldots, s_n) \xrightarrow{A_n} G_1(s)$$

the real convolution theorem states that

$$F(s_1, s_2, \ldots, s_n) \xrightarrow{A_n} G(s) = H(s)G_1(s)$$

Then, with

$$H(s_1, s_2, s_3) = \frac{1}{s_1 + s_2 + s_3 + a}$$

$$F_1(s_1, s_2, s_3) = \left[Db^3 \frac{1}{(s_1 - \lambda)s_1(s_2 - \lambda)s_2(s_3 - \lambda)s_3} \right]$$

From [Chen and Chiu 1973] a kernel of the form,

$$\frac{K}{\prod_{i=1}^{3}(s_i + a)(s_i + b)}$$

is *associated* into,

$$\frac{K}{(a-b)^3}\left(\frac{1}{s+3b} - \frac{1}{s+2a+b} + \frac{1}{s+a+2b} - \frac{1}{s+3a} \right)$$

Therefore,

$$F_1(s_1,s_2,s_3) \xrightarrow{A_2} G_1(s) = Db^3 \frac{1}{(-\lambda)^3}\left(\frac{1}{s} - \frac{3}{s-2\lambda} + \frac{3}{s-\lambda} - \frac{1}{s-3\lambda}\right)$$

and

$$F(s_1,s_2,s_3) = Db^3 \frac{1}{(-\lambda)^3}\frac{1}{s-\lambda}\left(\frac{1}{s} - \frac{3}{s-2\lambda} + \frac{3}{s-\lambda} - \frac{1}{s-3\lambda}\right)$$

Finally the third order terms in the time domain solution have the form,

$$y^3(t) = -F^3\beta\left[1-\left(\frac{5}{2}-\frac{3}{\tau}t\right)e^{-t/\tau} + 3e^{-2t/\tau} + \frac{1}{2}e^{-3t/\tau}\right]$$

with the full solution,

$$y(t) = y^1(t) + y^3(t) + \ldots$$

$$y(t) = F\left(1-e^{-t/\tau}\right) - F^3\beta\left[1-\left(\frac{5}{2}-\frac{3}{\tau}t\right)e^{-t/\tau} + 3e^{-2t/\tau} + \frac{1}{2}e^{-3t/\tau}\right] + \ldots \quad (5.40)$$

(5.40) agrees with that obtained in [Zhu *et al.* 1995] for the case of a step input signal. The analytical example has demonstrated the application of modal series which is based on multidimensional Laplace compared to the solution obtained by a different technique such as the Laplace-Borel transform.

5.5 THE TRANSFER FUNCTION IN NONLINEAR SYSTEMS

5.5.1 Introduction

The transfer function concept has been deeply analyzed as a powerful tool for either time or time varying linear systems with solid applications to control systems. The concept of transfer function itself attends the behavior between inputs and outputs of the dynamic system.

With respect to the application of transfer function concepts to power systems, it may be observed the following [Smith *et al.* 1993]:

- The order of any transfer function is as large as the number of state variables included in the model
- Most of poles or eigenvalues of the transfer function cannot be observed from any signal in the system; therefore, it is possible to identify the effective transfer function between two points in the system.
- An input signal applied to a power system will usually excite many modes which will be reflected in different output signals and locations in the system.
- It is important to point out that a transfer function is usually written as a ratio of polynomials; nevertheless it can be also expressed as a sum of residues over a first order pole.

- *Transfer function analysis assumes that initial condition effects have died away and that the output is a function of the input only.*

Several applications and definitions have been introduced into the analysis of power systems based on issues associated to the transfer functions. One important concept quite addressed by some authors is the computation of dominant poles of power system transfer functions. The concept arises over the consideration of a transfer function in which the poles and zeros are known. So, it is of concern to determine the main modes that are taking part in the frequency response to the oscillations in the power system. An algorithm based on Rayleigh iterations has been proposed, which exploits its characteristics of numerical properties of global cubic convergence [Martins *et al.* 1996]. The participation factors and the applications of such algorithm are remarked when a large scale power system is studied. An earlier work proposed the use of Prony analysis to determine the residues and with them, to obtain the transfer functions for the design of PSS applied to a multimachine power system [Trudnowski *et al*. 1991]. In this work the usefulness of transfer function concept arises in its determination of frequencies presented during oscillations in the power system and eventually damped by PSS design.

5.5.2 Theoretical Basis of Nonlinear Transfer Function

Transfer functions of nonlinear systems satisfy many properties that are expected from transfer functions [Halás *et al.* 2008]; *i.e.*

- They characterize a nonlinear system uniquely. This means that each nonlinear system has a unique transfer function, no matter what state space realization one starts with.
- They provide an input-output description of the nonlinear system.
- They allow the use of transfer function algebra, to combine systems in series, parallel or feedback connection.

Assuming a transfer function defined for a linear system, we have,

$$G(s) = \frac{Y(s)}{U(s)} \tag{5.41}$$

The time response of $Y(s)$ to an impulse disturbance applied in the input function U is equal to the inverse Laplace transform of $G(s)$ considering zero initial conditions in all system states [Gomes Jr. *et al.* 2000]. Thus,

$$y = \sum_i R_i e^{\lambda_i t} \tag{5.42}$$

where,

λ_i are the poles of $G(s)$

R_i the associated residues

The time response of $G(s)$ can be directly obtained by integrating in the time domain the impulse response of $G(s)$, that is,

$$y = \sum_i \frac{R_i}{\lambda_i}\left(e^{\lambda_i t} - 1\right) \tag{5.43}$$

This case is very illustrative since the time response contains two parts due to the generic disturbance [Rugh 1981]:

- The first part is called forced response which consists of the steady state part.
- The second one, so called natural response, consists of the transient part which is formed by a sum of exponentials, whose values depend on the applied disturbance.

The natural characteristic response depends on the location of the system poles in the complex plane [Gomes Jr. *et al.* 2000]. Therefore, it is important to point out that modal analysis consists on the computation of these poles and on the determination of their nature and sensitivities [Martins *et al.* 1996].

For instance, the transfer function of a single input-single output (SISO) system has the form [Rommes and Martins 2006],

$$\begin{aligned} \dot{z}(t) &= \mathbf{A}z(t) + \mathbf{B}u(t) \\ y(t) &= \mathbf{C}^T z(t) + \mathbf{D}u(t) \end{aligned} \tag{5.44}$$

whose transfer function is,

$$H(s) = \mathbf{C}^T \left(s\mathbf{I} - \mathbf{A}\right)^{-1} \mathbf{B} + \mathbf{D} \tag{5.45}$$

Being the eigenvalues the poles of *A* and the corresponding right and left eigenvectors given by $\left(\lambda_j, \mathbf{x}_j, \mathbf{v}_j\right)$, the transfer function can be expressed as a sum of residues R_j over first order poles, that is,

$$H(s) = \sum_{j=1}^{n} \frac{R_j}{s - \lambda_j} \tag{5.46}$$

where the residues R_j are,

$$R_j = \left(\mathbf{x}_j^T \mathbf{C}\right)\left(v_j^* \mathbf{B}\right) \tag{5.47}$$

A pole λ_j that corresponds to a residue R_j with large $\left|R_j\right| / \mathrm{Re}\left(\lambda_j\right)$ is called a dominant pole, which is observable and controllable in the transfer function [Rommes and Martins 2006]. Several efforts oriented to research the dominant poles in large power systems have been focused over the

transfer function concepts. Almost every approach developed is based on numerical algorithms that allow the determination of poles that have the biggest participation in power systems oscillations [Martins *et al.* 1996], [Martins and Quintao 2003], [Rommes and Martins 2006], [Rommes and Martins 2006a], [Gomes Jr. *et al.* 2009]. Their extension to frequency analysis is straightforward, since functional kernels expressed in Laplace domain are easily swifted to frequency domain. Both SISO and MIMO systems are described by each contribution following the properties of linear transfer functions. More recently, dominant zeros in computation of feedback transfer functions have been considered as well [Martins *et al.* 2007].

The calculation of dominant poles will not be addressed in this thesis. For now, only the theoretical basis of nonlinear transfer function is of concern, leaving for future developments this research topic.

5.5.3 Volterra Functional Expansion

The input-output behavior of a dynamic system of the form,

$$\begin{aligned} \dot{\mathbf{x}} &= \mathbf{A}\mathbf{x} + \mathbf{B}\mathbf{u} \\ \mathbf{y} &= \mathbf{C}\mathbf{x} \end{aligned} \tag{5.48}$$

may be represented by means of a generalized convolution integrals series [Isidori 1989]. A general convolution integral of order k is defined as follows: let $(i_k,\ldots,i_1)$ be a multiindex of length k with $i_k,\ldots,i_1$ of the set $\{1,\ldots,m\}$ and if $u_1,\ldots,u_m$ are real valued continuous functions defined on $[0,T]$; the generalized convolutions integral with kernel $\omega_{i_k,\ldots,i_1}$ is defined as [Isidori 1989],

$$\int_0^t \int_0^{\tau_k} \cdots \int_0^{\tau_2} \omega_{i_k,\ldots,i_1}(t,\tau_k,\ldots,\tau_1)\ldots u_{i_1}(\tau_1)\,d\tau_1\ldots d\tau_k \tag{5.49}$$

for $0 \le t \le T$

After some manipulations, it can be demonstrated that the series written as,

$$y(t) = \omega_0(t) + \sum_{k=1}^{\infty} \sum_{i_1,\ldots i_k=1}^{m} \int_0^t \int_0^{\tau_k} \cdots \int_0^{\tau_2} \omega_{i_k,\ldots,i_1}(t,\tau_k,\ldots,\tau_1) u_{i_k}(\tau_k)\ldots u_{i_1}(\tau_1)\,d\tau_1\ldots d\tau_k \tag{5.50}$$

is absolutely and uniformly convergent, and is called a *Volterra series expansion* [Isidori 1989], [Schetzen 1980].

The original application of the Volterra functional to the analysis of nonlinear circuits is due to Wiener [Bussgang *et al.* 1974]. Wiener established that an output function $y(t)$ of a nonlinear system is some functional of its input $u(t)$ and that the two functions can be related by a functional series. The first few terms (up to order three) of the functional expansion are,

$$y(t)=\int_{-\infty}^{\infty}h_1(\tau)u(t-\tau)d\tau+\int_{-\infty}^{\infty}\int_{-\infty}^{\infty}h_2(\tau_1,\tau_2)u(t-\tau_1)u(t-\tau_2)d\tau_1 d\tau_2 + \int_{-\infty}^{\infty}\int_{-\infty}^{\infty}\int_{-\infty}^{\infty}h_3(\tau_1,\tau_2,\tau_3)u(t-\tau_1)u(t-\tau_2)u(t-\tau_3)d\tau_1 d\tau_2 d\tau_3+\ldots \quad (5.51)$$

The n^{th} order kernel of (5.51) $h_n(\tau_1,\tau_2,\ldots,\tau_n)$ can be called a nonlinear impulse response of order *n* [Bussgang *et al.* 1974].

Its Fourier transform can be called the nonlinear transfer function of order n. Hence considering the input-output relation (5.51) and writing in the form

$$y(t)=\sum_{i=1}^{\infty}y_i(t)$$

in which,

$$y_n(t)=\int_{-\infty}^{\infty}\cdots\int_{-\infty}^{\infty}h_n(\tau_1,\ldots,\tau_n)u(t-\tau_1)\ldots u(t-\tau_n)d\tau_1\ldots d\tau_n \quad (5.52)$$

is the output component of order *n* [Bussgang *et al.* 1974].

Therefore, Equation (5.51) can be rewritten as [George 1959],

$$y=H_1[u]+H_2[u]+\ldots+H_n[u] \quad (5.53)$$

That is, the system H has been broken into a parallel combination of systems H_i as shown in Figure 5.1. The interpretation of such Figure can be resumed as [George 1959],

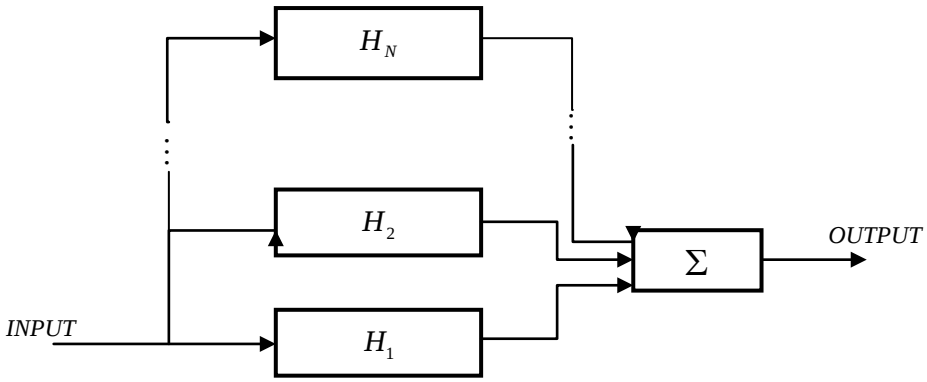

Figure 5.1 Block diagram for the generalized functional representation

- The generalized functional representation shows a nonlinear system as a parallel bank of systems H_i that are n^{th} order nonlinear systems.
- They have an impulse-response function $h_n(t_1,\ldots,t_n)$ associated with them.

Following the same reasoning, a nonlinear system of the form,

$$f\left(y(t),\dot{y}(t),\ddot{y}(t),\ldots\right)=x(t) \tag{5.54}$$

can be splitted-up into a sequence of components connected in parallel by the method of Volterra functional expansion [Schetzen 1980]. The process is illustrated by Figure 5.2. For this case, the first component is linear [Karmakar 1979], that is,

$$f_1(t)=\int h_1(\tau_1)\,x(t-\tau_1)\,d\tau_1 \tag{5.55}$$

Here, the procedure based on multidimensional Laplace transform described in Chapter 3, Section 3.3.2 can be used. In this way the linear case can be transformed as,

$$F_1(s)=H_1(s)U(s) \tag{5.56}$$

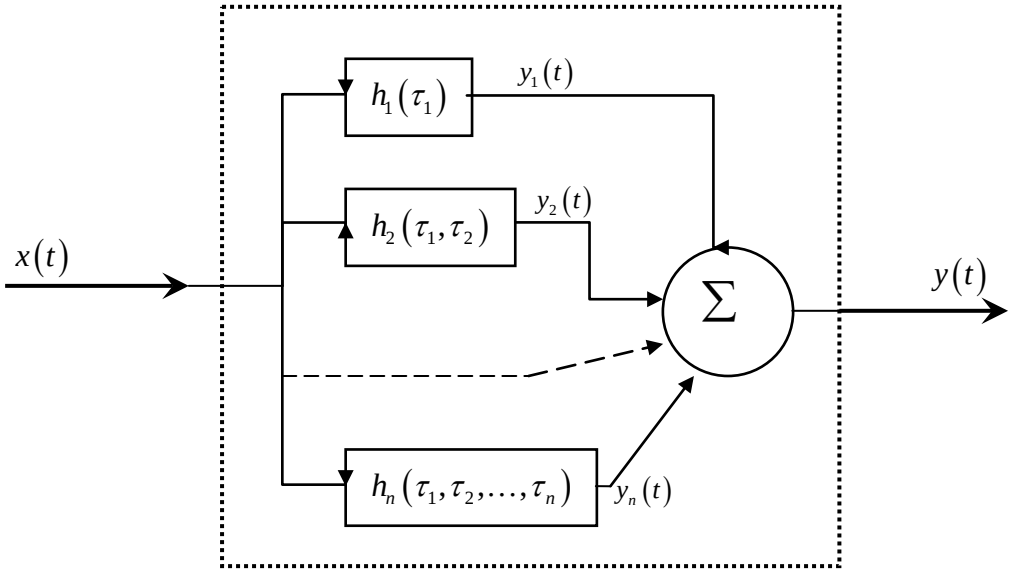

Figure 5.2. Functional expansion of the nonlinear system represented by (5.54)

The second component is of quadratic nature, *i.e.*

$$f_2(t)=\int\int h_2(\tau_1,\tau_2)\,x(t-\tau_1)\,x(t-\tau_2)\,d\tau_1 d\tau_2 \tag{5.57}$$

In order to use the theory of multidimensional Laplace transform, it is necessary to artificially introduce t_1 and t_2, *i.e.*

$$f_2(t)=\int\int h_2(\tau_1,\tau_2)\,x(t_1-\tau_1)\,x(t_2-\tau_2)\,d\tau_1 d\tau_2$$

and then,

$$F_2(s_1,s_2)=H_2(s_1,s_2)U(s_1)U(s_2) \tag{5.58}$$

Formally, at least $F_2(s_1,s_2)$ can be inverted to obtain $f_2(t_1,t_2)$ for which $f_2(t)$ is the desired output [George 1959]. Graphically, this can be illustrated in Figure 5.3. $f_2(t_1,t_2)$ can be plotted by contours on the (t_1,t_2) plane but we are interested only in the 45° line where $t_1 = t_2 = t$.

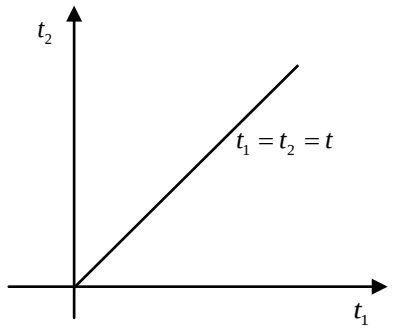

Figure 5.3. (t_1,t_2) plane for the case of $t_1 = t_2$ line

The method generalizes to higher order cases, hence the third is a cubic component; its output is,

$$f_3(t) = \int\int\int h_3(\tau_1,\tau_2,\tau_3)\,x(t-\tau_1)\,x(t-\tau_2)\,x(t-\tau_3)\,d\tau_1 d\tau_2 d\tau_3 \tag{5.59}$$

which in Laplace transform domain is,

$$F_3(s_1,s_2,s_3) = H_2(s_1,s_2,s_3)U(s_1)U(s_2)U(s_3) \tag{5.60}$$

The procedure of taking a number of variables $t_1,t_2,\ldots,t_n$ as equal is called *association of variables*, as it was described in Chapter 3.

The great value of making the associations in the transform domain lies on the fact that these associations can be made by inspection; being this application a class of problem adapted to this theory. Hence, the total system output is given by,

$$y(t) = \sum_{i=1}^{n} f_i(t) \tag{5.61}$$

assuming a finite number of terms represented as an n^{th} order nonlinear approximation. It is to be pointed out that terms associated to Volterra representation are denominated impulse response Volterra kernels [Rugh 1981]. Such kernels can be compared with those obtained by the modal series method in Equations (5.14) and (5.22).

Following the same reasoning, it is possible to represent a forced nonlinear system decomposed by the modal series method, in the same way as the Volterra framework. By comparing each kernel, similarities from a qualitative point of view for both kernels sets can be observed. Also, it is important to mention that one of the main applications of multidimensional Laplace transforms centers on the closed form solution of Volterra kernels. A detailed description of such procedure can be found in the

references [Rugh 1981] and [Mohler 1991], where an extension to the analysis is made to include bilinear systems.

5.6 NONLINEAR TRANSFER FUNCTION BASED ON MODAL SERIES ANALYSIS

Based on the modal series approach developed above, and considering the definition of the transfer function, this section is focused to obtain the analytical expressions which define the nonlinear transfer functions for the first, second and third order terms of the modal series closed form solution. Recalling the first and second order terms obtained previously, we have,

$$Y_j^1(s) = \frac{\hat{b}_j}{s-\lambda_j} U(s) \tag{5.62}$$

$$Y_j^2(s_1,s_2) = \sum_{k=1}^{n}\sum_{l=1}^{n} \frac{1}{(s_1+s_2-\lambda_j)} C_{kl}^j Y_k^1(s_1) Y_l^1(s_2) \tag{5.63}$$

where

$$Y_k^1(s_1) = \frac{\hat{b}_k}{s_1-\lambda_k} U(s_1) \tag{5.64}$$

$$Y_l^1(s_2) = \frac{\hat{b}_l}{s_2-\lambda_l} U(s_2) \tag{5.65}$$

Thus, substituting (5.64) and (5.65) in (5.63), the second order terms are,

$$Y_j^2(s_1,s_2) = \sum_{k=1}^{n}\sum_{l=1}^{n} C_{kl}^j \left\{ \hat{b}_k \hat{b}_l \frac{1}{(s_1+s_2-\lambda_j)} \frac{1}{(s_1-\lambda_k)(s_2-\lambda_l)} U(s_1)U(s_2) \right\} \tag{5.66}$$

An identical process can be applied to obtain third order terms, that is,

$$Y_j^2(s_1,s_2,s_3) = \sum_{p=1}^{n}\sum_{q=1}^{n}\sum_{r=1}^{n} D_{pqr}^j \left[\hat{b}_p \hat{b}_q \hat{b}_r \frac{1}{(s_1+s_2+s_3-\lambda_j)} \frac{1}{(s_1-\lambda_p)(s_2-\lambda_q)(s_3-\lambda_r)} U(s_1)U(s_2)U(s_3) \right] \tag{5.67}$$

Now, it is possible to follow the association of variables procedure, which will express in a single Laplace variable the terms referred to second and third orders, that is,

$$Y_j^1(s) = \frac{\hat{b}_j}{s-\lambda_j} U(s) \tag{5.68}$$

$$Y_j^2(s) = \sum_{k=1}^{n}\sum_{l=1}^{n} C_{kl}^j \left\{ \hat{b}_k \hat{b}_l \frac{1}{(s-\lambda_j)} \frac{1}{(s-\lambda_k-\lambda_l)} U(s) \right\} \tag{5.69}$$

$$Y_j^3(s)=\sum_{p=1}^{n}\sum_{q=1}^{n}\sum_{r=1}^{n}D_{pqr}^{j}\left[\hat{b}_p\hat{b}_q\hat{b}_r\frac{1}{(s-\lambda_j)}\frac{1}{(s-\lambda_p-\lambda_q-\lambda_r)}U(s)\right] \tag{5.70}$$

$$\vdots$$

where,

$$U(s_1)U(s_2) \xrightarrow{\text{Associated as}} U(s)$$

$$U(s_1)U(s_2)U(s_3) \xrightarrow{\text{Associated as}} U(s)$$

Equations (5.68)-(5.70) express the transfer functions of the nonlinear system, once the multidimensional Laplace domain kernels have been associated to a single Laplace variable. Here, (5.68) represents the linear case of the transfer functions, where the residues are defined; the rest of Equations are clearly representing the nonlinear contributions based on modal interactions to the total transfer function of the nonlinear system, that it was decomposed through the modal series method.

The same reasoning is extended to higher order terms, which are easily generated. It can be observed that the poles of a first order transfer function are given by the eigenvalues obtained from the state matrix Taylor series expansion of the nonlinear system. However, second and third order terms poles, besides the poles due to eigenvalues, are due to the combination of two and three eigenvalues respectively. In a schematic way, the transfer function can be represented by Figure 5.4.

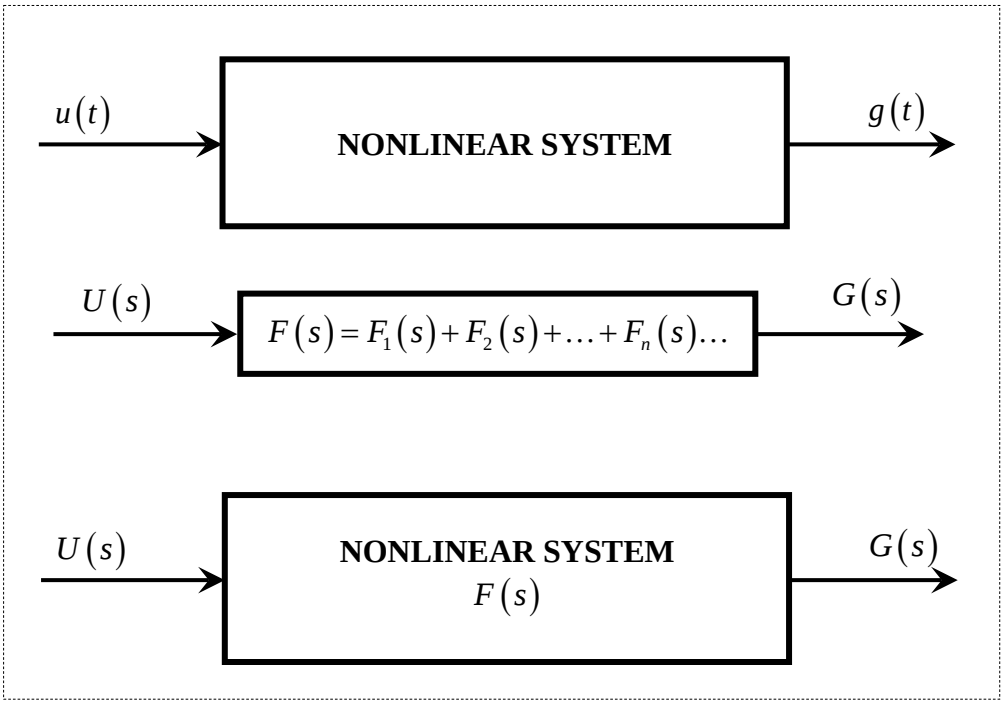

Figure 5.4 Schematic representation of transfer function for the nonlinear system

Assuming a transfer function,

$$F(s)=\frac{G(s)}{U(s)}$$

For the linear part, the time response of f to an impulse disturbance applied in $u(t)$ is equal to the inverse Laplace transform of $F(s)$ considering zero initial conditions in all system states [Gomes Jr. *et al*. 2000]. This is shown in Figure 5.5, where the decomposition of transfer function in individual kernels of first, second, third orders are denoted. Thus, the global output is dependent of the nonlinear contributions given by the modal combination included in the poles of the nonlinear transfer function.

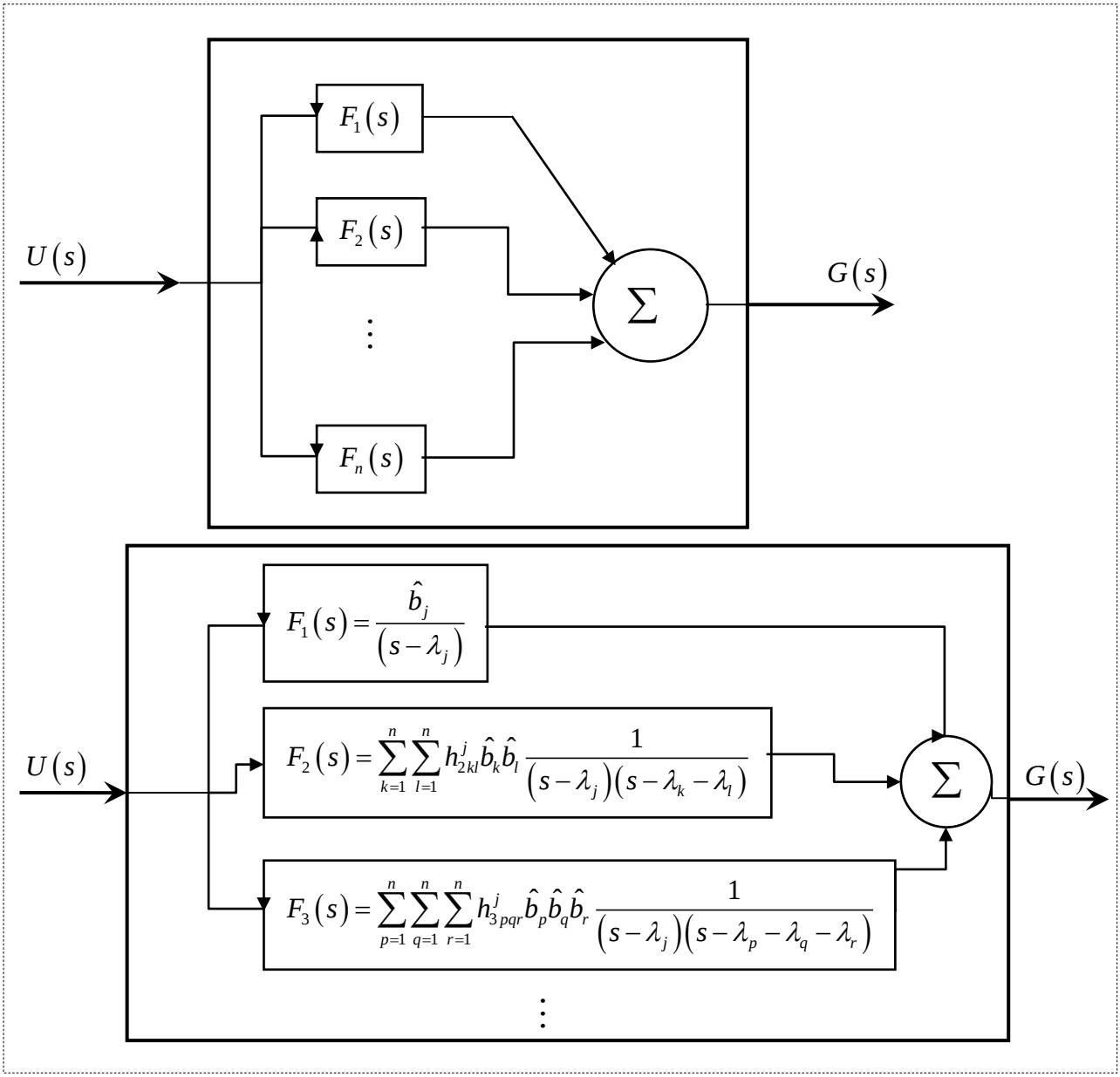

Figure 5.5 Schematic representation of individual transfer functions for the nonlinear system

5.7 EXAMPLE

5.7.1 SMIB Classical model

For the sake of exemplification, a simple power system consisting of a synchronous machine-infinite busbar power system is studied. The system is based on a classical model [Kundur 1994], with extended representation up to third order and assuming a single input-single output. The system has the form,

$$\dot{\mathbf{x}} = \begin{bmatrix} \Delta\delta \\ \Delta\omega \end{bmatrix} = \begin{bmatrix} \Delta\omega \\ -\frac{P_{\max}}{2H}\cos\delta_0\Delta\delta - \frac{D_m}{2H}\Delta\omega \end{bmatrix} + \frac{1}{2!}\begin{bmatrix} 0 \\ \frac{P_{\max}}{2H}\sin\delta_0\Delta\delta^2 \end{bmatrix} + \frac{1}{3!}\begin{bmatrix} 0 \\ \frac{P_{\max}}{2H}\cos\delta_0\Delta\delta^3 \end{bmatrix} + O(4) + \begin{bmatrix} 0 \\ \frac{1}{2H} \end{bmatrix}\Delta P_m \tag{5.71}$$

$$\boldsymbol{\psi} = \begin{bmatrix} 0 & 1 \end{bmatrix}\begin{bmatrix} \Delta\delta \\ \Delta\omega \end{bmatrix}$$

which includes only one transfer function given by,

$$F(s) = \frac{\Delta\omega(s)}{\Delta P_m(s)} \tag{5.72}$$

Applying modal series, it yields,

- First order terms:

$$\Delta x_i^1(s) = \sum_{j=1}^{n} \frac{\hat{b}_j}{s - \lambda_j} \qquad i = 1,\ 2$$

or

$$\begin{bmatrix} \Delta\tilde{\delta}(s) \\ \Delta\tilde{\omega}(s) \end{bmatrix} = \begin{bmatrix} \frac{\hat{b}_1}{s - \lambda_1} \\ \frac{\hat{b}_2}{s - \lambda_2} \end{bmatrix}\Delta P_m$$

Being, $\hat{C} = CU$,

$$\frac{\Delta\tilde{\omega}(s)}{\Delta P_m(s)} = \hat{c}_1\frac{\hat{b}_1}{s - \lambda_1} + \hat{c}_2\frac{\hat{b}_2}{s - \lambda_2} \tag{5.73}$$

- Second order terms:

The second order transfer function is expressed as a function of linear transfer functions. According to the theory above detailed, the kernels are function of the two-dimensional Laplace transform, which is associated to single variable kernels, that is,

$$\Delta x_j^2(s_1, s_2) = \sum_{k=1}^{n}\sum_{l=1}^{n} C_{kl}^j\hat{b}_k\hat{b}_l\frac{1}{(s_1 + s_2 - \lambda_j)(s_1 - \lambda_k)(s_2 - \lambda_l)} \qquad j = 1,\ 2$$

which is associated into,

$$\Delta x_j^2(s) = \sum_{k=1}^{n}\sum_{l=1}^{n} h_{2kl}^j \hat{b}_k \hat{b}_l \left\{ \frac{1}{(s-\lambda_k-\lambda_l)} - \frac{1}{(s-\lambda_j)} \right\} \tag{5.74}$$

that can be expanded for the state variables considered in the case study in the form,

$$\begin{bmatrix} \Delta\tilde{\delta}^2(s) \\ \Delta\tilde{\omega}^2(s) \end{bmatrix} = \begin{bmatrix} h_{2\,(1,1)}^1 \hat{b}_1^2 \left\{ \frac{1}{(s-2\lambda_1)} - \frac{1}{(s-\lambda_1)} \right\} + h_{2\,(1,2)}^1 \hat{b}_1 \hat{b}_2 \left\{ \frac{1}{(s-\lambda_1-\lambda_2)} - \frac{1}{(s-\lambda_1)} \right\} + \\ h_{2\,(2,1)}^1 \hat{b}_2 \hat{b}_1 \left\{ \frac{1}{(s-\lambda_2-\lambda_1)} - \frac{1}{(s-\lambda_1)} \right\} + h_{2\,(2,2)}^1 \hat{b}_2 \hat{b}_2 \left\{ \frac{1}{(s-2\lambda_2)} - \frac{1}{(s-\lambda_1)} \right\} \\ \hline h_{2\,(1,1)}^2 \hat{b}_1^2 \left\{ \frac{1}{(s-2\lambda_1)} - \frac{1}{(s-\lambda_2)} \right\} + h_{2\,(1,2)}^2 \hat{b}_1 \hat{b}_2 \left\{ \frac{1}{(s-\lambda_1-\lambda_2)} - \frac{1}{(s-\lambda_2)} \right\} + \\ h_{2\,(2,1)}^2 \hat{b}_2 \hat{b}_1 \left\{ \frac{1}{(s-\lambda_2-\lambda_1)} - \frac{1}{(s-\lambda_2)} \right\} + h_{2\,(2,2)}^2 \hat{b}_2^2 \left\{ \frac{1}{(s-2\lambda_2)} - \frac{1}{(s-\lambda_2)} \right\} \end{bmatrix} \Delta P_m$$

$$\begin{aligned} \frac{\Delta\tilde{\omega}^2(s)}{\Delta P_m} = \hat{c}_1 \Bigg[& h_{2\,(1,1)}^1 \hat{b}_1^2 \left\{ \frac{1}{(s-2\lambda_1)} - \frac{1}{(s-\lambda_1)} \right\} + h_{2\,(1,2)}^1 \hat{b}_1 \hat{b}_2 \left\{ \frac{1}{(s-\lambda_1-\lambda_2)} - \frac{1}{(s-\lambda_1)} \right\} + \\ & h_{2\,(2,1)}^1 \hat{b}_2 \hat{b}_1 \left\{ \frac{1}{(s-\lambda_2-\lambda_1)} - \frac{1}{(s-\lambda_1)} \right\} + h_{2\,(2,2)}^1 \hat{b}_2 \hat{b}_2 \left\{ \frac{1}{(s-2\lambda_2)} - \frac{1}{(s-\lambda_1)} \right\} \Bigg] + \\ \hat{c}_2 \Bigg[& h_{2\,(1,1)}^2 \hat{b}_1^2 \left\{ \frac{1}{(s-2\lambda_1)} - \frac{1}{(s-\lambda_2)} \right\} + h_{2\,(1,2)}^2 \hat{b}_1 \hat{b}_2 \left\{ \frac{1}{(s-\lambda_1-\lambda_2)} - \frac{1}{(s-\lambda_2)} \right\} + \\ & h_{2\,(2,1)}^2 \hat{b}_2 \hat{b}_1 \left\{ \frac{1}{(s-\lambda_2-\lambda_1)} - \frac{1}{(s-\lambda_2)} \right\} + h_{2\,(2,2)}^2 \hat{b}_2^2 \left\{ \frac{1}{(s-2\lambda_2)} - \frac{1}{(s-\lambda_2)} \right\} \Bigg] \end{aligned} \tag{5.75}$$

It can be observed from (5.75) that the transfer function residues are function of the nonlinear interaction matrix h_2^j, the elements of the transformed input matrix $\hat{B}$ and the combination of eigenvalues.

- Third order terms:

  Executing the same procedure described for the second order nonlinear transfer function, the third order is represented as,

$$\Delta x_j^3(s) = \sum_{p=1}^{n}\sum_{q=1}^{n}\sum_{r=1}^{n} h_{3\,pqr}^j \hat{b}_p \hat{b}_q \hat{b}_r \frac{1}{(s-\lambda_j)(s-\lambda_p-\lambda_q-\lambda_r)} \qquad j=1,\,2$$

  or in a single Laplace domain,

$$\Delta x_j^3(s) = \sum_{p=1}^{n}\sum_{q=1}^{n}\sum_{r=1}^{n} h_{3\,pqr}^j \hat{b}_p \hat{b}_q \hat{b}_r \left[\frac{1}{(s-\lambda_j)} - \frac{1}{(s-\lambda_p-\lambda_q-\lambda_r)} \right] \tag{5.76}$$

  Thus,

$$\begin{bmatrix}\Delta\tilde{\delta}^3(s)\\ \Delta\tilde{\omega}^3(s)\end{bmatrix}=\frac{\begin{bmatrix} h^1_{3(1,1,1)}\hat{b}_1^3\left[\frac{1}{(s-\lambda_1)}-\frac{1}{(s-3\lambda_1)}\right]+h^1_{3(1,1,2)}\hat{b}_1^2\hat{b}_2\left[\frac{1}{(s-\lambda_1)}-\frac{1}{(s-2\lambda_1-\lambda_2)}\right]+\\ h^1_{3(1,2,1)}\hat{b}_1^2\hat{b}_2\left[\frac{1}{(s-\lambda_1)}-\frac{1}{(s-2\lambda_1-\lambda_2)}\right]+h^1_{3(1,2,2)}\hat{b}_1\hat{b}_2^2\left[\frac{1}{(s-\lambda_1)}-\frac{1}{(s-\lambda_1-2\lambda_2)}\right]+\\ h^1_{3(2,1,1)}\hat{b}_1^2\hat{b}_2\left[\frac{1}{(s-\lambda_1)}-\frac{1}{(s-2\lambda_1-\lambda_2)}\right]+h^1_{3(2,1,2)}\hat{b}_1\hat{b}_2^2\left[\frac{1}{(s-\lambda_1)}-\frac{1}{(s-\lambda_1-2\lambda_2)}\right]+\\ h^1_{3(2,2,1)}\hat{b}_1\hat{b}_2^2\left[\frac{1}{(s-\lambda_1)}-\frac{1}{(s-\lambda_1-2\lambda_2)}\right]+h^1_{3(2,2,2)}\hat{b}_2^3\left[\frac{1}{(s-\lambda_1)}-\frac{1}{(s-3\lambda_2)}\right]\end{bmatrix}}{\begin{bmatrix} h^2_{3(1,1,1)}\hat{b}_1^3\left[\frac{1}{(s-\lambda_2)}-\frac{1}{(s-3\lambda_1)}\right]+h^2_{3(1,1,2)}\hat{b}_1^2\hat{b}_2\left[\frac{1}{(s-\lambda_2)}-\frac{1}{(s-2\lambda_1-\lambda_2)}\right]+\\ h^2_{3(1,2,1)}\hat{b}_1^2\hat{b}_2\left[\frac{1}{(s-\lambda_2)}-\frac{1}{(s-2\lambda_1-\lambda_2)}\right]+h^2_{3(1,2,2)}\hat{b}_1\hat{b}_2^2\left[\frac{1}{(s-\lambda_2)}-\frac{1}{(s-\lambda_1-2\lambda_2)}\right]+\\ h^2_{3(2,1,1)}\hat{b}_1^2\hat{b}_2\left[\frac{1}{(s-\lambda_2)}-\frac{1}{(s-2\lambda_1-\lambda_2)}\right]+h^2_{3(2,1,2)}\hat{b}_1\hat{b}_2^2\left[\frac{1}{(s-\lambda_2)}-\frac{1}{(s-\lambda_1-2\lambda_2)}\right]+\\ h^2_{3(2,2,1)}\hat{b}_1\hat{b}_2^2\left[\frac{1}{(s-\lambda_2)}-\frac{1}{(s-\lambda_1-2\lambda_2)}\right]+h^2_{3(2,2,2)}\hat{b}_2^3\left[\frac{1}{(s-\lambda_2)}-\frac{1}{(s-3\lambda_2)}\right]\end{bmatrix}}\Delta P_m \tag{5.77}$$

whose transfer function is expressed as,

$$\begin{aligned}\frac{\Delta\tilde{\omega}^3(s)}{\Delta P_m}=\hat{c}_1&\left\{h^1_{3(1,1,1)}\hat{b}_1^3\left[\frac{1}{(s-\lambda_1)}-\frac{1}{(s-3\lambda_1)}\right]+h^1_{3(1,1,2)}\hat{b}_1^2\hat{b}_2\left[\frac{1}{(s-\lambda_1)}-\frac{1}{(s-2\lambda_1-\lambda_2)}\right]+\right.\\ &h^1_{3(1,2,1)}\hat{b}_1^2\hat{b}_2\left[\frac{1}{(s-\lambda_1)}-\frac{1}{(s-2\lambda_1-\lambda_2)}\right]+h^1_{3(1,2,2)}\hat{b}_1\hat{b}_2^2\left[\frac{1}{(s-\lambda_1)}-\frac{1}{(s-\lambda_1-2\lambda_2)}\right]+\\ &h^1_{3(2,1,1)}\hat{b}_1^2\hat{b}_2\left[\frac{1}{(s-\lambda_1)}-\frac{1}{(s-2\lambda_1-\lambda_2)}\right]+h^1_{3(2,1,2)}\hat{b}_1\hat{b}_2^2\left[\frac{1}{(s-\lambda_1)}-\frac{1}{(s-\lambda_1-2\lambda_2)}\right]+\\ &\left.h^1_{3(2,2,1)}\hat{b}_1\hat{b}_2^2\left[\frac{1}{(s-\lambda_1)}-\frac{1}{(s-\lambda_1-2\lambda_2)}\right]+h^1_{3(2,2,2)}\hat{b}_2^3\left[\frac{1}{(s-\lambda_1)}-\frac{1}{(s-3\lambda_2)}\right]\right\}+\\ \hat{c}_2&\left\{h^2_{3(1,1,1)}\hat{b}_1^3\left[\frac{1}{(s-\lambda_2)}-\frac{1}{(s-3\lambda_1)}\right]+h^2_{3(1,1,2)}\hat{b}_1^2\hat{b}_2\left[\frac{1}{(s-\lambda_2)}-\frac{1}{(s-2\lambda_1-\lambda_2)}\right]+\right.\\ &h^2_{3(1,2,1)}\hat{b}_1^2\hat{b}_2\left[\frac{1}{(s-\lambda_2)}-\frac{1}{(s-2\lambda_1-\lambda_2)}\right]+h^2_{3(1,2,2)}\hat{b}_1\hat{b}_2^2\left[\frac{1}{(s-\lambda_2)}-\frac{1}{(s-\lambda_1-2\lambda_2)}\right]+\\ &h^2_{3(2,1,1)}\hat{b}_1^2\hat{b}_2\left[\frac{1}{(s-\lambda_2)}-\frac{1}{(s-2\lambda_1-\lambda_2)}\right]+h^2_{3(2,1,2)}\hat{b}_1\hat{b}_2^2\left[\frac{1}{(s-\lambda_2)}-\frac{1}{(s-\lambda_1-2\lambda_2)}\right]+\\ &\left.h^2_{3(2,2,1)}\hat{b}_1\hat{b}_2^2\left[\frac{1}{(s-\lambda_2)}-\frac{1}{(s-\lambda_1-2\lambda_2)}\right]+h^2_{3(2,2,2)}\hat{b}_2^3\left[\frac{1}{(s-\lambda_2)}-\frac{1}{(s-3\lambda_2)}\right]\right\}\end{aligned} \tag{5.78}$$

This process can be repeatedly applied up to the terms suitable to be considered. For this case, terms up to third order have been solved, hence the transfer function is represented by linear and second and third nonlinear terms. Figures 5.6 show the bode graphs for the transfer functions (5.73), (5.75) and (5.78) corresponding to the first, second and third order respectively, so related to the test power system considered in this experiment. Bode analysis has been performed by using Matlab® control toolbox, assuming individual transfer functions. The frequency contributions of second and third order terms can be observed in the gain of the transfer function.

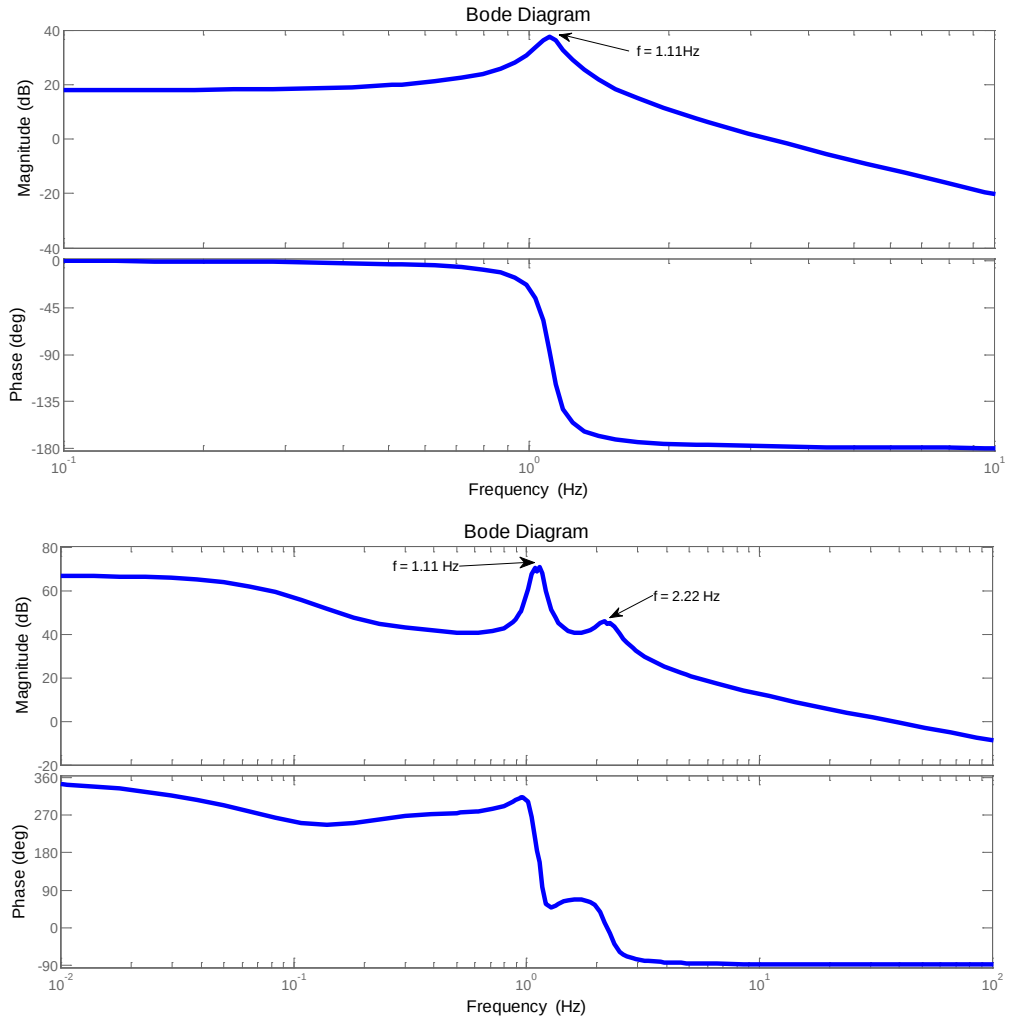

Figure 5.6 Bode graphics of first and second order transfer functions for the case of SMIB power system

The Bode graphs of Figure 5.6 show the frequency contributions of both linear and nonlinear transfer functions. Of course, the linear frequency transfer function is due to the poles of the oscillatory eigenvalues, with frequency $f = 1.1096\ Hz$, such as it is described in Table 5.1. Furthermore, the frequencies due to the second order transfer functions are due to the combination of oscillatory modes, resulting in two main frequencies contributions, also detailed in Table 5.1.

The same Table 5.1 is specifying the residue, pole, frequency and damping ratio associated to each mode for the case of the first order transfer function, and the resulting of modal combination for the case of the second order transfer function. A frequency of 2.2191 Hz (which can be observed in the Bode graph of Figure 5.6) is the resultant of modal combination (5.75). Also to be noted is the substantial increase on residue values of the second order transfer function, that are dependent of nonlinear coefficients.

Table 5.1 Residues, poles and frequency properties of transfer functions

	RESIDUES	**POLES**	**FREQUENCY**	**DAMPING RATIO**
First Order Transfer Function	27.0380i	$-0.3571 \pm 6.9715i$	1.1096	0.0512
Second Order Transfer Function	$223.24370479 - 11.4365329i$	$-0.7143 + 13.9430i$	2.2191	0.0512
	$-223.24370479 + 11.4365329i$	$-0.3571 + 6.9715i$	1.1096	0.0512
	$223.24370479 - 11.4365329i$	-0.7143	-	-
	$-223.24370479 + 11.4365329i$	$-0.3571 + 6.9715i$	1.1096	0.0512
	$223.24370479 - 11.4365329i$	-0.7143	-	-
	$-223.24370479 + 11.4365329i$	$-0.3571 + 6.9715i$	1.1096	0.0512
	$-74.58811208 - 1.27368937i$	$-0.7143 - 13.9430i$	2.2191	0.0512
	$74.58811208 + 1.27368937i$	$-0.3571 + 6.9715i$	1.1096	0.0512
	$-74.58811208 - 1.27368937i$	$-0.7143 + 13.9430i$	2.2191	0.0512
	$74.58811208 + 1.27368937i$	$-0.3571 - 6.9715i$	1.1096	0.0512
	$223.24370479 - 11.4365329i$	-0.7143	-	-
	$-223.24370479 + 11.4365329i$	$-0.3571 - 6.9715i$	1.1096	0.0512
	$223.24370479 - 11.4365329i$	-0.7143	-	-
	$-223.24370479 + 11.4365329i$	$-0.3571 - 6.9715i$	1.1096	0.0512
	$223.24370479 - 11.4365329i$	$-0.7143 - 13.9430i$	2.2191	0.0512
	$-223.24370479 + 11.4365329i$	$-0.3571 - 6.9715i$	1.1096	0.0512

Another schematic form to express the frequency response of the linear and nonlinear transfer functions is the application of the Nyquist plots or polar plots shown in Figure 5.7.

In this case study, the mechanical power input, as it was mentioned before, is applied as the input signal to the transfer function. Figure 5.7a shows the polar plot for the linear transfer function. According to the theory of Nyquist diagrams, the frequency evolution is demonstrating that the system is stable for the a defined perturbation, since the polar diagram is not circling the axis in -1 [Lazaro-Castillo 2008]. The analysis is made considering transfer functions in open loop.

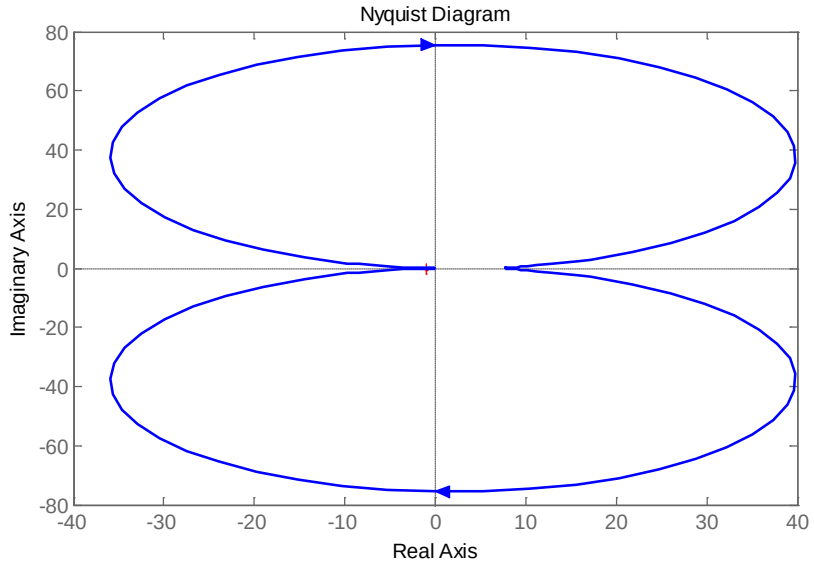

a) Linear transfer function

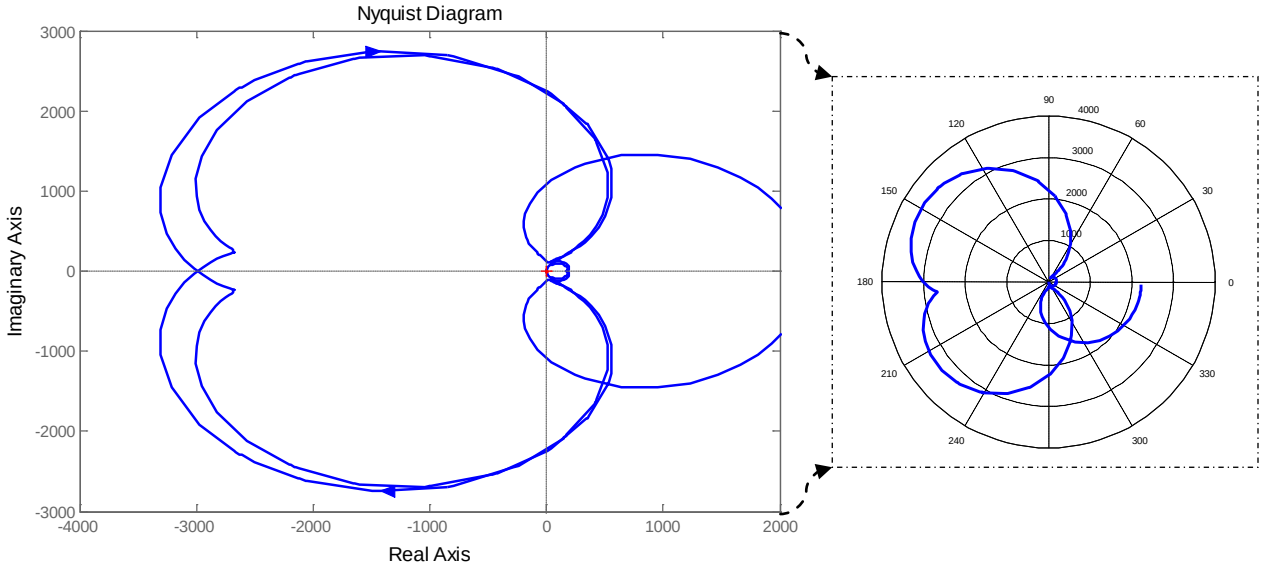

b) Second order transfer function

Figure 5.7 Nyquist plots for the linear and transfer functions of $\Delta\omega/\Delta P_m$

Also, the same reasoning is used for the second order transfer function. A zoomed vision of the diagram of Figure 5.7 is shown in Figure 5.8, where the frequency of 2.2 Hz which is contributed by second order modal terms is observed. In the same way as the linear case, referring to Figures 5.7b and 5.8, the trajectory obtained by the Nyquist plot is not closing the *x* axis point -1, thus demonstrating that the system is stable for the transfer function performed under the parameter conditions given.

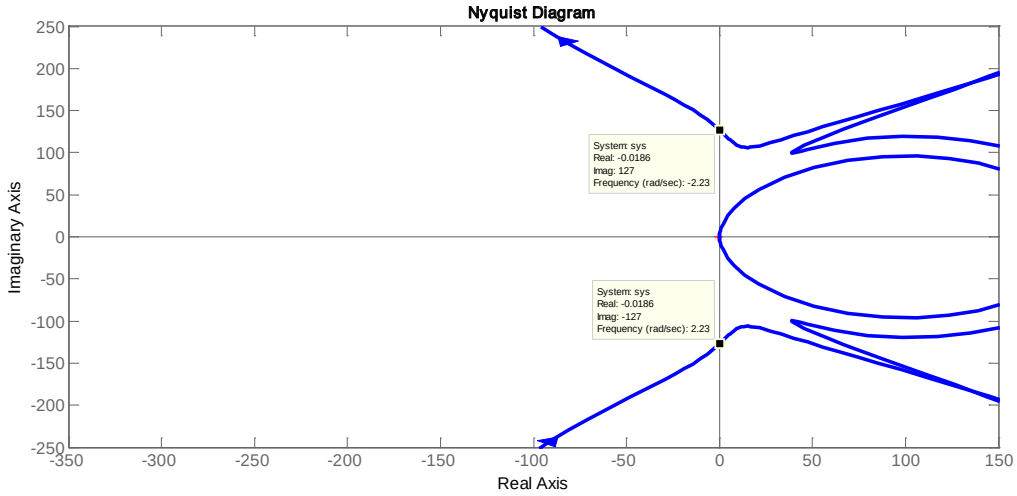

Figure 5.8 Detailed zoom of Nyquist plot of the second order transfer function

5.7.2 Step Input Response

The transfer functions previously defined are subjected to the application of a unit step function of the form [Ogata 1997],

$$f(t)=0 \qquad \text{for } t<0$$
$$f(t)=1 \qquad \text{for } t>0$$

The unit step function is undefined at $t=0$. In the Laplace domain it is defined as,

$$\Im[1]=\int_0^\infty e^{-st}dt=\frac{1}{s}$$

Taking the transfer functions (5.73) and (5.75) defined for linear and second order respectively, and applying the input unit step function, the closed form expressions in the Laplace domain are,

$$\Delta\tilde{\omega}(s)=\hat{c}_1\frac{\hat{b}_1}{s-\lambda_1}\frac{1}{s}+\hat{c}_2\frac{\hat{b}_2}{s-\lambda_2}\frac{1}{s} \tag{5.79}$$

$$\Delta\tilde{\omega}^2(s)=\hat{c}_1\begin{bmatrix} h^1_{2\,(1,1)}\hat{b}_1^2\left\{\frac{1}{2\lambda_1}\left[\frac{1}{(s-2\lambda_1)}-\frac{1}{s}\right]-\frac{1}{\lambda_1}\left[\frac{1}{(s-\lambda_1)}-\frac{1}{s}\right]\right\} \\ +h^1_{2\,(1,2)}\hat{b}_1\hat{b}_2\left\{\frac{1}{\lambda_1+\lambda_2}\left[\frac{1}{(s-\lambda_1-\lambda_2)}-\frac{1}{s}\right]-\frac{1}{\lambda_1}\left[\frac{1}{(s-\lambda_1)}-\frac{1}{s}\right]\right\}+ \\ h^1_{2\,(2,1)}\hat{b}_2\hat{b}_1\left\{\frac{1}{\lambda_1+\lambda_2}\left[\frac{1}{(s-\lambda_1-\lambda_2)}-\frac{1}{s}\right]-\frac{1}{\lambda_1}\left[\frac{1}{(s-\lambda_1)}-\frac{1}{s}\right]\right\}+ \\ h^1_{2\,(2,2)}\hat{b}_2\hat{b}_2\left\{\frac{1}{2\lambda_2}\left[\frac{1}{(s-2\lambda_2)}-\frac{1}{s}\right]-\frac{1}{\lambda_1}\left[\frac{1}{(s-\lambda_1)}-\frac{1}{s}\right]\right\} \end{bmatrix}+$$

$$\hat{c}_2\begin{bmatrix} h^2_{2\,(1,1)}\hat{b}_1^2\left\{\frac{1}{2\lambda_1}\left[\frac{1}{(s-2\lambda_1)}-\frac{1}{s}\right]-\frac{1}{\lambda_2}\left[\frac{1}{(s-\lambda_2)}-\frac{1}{s}\right]\right\}+ \\ h^2_{2\,(1,2)}\hat{b}_1\hat{b}_2\left\{\frac{1}{\lambda_1+\lambda_2}\left[\frac{1}{(s-\lambda_1-\lambda_2)}-\frac{1}{s}\right]-\frac{1}{\lambda_2}\left[\frac{1}{(s-\lambda_2)}-\frac{1}{s}\right]\right\}+ \\ h^2_{2\,(2,1)}\hat{b}_2\hat{b}_1\left\{\frac{1}{\lambda_1+\lambda_2}\left[\frac{1}{(s-\lambda_1-\lambda_2)}-\frac{1}{s}\right]-\frac{1}{\lambda_2}\left[\frac{1}{(s-\lambda_2)}-\frac{1}{s}\right]\right\}+ \\ h^2_{2\,(2,2)}\hat{b}_2^2\left\{\frac{1}{2\lambda_2}\left[\frac{1}{(s-2\lambda_2)}-\frac{1}{s}\right]-\frac{1}{\lambda_2}\left[\frac{1}{(s-\lambda_2)}-\frac{1}{s}\right]\right\} \end{bmatrix} \tag{5.80}$$

Now, applying the inverse Laplace transform, the closed form solutions in time domain are obtained as follows,

$$\Delta\tilde{\omega}^1(t)=\hat{c}_1\frac{\hat{b}_1}{\lambda_1}\left[e^{\lambda_1 t}-1\right]+\hat{c}_2\frac{\hat{b}_2}{\lambda_2}\left[e^{\lambda_2 t}-1\right] \tag{5.81}$$

$$\Delta\tilde{\omega}^2(t)=\hat{c}_1\begin{bmatrix} h^1_{2\,(1,1)}\hat{b}_1^2\left\{\frac{1}{2\lambda_1}\left[e^{2\lambda_1 t}-1\right]-\frac{1}{\lambda_1}\left[e^{\lambda_1 t}-1\right]\right\} \\ +h^1_{2\,(1,2)}\hat{b}_1\hat{b}_2\left\{\frac{1}{\lambda_1+\lambda_2}\left[e^{(\lambda_1+\lambda_2)t}-1\right]-\frac{1}{\lambda_1}\left[e^{\lambda_1 t}-1\right]\right\}+ \\ h^1_{2\,(2,1)}\hat{b}_2\hat{b}_1\left\{\frac{1}{\lambda_1+\lambda_2}\left[e^{(\lambda_1+\lambda_2)t}-1\right]-\frac{1}{\lambda_1}\left[e^{\lambda_1 t}-1\right]\right\}+ \\ h^1_{2\,(2,2)}\hat{b}_2\hat{b}_2\left\{\frac{1}{2\lambda_2}\left[e^{2\lambda_2 t}-1\right]-\frac{1}{\lambda_1}\left[e^{\lambda_1 t}-1\right]\right\} \end{bmatrix}+\hat{c}_2\begin{bmatrix} h^2_{2\,(1,1)}\hat{b}_1^2\left\{\frac{1}{2\lambda_1}\left[e^{2\lambda_1 t}-1\right]-\frac{1}{\lambda_2}\left[e^{\lambda_2 t}-1\right]\right\}+ \\ h^2_{2\,(1,2)}\hat{b}_1\hat{b}_2\left\{\frac{1}{\lambda_1+\lambda_2}\left[e^{(\lambda_1+\lambda_2)t}-1\right]-\frac{1}{\lambda_2}\left[e^{\lambda_2 t}-1\right]\right\}+ \\ h^2_{2\,(2,1)}\hat{b}_2\hat{b}_1\left\{\frac{1}{\lambda_1+\lambda_2}\left[e^{(\lambda_1+\lambda_2)t}-1\right]-\frac{1}{\lambda_2}\left[e^{\lambda_2 t}-1\right]\right\}+ \\ h^2_{2\,(2,2)}\hat{b}_2^2\left\{\frac{1}{2\lambda_2}\left[e^{2\lambda_2 t}-1\right]-\frac{1}{\lambda_2}\left[e^{\lambda_2 t}-1\right]\right\} \end{bmatrix} \tag{5.82}$$

Performing simulations through the time domain expressions (5.81) and (5.82) and according to the assumed parameter conditions for this case study, the waveforms of Figure 5.9 are obtained for the case of input step function response.

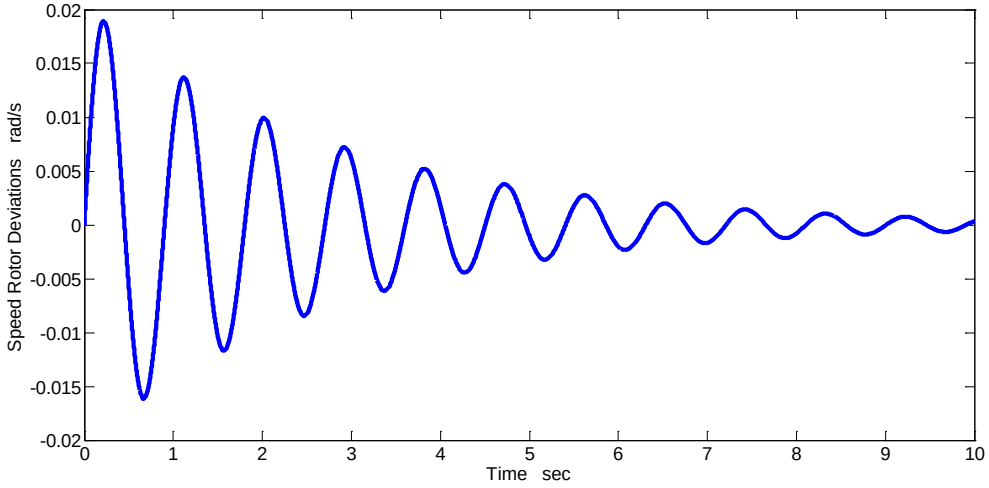

a) Linear transfer function

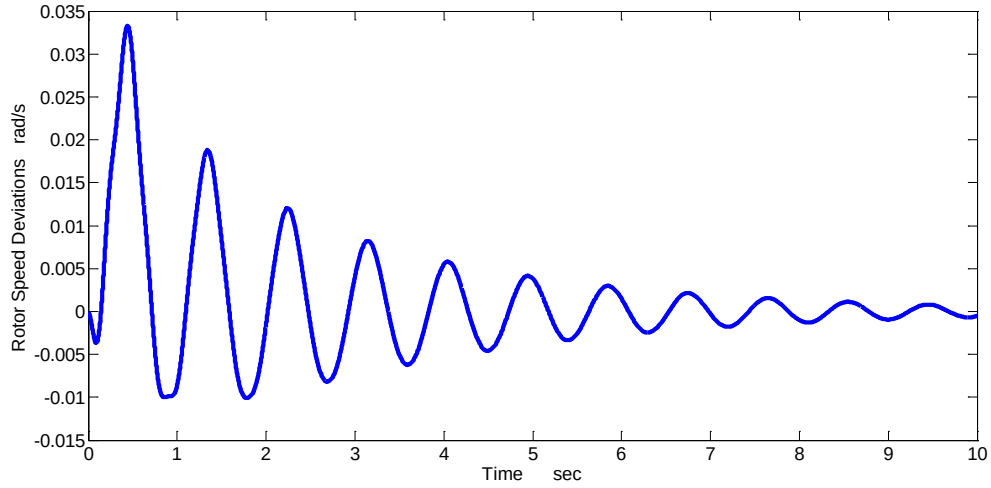

b) Second order transfer function

Figure 5.9 Time evolution after a unit step function applied to the transfer functions

Low frequency oscillations are observed in this Figure, where the second order evolution is considered. The graphs also show that the system keeps stable under this input signal, thus oscillating to eventually disappear. An additional exercise can be performed in this case study, now assuming various damping coefficients, resulting in different oscillation conditions. Figures 5.10a and 5.10b show this experiment for the linear and nonlinear transfer function, respectively, where the damping constant is varied from 0 to 5 and increased to the hypothetic values of 10 and 20 (over-damped conditions). Observe that the oscillations vary only in amplitude, keeping unchanged the frequency; as it was expected. For the higher values of damping conditions, oscillations disappear more rapidly than low damping constants.

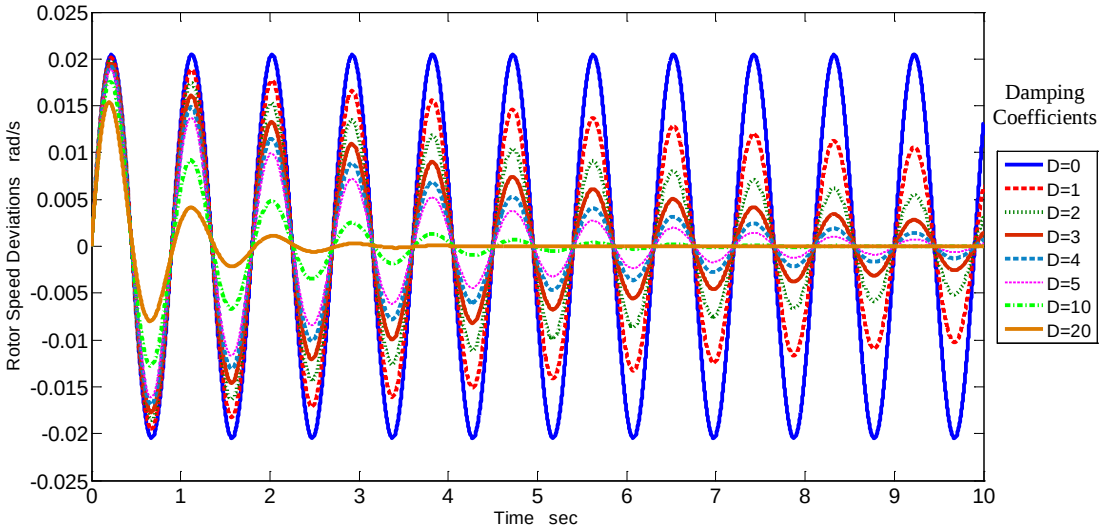

a) Linear transfer function

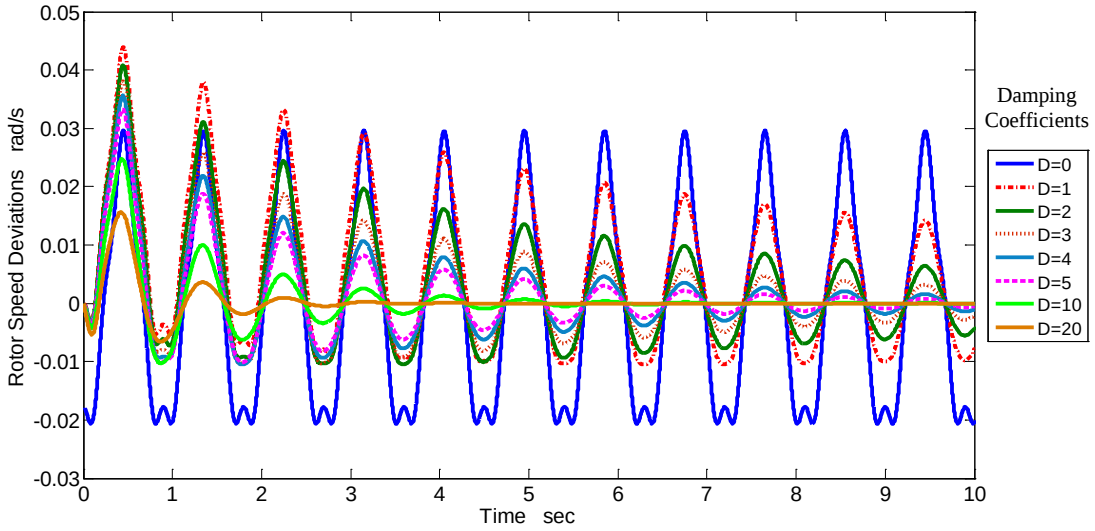

b) Second order transfer function

Figure 5.10 Time evolution after a unit step function applied to the transfer functions varying the damping coefficient

5.7.3 3 SM, 9 BUSES Test Power System

The application of the proposed method is illustrated on a 3 machines, 9 bus test power system. The generation and network parameters, load data and the system operating conditions are taken from [Anderson and Fouad 2003] and given in Appendix C. The power system is represented by a fourth-order model including the AVR representation. In Chapter 4 the model of this power system is detailed.

Expanding the nonlinear model into a truncated series, up to order 2, one has

$$\dot{\mathbf{x}} = \mathbf{A}\mathbf{x} + \mathbf{F}_2(\mathbf{x}) + \mathbf{B}\mathbf{u} = \mathbf{A}\mathbf{x} + \frac{1}{2}\mathbf{x}^{\mathrm{T}}\mathbf{H}^{\mathrm{i}}\mathbf{x} + O\left(\left|\mathbf{x}\right|^{3}\right) + \mathbf{B}\mathbf{u} \tag{5.83}$$

Once the nonlinear representation has been obtained, modal solutions can be calculated.

Nonlinear Transfer Functions

Taking into account the modeling of a multimachine power system, and considering the fourth order power system previously described in Chapter 4, the system is linearized considering the state variables of each generator and the input variables associated to the power system as the mechanical power inputs and the reference voltages of the automatic voltage regulator, that is,

$$\begin{aligned}\Delta\mathbf{x} = \Big[\big[\Delta\delta_1 \quad \Delta\delta_2 \quad \Delta\delta_3\big]\big[\Delta\omega_1 \quad \Delta\omega_2 \quad \Delta\omega_3\big]\big[\Delta E'_{q1} \quad \Delta E'_{q2} \quad \Delta E'_{q3}\big] \\ \big[\Delta E'_{d1} \quad \Delta E'_{d2} \quad \Delta E'_{d3}\big]\big[\Delta E_{fd1} \quad \Delta E_{fd2} \quad \Delta E_{fd3}\big]\Big]^T\end{aligned} \tag{5.84}$$

$$\Delta\mathbf{u} = \Big[\big[\Delta P_{m1} \quad \Delta P_{m2} \quad \Delta P_{m3}\big]\big[\Delta V_{ref1} \quad \Delta V_{ref2} \quad \Delta V_{ref3}\big]\Big]^T \tag{5.85}$$

Hence, the complete model including for the power system under study has the form (in a similar way to the linearized system described by (3.41)),

$$\dot{\mathbf{x}} = F_1(\mathbf{x}) + F_2(\mathbf{x}) + F_3(\mathbf{x}) + \ldots + \mathbf{B}\Delta\mathbf{u} \tag{5.86}$$

where, $F_1(\mathbf{x})$, $F_2(\mathbf{x})$ and $F_3(\mathbf{x})$ are defined by (3.43), (3.44) and (3.45), respectively. The input matrix **B** has the form,

$$\mathbf{B} = \begin{bmatrix} \frac{\partial f_1}{\partial u_1} & \frac{\partial f_1}{\partial u_2} & \cdots & \frac{\partial f_1}{\partial u_r} \\ \frac{\partial f_2}{\partial u_1} & \frac{\partial f_2}{\partial u_2} & \cdots & \frac{\partial f_2}{\partial u_r} \\ \vdots & \vdots & \ddots & \vdots \\ \frac{\partial f_n}{\partial u_1} & \frac{\partial f_n}{\partial u_2} & \cdots & \frac{\partial f_n}{\partial u_r} \end{bmatrix} \tag{5.87}$$

which for the assumed power system is a (15×6) order matrix.

For this case study, the transfer functions can be described choosing the rotor speed deviations as the set of output variables, resulting in a multivariable transfer function with 6 inputs-3 outputs, in the form shown by Figure 5.11. Since the system under study has multiple inputs-multiple outputs (MIMO system) it is necessary to incorporate the concept of superposition. Although this is a concept only valid for linear systems, it can be assumed the linearity of inputs and the nature of each kernel represented in terms of the multidimensional Laplace domain. For the sake of simplicity, each transfer

function will be calculated as a single input-single output system thus considering only the effect on the output variable due to a single input variable.

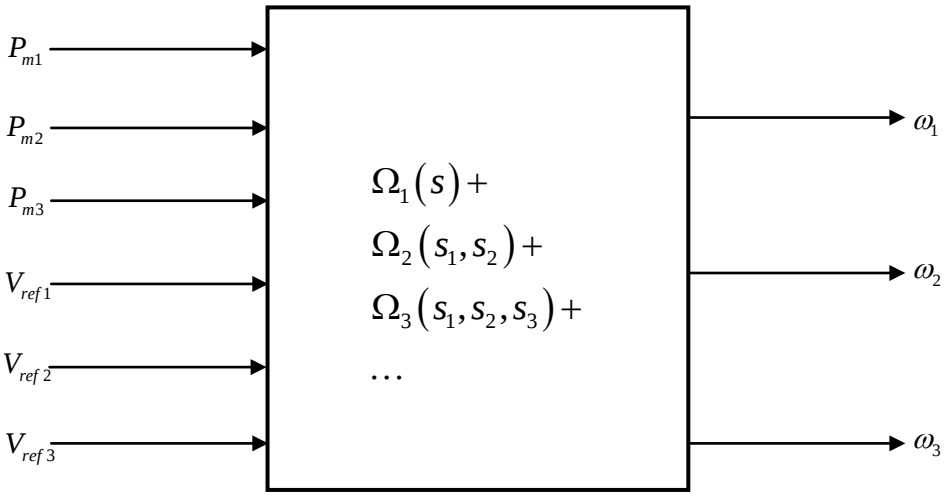

Figure 5.11 Multivariable transfer function $\Omega(s)$

Applying the modal series method, detailed transfer functions including second and third order terms can be described. Following the modal series reasoning, the complete system can be modeled according to linear rules, that is,

$$\begin{aligned} \dot{\mathbf{x}} &= \mathbf{A}\mathbf{x} + \frac{1}{2}\mathbf{x}^{\mathrm{T}}\mathbf{H}^{\mathrm{i}}\mathbf{x} + O\left(|\mathbf{x}|^{3}\right) + \mathbf{B}\mathbf{u} \\ \mathbf{y} &= \mathbf{C}\mathbf{x} \end{aligned} \tag{5.88}$$

which in its own can be expressed according to Jordan canonical form, *i.e.*,

$$\begin{aligned} \dot{\tilde{\mathbf{x}}} &= \mathbf{\Lambda}\tilde{\mathbf{x}} + \mathbf{F}_2(\tilde{\mathbf{x}}) + \mathbf{F}_3(\tilde{\mathbf{x}}) + \ldots + \mathbf{U}^{-1}\mathbf{B}\mathbf{u} \\ \mathbf{y} &= \mathbf{C}\mathbf{U}\mathbf{x} \end{aligned} \tag{5.89}$$

and then transformed into its Laplace transform domain as,

$$\begin{aligned} \tilde{\mathbf{X}}(s) &= \tilde{\mathbf{X}}_1(s) + \tilde{\mathbf{X}}_2(s) + \tilde{\mathbf{X}}_3(s) + \ldots + \tilde{\mathbf{B}}\mathbf{U}(s) \\ \tilde{\mathbf{Y}}(s) &= \tilde{\mathbf{C}}\tilde{\mathbf{X}}(s) \end{aligned} \tag{5.90}$$

Calculating $\tilde{\mathbf{B}} = \mathbf{U}^{-1}\mathbf{B}$,

$$\mathbf{B} = \begin{bmatrix} 0 & 0 & 0 & 0 & 0 & 0 \\ 0 & 0 & 0 & 0 & 0 & 0 \\ 0 & 0 & 0 & 0 & 0 & 0 \\ \frac{\omega_r}{2H_1} & 0 & 0 & 0 & 0 & 0 \\ 0 & \frac{\omega_r}{2H_2} & 0 & 0 & 0 & 0 \\ 0 & 0 & \frac{\omega_r}{2H_3} & 0 & 0 & 0 \\ 0 & 0 & 0 & 0 & 0 & 0 \\ 0 & 0 & 0 & 0 & 0 & 0 \\ 0 & 0 & 0 & 0 & 0 & 0 \\ 0 & 0 & 0 & 0 & 0 & 0 \\ 0 & 0 & 0 & 0 & 0 & 0 \\ 0 & 0 & 0 & 0 & 0 & 0 \\ 0 & 0 & 0 & \frac{K_{exc1}}{T_{exc1}} & 0 & 0 \\ 0 & 0 & 0 & 0 & \frac{K_{exc2}}{T_{exc2}} & 0 \\ 0 & 0 & 0 & 0 & 0 & \frac{K_{exc3}}{T_{exc3}} \end{bmatrix}$$

$$\tilde{\mathbf{B}} = \begin{array}{c} \\ \delta_1 \\ \delta_2 \\ \delta_3 \\ \omega_1 \\ \omega_2 \\ \omega_3 \\ E'_{q1} \\ E'_{q2} \\ E'_{q3} \\ E'_{d1} \\ E'_{d2} \\ E'_{d3} \\ E_{fd1} \\ E_{fd2} \\ E_{fd3} \end{array} \begin{array}{c} \begin{array}{ccc|ccc} P_{m1} & P_{m2} & P_{m3} & V_{ref1} & V_{ref2} & V_{ref3} \end{array} \\ \begin{bmatrix} \hat{b}_{11} & \hat{b}_{12} & \hat{b}_{13} & \hat{b}_{14} & \hat{b}_{15} & \hat{b}_{16} \\ \hat{b}_{21} & \hat{b}_{22} & \hat{b}_{23} & \hat{b}_{24} & \hat{b}_{25} & \hat{b}_{26} \\ \hat{b}_{31} & \hat{b}_{32} & \hat{b}_{33} & \hat{b}_{34} & \hat{b}_{35} & \hat{b}_{36} \\ \hat{b}_{41} & \hat{b}_{42} & \hat{b}_{43} & \hat{b}_{44} & \hat{b}_{45} & \hat{b}_{46} \\ \hat{b}_{51} & \hat{b}_{52} & \hat{b}_{53} & \hat{b}_{54} & \hat{b}_{55} & \hat{b}_{56} \\ \hat{b}_{61} & \hat{b}_{62} & \hat{b}_{63} & \hat{b}_{64} & \hat{b}_{65} & \hat{b}_{66} \\ \hat{b}_{71} & \hat{b}_{72} & \hat{b}_{73} & \hat{b}_{74} & \hat{b}_{75} & \hat{b}_{76} \\ \hat{b}_{81} & \hat{b}_{82} & \hat{b}_{83} & \hat{b}_{84} & \hat{b}_{85} & \hat{b}_{86} \\ \hat{b}_{91} & \hat{b}_{92} & \hat{b}_{93} & \hat{b}_{94} & \hat{b}_{95} & \hat{b}_{96} \\ \hat{b}_{10,1} & \hat{b}_{10,2} & \hat{b}_{10,3} & \hat{b}_{10,4} & \hat{b}_{10,5} & \hat{b}_{10,6} \\ \hat{b}_{11,1} & \hat{b}_{11,2} & \hat{b}_{11,3} & \hat{b}_{11,4} & \hat{b}_{11,5} & \hat{b}_{11,6} \\ \hat{b}_{12,1} & \hat{b}_{12,2} & \hat{b}_{12,3} & \hat{b}_{12,4} & \hat{b}_{12,5} & \hat{b}_{12,6} \\ \hat{b}_{13,1} & \hat{b}_{13,2} & \hat{b}_{13,3} & \hat{b}_{13,4} & \hat{b}_{13,5} & \hat{b}_{13,6} \\ \hat{b}_{14,1} & \hat{b}_{14,2} & \hat{b}_{14,3} & \hat{b}_{14,4} & \hat{b}_{14,5} & \hat{b}_{14,6} \\ \hat{b}_{15,1} & \hat{b}_{15,2} & \hat{b}_{15,3} & \hat{b}_{15,4} & \hat{b}_{15,5} & \hat{b}_{15,6} \end{bmatrix} \end{array}$$

(5.91)

$$\mathbf{C} = \begin{array}{c} \\ \omega_1 \\ \omega_2 \\ \omega_3 \end{array} \begin{array}{c} \begin{array}{ccccccccccccccc} \delta_1 & \delta_2 & \delta_3 & \omega_1 & \omega_2 & \omega_3 & E'_{q1} & E'_{q2} & E'_{q3} & E'_{d1} & E'_{d2} & E'_{d3} & E_{fd1} & E_{fd2} & E_{fd3} \end{array} \\ \begin{bmatrix} 0 & 0 & 0 & 1 & 0 & 0 & 0 & 0 & 0 & 0 & 0 & 0 & 0 & 0 & 0 \\ 0 & 0 & 0 & 0 & 1 & 0 & 0 & 0 & 0 & 0 & 0 & 0 & 0 & 0 & 0 \\ 0 & 0 & 0 & 0 & 0 & 1 & 0 & 0 & 0 & 0 & 0 & 0 & 0 & 0 & 0 \end{bmatrix} \end{array}$$

Or,

$$\tilde{\mathbf{C}} = \begin{bmatrix} \hat{c}_{1,1} & \hat{c}_{1,2} & \hat{c}_{1,3} & \hat{c}_{1,4} & \hat{c}_{1,5} & \hat{c}_{1,6} & \hat{c}_{1,7} & \hat{c}_{1,8} & \hat{c}_{1,9} & \hat{c}_{1,10} & \hat{c}_{1,11} & \hat{c}_{1,12} & \hat{c}_{1,13} & \hat{c}_{1,14} & \hat{c}_{1,15} \\ \hat{c}_{2,1} & \hat{c}_{2,2} & \hat{c}_{2,3} & \hat{c}_{2,4} & \hat{c}_{2,5} & \hat{c}_{2,6} & \hat{c}_{2,7} & \hat{c}_{2,8} & \hat{c}_{2,9} & \hat{c}_{2,10} & \hat{c}_{2,11} & \hat{c}_{2,12} & \hat{c}_{2,13} & \hat{c}_{2,14} & \hat{c}_{2,15} \\ \hat{c}_{3,1} & \hat{c}_{3,2} & \hat{c}_{3,3} & \hat{c}_{3,4} & \hat{c}_{3,5} & \hat{c}_{3,6} & \hat{c}_{3,7} & \hat{c}_{3,8} & \hat{c}_{3,9} & \hat{c}_{3,10} & \hat{c}_{3,11} & \hat{c}_{3,12} & \hat{c}_{3,13} & \hat{c}_{3,14} & \hat{c}_{3,15} \end{bmatrix}$$

From (5.90) it is possible to separate the terms corresponding to first, second, etc. order resulting in the next transfer functions that are expressed as a Multi Input-Multi Output system.

- First order transfer functions:

$$\Delta x_i^1(s) = \sum_{i=1}^{n} \sum_{j=1}^{n} \frac{\hat{b}_{ij}}{s - \lambda_j}$$

$$\begin{bmatrix} \tilde{\delta}_1(s) \\ \tilde{\delta}_2(s) \\ \tilde{\delta}_3(s) \\ \hline \tilde{\omega}_1(s) \\ \tilde{\omega}_2(s) \\ \tilde{\omega}_3(s) \\ \hline \tilde{E}'_{q1}(s) \\ \tilde{E}'_{q2}(s) \\ \tilde{E}'_{q3}(s) \\ \hline \tilde{E}'_{d1}(s) \\ \tilde{E}'_{d2}(s) \\ \tilde{E}'_{d3}(s) \\ \hline \tilde{E}_{fd1}(s) \\ \tilde{E}_{fd2}(s) \\ \tilde{E}_{fd3}(s) \end{bmatrix} = \left[\begin{array}{ccc|ccc} \frac{\hat{b}_{11}}{s-\lambda_1} & \frac{\hat{b}_{12}}{s-\lambda_1} & \frac{\hat{b}_{13}}{s-\lambda_1} & \frac{\hat{b}_{14}}{s-\lambda_1} & \frac{\hat{b}_{15}}{s-\lambda_1} & \frac{\hat{b}_{16}}{s-\lambda_1} \\ \frac{\hat{b}_{21}}{s-\lambda_2} & \frac{\hat{b}_{22}}{s-\lambda_2} & \frac{\hat{b}_{23}}{s-\lambda_2} & \frac{\hat{b}_{24}}{s-\lambda_2} & \frac{\hat{b}_{25}}{s-\lambda_2} & \frac{\hat{b}_{26}}{s-\lambda_2} \\ \frac{\hat{b}_{31}}{s-\lambda_3} & \frac{\hat{b}_{32}}{s-\lambda_3} & \frac{\hat{b}_{33}}{s-\lambda_3} & \frac{\hat{b}_{34}}{s-\lambda_3} & \frac{\hat{b}_{35}}{s-\lambda_3} & \frac{\hat{b}_{36}}{s-\lambda_3} \\ \hline \frac{\hat{b}_{41}}{s-\lambda_4} & \frac{\hat{b}_{42}}{s-\lambda_4} & \frac{\hat{b}_{43}}{s-\lambda_4} & \frac{\hat{b}_{44}}{s-\lambda_4} & \frac{\hat{b}_{45}}{s-\lambda_4} & \frac{\hat{b}_{46}}{s-\lambda_4} \\ \frac{\hat{b}_{51}}{s-\lambda_5} & \frac{\hat{b}_{52}}{s-\lambda_5} & \frac{\hat{b}_{53}}{s-\lambda_5} & \frac{\hat{b}_{54}}{s-\lambda_5} & \frac{\hat{b}_{55}}{s-\lambda_5} & \frac{\hat{b}_{56}}{s-\lambda_5} \\ \frac{\hat{b}_{61}}{s-\lambda_6} & \frac{\hat{b}_{62}}{s-\lambda_6} & \frac{\hat{b}_{63}}{s-\lambda_6} & \frac{\hat{b}_{64}}{s-\lambda_6} & \frac{\hat{b}_{65}}{s-\lambda_6} & \frac{\hat{b}_{66}}{s-\lambda_6} \\ \hline \frac{\hat{b}_{71}}{s-\lambda_7} & \frac{\hat{b}_{72}}{s-\lambda_7} & \frac{\hat{b}_{73}}{s-\lambda_7} & \frac{\hat{b}_{74}}{s-\lambda_7} & \frac{\hat{b}_{75}}{s-\lambda_7} & \frac{\hat{b}_{76}}{s-\lambda_7} \\ \frac{\hat{b}_{81}}{s-\lambda_8} & \frac{\hat{b}_{82}}{s-\lambda_8} & \frac{\hat{b}_{83}}{s-\lambda_8} & \frac{\hat{b}_{84}}{s-\lambda_8} & \frac{\hat{b}_{85}}{s-\lambda_8} & \frac{\hat{b}_{86}}{s-\lambda_8} \\ \frac{\hat{b}_{91}}{s-\lambda_9} & \frac{\hat{b}_{92}}{s-\lambda_9} & \frac{\hat{b}_{93}}{s-\lambda_9} & \frac{\hat{b}_{94}}{s-\lambda_9} & \frac{\hat{b}_{95}}{s-\lambda_9} & \frac{\hat{b}_{96}}{s-\lambda_9} \\ \hline \frac{\hat{b}_{10,1}}{s-\lambda_{10}} & \frac{\hat{b}_{10,2}}{s-\lambda_{10}} & \frac{\hat{b}_{10,3}}{s-\lambda_{10}} & \frac{\hat{b}_{10,4}}{s-\lambda_{10}} & \frac{\hat{b}_{10,5}}{s-\lambda_{10}} & \frac{\hat{b}_{10,6}}{s-\lambda_{10}} \\ \frac{\hat{b}_{11,1}}{s-\lambda_{11}} & \frac{\hat{b}_{11,2}}{s-\lambda_{11}} & \frac{\hat{b}_{11,3}}{s-\lambda_{11}} & \frac{\hat{b}_{11,4}}{s-\lambda_{11}} & \frac{\hat{b}_{11,5}}{s-\lambda_{11}} & \frac{\hat{b}_{11,6}}{s-\lambda_{11}} \\ \frac{\hat{b}_{12,1}}{s-\lambda_{12}} & \frac{\hat{b}_{12,2}}{s-\lambda_{12}} & \frac{\hat{b}_{12,3}}{s-\lambda_{12}} & \frac{\hat{b}_{12,4}}{s-\lambda_{12}} & \frac{\hat{b}_{12,5}}{s-\lambda_{12}} & \frac{\hat{b}_{12,6}}{s-\lambda_{12}} \\ \hline \frac{\hat{b}_{13,1}}{s-\lambda_{13}} & \frac{\hat{b}_{13,2}}{s-\lambda_{13}} & \frac{\hat{b}_{13,3}}{s-\lambda_{13}} & \frac{\hat{b}_{13,4}}{s-\lambda_{13}} & \frac{\hat{b}_{13,5}}{s-\lambda_{13}} & \frac{\hat{b}_{13,6}}{s-\lambda_{13}} \\ \frac{\hat{b}_{14,1}}{s-\lambda_{14}} & \frac{\hat{b}_{14,2}}{s-\lambda_{14}} & \frac{\hat{b}_{14,3}}{s-\lambda_{14}} & \frac{\hat{b}_{14,4}}{s-\lambda_{14}} & \frac{\hat{b}_{14,5}}{s-\lambda_{14}} & \frac{\hat{b}_{14,6}}{s-\lambda_{14}} \\ \frac{\hat{b}_{15,1}}{s-\lambda_{15}} & \frac{\hat{b}_{15,2}}{s-\lambda_{15}} & \frac{\hat{b}_{15,3}}{s-\lambda_{15}} & \frac{\hat{b}_{15,4}}{s-\lambda_{15}} & \frac{\hat{b}_{15,5}}{s-\lambda_{15}} & \frac{\hat{b}_{15,6}}{s-\lambda_{15}} \end{array}\right] \begin{bmatrix} \Delta P_{m1} \\ \Delta P_{m2} \\ \Delta P_{m3} \\ \hline \Delta V_{ref\,1} \\ \Delta V_{ref\,2} \\ \Delta V_{ref\,3} \end{bmatrix} \tag{5.92}$$

The transfer function matrix has the form,

$$\begin{bmatrix} \tilde{\boldsymbol{\omega}}_1(s) \\ \tilde{\boldsymbol{\omega}}_2(s) \\ \tilde{\boldsymbol{\omega}}_3(s) \end{bmatrix} = \begin{bmatrix} \Omega_{1,1}(s) & \Omega_{1,2}(s) & \Omega_{1,3}(s) & \Omega_{1,4}(s) & \Omega_{1,5}(s) & \Omega_{1,6}(s) \\ \Omega_{2,1}(s) & \Omega_{2,2}(s) & \Omega_{2,3}(s) & \Omega_{2,4}(s) & \Omega_{2,5}(s) & \Omega_{2,6}(s) \\ \Omega_{3,1}(s) & \Omega_{3,2}(s) & \Omega_{3,3}(s) & \Omega_{3,4}(s) & \Omega_{3,5}(s) & \Omega_{3,6}(s) \end{bmatrix} \begin{bmatrix} \mathbf{P}_{m1}(s) \\ \mathbf{P}_{m2}(s) \\ \mathbf{P}_{m3}(s) \\ \hline \mathbf{V}_{ref\,1}(s) \\ \mathbf{V}_{ref\,2}(s) \\ \mathbf{V}_{ref\,3}(s) \end{bmatrix} \tag{5.93}$$

where,

$$\Omega_{1,1}(s) = \frac{\Delta\tilde{\omega}_1{}^1(s)}{\Delta P_1(s)} = \frac{\hat{b}_{1,1}\hat{c}_{1,1}}{s-\lambda_1} + \frac{\hat{b}_{2,1}\hat{c}_{1,2}}{s-\lambda_2} + \frac{\hat{b}_{3,1}\hat{c}_{1,3}}{s-\lambda_3} + \cdots + \frac{\hat{b}_{15,1}\hat{c}_{1,15}}{s-\lambda_{15}}$$

$$\Omega_{2,1}(s) = \frac{\Delta\tilde{\omega}_2{}^1(s)}{\Delta P_{m1}(s)} = \frac{\hat{b}_{1,1}\hat{c}_{2,1}}{s-\lambda_1} + \frac{\hat{b}_{2,1}\hat{c}_{2,2}}{s-\lambda_2} + \frac{\hat{b}_{3,1}\hat{c}_{2,3}}{s-\lambda_3} + \cdots + \frac{\hat{b}_{15,1}\hat{c}_{2,15}}{s-\lambda_{15}}$$

$$\Omega_{3,1}(s) = \frac{\Delta\tilde{\omega}_3{}^1(s)}{\Delta P_{m1}(s)} = \frac{\hat{b}_{1,1}\hat{c}_{3,1}}{s-\lambda_1} + \frac{\hat{b}_{2,1}\hat{c}_{3,2}}{s-\lambda_2} + \frac{\hat{b}_{3,1}\hat{c}_{3,3}}{s-\lambda_3} + \cdots + \frac{\hat{b}_{15,1}\hat{c}_{3,15}}{s-\lambda_{15}}$$

$$\Omega_{1,2}(s)=\frac{\Delta\tilde{\omega}_1^{\,1}(s)}{\Delta P_{m2}(s)}=\frac{\hat{b}_{1,2}\hat{c}_{1,1}}{s-\lambda_1}+\frac{\hat{b}_{2,2}\hat{c}_{1,2}}{s-\lambda_2}+\frac{\hat{b}_{3,2}\hat{c}_{1,3}}{s-\lambda_3}+\cdots+\frac{\hat{b}_{15,2}\hat{c}_{1,15}}{s-\lambda_{15}}$$

$$\Omega_{2,2}(s)=\frac{\Delta\tilde{\omega}_2^{\,1}(s)}{\Delta P_{m2}(s)}=\frac{\hat{b}_{1,2}\hat{c}_{2,1}}{s-\lambda_1}+\frac{\hat{b}_{2,2}\hat{c}_{2,2}}{s-\lambda_2}+\frac{\hat{b}_{3,2}\hat{c}_{2,3}}{s-\lambda_3}+\cdots+\frac{\hat{b}_{15,2}\hat{c}_{2,15}}{s-\lambda_{15}}$$

$$\Omega_{2,3}(s)=\frac{\Delta\tilde{\omega}_3^{\,1}(s)}{\Delta P_{m2}(s)}=\frac{\hat{b}_{1,2}\hat{c}_{3,1}}{s-\lambda_1}+\frac{\hat{b}_{2,2}\hat{c}_{3,2}}{s-\lambda_2}+\frac{\hat{b}_{3,2}\hat{c}_{3,3}}{s-\lambda_3}+\cdots+\frac{\hat{b}_{15,2}\hat{c}_{3,15}}{s-\lambda_{15}}$$

$$\Omega_{1,3}(s)=\frac{\Delta\tilde{\omega}_1^{\,1}(s)}{\Delta P_{m3}(s)}=\frac{\hat{b}_{1,3}\hat{c}_{1,1}}{s-\lambda_1}+\frac{\hat{b}_{2,3}\hat{c}_{1,2}}{s-\lambda_2}+\frac{\hat{b}_{3,3}\hat{c}_{1,3}}{s-\lambda_3}+\cdots+\frac{\hat{b}_{15,3}\hat{c}_{1,15}}{s-\lambda_{15}}$$

$$\Omega_{2,3}(s)=\frac{\Delta\tilde{\omega}_2^{\,1}(s)}{\Delta P_{m3}(s)}=\frac{\hat{b}_{1,3}\hat{c}_{2,1}}{s-\lambda_1}+\frac{\hat{b}_{2,3}\hat{c}_{2,2}}{s-\lambda_2}+\frac{\hat{b}_{3,3}\hat{c}_{2,3}}{s-\lambda_3}+\cdots+\frac{\hat{b}_{15,3}\hat{c}_{2,15}}{s-\lambda_{15}}$$

$$\Omega_{3,3}(s)=\frac{\Delta\tilde{\omega}_3^{\,1}(s)}{\Delta P_{m3}(s)}=\frac{\hat{b}_{1,3}\hat{c}_{3,1}}{s-\lambda_1}+\frac{\hat{b}_{2,3}\hat{c}_{3,2}}{s-\lambda_2}+\frac{\hat{b}_{3,3}\hat{c}_{3,3}}{s-\lambda_3}+\cdots+\frac{\hat{b}_{15,3}\hat{c}_{3,15}}{s-\lambda_{15}}$$

$$\Omega_{1,4}(s)=\frac{\Delta\tilde{\omega}_1^{\,1}(s)}{\Delta V_{ref\,1}(s)}=\frac{\hat{b}_{1,4}\hat{c}_{1,1}}{s-\lambda_1}+\frac{\hat{b}_{2,4}\hat{c}_{1,2}}{s-\lambda_2}+\frac{\hat{b}_{3,4}\hat{c}_{1,3}}{s-\lambda_3}+\cdots+\frac{\hat{b}_{15,4}\hat{c}_{1,15}}{s-\lambda_{15}}$$

$$\Omega_{2,4}(s)=\frac{\Delta\tilde{\omega}_2^{\,1}(s)}{\Delta V_{ref\,1}(s)}=\frac{\hat{b}_{1,4}\hat{c}_{2,1}}{s-\lambda_1}+\frac{\hat{b}_{2,4}\hat{c}_{2,2}}{s-\lambda_2}+\frac{\hat{b}_{3,4}\hat{c}_{2,3}}{s-\lambda_3}+\cdots+\frac{\hat{b}_{15,4}\hat{c}_{2,15}}{s-\lambda_{15}}$$

$$\Omega_{3,4}(s)=\frac{\Delta\tilde{\omega}_3^{\,1}(s)}{\Delta V_{ref\,1}(s)}=\frac{\hat{b}_{1,4}\hat{c}_{3,1}}{s-\lambda_1}+\frac{\hat{b}_{2,4}\hat{c}_{3,2}}{s-\lambda_2}+\frac{\hat{b}_{3,4}\hat{c}_{3,3}}{s-\lambda_3}+\cdots+\frac{\hat{b}_{15,4}\hat{c}_{3,15}}{s-\lambda_{15}}$$

$$\Omega_{1,5}(s)=\frac{\Delta\tilde{\omega}_1^{\,1}(s)}{\Delta V_{ref\,2}(s)}=\frac{\hat{b}_{1,5}\hat{c}_{1,1}}{s-\lambda_1}+\frac{\hat{b}_{2,5}\hat{c}_{1,2}}{s-\lambda_2}+\frac{\hat{b}_{3,5}\hat{c}_{1,3}}{s-\lambda_3}+\cdots+\frac{\hat{b}_{15,5}\hat{c}_{1,15}}{s-\lambda_{15}}$$

$$\Omega_{2,5}(s)=\frac{\Delta\tilde{\omega}_2^{\,1}(s)}{\Delta V_{ref\,2}(s)}=\frac{\hat{b}_{1,5}\hat{c}_{2,1}}{s-\lambda_1}+\frac{\hat{b}_{2,5}\hat{c}_{2,2}}{s-\lambda_2}+\frac{\hat{b}_{3,5}\hat{c}_{2,3}}{s-\lambda_3}+\cdots+\frac{\hat{b}_{15,5}\hat{c}_{2,15}}{s-\lambda_{15}}$$

$$\Omega_{3,5}(s)=\frac{\Delta\tilde{\omega}_3^{\,1}(s)}{\Delta V_{ref\,2}(s)}=\frac{\hat{b}_{1,5}\hat{c}_{3,1}}{s-\lambda_1}+\frac{\hat{b}_{2,5}\hat{c}_{3,2}}{s-\lambda_2}+\frac{\hat{b}_{3,5}\hat{c}_{3,3}}{s-\lambda_3}+\cdots+\frac{\hat{b}_{15,5}\hat{c}_{3,15}}{s-\lambda_{15}}$$

$$\Omega_{1,6}(s)=\frac{\Delta\tilde{\omega}_1^{\,1}(s)}{\Delta V_{ref\,3}(s)}=\frac{\hat{b}_{1,6}\hat{c}_{1,1}}{s-\lambda_1}+\frac{\hat{b}_{2,6}\hat{c}_{1,2}}{s-\lambda_2}+\frac{\hat{b}_{3,6}\hat{c}_{1,3}}{s-\lambda_3}+\cdots+\frac{\hat{b}_{15,6}\hat{c}_{1,15}}{s-\lambda_{15}}$$

$$\Omega_{2,6}(s)=\frac{\Delta\tilde{\omega}_2^{\,1}(s)}{\Delta V_{ref\,3}(s)}=\frac{\hat{b}_{1,6}\hat{c}_{2,1}}{s-\lambda_1}+\frac{\hat{b}_{2,6}\hat{c}_{2,2}}{s-\lambda_2}+\frac{\hat{b}_{3,6}\hat{c}_{2,3}}{s-\lambda_3}+\cdots+\frac{\hat{b}_{15,6}\hat{c}_{2,15}}{s-\lambda_{15}}$$

$$\Omega_{3,6}(s)=\frac{\Delta\tilde{\omega}_3^{\,1}(s)}{\Delta V_{ref\,3}(s)}=\frac{\hat{b}_{1,6}\hat{c}_{3,1}}{s-\lambda_1}+\frac{\hat{b}_{2,6}\hat{c}_{3,2}}{s-\lambda_2}+\frac{\hat{b}_{3,6}\hat{c}_{3,3}}{s-\lambda_3}+\cdots+\frac{\hat{b}_{15,6}\hat{c}_{3,15}}{s-\lambda_{15}}$$

In general, the linear transfer functions are,

$$\Omega^1_{i,j}(s) = \sum_{k=1}^{n} \frac{\hat{b}_{k,j}\hat{c}_{i,k}}{s-\lambda_k} \tag{5.94}$$

with $i = 1,\ldots,o$ $o = 3 =$ number of output variables

$j = 1,\ldots,r$ $r = 6 =$ number of input variables

$n = 15 =$ number of state variables

- Second order transfer functions

To formulate the second order transfer function, it is necessary to consider the system as a Single Input-Single Output in order to form the transfer function matrix, that is,

$$\begin{bmatrix} \tilde{\delta}^2_1(s) \\ \tilde{\delta}^2_2(s) \\ \tilde{\delta}^2_3(s) \\ \hline \tilde{\omega}^2_1(s) \\ \tilde{\omega}^2_2(s) \\ \tilde{\omega}^2_3(s) \\ \hline \tilde{E}'^2_{q1}(s) \\ \tilde{E}'^2_{q2}(s) \\ \tilde{E}'^2_{q3}(s) \\ \hline \tilde{E}'^2_{d1}(s) \\ \tilde{E}'^2_{d2}(s) \\ \tilde{E}'^2_{d3}(s) \\ \hline \tilde{E}^2_{fd1}(s) \\ \tilde{E}^2_{fd2}(s) \\ \tilde{E}^2_{fd3}(s) \end{bmatrix} = \left[\begin{array}{ccc|ccc} G^2_{1,1}(s) & G^2_{1,2}(s) & G^2_{1,3}(s) & G^2_{1,4}(s) & G^2_{1,5}(s) & G^2_{1,6}(s) \\ G^2_{2,1}(s) & G^2_{2,2}(s) & G^2_{2,3}(s) & G^2_{2,4}(s) & G^2_{2,5}(s) & G^2_{2,6}(s) \\ G^2_{3,1}(s) & G^2_{3,2}(s) & G^2_{3,3}(s) & G^2_{3,4}(s) & G^2_{3,5}(s) & G^2_{3,6}(s) \\ \hline G^2_{4,1}(s) & G^2_{4,2}(s) & G^2_{4,3}(s) & G^2_{4,4}(s) & G^2_{4,5}(s) & G^2_{4,6}(s) \\ G^2_{5,1}(s) & G^2_{5,2}(s) & G^2_{5,3}(s) & G^2_{5,4}(s) & G^2_{5,5}(s) & G^2_{5,6}(s) \\ G^2_{6,1}(s) & G^2_{6,2}(s) & G^2_{6,3}(s) & G^2_{6,4}(s) & G^2_{6,5}(s) & G^2_{6,6}(s) \\ \hline G^2_{7,1}(s) & G^2_{7,2}(s) & G^2_{7,3}(s) & G^2_{7,4}(s) & G^2_{7,5}(s) & G^2_{7,6}(s) \\ G^2_{8,1}(s) & G^2_{8,2}(s) & G^2_{8,3}(s) & G^2_{8,4}(s) & G^2_{8,5}(s) & G^2_{8,6}(s) \\ G^2_{9,1}(s) & G^2_{9,2}(s) & G^2_{9,3}(s) & G^2_{9,4}(s) & G^2_{9,5}(s) & G^2_{9,6}(s) \\ \hline G^2_{10,1}(s) & G^2_{10,2}(s) & G^2_{10,3}(s) & G^2_{10,4}(s) & G^2_{10,5}(s) & G^2_{10,6}(s) \\ G^2_{11,1}(s) & G^2_{11,2}(s) & G^2_{11,3}(s) & G^2_{11,4}(s) & G^2_{11,5}(s) & G^2_{11,6}(s) \\ G^2_{12,1}(s) & G^2_{12,2}(s) & G^2_{12,3}(s) & G^2_{12,4}(s) & G^2_{12,5}(s) & G^2_{12,6}(s) \\ \hline G^2_{13,1}(s) & G^2_{13,2}(s) & G^2_{13,3}(s) & G^2_{13,4}(s) & G^2_{13,5}(s) & G^2_{13,6}(s) \\ G^2_{14,1}(s) & G^2_{14,2}(s) & G^2_{14,3}(s) & G^2_{14,4}(s) & G^2_{14,5}(s) & G^2_{14,6}(s) \\ G^2_{15,1}(s) & G^2_{15,2}(s) & G^2_{15,3}(s) & G^2_{15,4}(s) & G^2_{15,5}(s) & G^2_{15,6}(s) \end{array}\right] \begin{bmatrix} \mathbf{P}_{m1}(s) \\ \mathbf{P}_{m2}(s) \\ \mathbf{P}_{m3}(s) \\ \hline \mathbf{V}_{ref\,1}(s) \\ \mathbf{V}_{ref\,2}(s) \\ \mathbf{V}_{ref\,3}(s) \end{bmatrix} \tag{5.95}$$

where $G^2_{p,q}(s) = \sum_{j=1}^{n}\sum_{k=1}^{n}\sum_{l=1}^{n} h^j_{2kl}\hat{b}_{pk}\hat{b}_{ql}\left\{\frac{1}{(s-\lambda_k-\lambda_l)} - \frac{1}{(s-\lambda_j)}\right\}$ with $p = 1,2,\ldots,n$ $n = 15$

$q = 1,2,\ldots,r$ $r = 6$

From here, (5.95) is developed considering the selected output variables, which in this case study are the rotor speed deviations ($\omega_1, \omega_2, \omega_3$), to obtain individual transfer functions that are grouped to form the transfer function matrix. For instance, the first transfer function is formed as,

$$
\begin{aligned}
\frac{\Delta\tilde{\omega}_1^2(s)}{\Delta P_{m1}} = \hat{c}_{1,1}&\left[\begin{array}{l}
h^1_{2(1,1)}\hat{b}_{1,1}\hat{b}_{1,1}\left\{\frac{1}{(s-\lambda_1-\lambda_1)}-\frac{1}{(s-\lambda_1)}\right\}+h^1_{2(1,2)}\hat{b}_{1,1}\hat{b}_{1,2}\left\{\frac{1}{(s-\lambda_1-\lambda_2)}-\frac{1}{(s-\lambda_1)}\right\}+\cdots+\\
h^1_{2(1,15)}\hat{b}_{1,1}\hat{b}_{1,15}\left\{\frac{1}{(s-\lambda_1-\lambda_{15})}-\frac{1}{(s-\lambda_1)}\right\}+h^1_{2(2,1)}\hat{b}_{1,2}\hat{b}_{1,1}\left\{\frac{1}{(s-\lambda_2-\lambda_1)}-\frac{1}{(s-\lambda_1)}\right\}+\\
h^1_{2(2,2)}\hat{b}_{1,2}\hat{b}_{1,2}\left\{\frac{1}{(s-\lambda_2-\lambda_2)}-\frac{1}{(s-\lambda_1)}\right\}+\cdots+h^1_{2(2,15)}\hat{b}_{1,2}\hat{b}_{1,15}\left\{\frac{1}{(s-\lambda_2-\lambda_{15})}-\frac{1}{(s-\lambda_1)}\right\}+\ldots+\\
h^1_{2(15,1)}\hat{b}_{1,15}\hat{b}_{1,1}\left\{\frac{1}{(s-\lambda_{15}-\lambda_1)}-\frac{1}{(s-\lambda_1)}\right\}+h^1_{2(15,2)}\hat{b}_{1,15}\hat{b}_{1,2}\left\{\frac{1}{(s-\lambda_{15}-\lambda_2)}-\frac{1}{(s-\lambda_1)}\right\}+\cdots+\\
h^1_{2(15,15)}\hat{b}_{1,15}\hat{b}_{1,15}\left\{\frac{1}{(s-\lambda_{15}-\lambda_{15})}-\frac{1}{(s-\lambda_1)}\right\}
\end{array}\right]+\\
&\hat{c}_{1,2}\left[\begin{array}{l}
h^1_{2(1,1)}\hat{b}_{1,1}\hat{b}_{1,1}\left\{\frac{1}{(s-\lambda_1-\lambda_1)}-\frac{1}{(s-\lambda_1)}\right\}+h^1_{2(1,2)}\hat{b}_{1,1}\hat{b}_{1,2}\left\{\frac{1}{(s-\lambda_1-\lambda_2)}-\frac{1}{(s-\lambda_1)}\right\}+\cdots+\\
h^1_{2(1,15)}\hat{b}_{1,1}\hat{b}_{1,15}\left\{\frac{1}{(s-\lambda_1-\lambda_{15})}-\frac{1}{(s-\lambda_1)}\right\}+h^1_{2(2,1)}\hat{b}_{1,2}\hat{b}_{1,1}\left\{\frac{1}{(s-\lambda_2-\lambda_1)}-\frac{1}{(s-\lambda_1)}\right\}+\\
h^1_{2(2,2)}\hat{b}_{1,2}\hat{b}_{1,2}\left\{\frac{1}{(s-\lambda_2-\lambda_2)}-\frac{1}{(s-\lambda_1)}\right\}+\cdots+h^1_{2(2,15)}\hat{b}_{1,2}\hat{b}_{1,15}\left\{\frac{1}{(s-\lambda_2-\lambda_{15})}-\frac{1}{(s-\lambda_1)}\right\}+\ldots+\\
h^1_{2(15,1)}\hat{b}_{1,15}\hat{b}_{1,1}\left\{\frac{1}{(s-\lambda_{15}-\lambda_1)}-\frac{1}{(s-\lambda_1)}\right\}+h^1_{2(15,2)}\hat{b}_{1,15}\hat{b}_{1,2}\left\{\frac{1}{(s-\lambda_{15}-\lambda_2)}-\frac{1}{(s-\lambda_1)}\right\}+\cdots+\\
h^1_{2(15,15)}\hat{b}_{1,15}\hat{b}_{1,15}\left\{\frac{1}{(s-\lambda_{15}-\lambda_{15})}-\frac{1}{(s-\lambda_1)}\right\}
\end{array}\right]+\cdots\\
&\hat{c}_{1,15}\left[\begin{array}{l}
h^1_{2(1,1)}\hat{b}_{1,1}\hat{b}_{1,1}\left\{\frac{1}{(s-\lambda_1-\lambda_1)}-\frac{1}{(s-\lambda_1)}\right\}+h^1_{2(1,2)}\hat{b}_{1,1}\hat{b}_{1,2}\left\{\frac{1}{(s-\lambda_1-\lambda_2)}-\frac{1}{(s-\lambda_1)}\right\}+\cdots+\\
h^1_{2(1,15)}\hat{b}_{1,1}\hat{b}_{1,15}\left\{\frac{1}{(s-\lambda_1-\lambda_{15})}-\frac{1}{(s-\lambda_1)}\right\}+h^1_{2(2,1)}\hat{b}_{1,2}\hat{b}_{1,1}\left\{\frac{1}{(s-\lambda_2-\lambda_1)}-\frac{1}{(s-\lambda_1)}\right\}+\\
h^1_{2(2,2)}\hat{b}_{1,2}\hat{b}_{1,2}\left\{\frac{1}{(s-\lambda_2-\lambda_2)}-\frac{1}{(s-\lambda_1)}\right\}+\cdots+h^1_{2(2,15)}\hat{b}_{1,2}\hat{b}_{1,15}\left\{\frac{1}{(s-\lambda_2-\lambda_{15})}-\frac{1}{(s-\lambda_1)}\right\}+\ldots+\\
h^1_{2(15,1)}\hat{b}_{1,15}\hat{b}_{1,1}\left\{\frac{1}{(s-\lambda_{15}-\lambda_1)}-\frac{1}{(s-\lambda_1)}\right\}+h^1_{2(15,2)}\hat{b}_{1,15}\hat{b}_{1,2}\left\{\frac{1}{(s-\lambda_{15}-\lambda_2)}-\frac{1}{(s-\lambda_1)}\right\}+\cdots+\\
h^1_{2(15,15)}\hat{b}_{1,15}\hat{b}_{1,15}\left\{\frac{1}{(s-\lambda_{15}-\lambda_{15})}-\frac{1}{(s-\lambda_1)}\right\}
\end{array}\right]
\end{aligned}
\tag{5.96}
$$

In the same way, the rest of transfer functions are defined and then grouped in matrix form in order to complete the transfer function matrix as,

$$
\begin{bmatrix}\tilde{\boldsymbol{\omega}}_1(s)\\ \tilde{\boldsymbol{\omega}}_2(s)\\ \tilde{\boldsymbol{\omega}}_3(s)\end{bmatrix}=\begin{bmatrix}\Omega^2{}_{1,1}(s) & \Omega^2{}_{1,2}(s) & \Omega^2{}_{1,3}(s) & \Omega^2{}_{1,4}(s) & \Omega^2{}_{1,5}(s) & \Omega^2{}_{1,6}(s)\\ \Omega^2{}_{2,1}(s) & \Omega^2{}_{2,2}(s) & \Omega^2{}_{2,3}(s) & \Omega^2{}_{2,4}(s) & \Omega^2{}_{2,5}(s) & \Omega^2{}_{2,6}(s)\\ \Omega^2{}_{3,1}(s) & \Omega^2{}_{3,2}(s) & \Omega^2{}_{3,3}(s) & \Omega^2{}_{3,4}(s) & \Omega^2{}_{3,5}(s) & \Omega^2{}_{3,6}(s)\end{bmatrix}\begin{bmatrix}\mathbf{P}_{m1}(s)\\ \mathbf{P}_{m2}(s)\\ \mathbf{P}_{m3}(s)\\ \hline \mathbf{V}_{ref\,1}(s)\\ \mathbf{V}_{ref\,2}(s)\\ \mathbf{V}_{ref\,3}(s)\end{bmatrix}
\tag{5.97}
$$

where

$$\Omega^2_{(1,1)}(s)=\frac{\tilde{\omega}_1^2(s)}{\Delta P_{m1}(s)}=\hat{c}_{1,1}\left[\sum_{k=1}^{n}\sum_{l=1}^{n}h^1_{2kl}\hat{b}_{k1}\hat{b}_{l1}\left\{\frac{1}{(s-\lambda_k-\lambda_l)}-\frac{1}{(s-\lambda_1)}\right\}\right]+\hat{c}_{1,2}\left[\sum_{k=1}^{n}\sum_{l=1}^{n}h^1_{2kl}\hat{b}_{k1}\hat{b}_{l1}\left\{\frac{1}{(s-\lambda_k-\lambda_l)}-\frac{1}{(s-\lambda_1)}\right\}\right]$$
$$+\cdots+\hat{c}_{1,15}\left[\sum_{k=1}^{n}\sum_{l=1}^{n}h^1_{2kl}\hat{b}_{k1}\hat{b}_{l1}\left\{\frac{1}{(s-\lambda_k-\lambda_l)}-\frac{1}{(s-\lambda_1)}\right\}\right]$$

$$\Omega^2_{(1,2)}(s)=\frac{\tilde{\omega}_1^2(s)}{\Delta P_{m2}(s)}=\hat{c}_{1,1}\left[\sum_{k=1}^{n}\sum_{l=1}^{n}h^2_{2kl}\hat{b}_{k2}\hat{b}_{l2}\left\{\frac{1}{(s-\lambda_k-\lambda_l)}-\frac{1}{(s-\lambda_2)}\right\}\right]+\hat{c}_{1,2}\left[\sum_{k=1}^{n}\sum_{l=1}^{n}h^2_{2kl}\hat{b}_{k2}\hat{b}_{l2}\left\{\frac{1}{(s-\lambda_k-\lambda_l)}-\frac{1}{(s-\lambda_2)}\right\}\right]$$
$$+\cdots+\hat{c}_{1,15}\left[\sum_{k=1}^{n}\sum_{l=1}^{n}h^2_{2kl}\hat{b}_{k2}\hat{b}_{l2}\left\{\frac{1}{(s-\lambda_k-\lambda_l)}-\frac{1}{(s-\lambda_2)}\right\}\right]$$

$$\Omega^2_{(1,3)}(s)=\frac{\tilde{\omega}_1^2(s)}{\Delta P_{m3}(s)}=\hat{c}_{1,1}\left[\sum_{k=1}^{n}\sum_{l=1}^{n}h^3_{2kl}\hat{b}_{k3}\hat{b}_{l3}\left\{\frac{1}{(s-\lambda_k-\lambda_l)}-\frac{1}{(s-\lambda_3)}\right\}\right]+\hat{c}_{1,2}\left[\sum_{k=1}^{n}\sum_{l=1}^{n}h^3_{2kl}\hat{b}_{k3}\hat{b}_{l3}\left\{\frac{1}{(s-\lambda_k-\lambda_l)}-\frac{1}{(s-\lambda_3)}\right\}\right]$$
$$+\cdots+\hat{c}_{1,15}\left[\sum_{k=1}^{n}\sum_{l=1}^{n}h^3_{2kl}\hat{b}_{k3}\hat{b}_{l3}\left\{\frac{1}{(s-\lambda_k-\lambda_l)}-\frac{1}{(s-\lambda_3)}\right\}\right]$$

$$\Omega^2_{(1,4)}(s)=\frac{\tilde{\omega}_1^2(s)}{\Delta V_{ref1}(s)}=\hat{c}_{1,1}\left[\sum_{k=1}^{n}\sum_{l=1}^{n}h^4_{2kl}\hat{b}_{k4}\hat{b}_{l4}\left\{\frac{1}{(s-\lambda_k-\lambda_l)}-\frac{1}{(s-\lambda_4)}\right\}\right]+\hat{c}_{1,2}\left[\sum_{k=1}^{n}\sum_{l=1}^{n}h^4_{2kl}\hat{b}_{k4}\hat{b}_{l4}\left\{\frac{1}{(s-\lambda_k-\lambda_l)}-\frac{1}{(s-\lambda_4)}\right\}\right]$$
$$+\cdots+\hat{c}_{1,15}\left[\sum_{k=1}^{n}\sum_{l=1}^{n}h^4_{2kl}\hat{b}_{k4}\hat{b}_{l4}\left\{\frac{1}{(s-\lambda_k-\lambda_l)}-\frac{1}{(s-\lambda_4)}\right\}\right]$$

$$\Omega^2_{(1,5)}(s)=\frac{\tilde{\omega}_1^2(s)}{\Delta V_{ref2}(s)}=\hat{c}_{1,1}\left[\sum_{k=1}^{n}\sum_{l=1}^{n}h^5_{2kl}\hat{b}_{k5}\hat{b}_{l5}\left\{\frac{1}{(s-\lambda_k-\lambda_l)}-\frac{1}{(s-\lambda_5)}\right\}\right]+\hat{c}_{1,2}\left[\sum_{k=1}^{n}\sum_{l=1}^{n}h^5_{2kl}\hat{b}_{k5}\hat{b}_{l5}\left\{\frac{1}{(s-\lambda_k-\lambda_l)}-\frac{1}{(s-\lambda_5)}\right\}\right]$$
$$+\cdots+\hat{c}_{1,15}\left[\sum_{k=1}^{n}\sum_{l=1}^{n}h^5_{2kl}\hat{b}_{k5}\hat{b}_{l5}\left\{\frac{1}{(s-\lambda_k-\lambda_l)}-\frac{1}{(s-\lambda_5)}\right\}\right]$$

$$\Omega^2_{(1,6)}(s)=\frac{\tilde{\omega}_1^2(s)}{\Delta V_{ref3}(s)}=\hat{c}_{1,1}\left[\sum_{k=1}^{n}\sum_{l=1}^{n}h^6_{2kl}\hat{b}_{k6}\hat{b}_{l6}\left\{\frac{1}{(s-\lambda_k-\lambda_l)}-\frac{1}{(s-\lambda_6)}\right\}\right]+\hat{c}_{1,2}\left[\sum_{k=1}^{n}\sum_{l=1}^{n}h^6_{2kl}\hat{b}_{k6}\hat{b}_{l6}\left\{\frac{1}{(s-\lambda_k-\lambda_l)}-\frac{1}{(s-\lambda_6)}\right\}\right]$$
$$+\cdots+\hat{c}_{1,15}\left[\sum_{k=1}^{n}\sum_{l=1}^{n}h^6_{2kl}\hat{b}_{k6}\hat{b}_{l6}\left\{\frac{1}{(s-\lambda_k-\lambda_l)}-\frac{1}{(s-\lambda_6)}\right\}\right]$$

$$\vdots$$

In the general case,

$$\Omega^2_{(i,j)}(s)=\frac{\tilde{\omega}_i^2(s)}{U_j(s)}=\sum_{p=1}^{n}\hat{c}_{i,p}\left[\sum_{k=1}^{n}\sum_{l=1}^{n}h^j_{2kl}\hat{b}_{kj}\hat{b}_{lj}\left\{\frac{1}{(s-\lambda_k-\lambda_l)}-\frac{1}{(s-\lambda_j)}\right\}\right] \tag{5.98}$$

with $i=1,\ldots,o \qquad o=3$

$j=1,\ldots,r \qquad r=6$

That is, the input signal is chosen as the input mechanical torque, for which it is possible to determine the transfer function of any state variable. Upon rearranging terms, we obtain the transfer functions defined by Equation (5.98). These equations are amenable to multidimensional Laplace

analysis using the detailed theory of Chapter 3. We emphasize that, unlike previous approaches, the above formulations allows the study of the system behavior in both, the time and frequency domains.

Finally, the complete transfer function for this MIMO system is expressed in matrix form as,

$$\frac{\mathbf{\Omega}(s)}{\Delta\mathbf{U}(s)}=\begin{bmatrix}\frac{\Delta\omega_1(s)}{\Delta P_{m1}(s)}\\ \frac{\Delta\omega_2(s)}{\Delta P_{m2}(s)}\\ \frac{\Delta\omega_3(s)}{\Delta P_{m3}(s)}\\ \frac{\Delta\omega_1(s)}{\Delta V_{ref1}(s)}\\ \frac{\Delta\omega_2(s)}{\Delta V_{ref2}(s)}\\ \frac{\Delta\omega_3(s)}{\Delta V_{ref3}(s)}\end{bmatrix}=\begin{bmatrix}\frac{\Delta\omega_1^1(s)}{\Delta P_{m1}(s)}+\frac{\Delta\omega_1{}^2(s)}{\Delta P_{m1}(s)}+\frac{\Delta\omega_1{}^3(s)}{\Delta P_{m1}(s)}+\dots\\ \frac{\Delta\omega_2^1(s)}{\Delta P_{m2}(s)}+\frac{\Delta\omega_2{}^2(s)}{\Delta P_{m2}(s)}+\frac{\Delta\omega_2{}^3(s)}{\Delta P_{m2}(s)}+\dots\\ \frac{\Delta\omega_3^1(s)}{\Delta P_{m3}(s)}+\frac{\Delta\omega_3{}^2(s)}{\Delta P_{m3}(s)}+\frac{\Delta\omega_3{}^3(s)}{\Delta P_{m3}(s)}+\dots\\ \frac{\Delta\omega_1^1(s)}{\Delta V_{ref1}(s)}+\frac{\Delta\omega_1{}^2(s)}{\Delta V_{ref1}(s)}+\frac{\Delta\omega_1{}^3(s)}{\Delta V_{ref1}(s)}+\dots\\ \frac{\Delta\omega_2^1(s)}{\Delta V_{ref2}(s)}+\frac{\Delta\omega_2{}^2(s)}{\Delta V_{ref2}(s)}+\frac{\Delta\omega_2{}^3(s)}{\Delta V_{ref2}(s)}+\dots\\ \frac{\Delta\omega_3^1(s)}{\Delta V_{ref3}(s)}+\frac{\Delta\omega_3{}^2(s)}{\Delta V_{ref3}(s)}+\frac{\Delta\omega_3{}^3(s)}{\Delta V_{ref3}(s)}+\dots\end{bmatrix} \tag{5.99}$$

5.7.4 Numerical Analysis

The example is conducted following the theory of nonlinear transfer functions through modal series described above. In this study case, the linear transfer functions were defined by (5.93) which are expressed in partial fractions as a result of the modal series expansion.

5.7.4.1 Linear transfer functions

The form of the transfer function is as follows (in this case, only the first transfer function $\Omega^1_{(1,1)}(s)$ is shown as a sake of exemplification) once the parameters of the test power system are substituted in the analytical expressions and the eigenvalues obtained. Hence,

$$\begin{aligned}\Omega^1_{1,1}(s)=&\frac{0.0453-0.0066i}{s-(-1.0618+13.0572i)}+\frac{0.0453+0.0066i}{s-(-1.0618-13.0572i)}+\frac{1.1701+0.0154i}{s-(-0.3744+8.5858i)}+\frac{1.1701-0.0154i}{s-(-0.3744-8.5858i)}-\frac{0.0173}{s+5.8688}+\\ &\frac{0.0516-0.0885i}{s-(-1.5421+2.4311i)}+\frac{0.0516+0.0885i}{s-(-1.5421-2.4311i)}-\frac{0.3588}{s+3.4589}+\frac{0.0864-0.0465i}{s-(-3.2841+0.1123i)}+\frac{0.0864+0.0465i}{s+(3.2841+0.1123i)}+\\ &\frac{0.0403-0.0549i}{s-(-1.8002+1.2864i)}+\frac{0.0403+0.0549i}{s+(1.8002+1.2864i)}+\frac{5.5573}{s+0.1401}+\frac{0.0051}{s+0.9943}\end{aligned} \tag{5.100}$$

This transfer function is of 15th order, being the individual poles the linear combination of original eigenvalues. Similar expressions are obtained for the rest of transfer functions that complete the transfer function matrix in (5.93). In order to obtain the frequency characteristics of the transfer

functions, a Bode analysis is performed using the tools for these purposes developed in Matlab® platform. The Matlab® Control Toolbox possesses well defined routines of Bode and Nyquist analysis that are exploited in this case study. Figure 5.12 shows the Bode and Nyquist graphics for the linear transfer functions $\Omega_{(1,1)}(s)$, $\Omega_{(1,2)}(s)$, $\Omega_{(1,3)}(s)$, $\Omega_{(2,2)}(s)$ and $\Omega_{(3,3)}(s)$ selected due to they present the highest contributions (highest residues).

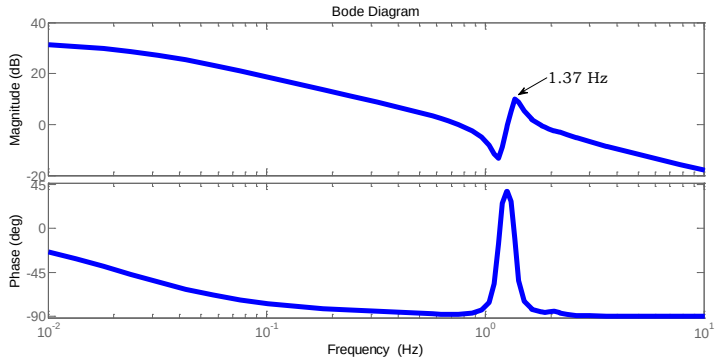

Bode graphic

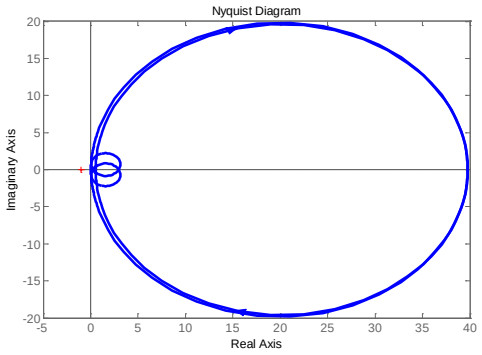

Nyquist Graphic

a) $\Omega^{1}_{(1,1)}$

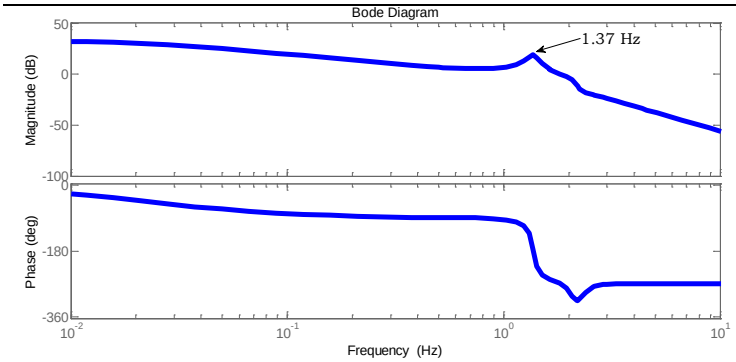

Bode graphic

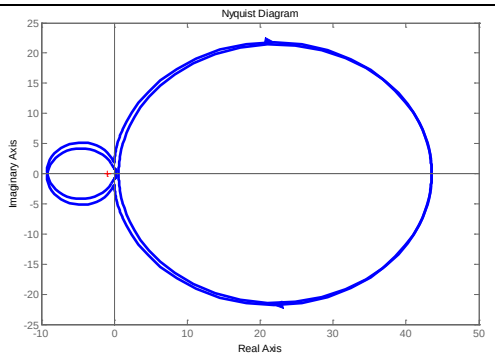

Nyquist Graphic

b) $\Omega^{1}_{(1,2)}$

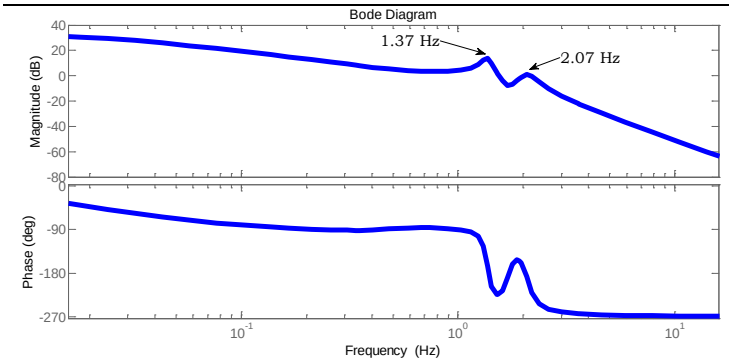

Bode graphic

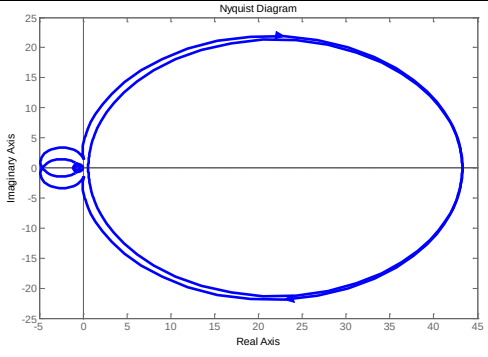

Nyquist Graphic

c) $\Omega^{1}_{(1,3)}$

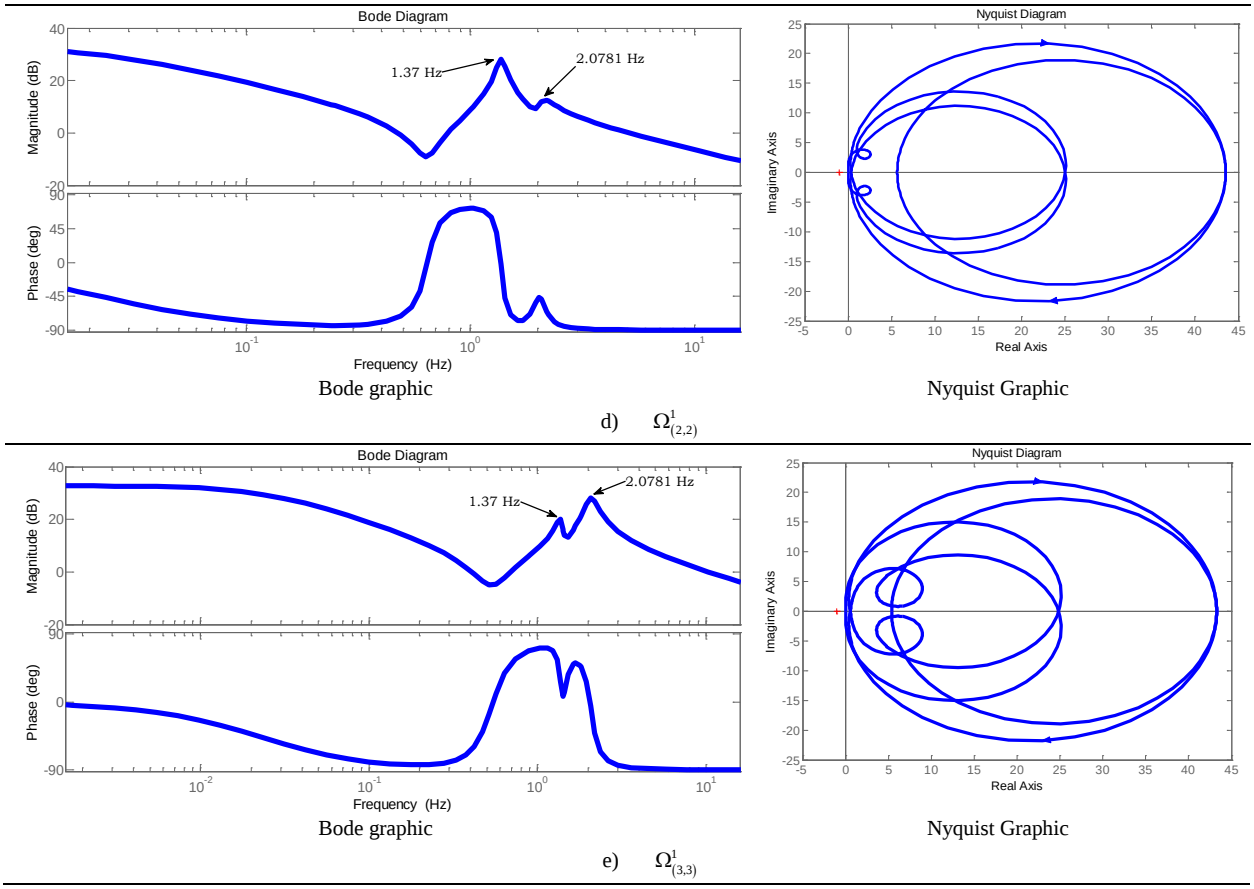

Figure 5.12 Bode and Nyquist diagrams from the linear transfer functions of the 3SM-9 Buses test power system

The frequency combinations observed in this Figure are 2.0781 Hz and 1.3665 Hz. Regarding the details observed in the Figure 5.12, it can be denoted that transfer functions $\Omega_{(1,1)}(s)$ and $\Omega_{(1,2)}(s)$ have predominant frequency contribution of 1.3665 Hz while transfer functions $\Omega_{(1,3)}(s)$, $\Omega_{(2,2)}(s)$ and $\Omega_{(3,3)}(s)$ have resonant contributions of both frequencies 2.0781 Hz and 1.3665 Hz

5.7.4.2 Nonlinear transfer functions

Now, the nonlinear transfer functions are analyzed. Please observe the Figure 5.13, which denotes the Bode and Nyquist graphics for the transfer function $\Omega^2_{(1,2)}(s_1, s_2)$. It is important to notice the several frequency contributions that the Bode graph is showing. This transfer function is an element of the nonlinear transfer function matrix obtained above and detailed in (5.97) for the MIMO system under analysis. Also, there is a fact that the system may be of a huge size since the partial fractions of the transfer functions obtained by modal series are the result of combination of all the possible second order modal combinations. Considering these modal combinations, the poles can originate a transfer

function of almost 6750 order in the system under study. Of course, a higher number is very complicate to handle by a Bode and Nyquist routine.

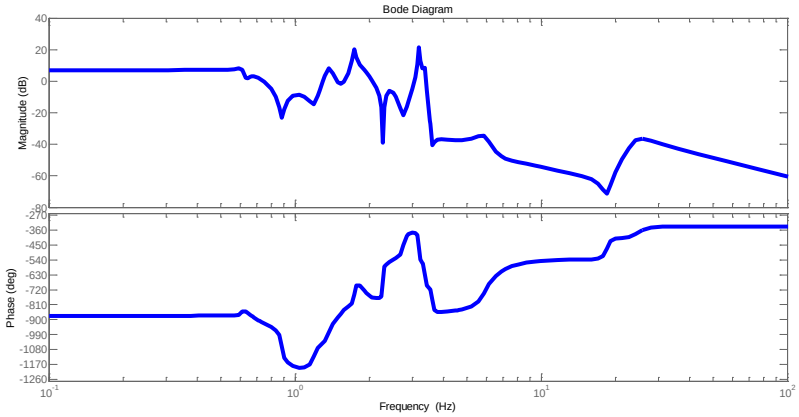

$\Omega^2_{(1,2)}(s_1, s_2)$

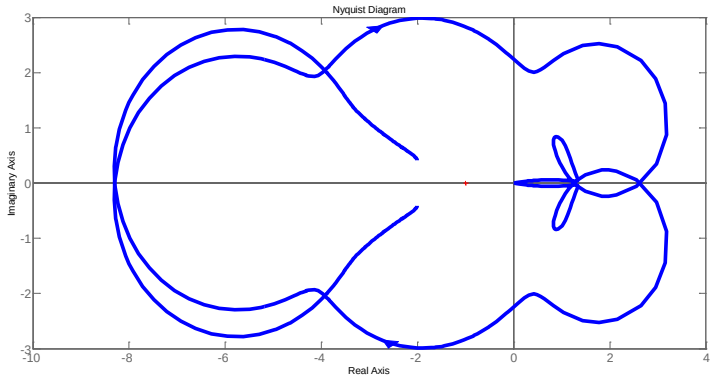

Figure 5.13 Bode and Nyquist diagrams for the second order transfer function $\Omega^2_{(1,2)}(s_1, s_2)$ for the case study of the test power system 3SM-9BUSES

In order to obtain an easier expression, a simple analysis based on the highest residues is applied to the nonlinear terms. Figure 5.14 shows the residues location in the complex plane. Thus, due to the excessive number of residues and therefore, the same number of poles, only those with highest absolute magnitude are considered to characterize the nonlinear transfer function. The zoomed Figure 5.14 details the residues that are out of bounds, that is, residues whose magnitude are $|r_i| < 0.1$.

Agreeing to the reasoning of residues, the corresponding poles (modal combination) referred to the resultant residues are shown in Figure 5.15. This analysis can be compared with the proposal of dominant poles calculation [Martins *et al.* 1996], [Rommes and Martins 2006] where the main residues and their corresponding poles are obtained using an iterative process.

With respect to the complete poles of the transfer functions, the main frequencies detected in the wide range spectrum are 4.16Hz, 3.44 Hz, 2.73 Hz, 2.47, 2.28, 2.1, 2.08, 1.87, 1.75, 1.69, 1.57 and 0.98 Hz.

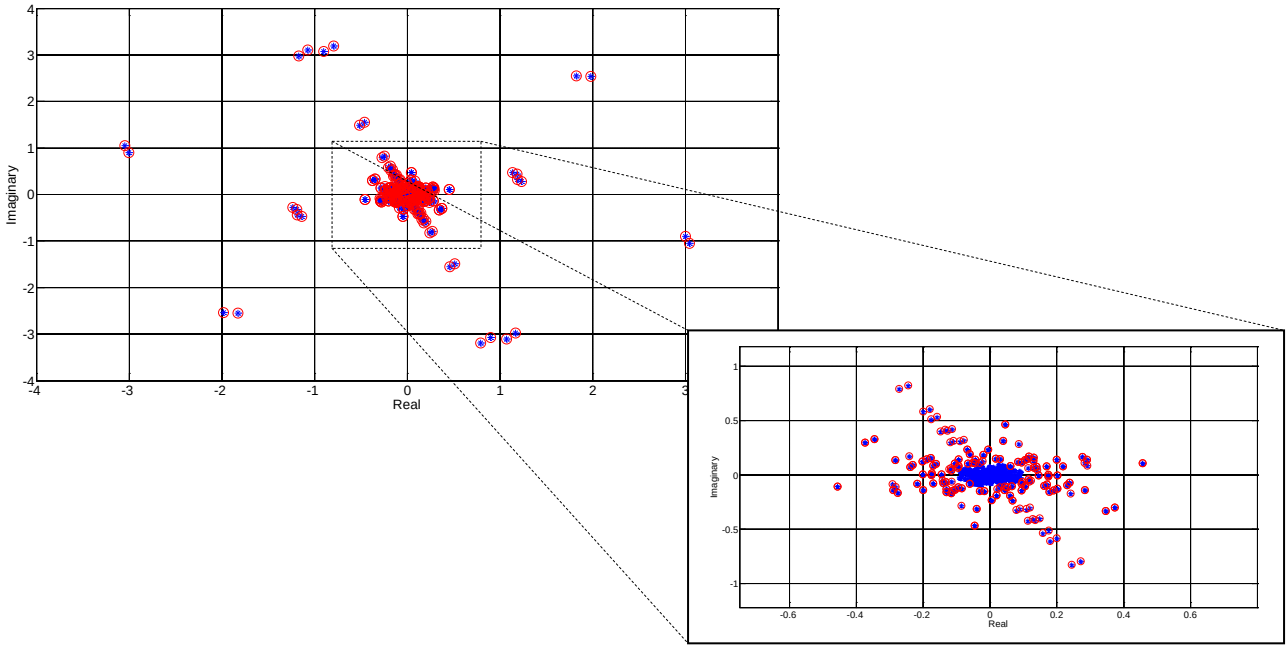

Figure 5.14 Residues spectrum for the nonlinear transfer function $\Omega^2_{(1,2)}(s_1, s_2)$ for the case study of the test power system 3SM-9BUSES

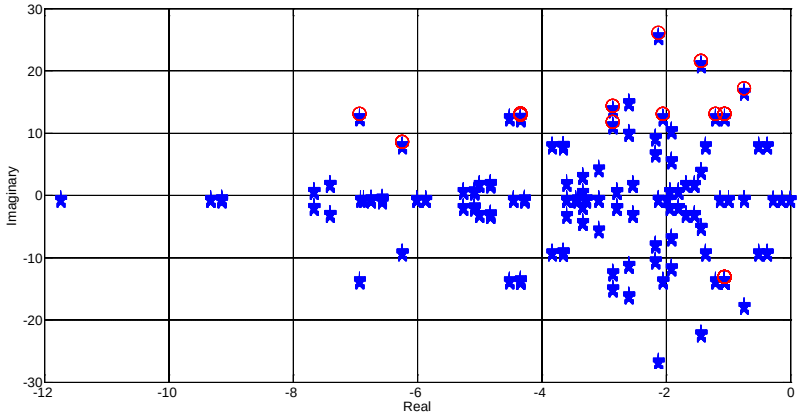

Figure 5.15 Poles spectrum for the nonlinear transfer function $\Omega^2_{(1,2)}(s_1, s_2)$ for the case study of the test power system 3SM-9BUSES

A spectrum characteristic of the nonlinear transfer function is obtained, as shown in Figure 5.16. The Figure shows the full frequency content of the nonlinear transfer function of order 6750th. A zoomed window denotes the content of some of the terms, *i.e.* through order 300. It is clear that there is a predominant frequency detected in the spectrum (2.08 Hz) which is a low frequency due to the electromechanical modes of the power system.

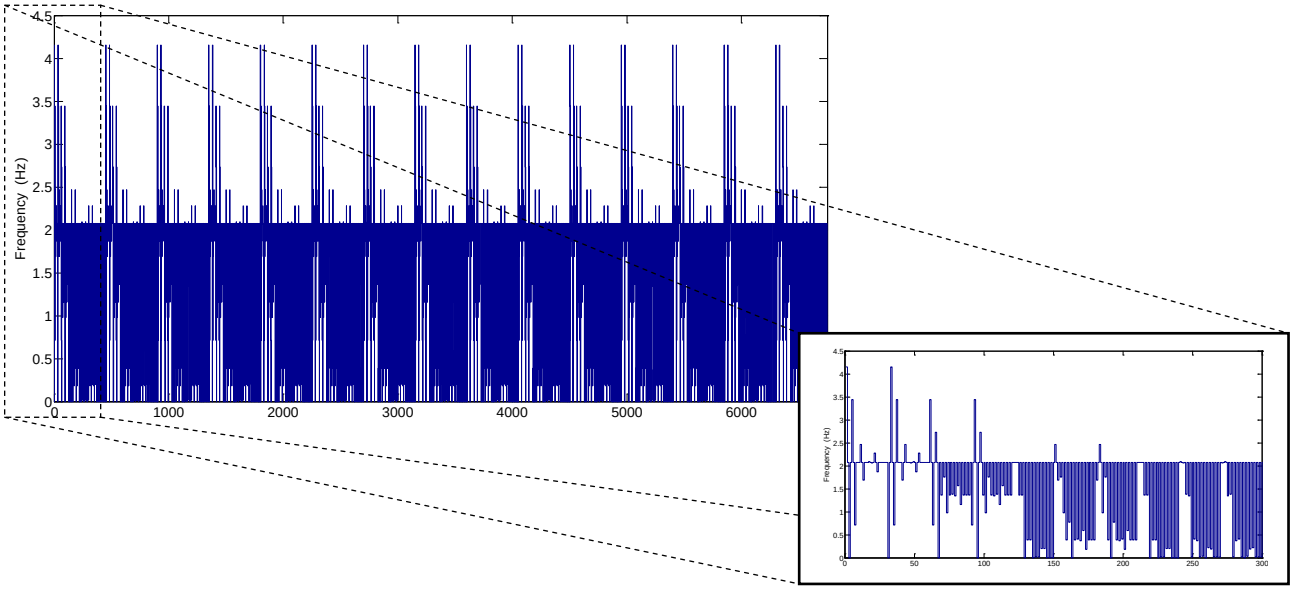

Figure 5.16 Frequency spectrum of the nonlinear transfer function $\Omega^{2}_{(1,2)}(s_1, s_2)$ for the case study of the test power system 3SM-9BUSES

Once the reduction in the nonlinear transfer function order is performed, an approximate frequency content is obtained; please see Figure 5.17. From this Figure, the similarity on frequency content with respect to the full spectrum already commented with reference to the Figure 5.16 is observed. In such case, it can be said that the reduced model keeps almost the same frequency characteristics of the full system.

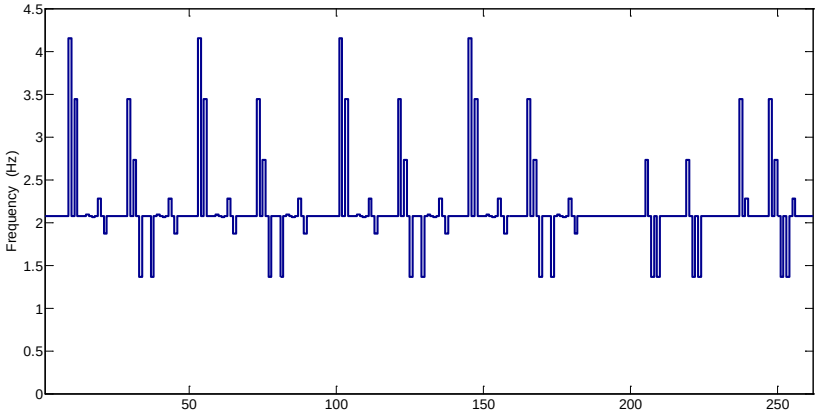

Figure 5.17 Pole spectrum of the reduced nonlinear transfer function for the case study of the test power system 3SM-9BUSES

Finally, the Figure 5.18 shows the Bode and Nyquist graphs of some of the main nonlinear transfer functions, where the frequency content of each of them can be observed. In some cases, for instance

$\Omega^2_{(1,3)}(s)$ various resonant frequencies are presented, being of predominance the frequencies in the range of 2 to 3 Hz.

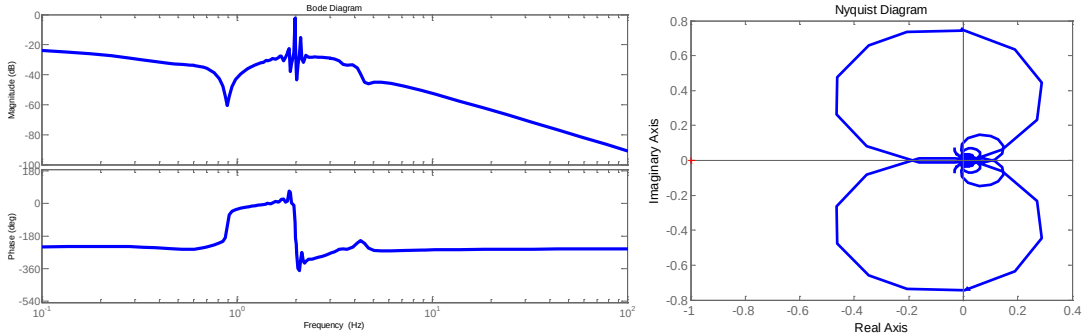

$\Omega^2_{(1,3)}(s)$

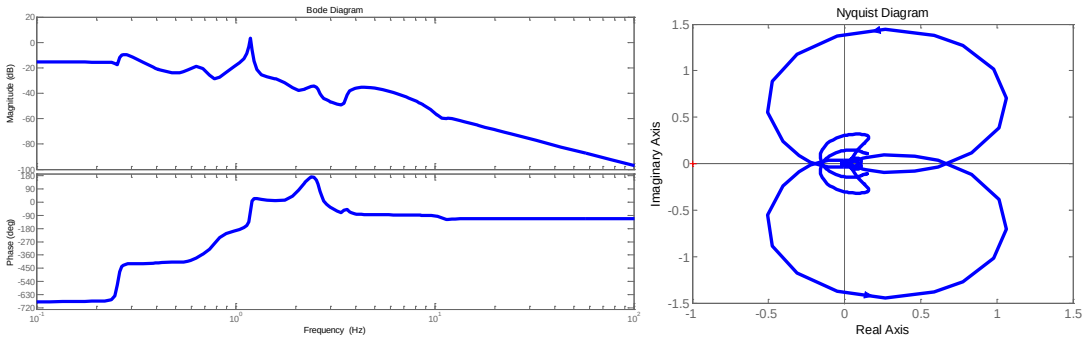

$\Omega^2_{(1,4)}(s)$

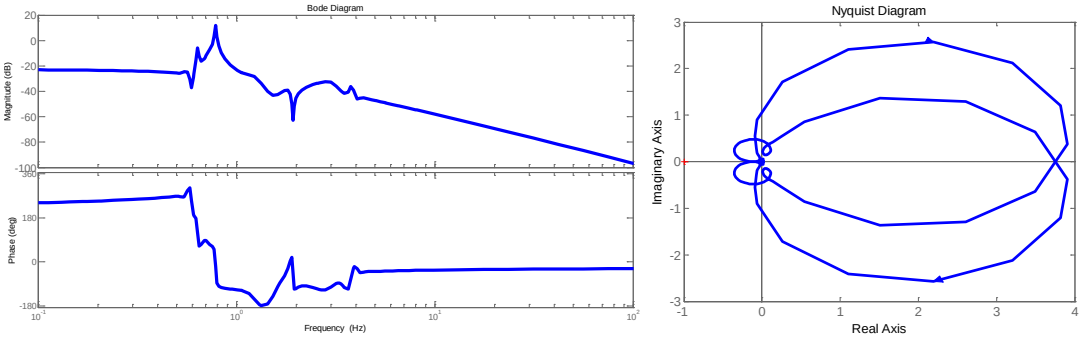

$\Omega^2_{(1,5)}(s)$

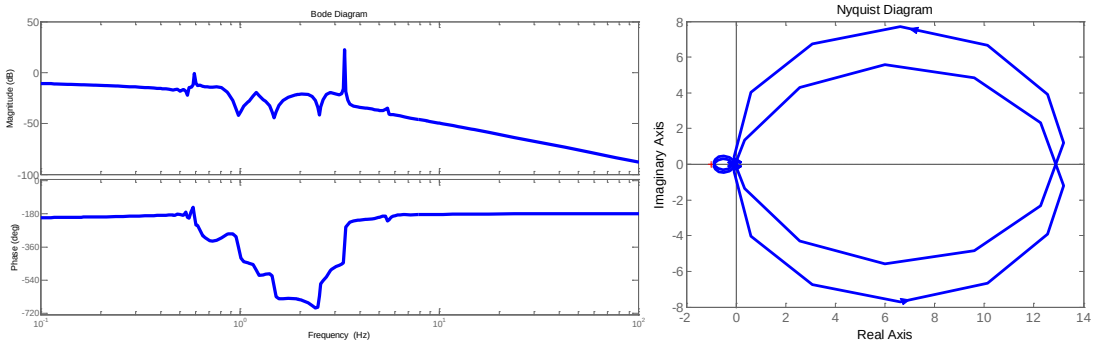

$\Omega^2_{(1,6)}(s)$

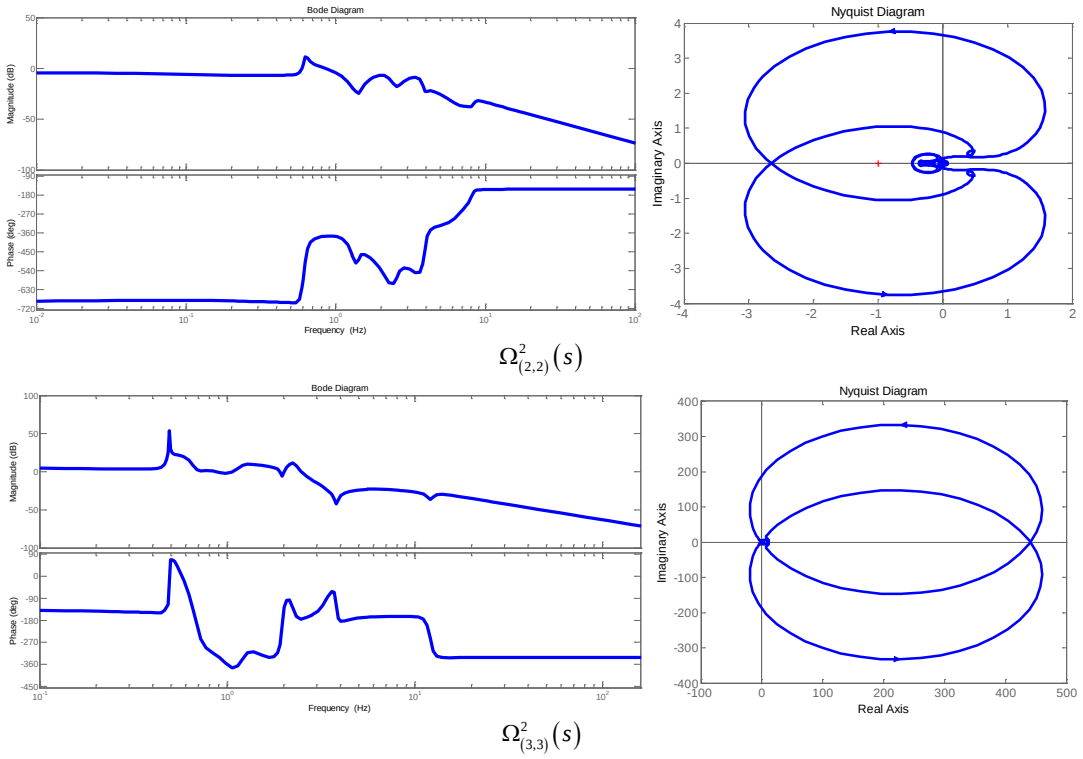

Figure 5.18 Bode and Nyquist graphics of nonlinear transfer functions

5.8 DISCUSSION

This chapter has described in detail the theory related to the linear transfer functions concepts and its extension to the nonlinear transfer function through the application of the modal series method, as the basis of nonlinear system expansion, assuming an input force response. The method has the great advantage of analyzing in both time and frequency domains, in a numerical and analytical way, the transfer functions of nonlinear systems. Application of the multidimensional Laplace transform and association of variables techniques are the core of modal series technique, which allows a closed form analytical solution of the nonlinear system, being the extension of including the control forced response. The examples were focused on applications to simple power systems, however, it is possible following the same definitions, to extend it easily in a straightforward manner to the analysis of large scale power systems. It is clear that dealing with bigger systems, the complexity of analysis is increased, being necessary the inclusion of sparsity techniques, effective algorithms of eigenvalues determination, etc. Future developments based on this contribution will take this problem adding the determination of dominant poles and the analysis of large scale power systems.

THIS PAGE IS INTENTIONALLY LEFT BLANK

6

CASE STUDIES: APPLICATION OF MODAL SERIES TO THE ANALYSIS OF NONLINEAR OSCILLATIONS

This chapter consolidates with the theory detailed along this research. To exemplify it, two test power systems are considered, i.e. the 9 buses, 3 generators [Anderson and Fouad 2003] and the version of New England test power system with 10 generators, 39 buses [Pai 1989]. Experiments with both methods are conducted using the modal series method, analyzing the linear and nonlinear contributions to the closed form solution through numerical simulations and linear and nonlinear participation factors and interaction modal indices on the test systems.

6.1 INTRODUCTION

The theory of modal series method described along this thesis is exemplified in this Chapter through the study of two test power systems. The first one was already analyzed in Chapter 5, where the concept of nonlinear transfer function was introduced; the main goal of the experiment with the same test power system is to clarify the application of the modal series method, the modal analysis, the nonlinear modal interaction, the frequency contribution of nonlinear terms considered in the study and also the analysis of nonlinearity when a time disturbance clearance is changed.

On the second part, a larger power system based on the WSCC test power system of 10 machines, 39 buses is exemplified; the nature of linear and nonlinear oscillations are clarified, following a similar procedure of the previous case study, in fact, modal analysis and nonlinear modal interaction are of concern. Also, the system is simulated when the modal analysis results in unstable working conditions. One of the main advantages of the modal series method is its facility of application even under modal resonance conditions.

6.2 CASE STUDY 1: 3 SYNCHRONOUS MACHINES, 9 BUSES TEST POWER SYSTEM

The first study case is oriented to the study of the 9-bus test power system shown in Figure 6.1 [Anderson and Fouad 2003]. The generation and network parameters, load data and the system operating conditions are given in Appendix A. For the purposes of analysis, the power system is represented by a fourth-order model including the AVR representation such as it was described in

Chapter 4. The network is represented by a quasi-stationary model; loads are treated as constant impedances and the generator impedances are included in the augmented network admittance matrix.

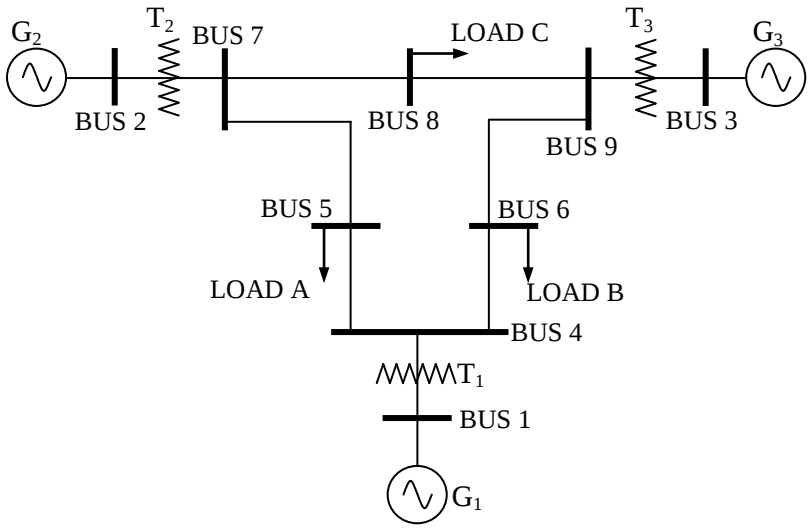

Figure 6.1. Nine-bus, three-machine test power system

The state variables vector in that represent the nonlinear power system model are defined as $\mathbf{x}(t) = [\mathbf{x}_{\delta} \quad \mathbf{x}_{\omega} \quad \mathbf{x}_{E'_q} \quad \mathbf{x}_{E'_d} \quad \mathbf{x}_{E_{fd}}]^T$, where,

$\mathbf{x}_{\delta} = \begin{bmatrix} \delta_1 & \delta_2 & \delta_3 \end{bmatrix}^T$

$\mathbf{x}_{\omega} = \begin{bmatrix} \omega_1 & \omega_2 & \omega_3 \end{bmatrix}^T$

$\mathbf{x}_{E'_q} = \begin{bmatrix} E'_{q1} & E'_{q2} & E'_{q3} \end{bmatrix}^T$

$\mathbf{x}_{E'_d} = \begin{bmatrix} E'_{d1} & E'_{d2} & E'_{d3} \end{bmatrix}^T$

$\mathbf{x}_{E_{fd}} = \begin{bmatrix} E_{fd1} & E_{fd2} & E_{fd3} \end{bmatrix}^T$

The state matrix obtained by the linearization process detailed in Section 2.2, Chapter 2, is evaluated to obtain the Jacobian equation which has the form,

$J =$

0	0	0	1	0	0	0	0	0	0	0	0	0	0
0	0	0	0	1	0	0	0	0	0	0	0	0	0
0	0	0	0	0	1	0	0	0	0	0	0	0	0
-24.1837	13.5322	10.6514	-0.0997	0	0	9.6542	7.0316	22.5939	-8.6678	-7.7655	0	0	0
44.3537	-77.584	33.2302	0	-0.2	0	-92.879	13.5713	-42.4814	16.6473	-31.4914	0	0	0
78.3229	73.9174	-152.2403	0	0	-0.3	42.3338	-150.9938	-74.7438	-56.5049	67.1463	0	0	0
0.0014	-0.0014	0	0	0	0	0.01	0.0089	-0.008	0.0107	0.0077	0.1116	0	0
0.1972	-0.3222	0.125	0	0	0	-0.519	0.1363	-0.185	-0.0543	-0.0444	0	0.1667	0
0.2219	0.1595	-0.3814	0	0	0	0.2124	-0.6246	-0.2073	-0.0153	-0.0532	0	0	0.1698
0.3347	-0.1875	-0.1473	0	0	0	-0.1307	-0.0947	-3.5738	0.1228	0.1095	0	0	0
-0.7905	1.5983	-0.8077	0	0	0	0.5846	0.4782	0.794	-5.6607	1.4672	0	0	0
-1.1223	-1.4642	2.5865	0	0	0	0.1432	0.497	1.1068	1.9839	-5.9155	0	0	0
-1.274	0.9783	0.2957	0	0	0	-3.8051	-3.4385	0.008	-4.5919	-3.371	-3.1847	0	0
-3.786	4.865	-1.079	0	0	0	-29.0439	-7.0326	3.3255	-31.7483	-4.7018	0	-3.1847	0
-3.1797	0.9322	2.2475	0	0	0	-8.9983	-26.0508	2.6864	-9.1065	-25.5488	0	0	-3.1847

with the sparsity structure shown in Figure 6.2. The coupling existing between the main state variables can be observed.

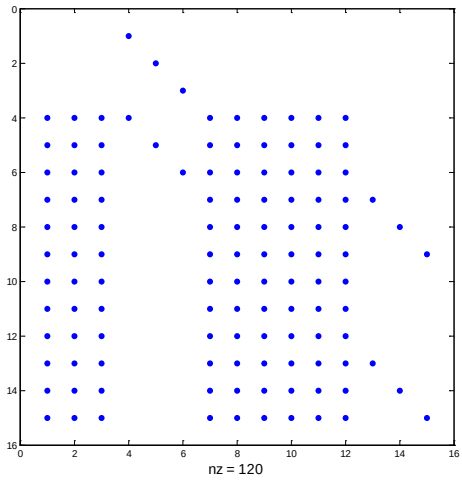

Figure 6.2 Jacobian matrix structure

In the same way, the second order partial derivatives of the power system model are represented by the Hessian matrix whose sparse structure has the form illustrated by Figure 6.3. The Hessian is a sparse matrix, requieres of an efficient technique for matrices storage mostly in cases where the system explodes in dimension, for instance, large scale power systems. In particular for this study case the Hessian matrix has size of 15×225 elements.

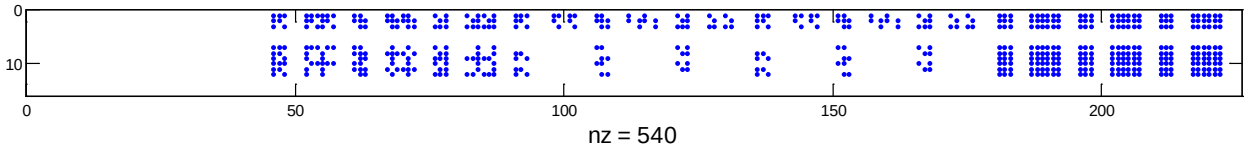

Figure 6.3 Hessian matrix structure

The sparsity structure of the Jacobian and Hessian matrices is illustrated for visual and qualitative evaluation objectives. Both matrices in computational implementation are obtained in a symbolic way: the original set of differential equations is linearized obtaining the first and second order partial derivatives using the symbolic properties of Matlab®. It is very important to remark the importance of using symbolic applications. Powerful tools as Mathematica® can be very useful in order to obtain the analytical expressions, since the modal series method is based on analytical solutions instead on numerical calculations. Despite the Symbolic Toolbox of Matlab® is not the best option to write a symbolic math program, the developed software for the case studies reported in this thesis includes routines written using the symbolic toolbox. Further developments consider the extension of some other routines, thought to be used with a better analytical platform, such as Mathematica®.

6.2.1 Small Signal Analysis

The small signal analysis in the case study is resumed in the Table 6.1.

Table 6.1 Modal analysis of 3SM, 9 buses test power system

Mode	Eigenvalue	Damping Ratio	Frequency
1,2	$-1.0618 \pm 13.0572i$ -	0.081	2.0781
3,4	$-0.3744 \pm 8.5858i$	0.0436	1.3665
5	-5.8688	1	0
6,7	$-1.5421 \pm 2.4311i$	0.5357	0.3869
8	-3.4589	1	0
9,10	$-3.2841 \pm 0.1123i$	0.9994	0.0179
11,12	$-1.8002 \pm 1.2864i$	0.8136	0.2047
13	0	1	0
14	-0.1401	1	0
15	-0.9943	1	0

From Table 6.1 we can observe that there are 10 oscillatory modes, being the electromechanical modes 1,2 and 3,4 of main importance. With respect to the analysis of participation factors, the bar diagrams illustrated in Figure 6.4 show the variables with the highest participation factors, only for the oscillatory modes. For this case study, the set of highest participation factors are resumed in Table 6.2.

Table 6.2 Most dominant participation factors

Mode	Participation Factor	State Variables
1,2	0.3823	δ_3, ω_3
3,4	0.3011	δ_2, ω_2
5	0.5195	E'_{d2}
6,7	0.2437	E'_{q1}, E_{fd1}
8	0.4209	E'_{d3}
9,10	0.4367	E_{fd3}
11,12	0.2186	E_{fd2}
13	0.4971	δ_1
14	0.4944	ω_1
15	0.4601	E'_{q3}

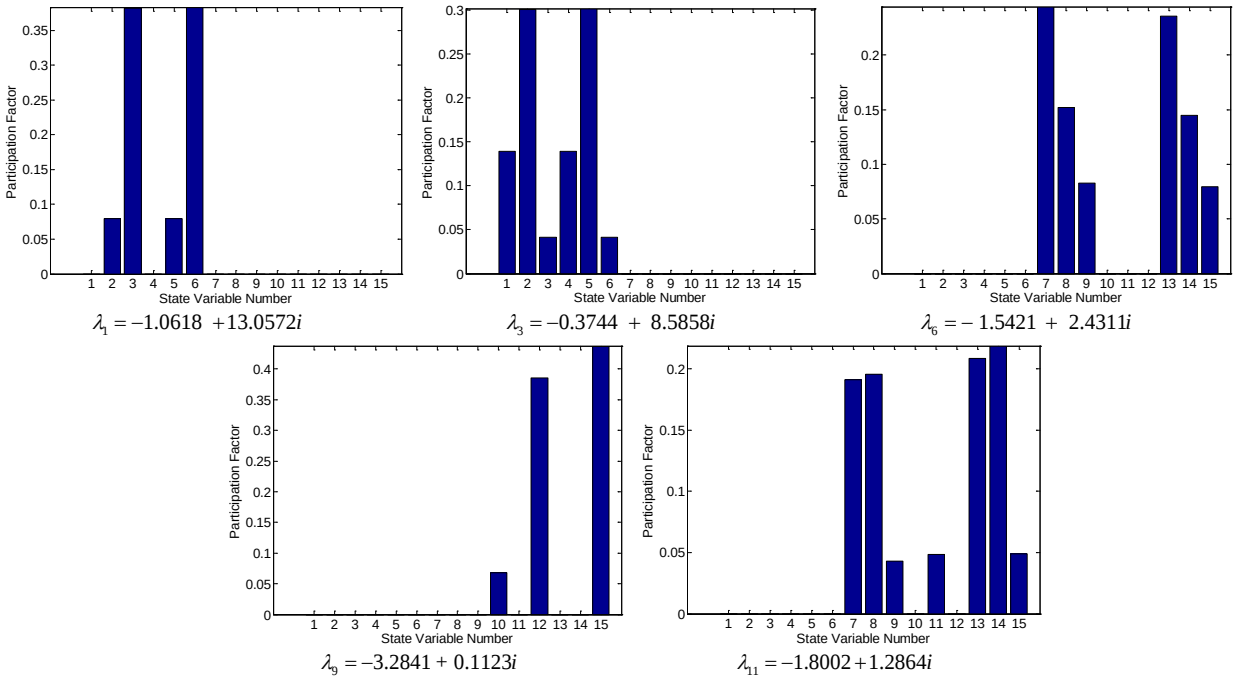

Figure 6.4 Linear Participation Factors

The participation factors listed in Table 6.2 denotes that the oscillatory modes 1,2 with frequency 2.0781 Hz are associated to rotor angle and speed of generators 2 and 3, acting as local modes, while the modes 3,4 with frequencies 1.3665 Hz are with generator 2. The rest are modes due to control interactions between field and stator windings. In this particular case, there are no any inter-area modes presented. The modal analysis establishes the main characteristics of frequency, damping ratio and participation factors, which interact in the analysis of the nonlinear system when modal combination is present.

6.2.2 Approximate Time-Domain Solutions to System Motion

To test the accuracy of the method, a three-phase fault is applied at bus 8 cleared in 6 cycles followed by 10 MW load rejection. The state variables perturbation constraint is,

$$disturb = \begin{bmatrix} 0.0036 & 0.2384 & 0.1384 & 0.0958 & 4.7531 & 2.6458 & 0.0031 & -0.0049 & -0.0043 & -0.0019 & -0.4258 & -0.2308 & 1.0502 & 3.9079 & 2.4613 \end{bmatrix}^T$$

The time domain validation of the nonlinear power system is performed by comparing the time domain solution obtained with the modal series method with the full non-linear system behavior obtained through numerical integration. Also the linear approximation is studied and compared. Figures 6.5 a) to f) provide a comparison of the full system solution for selected states with the solution obtained from the modal series approach for the already described conditions.

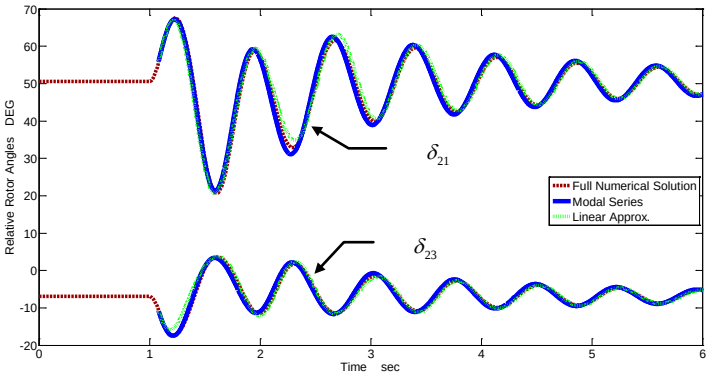

a) Relative rotor angles δ_{21} and δ_{23}

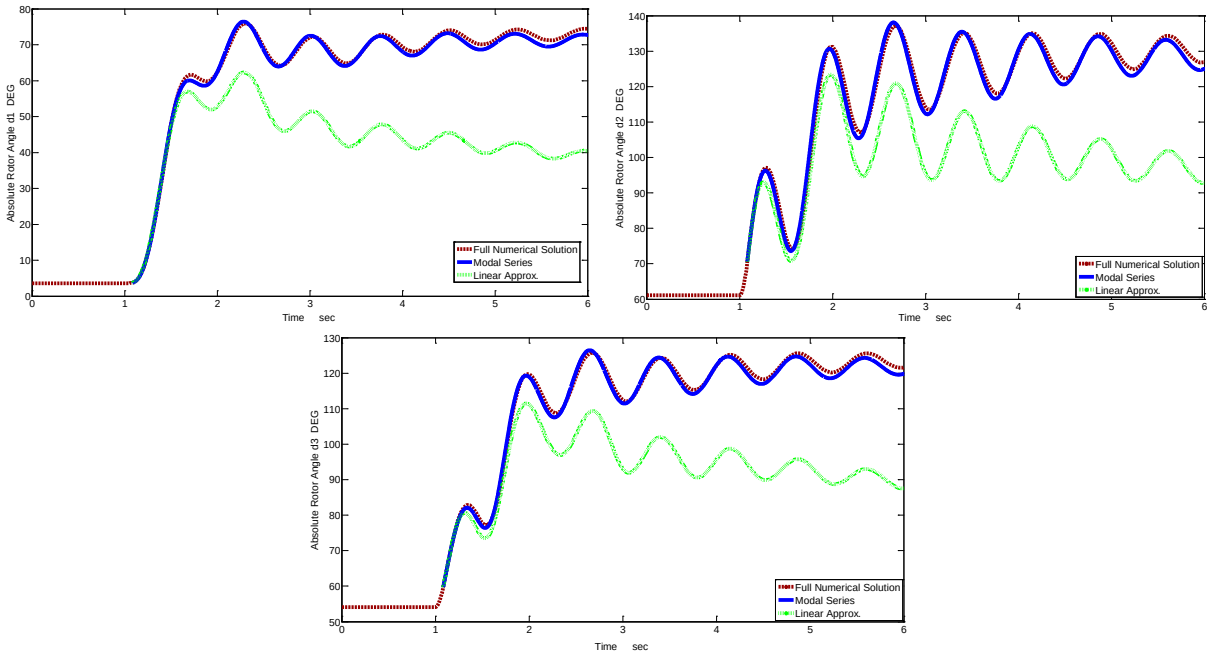

b) Absolute rotor angles of δ_1, δ_2 and δ_3

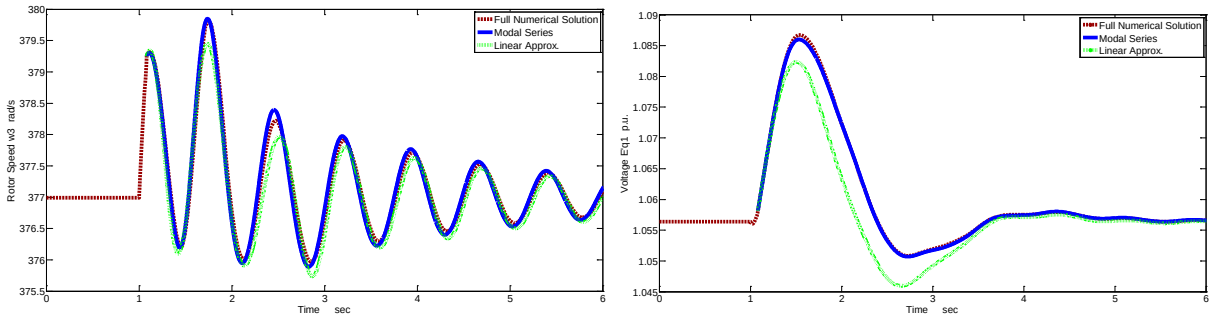

c) Rotor Speed ω_1

d) Voltage E'_{q1}

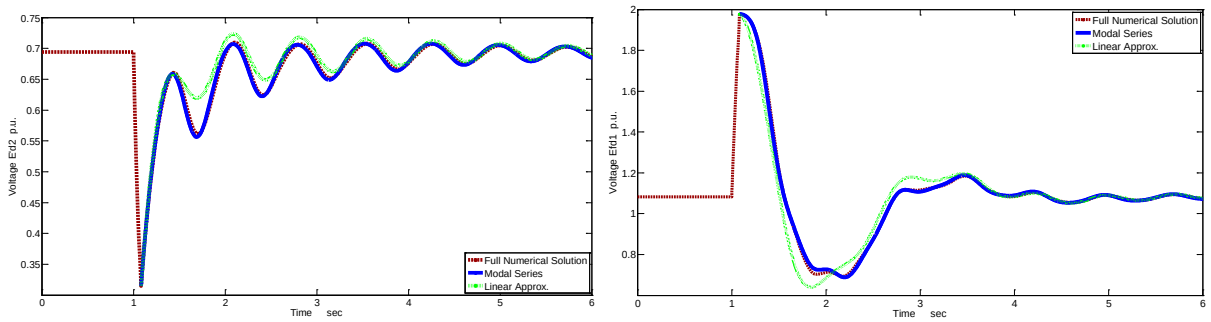

e) Voltage E'_{d3} f) Voltage E_{fd1}

Figure 6.5 Time domain validation of the 3 SM, 9 buses test power system

Figure 6.5a) is related to the relative rotor angles, it does not reflect almost any considerable difference between solutions; the angles δ_{21} and δ_{23} follow similar trajectories for the three methods during the transient. A slight difference with respect the linear approximation is observed in the rotor angle δ_{21} although it is not of concern. However, the absolute rotor angles shown in Figures 6.5b) have the largest differences with respect to the linear approximation. The modal series response closely follows the full numerical solution during the transient and eventually reaches an identical steady state solution, not shown, which is considerably different to that obtained by the linear approximation approach. The reason is based on the angles are the variable with the highest nonlinear characteristic of the model that is clearly appreciable.

The transient evolution of the rest of variables present differences with respect to the linear approximation but closely agree in steady state. For instance, referring to Figures 6.5d) e) and f), there is a noticeable difference between linear approximation with respect to modal series and full numerical solution, but it practically follows the same trajectory just before the steady state solution is reached. A smaller difference is observed for the rotor speed in Figure 6.5 c).

It can be concluded that for all the cases here described, the modal series solution is always closer to the time domain response described by the full numerical solution, while linear approximation may fail for the cases where the nonlinear characteristic is presented.

A new condition of operation is considered in this case study, when the fault duration is increased to 10 cycles, accompanied with the absence of damping conditions (damping factor $D=0$) for each generator. The simulation is shown throughout Figure 6.6. The variables exhibit higher differences between modal series and linear approximation.

The solution obtained by the modal series method, detailed for the variables of rotor angle δ_i, rotor speed ω_i and voltage E'_{qi} are described; significative differences are observed, when compared against

the linear approximation for the case of rotor angle variables, since the linear approximation follows a different direction of solution with respect to modal series and the full numerical solution.

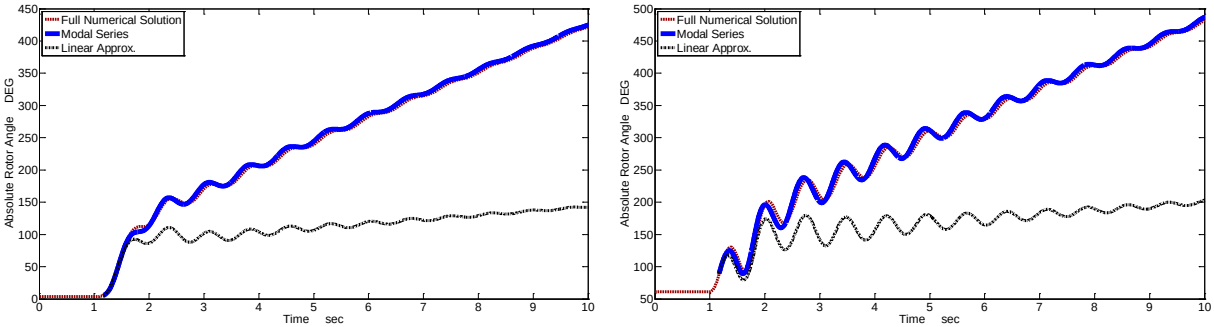

a) δ_1 b) δ_2

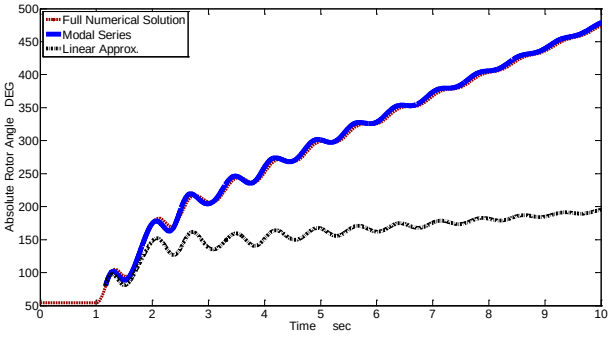

c) δ_3

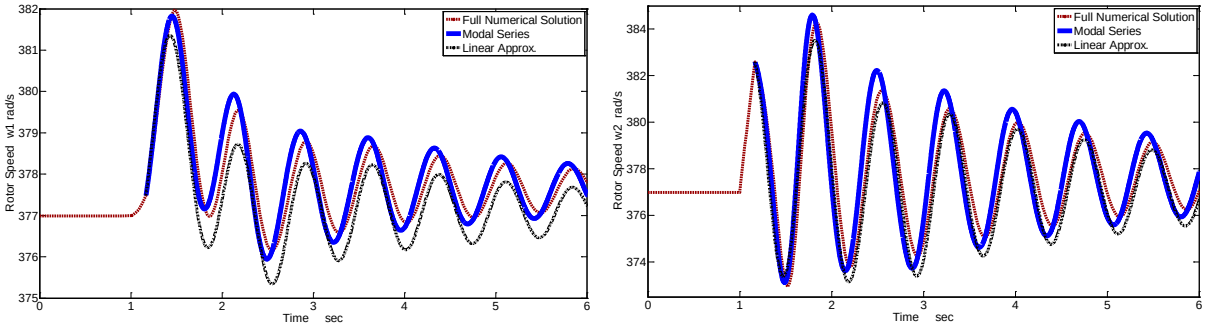

d) ω_1 e) ω_2

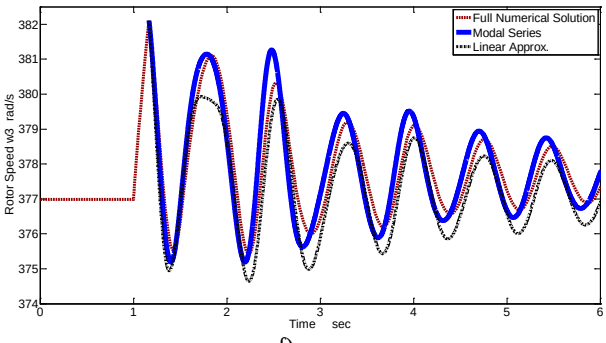

f) ω_3

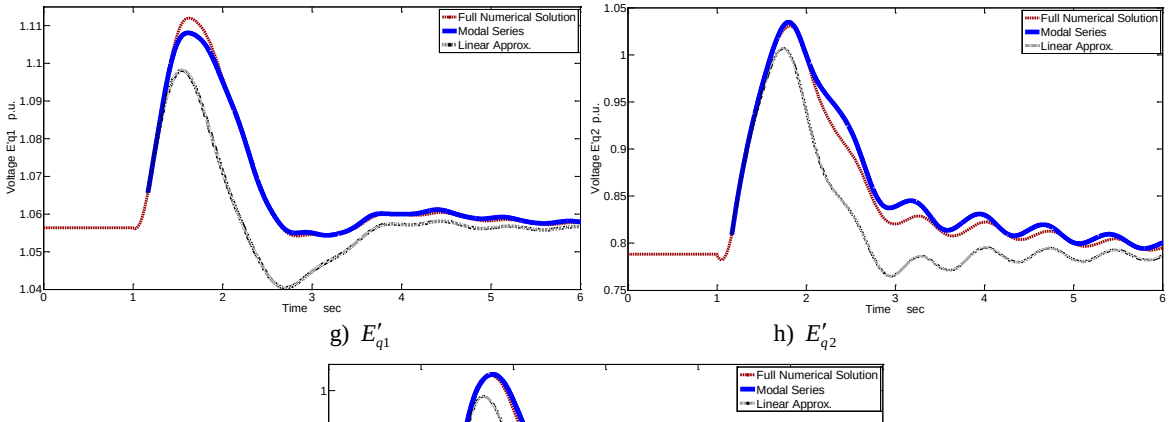

g) E'_{q1} h) E'_{q2}

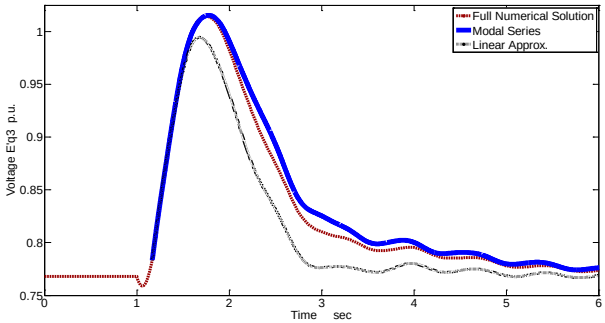

i) E'_{q3}

Figure 6.6 Time domain validation of 3SM 9 buses test power system under different perturbation conditions

6.2.3 Nonlinear Modal Interaction Through Nonlinear Indices

To analyze the nonlinear contribution of the modal series terms, several nonlinear indices are taken into account as follows:

a) The first nonlinear index is defined by,

$$I1=\max\left|h2_{kl}^{j}\, y_k(0)\, y_l(0)\right| \tag{6.1}$$

which provides the maximum measure of the nonlinearity to the closed form solution. Also, it can be the contribution of modes k, l to the j^{th} mode.

b) Other nonlinear index is defined as,

$$I2=\left|\frac{\max\limits_{k,l}\left|h2_{kl}^{j}\, y_k(0)\, y_l(0)\right|}{y_j(0)}\right| \tag{6.2}$$

which determines the second order nonlinear effects, indicating a strong modal interaction [Barocio 2003].

c) A new coefficient of nonlinearity taken from [Barocio 2003] that is defined from the theory of nonlinear distorsion interference criteria, has been applied to estimate the nonlinear interaction in terms of normal forms variables. The same index is adapted in terms of Jordan canonical variables, resulting in,

$$I3 = \frac{\sqrt{\sum_{k=1}^{n}\sum_{l=1}^{n}\left|h2_{kl}^{j}\, y_k(0)\, y_l(0)\right|^2}}{\left|y_j(0)\right|\sqrt{\quad}} \tag{6.3}$$

d) Finally, a fundamental mode nonlinearity index provides a measure of the effect of modal interactions on the fundamental mode in the original coordinates [Chen *et al.* 2010], that is,

$$I4(j) = \frac{\left[y_j(0) - \sum_{k=1}^{n}\sum_{l=1}^{n} h2_{kl}^{j}\, y_k(0)\, y_l(0) \right]}{y_j(0)} \tag{6.4}$$

To demonstrate the contribution of the nonlinear part to the system dynamics, the experiment is conducted applying a three phase fault at bus 8 during 15 cycles (0.25s), clearing the fault without any change on network topology. The Figure 6.7 shows a comparison between the nonlinear solution (closed form solution by modal series method) and the linear approximation for the rotor angle and rotor speed of generator 1.

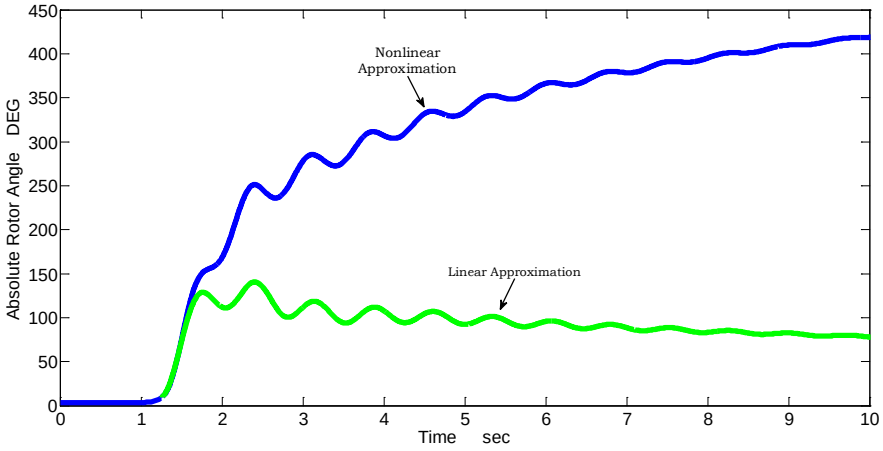

a) Rotor angle δ_1

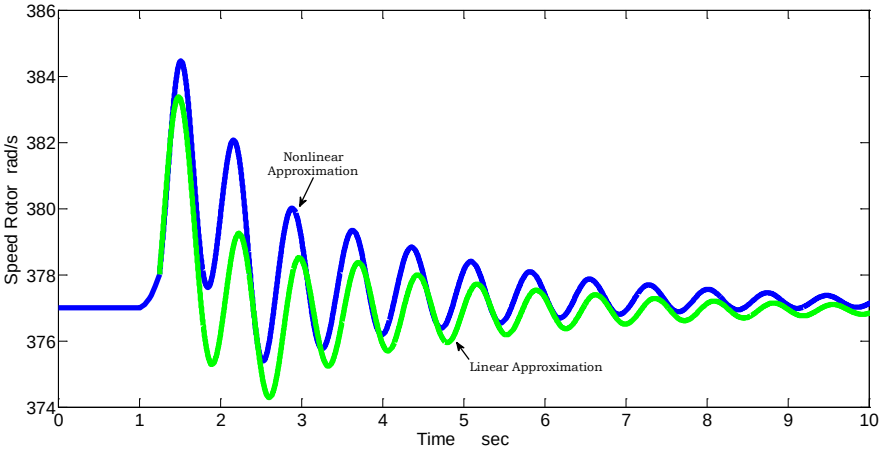

b) Rotor speed ω_1

Figure 6.7 Comparison of linear and nonlinear approximation

A qualitative clear difference between linear and nonlinear solutions is observed from Figure 6.7. After the fault, the rotor angle 1 increases trying to maintain the synchronism of the power system. This causes an acceleration of the rotor speed, which starts an oscillation that eventually disappears. However, apparently the linear solution estimates a very low damped oscillation in rotor angle, quickly finding the steady state solution. A large difference between linear and nonlinear solution, mostly for the particular case of rotor angle is observed. In the case of rotor speed, Figure 6.7b), the linear solution closely follows to the nonlinear solution, with the solution difference being kept over the first 5 cycles of oscillation.

With respect to the nonlinear indices, the nonlinear coefficients $h2_{kl}^{j}$ can be analyzed. For this case, the largest coefficient for each mode is considered. The Figure 6.8 shows a bar diagram of coefficients magnitude. For this particular case, the main contribution is due to the modes 11 and 12, which are control modes of the test power system

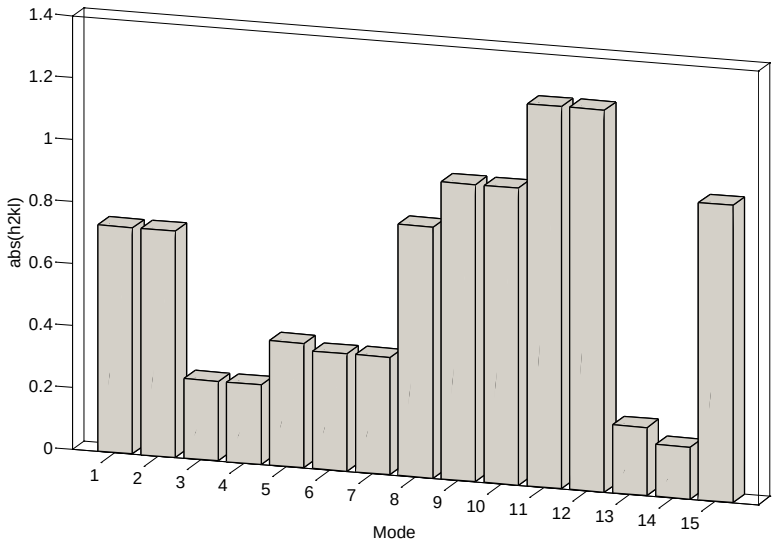

Figure 6.8 Second order coefficients $\max\left(\left|h2_{kl}^{j}\right|\right)$

The four nonlinear indices given by (6.1) to (6.4) are now taken into account. Calculating the indices magnitude in the same way as the nonlinear coefficients, the graphs shown in Figure 6.9 denotes the absolute value of each index. From this Figure, it can be commented that:

- The main contribution index is $I1$, which means that the modes 5, 8, 9 and 10 are the modes that have major contributions to the closed form solution.
- The indices which show less contribution are $I3$ and $I4$. This may imply that there is no strong modal interaction on the fundamental modes. Their values are quite small compared with indices $I1$ and $I2$, as it can be noticed from Figure 6.9

- The index I2 has its largest value in the mode 5. Thus, there is a strong modal interaction due to the mode 5 with the rest of modes.

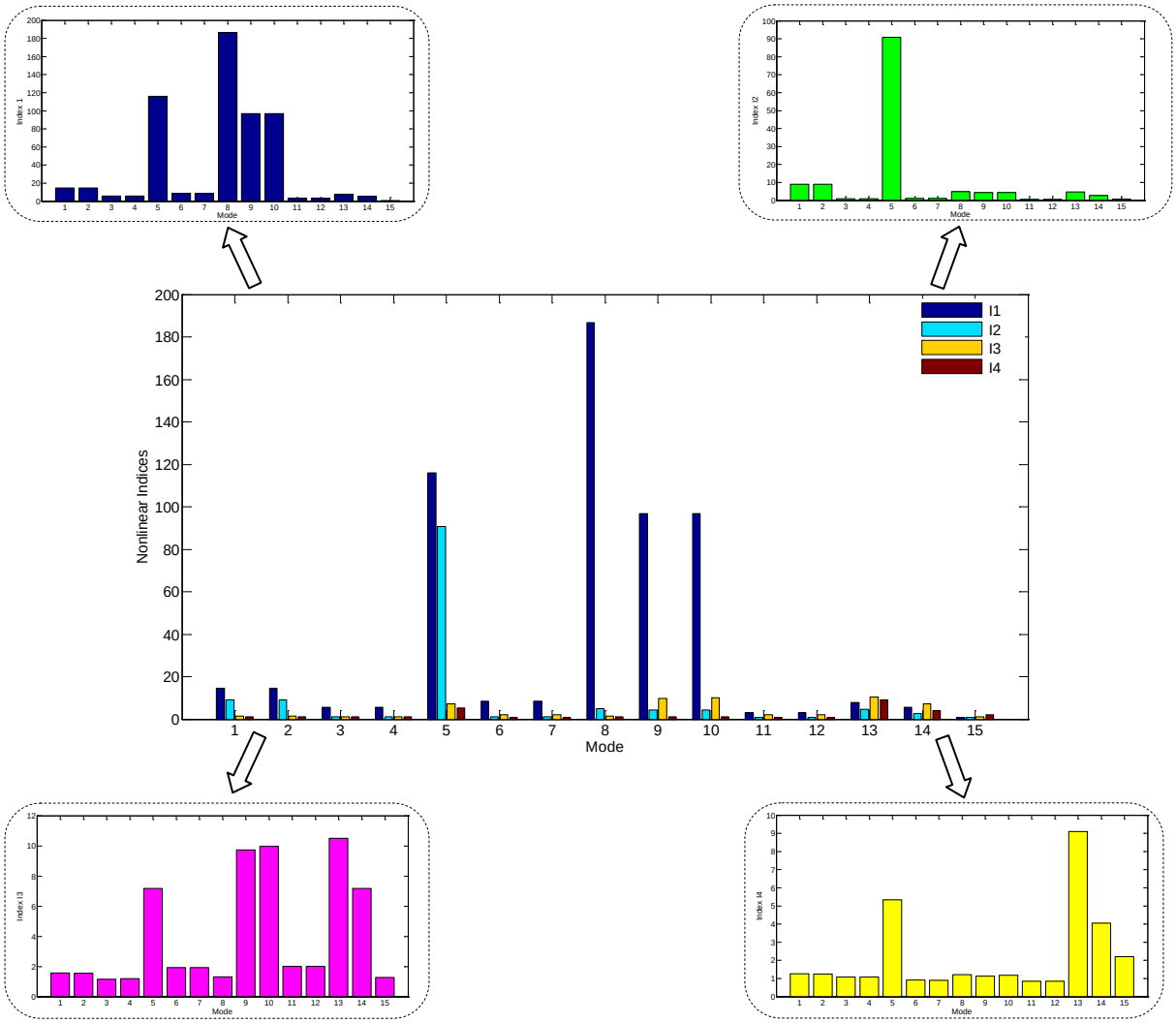

Figure 6.9 Nonlinear indices *I*1, *I*2, *I*3 and *I*4

6.2.3.1 Nonlinear participation factors

The participation factors are applied to the analysis of nonlinear power system assuming the linear definition and introducing the nonlinear definition. The linear participation factors are used as a measure of mode-machine interactions [Pérez-Arriaga *et al.* 1982]. The participation factor represents a measure of the participation of the k^{th} machine state trajectory of the i^{th} mode, and it is defined as,

$$p_{ki} = u_{ik} v_{ki} \tag{6.5}$$

With reference to the normal forms method, the nonlinear participation factors are defined based on the second order solution given by,

$$x_i(t) = \sum_{j=1}^{n} u_{ij} z_j(0) e^{\lambda_j t} + \sum_{k=1}^{n}\sum_{l=1}^{n} u_{2ikl} z_k(0) z_l(0) e^{(\lambda_k+\lambda_l)t} \tag{6.6}$$

where u_{ij} is an element of the i^{th} right-eigenvector and,

$$u_{2ikl} = \sum_{j=1}^{n} u_{ij} h2_{kl}^{j} \tag{6.7}$$

and $h2_{kl}^{j}$ is the second order normal form transformation coefficient of the *kl* product in the j^{th} equation [Starret, S. K. 1994].

From (6.6) the next statements can be observed:

- u_{2ikl} performs the same function for the second order mode $\lambda_k + \lambda_l$ as u_{ij} does for the linear mode *j*.
- Right-eigenvectors terms (linear and second order) indicate how the modal oscillations are translated to the machine states.

Following the same reasoning than the normal forms method, it is possible to determine the nonlinear participation factors derived for the closed form solution of the modal series method. Since there are similarities between both methods, the deduction can be made in a direct way.

Recalling that the modal series method has the closed form solution represented as,

$$x_i(t) = \left[\sum_{j=1}^{n} u_{ij} y_j(0) - \sum_{k=1}^{n}\sum_{l=1}^{n} u_{2ikl} y_k(0) y_l(0) \right] e^{\lambda_j t} + \sum_{k=1}^{n}\sum_{l=1}^{n} u_{2ikl} y_k(0) y_l(0) e^{(\lambda_k+\lambda_l)t} \tag{6.8}$$

or, it can be written as,

$$x_i(t) = u1_{ij} e^{\lambda_j t} + u2_{ikl} e^{(\lambda_k+\lambda_l)t} \tag{6.9}$$

where,

$$u1_{ij} = \left[\sum_{j=1}^{n} u_{ij} y_j(0) - \sum_{k=1}^{n}\sum_{l=1}^{n} u_{2ikl} y_k(0) y_l(0) \right] \tag{6.10}$$

$$u2_{ikl} = \sum_{k=1}^{n}\sum_{l=1}^{n} u_{2ikl} y_k(0) y_l(0) \tag{6.11}$$

Some observations can be made from this simple algebraic step:

- From a comparative point of view, the modal series solution has the same form as the normal forms solution, that is, linear terms are associated to the right eigenvectors, while the second order coefficients are associated to the modal combination $(\lambda_k + \lambda_l)$.

- However, with respect to the linear mode, the linear coefficient $u1_{ij}$ is also function of nonlinear coefficients $h2_{kl}^{j}$. This means that the linear terms are influenced by the action of nonlinear modal combination, since $h2_{kl}^{j}$ is a function of modal combination $\left(\lambda_k + \lambda_l - \lambda_j\right)$

Equation (6.8) describes the linear and nonlinear combination of the solution, however, it is necessary to re-define it, in order to obtain the nonlinear participation factors oriented to the closed form solution obtained through the modal series method. The deduction can be made considering that the initial condition vector is $x_0 = e_k$, which implies that the Jordan form initial condition can be expressed as,

$$y_{j0} = v_{jk} \tag{6.12}$$

It is important to remark the meaning of (6.12): the participation factors are due to the excitation of one mode at the time, by which it is possible to apply superposition procedure. If in the initial condition only one mode is considered, the initial condition in Jordan variables is a column corresponding to the left eigenvectors.

Thus, the solution for the k^{th} machine state variable (with $x_{i0} = 0$ for all $i \neq k$),

$$x_i\left(t\right) = \sum_{j=1}^{n}\left[u_{ij}v_{ji} - \sum_{k=1}^{n}\sum_{l=1}^{n}u_{ij}h2_{kl}^{j}v_{ki}v_{li}\right]e^{\lambda_j t} + \sum_{j=1}^{n}\sum_{k=1}^{n}\sum_{l=1}^{n}u_{ij}h2_{kl}^{j}v_{ki}v_{li}e^{(\lambda_k+\lambda_l)t} \tag{6.13}$$

or,

$$x_i\left(t\right) = \sum_{j=1}^{n}\left[P_{ij} - P2_{kl}^{j}\right]e^{\lambda_j t} + \sum_{j=1}^{n}P2_{kl}^{j}\,e^{(\lambda_k+\lambda_l)t} \tag{6.14}$$

where,

$$P_{ij} = u_{ij}v_{ji}$$

$$P2_{kl}^{j} = \sum_{k=1}^{n}\sum_{l=1}^{n}u_{ij}h2_{kl}^{j}v_{ki}v_{li}$$

Also,

$$x_i\left(t\right) = \sum_{j=1}^{n}P1_{kl}^{j}\,e^{\lambda_j t} + \sum_{j=1}^{n}P2_{kl}^{j}\,e^{(\lambda_k+\lambda_l)t} \tag{6.15}$$

where,

$$P1_{kl}^{j} = P_{ij} - P2_{kl}^{j}$$

There is a very important result in the expression (6.14): the linear participation factors are due to two terms, the linear definition of participation factors given by (6.5) and a correction term given by the contribution of nonlinear coefficients. $P2_{kl}^{j}$ represents the second order participation of the j^{th}

machine to the modal combination obtained from $(\lambda_k + \lambda_l)$ which also has influence on the participation of linear modes λ_j. Figure 6.10 shows the nonlinear participation factors, basically focusing on factors $P2_{kl}^{j}$.

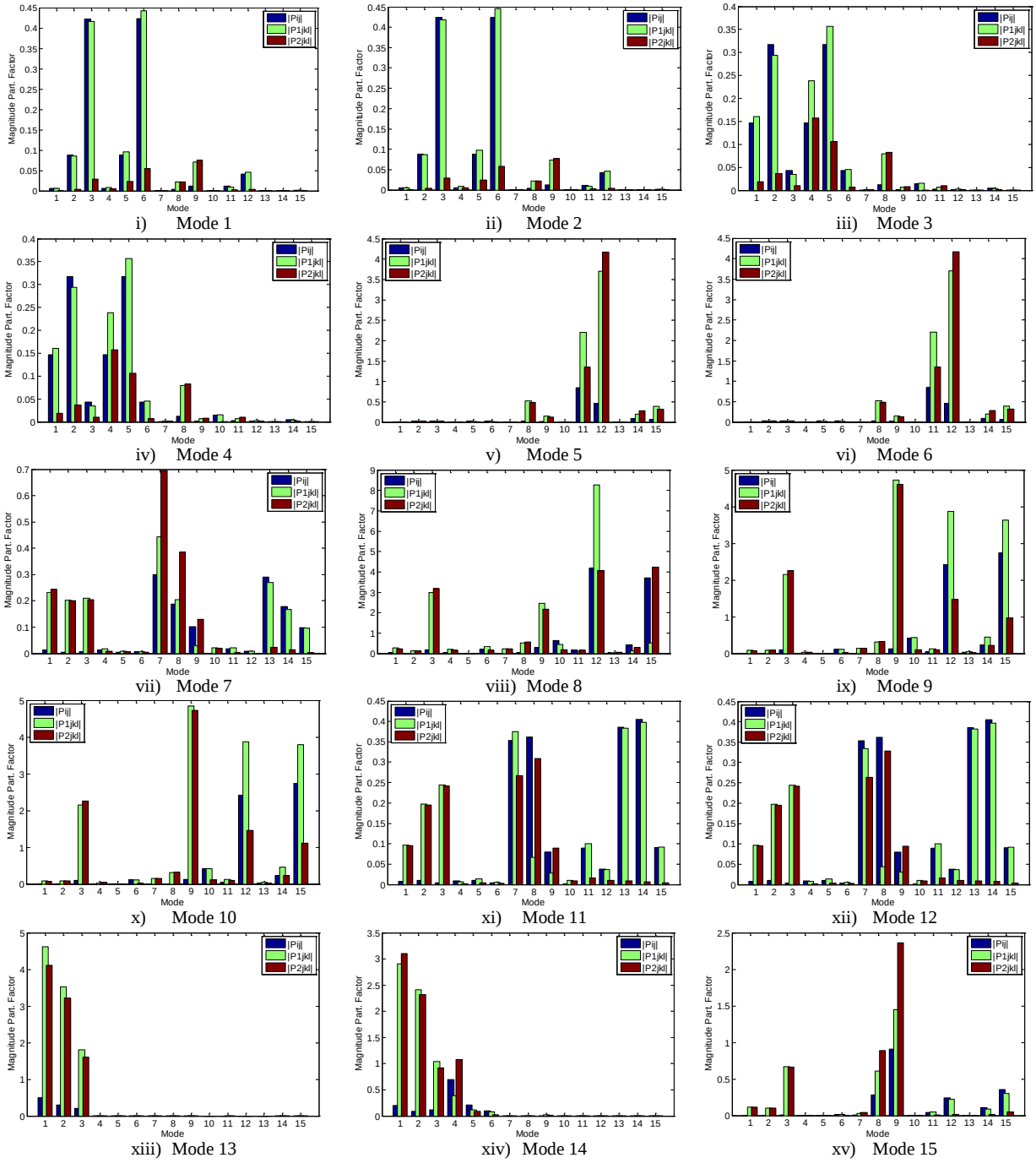

Figure 6.10 Nonlinear participations factors for the 3SM-9 Buses power system

Each bar diagram corresponds to the contribution of the modal combination with each mode. The modes with higher contributions due to modal combination are the 5, 8, 9, 10 and 13.

6.2.4 Algebraic Variables

The dynamic analysis in this section is oriented to the algebraic variables, *e.g.*, currents, active and reactive powers and generator voltages. Once the dynamic behavior of state variables has been obtained, it is straightforward to obtain the adequate conditions for algebraic variables. Basically, the solution is obtained solving the algebraic set of equations (4.37), (4.38) and (4.62) of Chapter 4. That is,

$$\begin{bmatrix} I_{d1} \\ I_{d2} \\ I_{d3} \end{bmatrix} = \begin{bmatrix} G_{11} & F_{G+B}(\delta_{12}) & F_{G+B}(\delta_{13}) \\ F_{G+B}(\delta_{21}) & G_{22} & F_{G+B}(\delta_{23}) \\ F_{G+B}(\delta_{31}) & F_{G+B}(\delta_{32}) & G_{33} \end{bmatrix} \begin{bmatrix} E'_{d1} \\ E'_{d2} \\ E'_{d3} \end{bmatrix} - \begin{bmatrix} B_{11} & F_{B-G}(\delta_{12}) & F_{B-G}(\delta_{13}) \\ F_{B-G}(\delta_{21}) & B_{22} & F_{B-G}(\delta_{23}) \\ F_{B-G}(\delta_{31}) & F_{B-G}(\delta_{32}) & B_{33} \end{bmatrix} \begin{bmatrix} E'_{q1} \\ E'_{q2} \\ E'_{q3} \end{bmatrix} \tag{6.16}$$

$$\begin{bmatrix} I_{q1} \\ I_{q2} \\ I_{q3} \end{bmatrix} = \begin{bmatrix} G_{11} & F_{G+B}(\delta_{12}) & F_{G+B}(\delta_{13}) \\ F_{G+B}(\delta_{21}) & G_{22} & F_{G+B}(\delta_{23}) \\ F_{G+B}(\delta_{31}) & F_{G+B}(\delta_{32}) & G_{33} \end{bmatrix} \begin{bmatrix} E'_{q1} \\ E'_{q2} \\ E'_{q3} \end{bmatrix} + \begin{bmatrix} B_{11} & F_{B-G}(\delta_{12}) & F_{B-G}(\delta_{13}) \\ F_{B-G}(\delta_{21}) & B_{22} & F_{B-G}(\delta_{23}) \\ F_{B-G}(\delta_{31}) & F_{B-G}(\delta_{32}) & B_{33} \end{bmatrix} \begin{bmatrix} E'_{d1} \\ E'_{d2} \\ E'_{d3} \end{bmatrix} \tag{6.17}$$

and,

$$\begin{bmatrix} P_{m1} \\ P_{m2} \\ P_{m3} \end{bmatrix} = \begin{bmatrix} E'_{d1} & E'_{d2} & E'_{d3} \end{bmatrix} \begin{bmatrix} I_{d1} \\ I_{d2} \\ I_{d3} \end{bmatrix} + \begin{bmatrix} E'_{q1} & E'_{q2} & E'_{q3} \end{bmatrix} \begin{bmatrix} I_{q1} \\ I_{q2} \\ I_{q3} \end{bmatrix} + \begin{bmatrix} D_1\omega_1 \\ D_2\omega_2 \\ D_3\omega_3 \end{bmatrix} \tag{6.18}$$

$$\begin{bmatrix} Q_{m1} \\ Q_{m2} \\ Q_{m3} \end{bmatrix} = \begin{bmatrix} E'_{q1} & E'_{q2} & E'_{q3} \end{bmatrix} \begin{bmatrix} I_{d1} \\ I_{d2} \\ I_{d3} \end{bmatrix} - \begin{bmatrix} E'_{d1} & E'_{d2} & E'_{d3} \end{bmatrix} \begin{bmatrix} I_{q1} \\ I_{q2} \\ I_{q3} \end{bmatrix} - \begin{bmatrix} x'_{d1} & x'_{d2} & x'_{d3} \end{bmatrix} \begin{bmatrix} I_{d1} \\ I_{d2} \\ I_{d3} \end{bmatrix}^2 - \begin{bmatrix} x'_{q1} & x'_{q2} & x'_{q3} \end{bmatrix} \begin{bmatrix} I_{q1} \\ I_{q2} \\ I_{q3} \end{bmatrix}^2 \tag{6.19}$$

The comparison is made considering the solution of (6.16) and (6.17) using the modal series solution and the full numerical solution of the nonlinear set of differential equations. The results are shown in Figure 6.11. According to the constraints defined in Section 6.6.2, the solutions obtained

using the modal series state variables is nearly identical to those obtained by the full numerical solution for each algebraic variables.

Low frequency oscillations are presented in the variables, which are the result of modal behavior of the original state variables, combined with their algebraic relationships. It is observed the transient presented after the fault, for which both trajectories are in very similar form. Thus, through this numerical proof, it can be concluded that even in the case of algebraic equations, that depend on state variables solution, the modal series approximation is giving good results.

6.2.5 Frequency analysis of linear and nonlinear contributions

In order to further assess the method ability to accurately capture the essential system behavior, the nonlinear contributions to the system response were computed by extracting the nonlinear part from the closed form solution obtained by the modal series method (Equation (3.30), Chapter 3), that is,

$$x_{i\,LINEAR}(t) = \sum_{j=1}^{N}\left(u_{ij} y_j^1(0) - \sum_{k=1}^{N}\sum_{l=1}^{N} u_{ij} h_{2kl}^j y_k^1(0) y_l^1(0) \right) e^{\lambda_j t} \tag{6.20}$$

and

$$x_{i\,NONLINEAR}(t) = \sum_{j=1}^{N}\sum_{k=1}^{N}\sum_{l=1}^{N} u_{ij} h_{2kl}^j y_k^1(0) y_l^1(0) e^{(\lambda_k+\lambda_l)t} \tag{6.21}$$

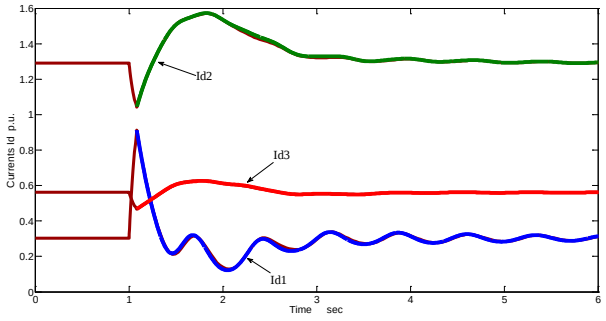

d axis currents

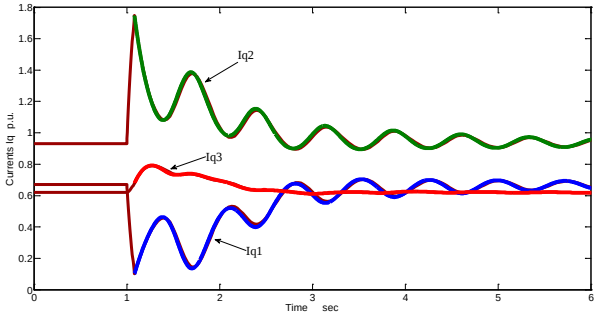

q axis currents

a) Stator Currents

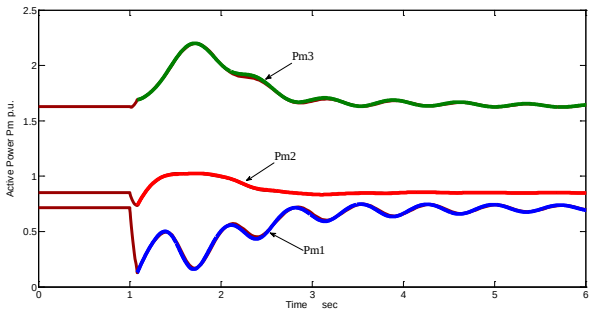

b) Active Powers

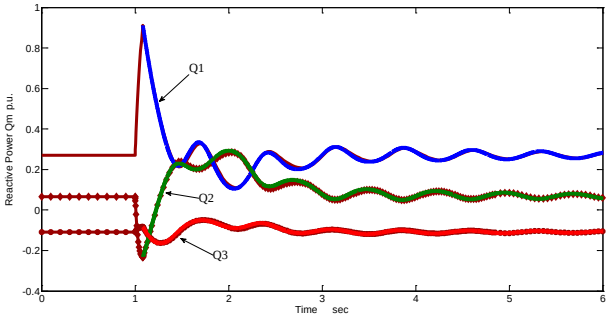

c) Reactive Powers

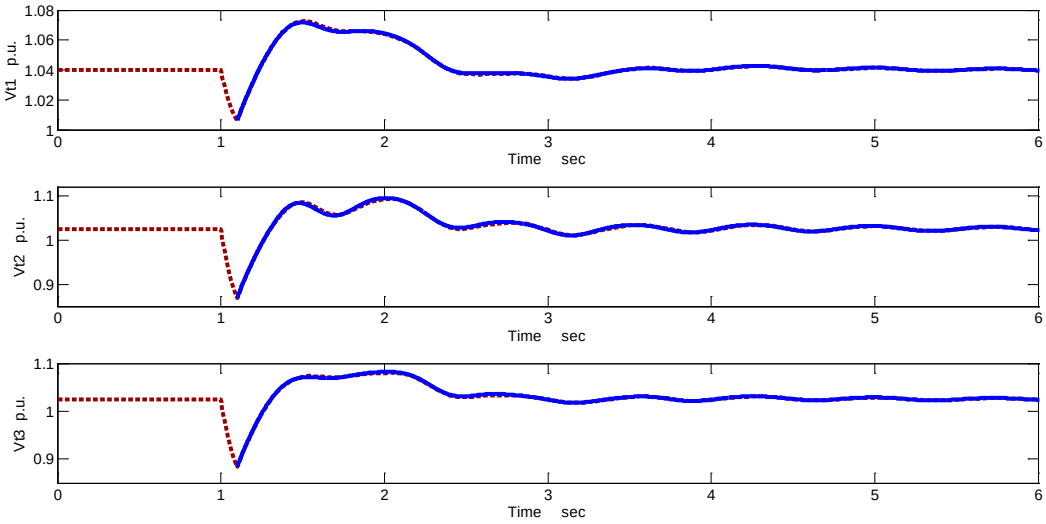

d) Terminal Voltages V_{ti}

Figure 6.11 Algebraic variables comparison between full solution and modal series method

This is shown in Figure 6.12 where the speed deviations at each synchronous machine are shown. These waveforms result from the consideration of the second order terms in the modal series method, and represent the nonlinear contribution to the total oscillation given by (6.21).

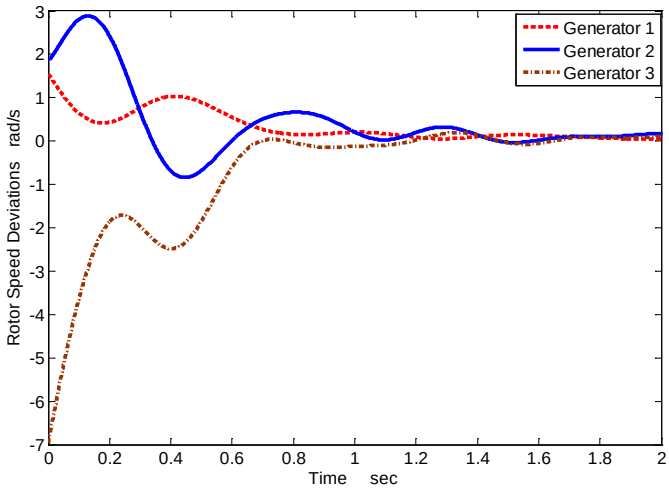

Figure 6.12 Nonlinear contribution associated to the speed deviations in the time domain

For comparison, using the Fast Fourier Transform (FFT) the rotor angle deviations for the nonlinear linear part were computed and plotted in Figure 6.13. Analysis of the peaks in the FFT of Figure 6.13 shows a good correlation with the system electromechanical modes of the state matrix **A** in Table 6.1.

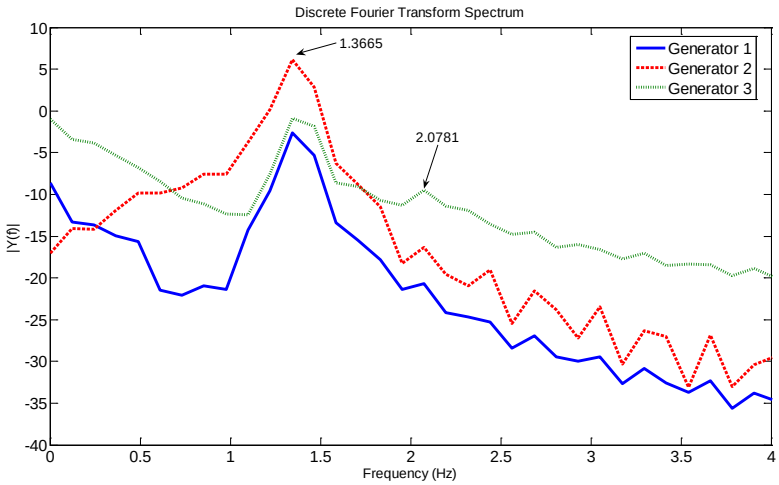

Figure 6.13 Spectral analysis by FFT of the nonlinear contribution of the speed deviations

As shown in Figure 6.14, the linear and nonlinear contributions to the speed deviations identify the presence of the electromechanical modes 3 and 4. The nonlinear contribution shows resonant frequencies at 1.3665 and 2.0781 Hz.

6.2.6 Comparisons with other Approaches

The proposed method generalizes modal analysis to high-dimensional systems and allows the computation of nonlinear input-output functions, which has been absent in previous work.

Table 6.3 Computational times comparison*

Activity	Full Numerical Solution	Linear Approximation	Modal Series	CPU-Time
Initialization	2.992638	2.992638	2.992638	
State Matrix	-	0.121824	0.121824	
Eigenvalues Eigenvectors	-	0.001278	0.001278	
Hessian Matrix	-	-	0.967034	
C^{j}_{kl} , h_{2kl}	-	-	0.025406	
Full Solution	0.193144		-	
Linear Approximation	-	0.246577	-	
Modal Series Formula	-	-	4.059203	
Total	**3.185782**	**3.362317**	**8.167383**	**10.3429**

*All times are expressed in seconds

An insight into the involved computational effort can be resumed from the study of CPU time required for the analysis of the test system using various approaches. Table 6.3 summarizes the CPU

times required for analysis of the above test system using linear solution and the modal series method. The software is executed using a PC/2.30 GHz; the code is written in MATLAB. All CPU times are in seconds.

In this study, the CPU time required to compute the linearized system (basically state matrix and its parameter obtained from symbolic analysis of the overall power system model) representation is about 0.121824 seconds, whereas the time spent to compute the Hessian matrix is 0.967034 s. The total time required to compute higher-order modal solutions is about 4.059203 seconds, compared to 0.246577 seconds needed for the linear approximation, and 0.193144 seconds for the full numerical solution. As suggested in this Table, the cost of nonlinear modal analysis drastically increases with the number of states, which requires the application of efficient sparsity-based techniques.

6.3 CASE STUDY 2: NEW ENGLAND TEST POWER SYSTEM (10 SM, 39 BUSES)

The 10 machines 39 buses New England test power system is considered in this case study. This system is a reduced equivalent of the WSCC power system, first introduced by [Pai 1989] and shown in Figure 6.14. The data of such system are given in Appendix C. The system is modeled according to the power system model previously described in Chapter 4, that is, a fourth order model for each synchronous machine combined with an AVR. The constraints of operation followed in this case study are:

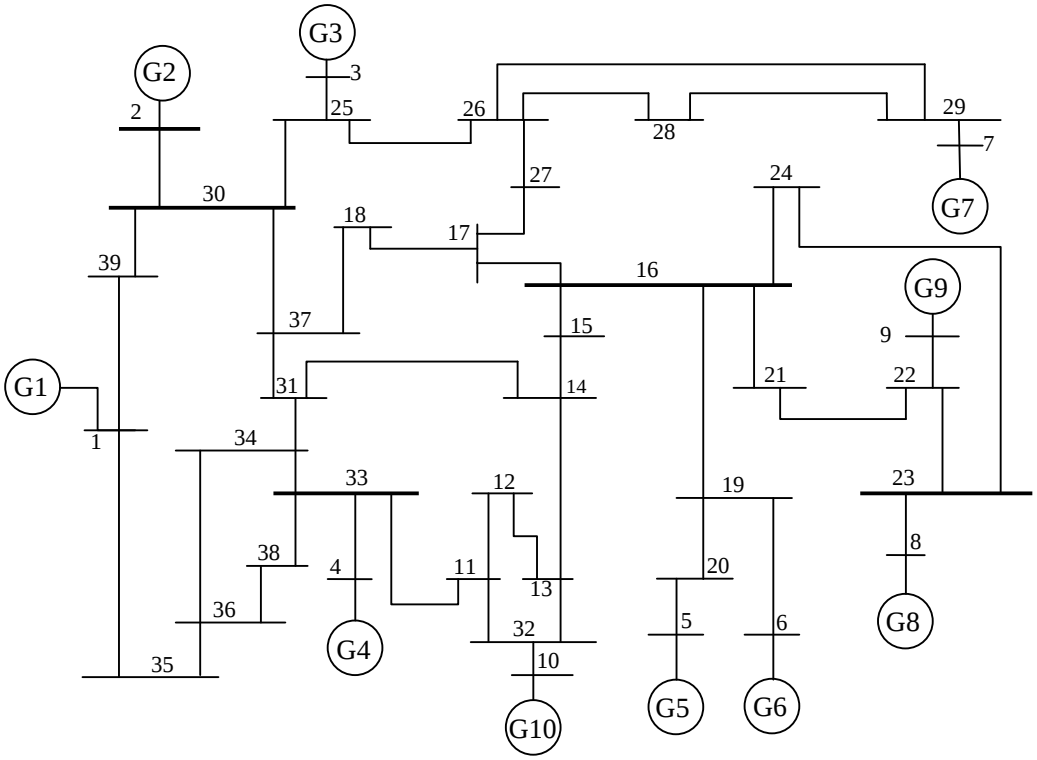

Figure 6.14 New England test power system

- A three phase fault is applied at the bus 31 during 0.083 seconds, and removed without any line switched.
- A three phase fault is applied at bus 26, leaving out of operation the transmission line 26-29. The fault is sustained during 5 cycles.

Also, the case study is structured as follows:

a) The small signal analysis is performed in order to obtain the linear characteristics of the system through the eigenvalues, eigenvectors and participation factors.

b) The nonlinear characteristics are obtained through the time domain simulation of the nonlinear power system operating under the constraints above described. The system is evaluated with respect to the numerical solution of the nonlinear model and with the linear approximation.

c) The fault clearance time is changed in the simulation, and analyzed with respect to the accuracy of the modal series method. In this case, the fault is sustained during 5, 8, 10 and 15 cycles and observed the dynamic of the nonlinear model.

d) Unstable conditions are also considered varying the system parameters (decreasing the time constant T'_{q0} up to 0.7, together with adding a damping coefficient $D_1 = 3.5$) and removing the fault at bus 31 by opening the line 31-14.

6.3.1 Small Signal Analysis

The modal analysis is performed on the power system under study. Table 6.4 describes the modes that are obtained from small signal analysis; 13 of them are oscillatory modes, and the rest are real eigenvalues.

Considering the participation factors analysis, dominant machines are obtained. In this case, only participation factors greater larger in magnitude than 0.09 have been considered. After the modal analysis, the system is exhibiting dominant modes that are related to local and control modes. However, a single interarea mode is observed (highlighted in Table 6.4), which represents an oscillation between machines 5 and 7.

6.3.2 Nonlinear model

To perform the study of nonlinear characteristics of the power system under study, the modal series approach is incorporated into the modeling. The set of nonlinear differential equations are treated once the linearization process and Jordan canonical form transformation are performed, resulting in the new set of equations, which is processed by the modal series approach. In the same way as the earlier case study, it is important to remark that the closed form analytical solution obtained by modal series is not

Table 6.4 Small Signal Analysis of the 10 unit,39 bus New England test power system

Mode	Eigenvalue	Frequency (Hz)	Damping Ratio	Associated State Variables	Participation Factor
1	-49.7818	0	1	E_{fd9}	0.9789
2	-49.5617	0	1	E_{fd7}	0.9825
3	-47.6599	0	1	E_{fd1}	0.9246
4	-46.8122	0	1	E_{fd8}	0.8976
5	-19.7051	0	1	E_{fd4}	0.9827
6	-16.3053	0	1	E_{fd6}, E_{fd10}	0.5367, 0.4373
7	-16.3721	0	1	E_{fd6}, E_{fd10}	0.4395, 0.5397
8,9	-0.3980 ± 9.4390i	1.5023	0.0421	δ_2, δ_3 ω_2, ω_3	0.2225, 0.2418
10,11	-0.4927 ± 9.4525i	1.5044	0.0521	δ_8, δ_9 ω_8, ω_9	0.2759, 0.1363
12,13	-0.4941 ± 9.0491i	1.4402	0.0545	δ_6, ω_6	0.3397, 0.3397
14,15	-0.2228 ± 7.8150i	1.2438	0.0285	δ_2, δ_3, ω_2, ω_3	0.1936, 0.1896
16,17	-0.2877 ± 7.8529i	1.2498	0.0366	δ_4, δ_{10}, ω_4, ω_{10}	0.2244, 0.2518
18	-8.0753	0	1	E'_{d5}	0.8586
19,20	-0.2251 ± 6.8802i	1.095	0.0327	δ_8, δ_9, ω_8, ω_9	0.0939, 0.2052
21,22	-0.1098 ± 6.1822i	0.9839	0.0178	$\delta_4, \delta_7, \delta_{10}$, $\omega_4, \omega_7, \omega_{10}$	0.1192, 0.1723, 0.1203
23,24	-0.0431 ± 5.6759i	0.9033	0.0076	δ_5, δ_7, ω_5, ω_7	0.2393, 0.1701
25	-6.8386	0	1	E'_{d3}, E'_{d9}	0.3197, 0.4557
26	-6.3624	0	1	E'_{d3}, E'_{d9}	0.5312, 0.2064
27,28	-0.0455 ± 3.0717i	0.4889	0.0148	δ_1, ω_1	0.1483, 0.1370
29	-4.5902	0	1	E'_{q8}, E'_{d8}	0.6603
30,31	-2.6975 ± 2.0940i	0.3333	0.7899	E'_{q5}, E'_{fd5}	0.3560, 0.3543
32,33	-2.9332 ± 1.2846i	0.2044	0.916	E'_{q3}, E'_{d3}, E_{fd3}	0.3095, 0.1311, 0.3868
34,35	-1.0443 ± 1.7357i	0.2762	0.5155	E'_{q2}, E'_{fd2}	0.4144, 0.4318
36	-2.6254	0	1	E'_{q5}, E'_{d6}, E_{fd5}	0.1429, 0.5947, 0.1366
37	-2.4591	0	1	ω_1, E'_{q1}, E'_{q3}, E_{fd3}	0.1028, 0.4686, 0.1064, 0.0960
38	-1.9331	0	1	E'_{d4}, E'_{d10}	0.3003, 0.5692
39	-1.7251	0	1	E'_{d4}, E'_{d10}	0.4790, 0.2519
40	0	0	-1	δ_1	1.0000
41	-1.3269	0	1	E'_{q8}, E'_{d7}, E'_{d8}	0.1219, 0.1031, 0.6707
42	-1.2462	0	1	E'_{q7}, E'_{d7}, E'_{d8}	0.1910, 0.5810, 0.1045
43,44	-1.0162 ± 0.0312i	0.005	0.9995	ω_1, E'_{d1}	0.2656, 0.3096
45	-0.725	0	1	E'_{d2}	0.9826
46	-0.6357	0	1	E'_{q7}, E'_{d7}	0.5996, 0.1972
47	-0.5268	0	1	E'_{q4}, E'_{q10}	0.3144, 0.3726
48	-0.4051	0	1	E'_{q6}, E'_{d6}	0.8194, 0.0929
49	-0.4499	0	1	E'_{q9}	0.8758
50	-0.4341	0	1	E'_{q4}, E'_{q10}	0.4771, 0.3943

affected by the estimation of the initial conditions, since they are calculated based on the perturbation conditions; therefore, their calculation do not need any numerical process.

Writing the set of differential equations for this case study and according to the modal series process, it can be represented in the Laplace domain as,

$$\mathbf{X}(s)=\begin{bmatrix} x_1(s) \\ x_2(s) \\ \vdots \\ x_n(s) \end{bmatrix}= \begin{bmatrix} \sum_{j=1}^{n}\left\{ \begin{array}{l} u_{1j}\dfrac{y_j(0)}{s-\lambda_j}+\sum_{k=1}^{n}\sum_{l=1}^{n}C_{kl}^{j}u_{1j}y_k(0)y_l(0)\dfrac{1}{(\lambda_k+\lambda_l-\lambda_j)}\left(\dfrac{1}{s-\lambda_k-\lambda_l}-\dfrac{1}{s-\lambda_j}\right)+ \\ \sum_{k=1}^{n}\sum_{l=1}^{n}\sum_{p=1}^{n}\sum_{q=1}^{n}u_{1j}C_{kl}^{j}C_{pq}^{k}Y_p^1(0)Y_q^1(0)Y_l^1(0)\dfrac{1}{(\lambda_j-\lambda_p-\lambda_q-\lambda_l)}\left[\dfrac{1}{(\lambda_j-\lambda_l-\lambda_k)}\dfrac{1}{(s-\lambda_j)}-\dfrac{1}{(\lambda_p+\lambda_q-\lambda_k)}\dfrac{1}{(s-\lambda_p-\lambda_q-\lambda_l)}\right]+ \\ \sum_{k=1}^{n}\sum_{l=1}^{n}\sum_{p=1}^{n}\sum_{q=1}^{n}u_{1j}C_{kl}^{j}C_{pq}^{l}Y_k^1(0)Y_p^1(0)Y_q^1(0)\dfrac{1}{(\lambda_j-\lambda_p-\lambda_q-\lambda_k)}\dfrac{1}{(\lambda_p+\lambda_q-\lambda_l)}\left[\dfrac{1}{(s-\lambda_j)}-\dfrac{1}{(s_1-\lambda_p-\lambda_q-\lambda_k)}\right]+ \\ \sum_{p=1}^{n}\sum_{q=1}^{n}\sum_{r=1}^{n}u_{1j}D_{pqr}^{j}Y_p^1(0)Y_q^1(0)Y_r^1(0)\dfrac{1}{(\lambda_j-\lambda_p-\lambda_q-\lambda_r)}\left[\dfrac{1}{(s-\lambda_j)}-\dfrac{1}{(s-\lambda_p-\lambda_q-\lambda_r)}\right] \end{array} \right\} \\ \sum_{j=1}^{n}\left\{ \begin{array}{l} u_{2j}\dfrac{y_j(0)}{s-\lambda_j}+\sum_{k=1}^{n}\sum_{l=1}^{n}C_{kl}^{j}u_{2j}y_k(0)y_l(0)\dfrac{1}{(\lambda_k+\lambda_l-\lambda_j)}\left(\dfrac{1}{s-\lambda_k-\lambda_l}-\dfrac{1}{s-\lambda_j}\right)+ \\ \sum_{k=1}^{n}\sum_{l=1}^{n}\sum_{p=1}^{n}\sum_{q=1}^{n}u_{2j}C_{kl}^{j}C_{pq}^{k}Y_p^1(0)Y_q^1(0)Y_l^1(0)\dfrac{1}{(\lambda_j-\lambda_p-\lambda_q-\lambda_l)}\left[\dfrac{1}{(\lambda_j-\lambda_l-\lambda_k)}\dfrac{1}{(s-\lambda_j)}-\dfrac{1}{(\lambda_p+\lambda_q-\lambda_k)}\dfrac{1}{(s-\lambda_p-\lambda_q-\lambda_l)}\right]+ \\ \sum_{k=1}^{n}\sum_{l=1}^{n}\sum_{p=1}^{n}\sum_{q=1}^{n}u_{2j}C_{kl}^{j}C_{pq}^{l}Y_k^1(0)Y_p^1(0)Y_q^1(0)\dfrac{1}{(\lambda_j-\lambda_p-\lambda_q-\lambda_k)}\dfrac{1}{(\lambda_p+\lambda_q-\lambda_l)}\left[\dfrac{1}{(s-\lambda_j)}-\dfrac{1}{(s_1-\lambda_p-\lambda_q-\lambda_k)}\right]+ \\ \sum_{p=1}^{n}\sum_{q=1}^{n}\sum_{r=1}^{n}u_{2j}D_{pqr}^{j}Y_p^1(0)Y_q^1(0)Y_r^1(0)\dfrac{1}{(\lambda_j-\lambda_p-\lambda_q-\lambda_r)}\left[\dfrac{1}{(s-\lambda_j)}-\dfrac{1}{(s-\lambda_p-\lambda_q-\lambda_r)}\right] \end{array} \right\} \\ \vdots \\ \sum_{j=1}^{n}\left\{ \begin{array}{l} u_{nj}\dfrac{y_j(0)}{s-\lambda_j}+\sum_{k=1}^{n}\sum_{l=1}^{n}C_{kl}^{j}u_{nj}y_k(0)y_l(0)\dfrac{1}{(\lambda_k+\lambda_l-\lambda_j)}\left(\dfrac{1}{s-\lambda_k-\lambda_l}-\dfrac{1}{s-\lambda_j}\right)+ \\ \sum_{k=1}^{n}\sum_{l=1}^{n}\sum_{p=1}^{n}\sum_{q=1}^{n}u_{nj}C_{kl}^{j}C_{pq}^{k}Y_p^1(0)Y_q^1(0)Y_l^1(0)\dfrac{1}{(\lambda_j-\lambda_p-\lambda_q-\lambda_l)}\left[\dfrac{1}{(\lambda_j-\lambda_l-\lambda_k)}\dfrac{1}{(s-\lambda_j)}-\dfrac{1}{(\lambda_p+\lambda_q-\lambda_k)}\dfrac{1}{(s-\lambda_p-\lambda_q-\lambda_l)}\right]+ \\ \sum_{k=1}^{n}\sum_{l=1}^{n}\sum_{p=1}^{n}\sum_{q=1}^{n}u_{nj}C_{kl}^{j}C_{pq}^{l}Y_k^1(0)Y_p^1(0)Y_q^1(0)\dfrac{1}{(\lambda_j-\lambda_p-\lambda_q-\lambda_k)}\dfrac{1}{(\lambda_p+\lambda_q-\lambda_l)}\left[\dfrac{1}{(s-\lambda_j)}-\dfrac{1}{(s_1-\lambda_p-\lambda_q-\lambda_k)}\right]+ \\ \sum_{p=1}^{n}\sum_{q=1}^{n}\sum_{r=1}^{n}u_{nj}D_{pqr}^{j}Y_p^1(0)Y_q^1(0)Y_r^1(0)\dfrac{1}{(\lambda_j-\lambda_p-\lambda_q-\lambda_r)}\left[\dfrac{1}{(s-\lambda_j)}-\dfrac{1}{(s-\lambda_p-\lambda_q-\lambda_r)}\right] \end{array} \right\} \end{bmatrix} \tag{6.22}$$

where,

$$\mathbf{X}(s)=\left[\delta_1(s) \quad \ldots \quad \delta_{10}(s) \quad \omega_1(s) \quad \ldots \quad \omega_{10}(s) \quad E'_{q1}(s) \quad \ldots \quad E'_{q10}(s) \quad E'_{d1}(s) \quad \ldots \quad E'_{d10}(s) \quad E_{fd1}(s) \quad \ldots \quad E_{fd10}(s)\right]^T$$

Upon rearranging terms, we obtain,

$$\mathbf{X}(s)=\begin{bmatrix}\sum_{j=1}^{n}\left\{\begin{array}{l}u_{1j}F_j^1(s)+\sum_{k=1}^{n}\sum_{l=1}^{n}C_{kl}^{j}u_{1j}y_k(0)y_l(0)F_j^2(s)+\sum_{k=1}^{n}\sum_{l=1}^{n}\sum_{p=1}^{n}\sum_{q=1}^{n}C_{kl}^{j}C_{pq}^{k}u_{1j}Y_p^1(0)Y_q^1(0)Y_l^1(0)F_1^3(s)+\\ \sum_{k=1}^{n}\sum_{l=1}^{n}\sum_{p=1}^{n}\sum_{q=1}^{n}C_{kl}^{j}C_{pq}^{l}u_{1j}Y_k^1(0)Y_p^1(0)Y_q^1(0)F_2^3(s)+\sum_{p=1}^{n}\sum_{q=1}^{n}\sum_{r=1}^{n}D_{pqr}^{j}u_{1j}Y_p^1(0)Y_q^1(0)Y_r^1(0)F_3^3(s)\end{array}\right\}\\ \sum_{j=1}^{n}\left\{\begin{array}{l}u_{2j}\frac{y_j(0)}{s-\lambda_j}+\sum_{k=1}^{n}\sum_{l=1}^{n}C_{kl}^{j}u_{2j}y_k(0)y_l(0)F_j(s)++\sum_{k=1}^{n}\sum_{l=1}^{n}\sum_{p=1}^{n}\sum_{q=1}^{n}C_{kl}^{j}C_{pq}^{k}u_{2j}Y_p^1(0)Y_q^1(0)Y_l^1(0)F_1^3(s)+\\ \sum_{k=1}^{n}\sum_{l=1}^{n}\sum_{p=1}^{n}\sum_{q=1}^{n}C_{kl}^{j}C_{pq}^{l}u_{2j}Y_k^1(0)Y_p^1(0)Y_q^1(0)F_2^3(s)+\sum_{p=1}^{n}\sum_{q=1}^{n}\sum_{r=1}^{n}D_{pqr}^{j}u_{2j}Y_p^1(0)Y_q^1(0)Y_r^1(0)F_3^3(s)\end{array}\right\}\\ \vdots\\ \sum_{j=1}^{n}\left\{\begin{array}{l}u_{nj}\frac{y_j(0)}{s-\lambda_j}+\sum_{k=1}^{n}\sum_{l=1}^{n}C_{kl}^{j}u_{nj}y_k(0)y_l(0)F_j(s)++\sum_{k=1}^{n}\sum_{l=1}^{n}\sum_{p=1}^{n}\sum_{q=1}^{n}C_{kl}^{j}C_{pq}^{k}u_{nj}Y_p^1(0)Y_q^1(0)Y_l^1(0)F_1^3(s)+\\ \sum_{k=1}^{n}\sum_{l=1}^{n}\sum_{p=1}^{n}\sum_{q=1}^{n}C_{kl}^{j}C_{pq}^{l}u_{nj}Y_k^1(0)Y_p^1(0)Y_q^1(0)F_2^3(s)+\sum_{p=1}^{n}\sum_{q=1}^{n}\sum_{r=1}^{n}D_{pqr}^{j}u_{nj}Y_p^1(0)Y_q^1(0)Y_r^1(0)F_3^3(s)\end{array}\right\}\end{bmatrix} \tag{6.23}$$

where,

$$F_j^1(s)=\frac{y_j(0)}{s-\lambda_j}$$

$$F_j^2(s)=\frac{1}{\left(\lambda_k+\lambda_l-\lambda_j\right)}\left(\frac{1}{s-\lambda_k-\lambda_l}-\frac{1}{s-\lambda_j}\right)$$

$$F_1^3(s)=\frac{1}{\left(\lambda_j-\lambda_p-\lambda_q-\lambda_l\right)}\left[\frac{1}{\left(\lambda_j-\lambda_l-\lambda_k\right)}F_j^1(s)-\frac{1}{\left(\lambda_p+\lambda_q-\lambda_k\right)}\frac{1}{\left(s-\lambda_p-\lambda_q-\lambda_l\right)}\right]$$

$$F_2^3(s)=\frac{1}{\left(\lambda_j-\lambda_p-\lambda_q-\lambda_k\right)}\frac{1}{\left(\lambda_p+\lambda_q-\lambda_l\right)}\left[F_j^1(s)-\frac{1}{\left(s_1-\lambda_p-\lambda_q-\lambda_k\right)}\right]$$

$$F_3^3(s)=\frac{1}{\left(\lambda_j-\lambda_p-\lambda_q-\lambda_r\right)}\left[F_j^1(s)-\frac{1}{\left(s-\lambda_p-\lambda_q-\lambda_r\right)}\right]$$

These equations are amenable to multidimensional Laplace analysis using the theory of Chapter 3 and 5. We emphasize that, unlike other approaches (such as normal forms), the above formulations allows the study of system behavior in both, time and frequency domains. To allow a comparison with full nonlinear results, the following study is constrained to time-domain solution. The closed form time evolutions of the linear and nonlinear parts of $x_i(t)$ with second-order accuracy are, respectively:

$$x_{i\,LINEAR}(t)=\sum_{j=1}^{N}\left(\sigma 1_{kl}^{j}\right)e^{\lambda_j t}$$

$$\sigma 1_{kl}^{j}=u_{ij}y_j^1(0)-\sum_{k=1}^{N}\sum_{l=1}^{N}u_{ij}h_{2kl}^{j}y_k^1(0)y_l^1(0)+\sum_{p=1}^{n}\sum_{q=1}^{n}\sum_{r=1}^{n}u_{ij}h_{3\,pqr}^{\ j}y_p^1(0)y_q^1(0)y_r^1(0)$$
$$+\sum_{k=1}^{n}\sum_{l=1}^{n}\sum_{p=1}^{n}\sum_{q=1}^{n}u_{ij}\frac{y_p^1(0)y_q^1(0)y_l^1(0)}{\left(\lambda_j-\lambda_p-\lambda_q-\lambda_l\right)}h_{2kl}^{\ j}+\sum_{k=1}^{n}\sum_{l=1}^{n}\sum_{p=1}^{n}\sum_{q=1}^{n}u_{ij}h_{2\,pq}^{\ l}C_{kl}^{j}\frac{y_k^1(0)y_p^1(0)y_q^1(0)}{\left(\lambda_j-\lambda_p-\lambda_q-\lambda_k\right)}$$

and

$$x_{i\ NONLINEAR}(t)=\sum_{j=1}^{N}\sigma 2_{kl}^{j}e^{(\lambda_k+\lambda_l)t}-\sum_{p=1}^{n}\sum_{q=1}^{n}\sum_{r=1}^{n}\sigma 3_{1,pqr}^{j}e^{(\lambda_p+\lambda_q+\lambda_r)t}-\sum_{k=1}^{n}\sum_{l=1}^{n}\sum_{p=1}^{n}\sum_{q=1}^{n}\sigma 3_{2,klpq}^{j}e^{(\lambda_p+\lambda_q+\lambda_l)t}$$
$$-\sum_{k=1}^{n}\sum_{l=1}^{n}\sum_{p=1}^{n}\sum_{q=1}^{n}\sigma 3_{3,klpq}^{j}e^{(\lambda_p+\lambda_q+\lambda_k)t}$$

$$\sigma 2_{kl}^{j}=\sum_{j=1}^{N}\sum_{k=1}^{N}\sum_{l=1}^{N}u_{ij}h_{2kl}^{j}y_k^1(0)y_l^1(0)$$

$$\sigma 3_{1,pqr}^{j}=\sum_{p=1}^{n}\sum_{q=1}^{n}\sum_{r=1}^{n}u_{ij}h_{3pqr}^{j}y_p^1(0)y_q^1(0)y_r^1(0)$$

$$\sigma 3_{2,klpq}^{j}=\sum_{k=1}^{n}\sum_{l=1}^{n}\sum_{p=1}^{n}\sum_{q=1}^{n}u_{ij}\frac{y_p^1(0)y_q^1(0)y_l^1(0)}{(\lambda_j-\lambda_p-\lambda_q-\lambda_l)}h_{2pq}^{l}$$

$$\sigma 3_{3,klpq}^{j}=\sum_{k=1}^{n}\sum_{l=1}^{n}\sum_{p=1}^{n}\sum_{q=1}^{n}u_{ij}h_{2pq}^{l}C_{kl}^{j}\frac{y_k^1(0)y_p^1(0)y_q^1(0)}{(\lambda_j-\lambda_p-\lambda_q-\lambda_k)}$$

6.3.3 Time Domain Validation

The experiment in this section is conducted to validate the nonlinear approximation with respect to the linear approximation and the full numerical solution of the nonlinear set of differential equations. The first study shows the results obtained for the relative rotor angles (Figure 6.15) according to the constraints defined previously, that is, a three phase stub at bus 31 maintained over 5 cycles and liberated without network change. The waveforms show identical responses between modal series and full numerical solution. More noticeable differences between the solution obtained by modal series and linear approximation are observed for the selected variables.

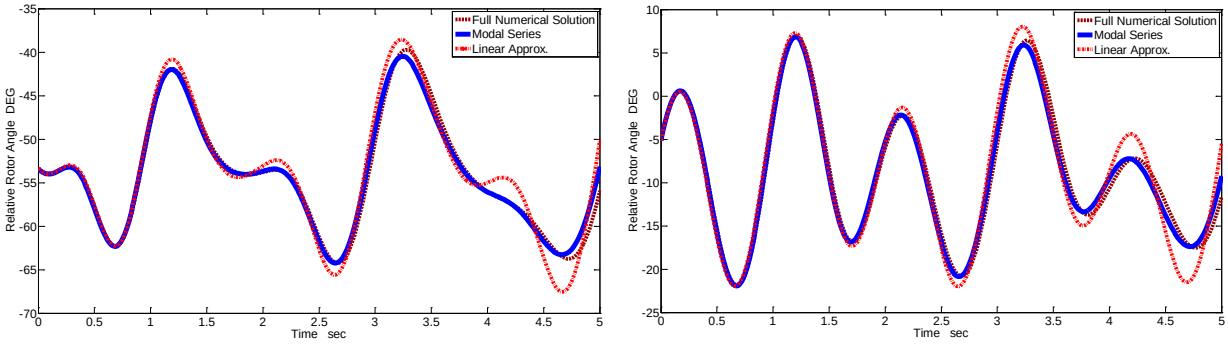

a) Relative rotor angle $\delta_{2,7}$

b) Relative rotor angle $\delta_{10,7}$

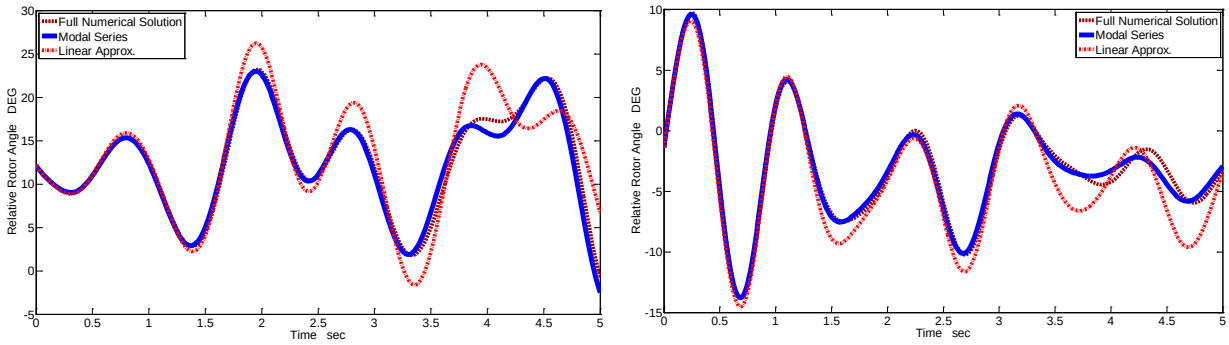

c) Relative rotor angle $\delta_{5,9}$ d) Relative rotor angle $\delta_{4,3}$

Figure 6.15 Relative rotor angle graphics of selected angles

Now, continuing with the experiment, the same fault is applied extending the faulted time to 8 cycles (0.1333 seconds) and removing the fault by switching-off the line 37-31. The Figure 6.16 shows the time domain evolution of rotor angle variables. In all cases, the modal series solution closely follows the full numerical solution, while a large solution deviation results when the linear approximation method is used.

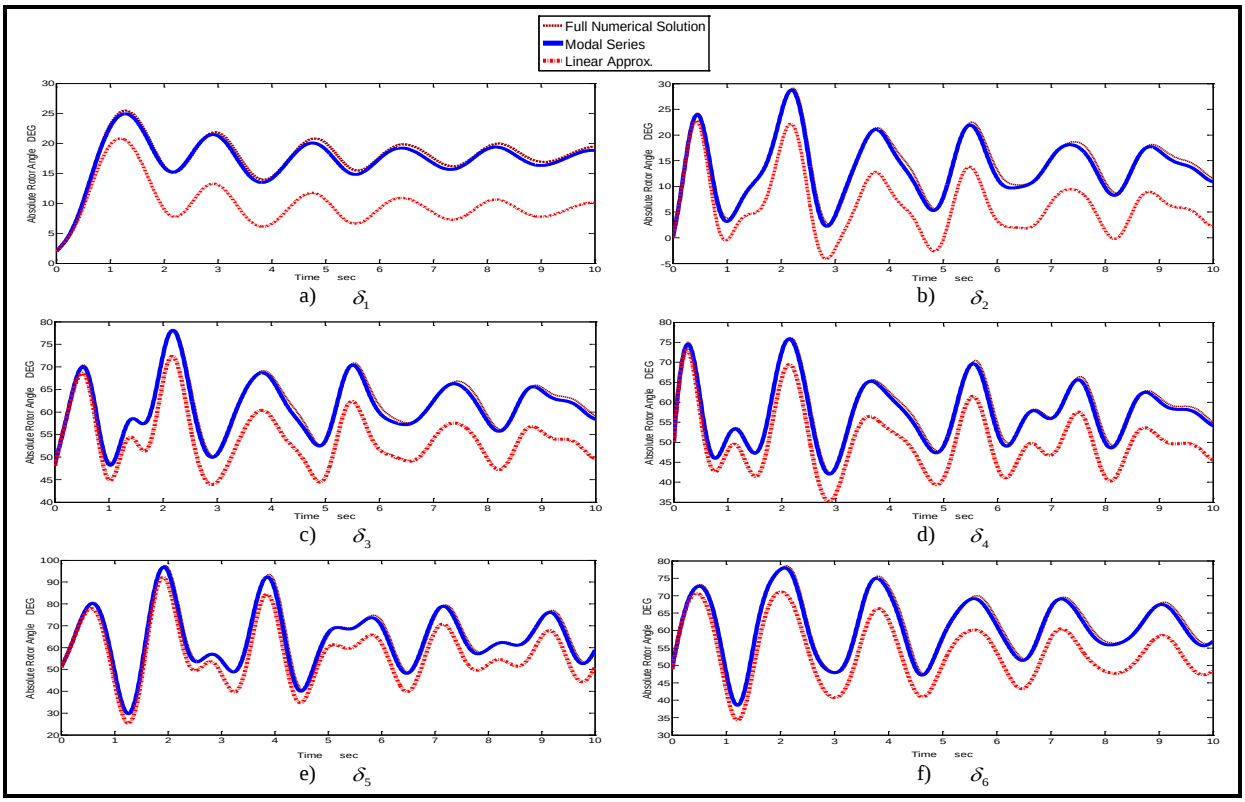

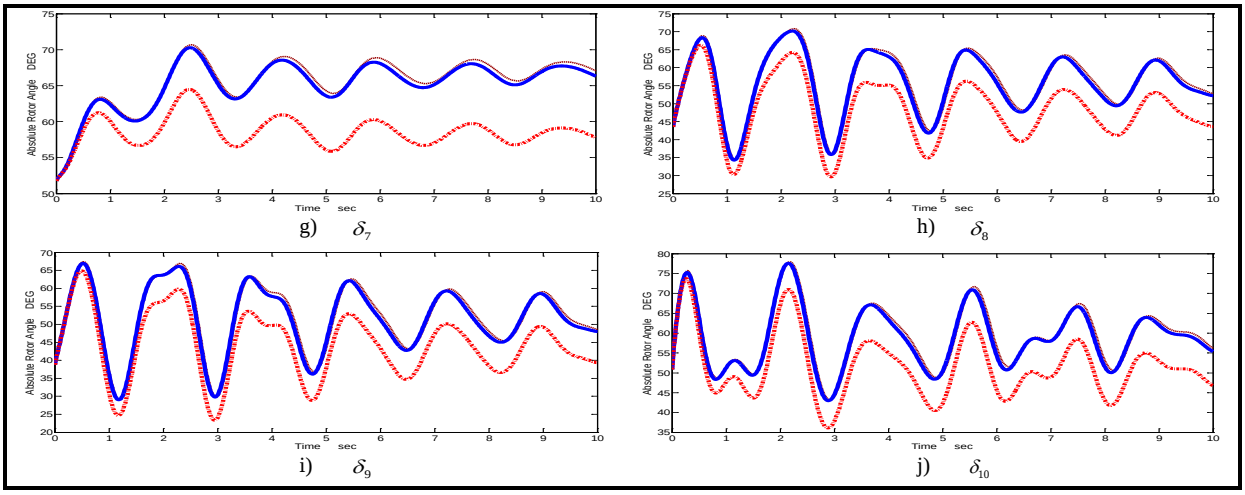

Figure 6.16 Absolute rotor angle graphics of generators in the study case of the New England test power system

Similar evolution is observed in the variables of E'_{qi} voltages that are shown in Figure 6.17. Again, the trajectories obtained by the linear approximation are with notorious differences with respect to modal series and full numerical solution, respectively. The last two are in closed agreement.

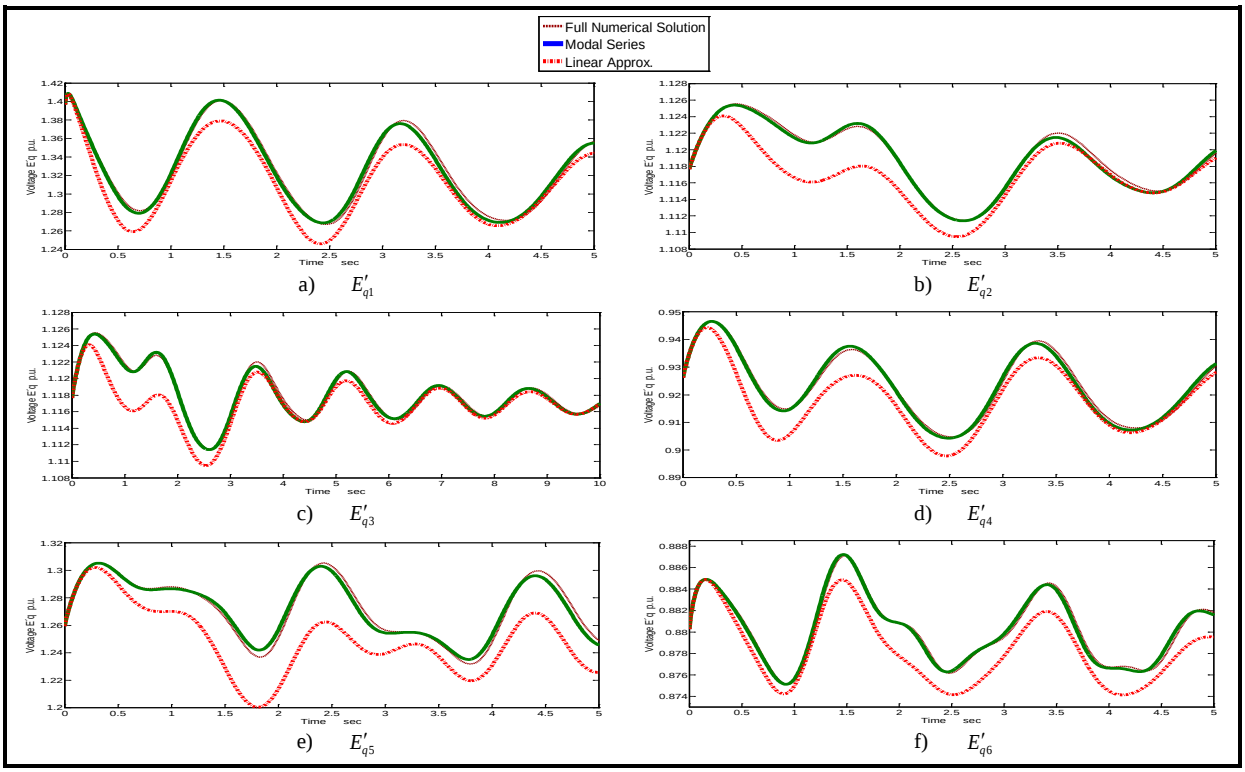

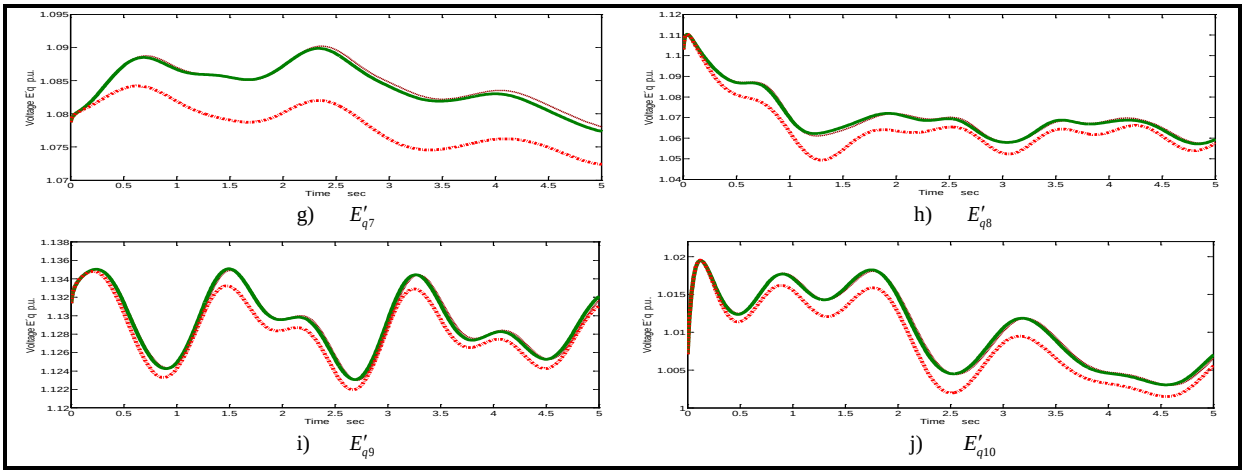

g) E'_{q7} h) E'_{q8}

i) E'_{q9} j) E'_{q10}

Figure 6.17 Voltage E'_{qi} graphics of generators in the study case of the New England test power system

The rest of state variables involved in the power system model, are exemplified. Let us consider the Figure 6.18 that illustrates the rotor velocity ω_3 and ω_5. The nonlinear contribution of such state variables may seem to be less relevant than the rotor angles and *q* axis voltages, since the waveforms of linear approximation, modal series and full numerical solution follow similar patterns. Small differences in the trajectory of linear approximation are noticed in the two variables illustrated in this Figure. Also, a graph of sixty seconds of simulation is shown in Figure 6.18 c), where it can be observed that the solutions reproduce similar waveforms, but oscillate with differences in both, phase angle and amplitude.

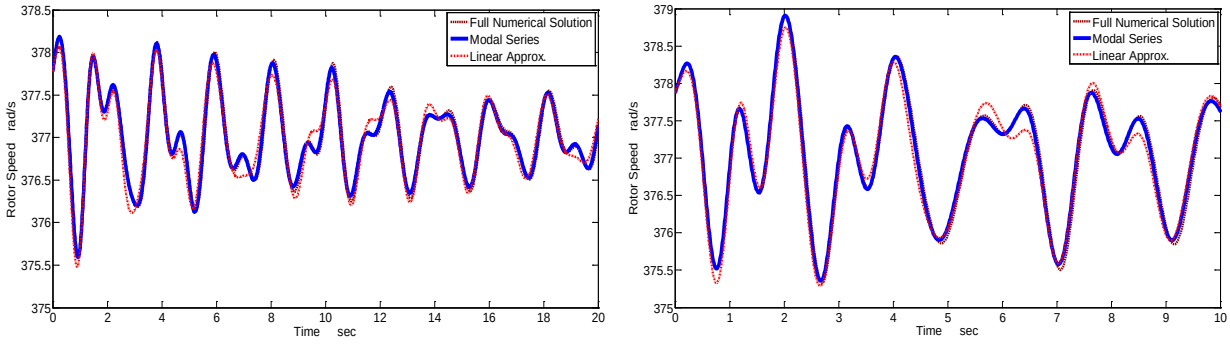

a) Rotor Speed ω_3 b) Rotor Speed ω_5

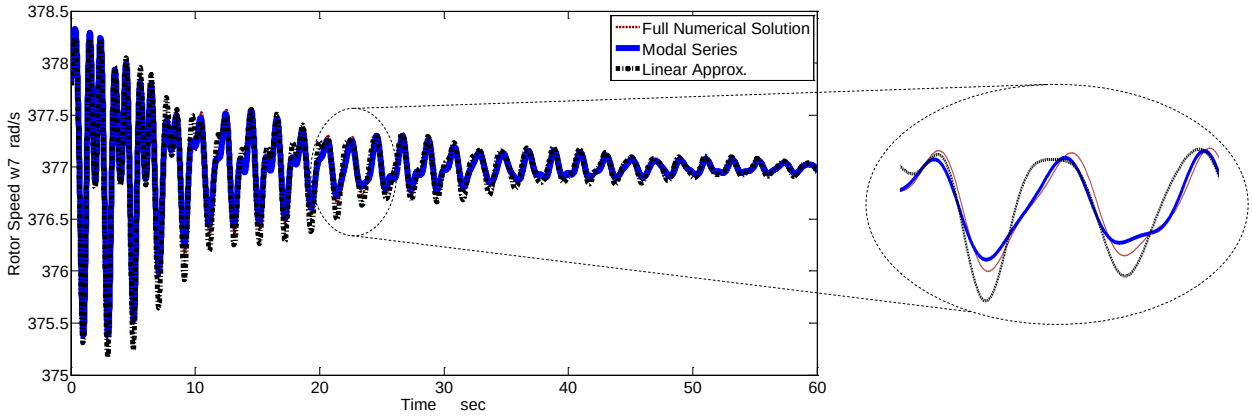

c) Long simulation of Rotor Speed ω_5

Figure 6.18 Rotor Speed graphics of generators 3 and 5 in the study case of the New England test power system

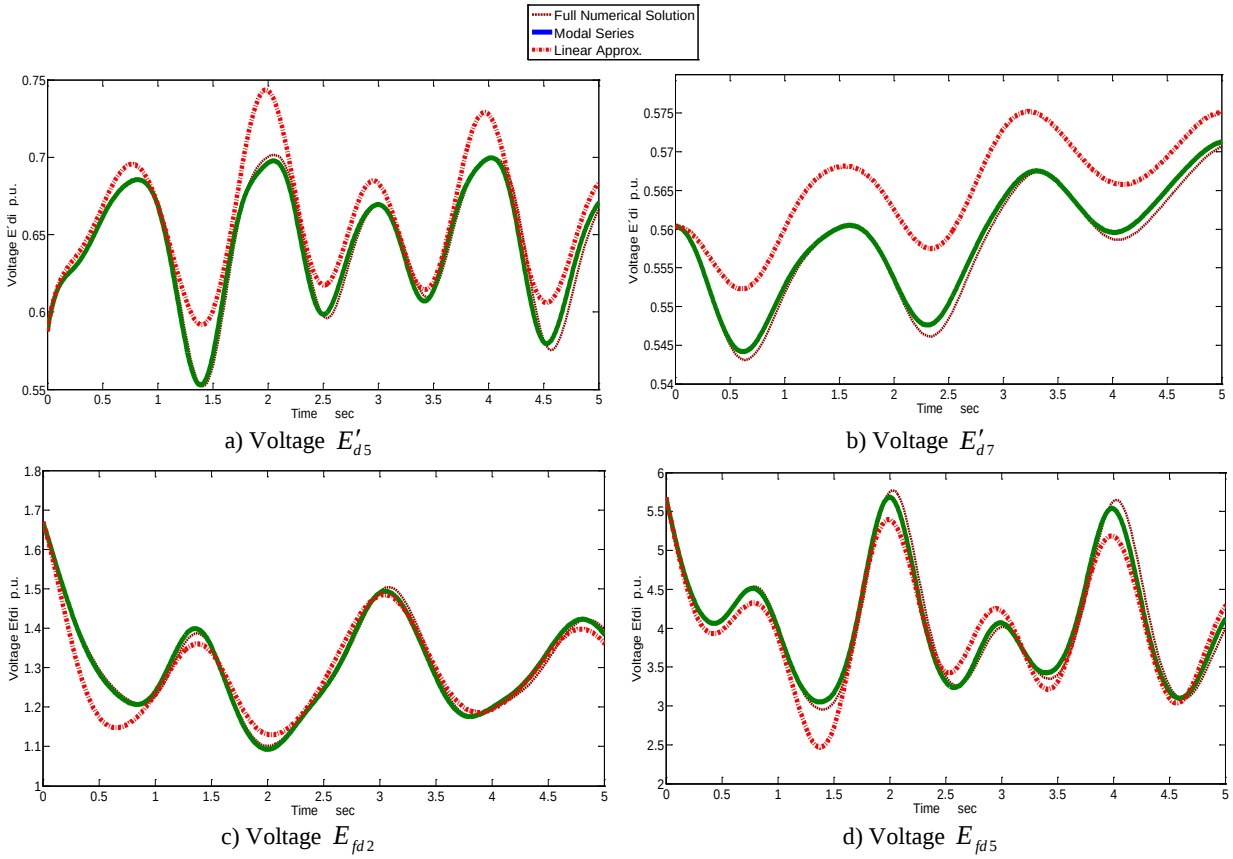

a) Voltage E'_{d5}

b) Voltage E'_{d7}

c) Voltage E_{fd2}

d) Voltage E_{fd5}

Figure 6.19 Voltages E'_{di} E'_{fdi} graphics of generators 2, 5 and 7 in the study case of the New England test power system

With reference to the direct axis voltages E'_{di} and controlled field voltage E_{fdi}, there are also visible differences in the simulations that are compared between linear approximation and modal series and full numerical solution. Figures 6.19 a) and b) detail the experiment for the voltages E'_{d5} and E'_{d7} where linear approximation maintains different trajectory than that followed by modal series and full

numerical solution in both cases, while for the field voltages variables E_{fd2} and E_{fd5} shown in Figure 6.19 c) and d), these differences are smaller.

This behavior confirms the presence of nonlinear contribution to the full solution, which is not considered when only the linear approximation is considered. Finally, Figure 6.20 shows a three-dimensional graph to detail the differences in trajectories followed when the rotor angle, rotor speed and *q* axis voltage are compared. In section 6.3.5 the nonlinear factors extend in a mathematical frame the meaning of these differences here illustrated in a qualitative way.

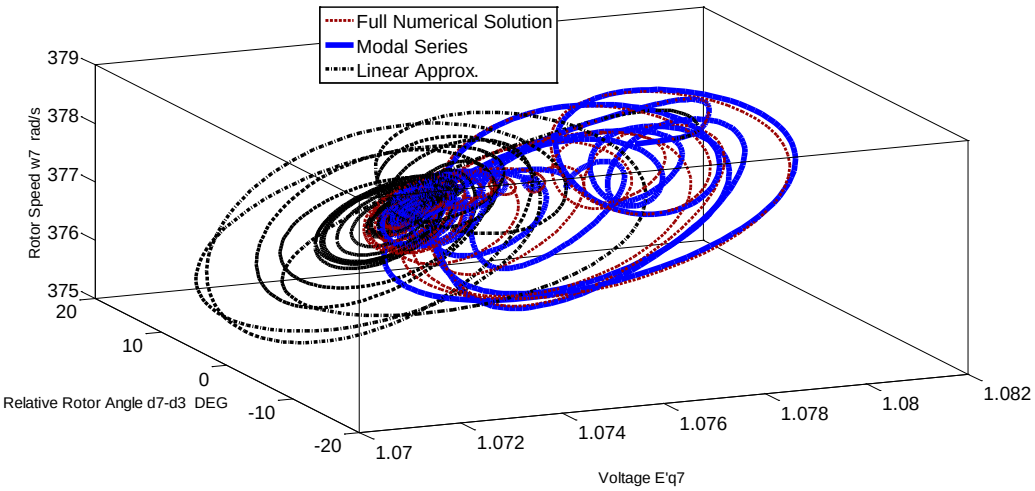

Figure 6.20 Three-dimensional comparison of modal series solution with respect to linear approximation and full numerical solution

6.3.4 Nonlinear oscillation analysis

In the same way as in the previous case study, the nonlinear indexes given by (6.1)-(6.4) are considered now. Recalling that such indexes establish some of the main nonlinear characteristics with respect to the nonlinear modal interaction, they are used here to express the nonlinear contribution to the closed form solution.

In the first instance, observing the nonlinear coefficients C_{kl}^{j} and h_{2kl}^{j} that link the earlier nonlinear frame; the Figure 6.21 shows the coefficient C_{kl}^{j} under two different damping constraints: 6.21a) refers to the damping coefficients of generators set to zero except in generator 1 where $D_1 = 3.5$. In 6.21b) all the damping coefficients are zero. This slight change results in a large difference: the values of coefficients in 6.21b) are bigger that those obtained in the case of Figure 6.21a). The damping helps to decrease the stress conditions, thus decreasing the nonlinear contributions.

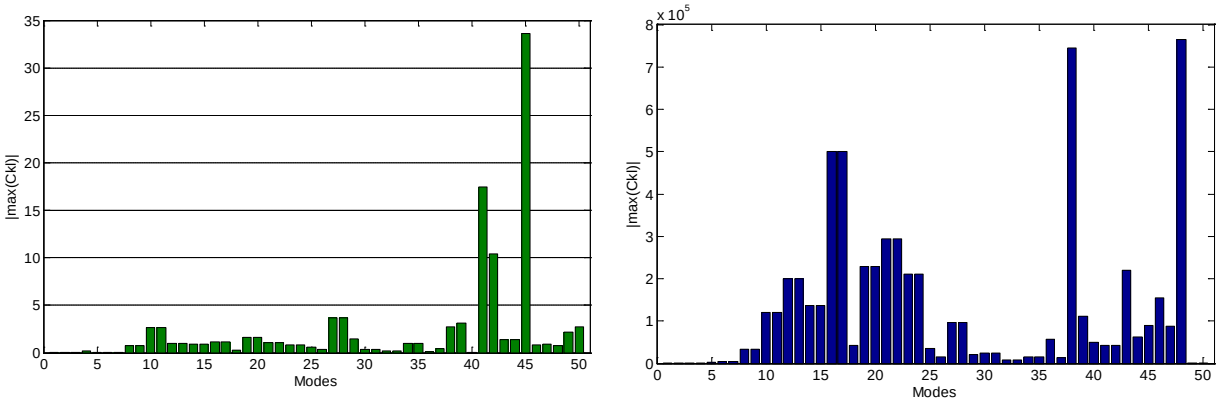

a) $D_i = 0$, except $D_1 = 3.5$ b) $D_i = 0$

Figure 6.21 C_{kl}^{j} Coefficients for different damping constant conditions

The same behavior is observed in Figure 6.22 where the coefficients h_{2kl}^{j} are shown. Again, the case with zero damping (Figure 6.22a) exhibits much higher values of the coefficient magnitudes with respect to that obtained assuming $D_1 = 3.5$ (Figure 6.22b).

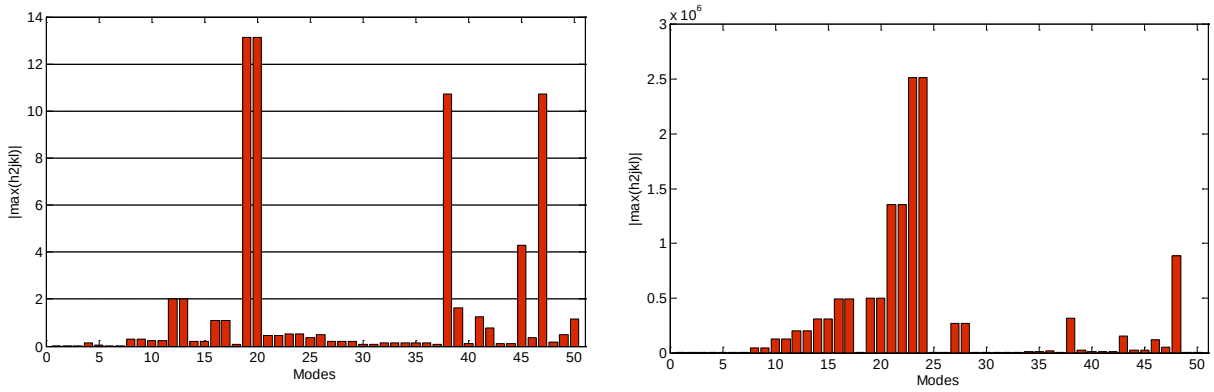

a) $D_i = 0$, except $D_1 = 3.5$ b) $D_i = 0$

Figure 6.22 $\max\left|h_{2kl}^{j}\right|$ Coefficients for different damping constant conditions

The analysis of bar diagrams obtained for the nonlinear coefficients results in different contributions. For instance, from Figure 6.21a), the most relevant generators are G1, G2 and G5, although, the situation changes without damping conditions, being now the generators G6, G7 and G8 besides G1 and G2 the relevant ones (Figure 6.21b). Now, considering the nonlinear coefficients h_{2kl}^{j}, the most relevant contribution are the electromechanical modes of generators G9 and G10, followed by G7 and G8 shown in Figure 6.22a. In turn, in the absence of damping conditions, the relevant generator modes are G1-G4, according to the results observed in Figure 6.22b.

Now, the nonlinear indexes are calculated, assuming the operation condition with $D_1 = 3.5$. This is observed in the bar diagram of Figure 6.23. The analysis of nonlinear indices allows to determine the different contributions of modal interactions. The index with highest value is *I*4 followed by index *I*3.

The index with lowest values is *I*1. Thus it can be concluded that there is a strong interaction on the fundamental modes of the system, being highest for the modes 25, 40, 46 and 49 (generators G5, G10, G6 and G9, respectively).

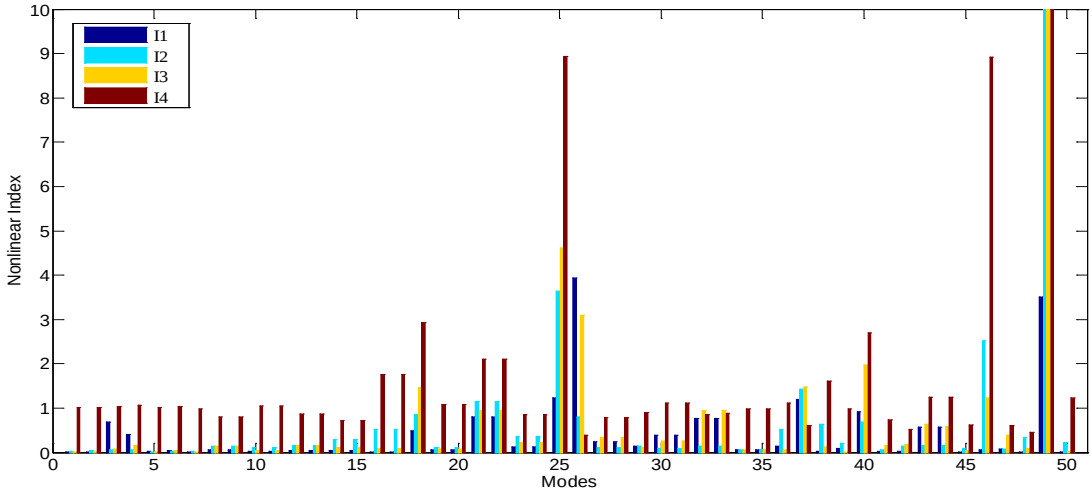

Figure 6.23 Nonlinear indices for the study case of the New England test power system

Another parameter to characterize the modal interaction is through the nonlinear participation factors. Figure 6.24 shows the participation factors of the system, according to (6.14)-(6.15). Each bar diagram represents the magnitudes of the linear participation factor ($\left|P_{ij}\right|$), the first order participation factor ($\left|P1_{kl}^{j}\right|$) and second order participation factors ($\left|P2_{kl}^{j}\right|$) for the modes with magnitude higher than 1.0. Some observations can be draw from these results:

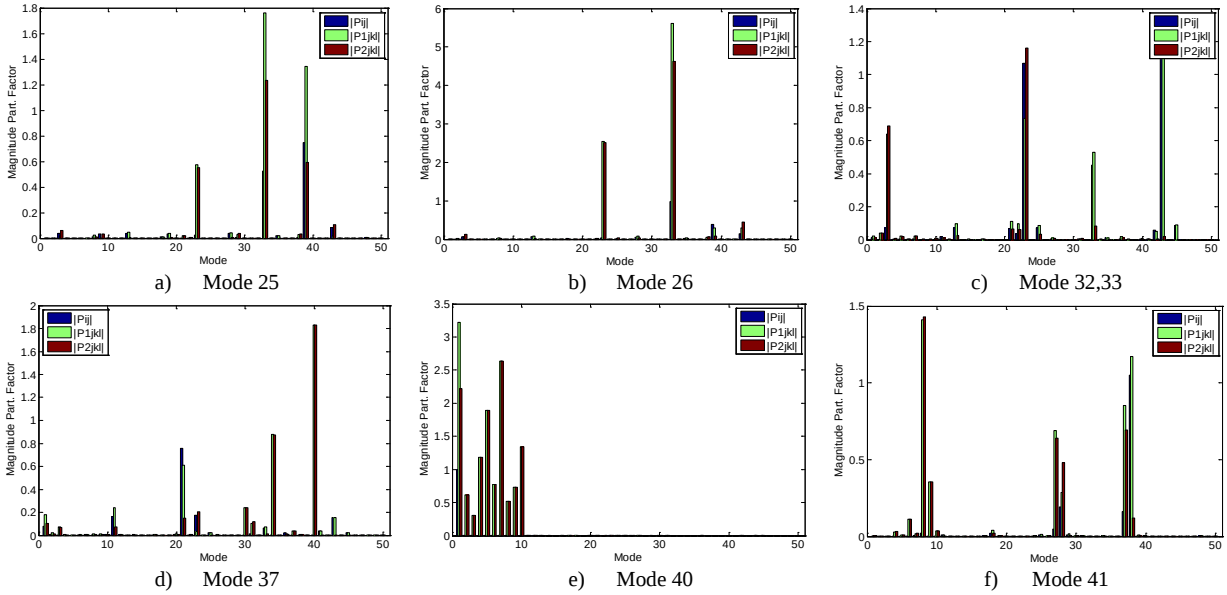

a) Mode 25 b) Mode 26 c) Mode 32,33

d) Mode 37 e) Mode 40 f) Mode 41

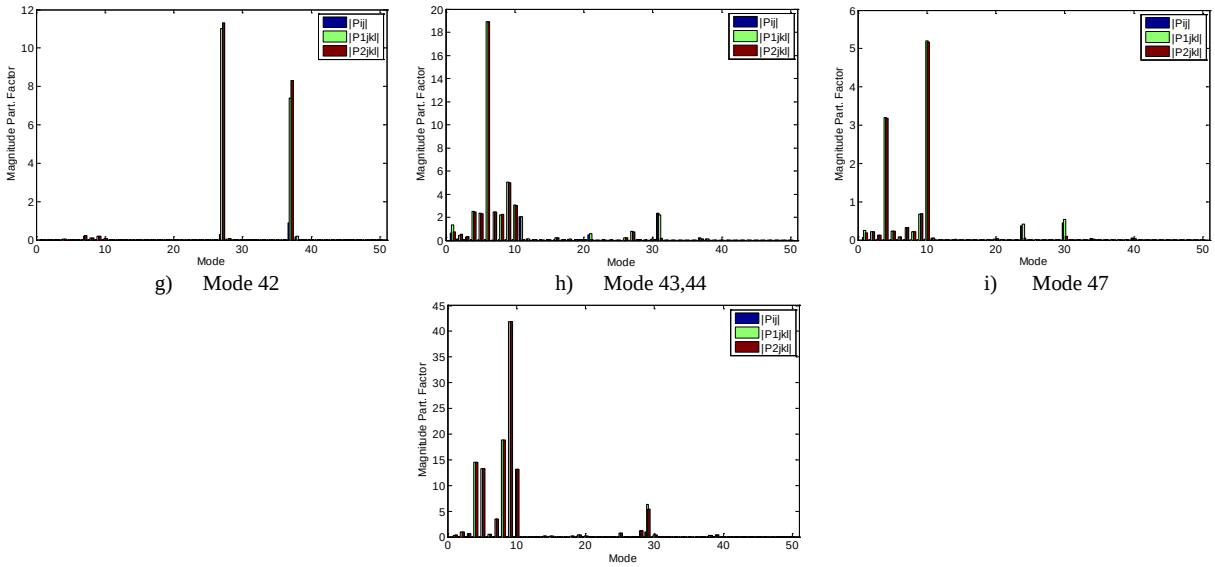

g) Mode 42 h) Mode 43,44 i) Mode 47

j) Mode 49

Figure 6.24 Linear and nonlinear participation factors of the New England test power system

- For all the modes, the linear participation factor has the lowest value, which means that the linear participation factor represents the smallest contribution to modal interaction.
- The second order participation factors have the highest values associated to the modal combination (43,6) (Figure 24h) and (49,9) (Figure 24j). This represents a modal combination effect due to interaction between generators G3-G6 and G9.

Graphically, the nonlinear contributions of the mechanical state variables calculated by the modal series method is illustrated in Figure 6.25. The absolute rotor angles of each generator are shown in 6.25a), with its zoomed graph. From this Figure the contributions of each variable to the total oscillations presented in the power system can be noticed. In the same way, the contributions of rotor speed deviations are shown in Figure 6.25b) and zoomed in its attached graph. Please observe that the nonlinear oscillations associated to each variable are not the same, being the less oscillatory the rotor speed ω_3 and the largest ω_4 and ω_5.

Therefore, Figure 6.25 is illustrating the total contributions to the oscillation due to a small perturbation of the nonlinear terms included in the closed form solutions obtained with the modal series method.

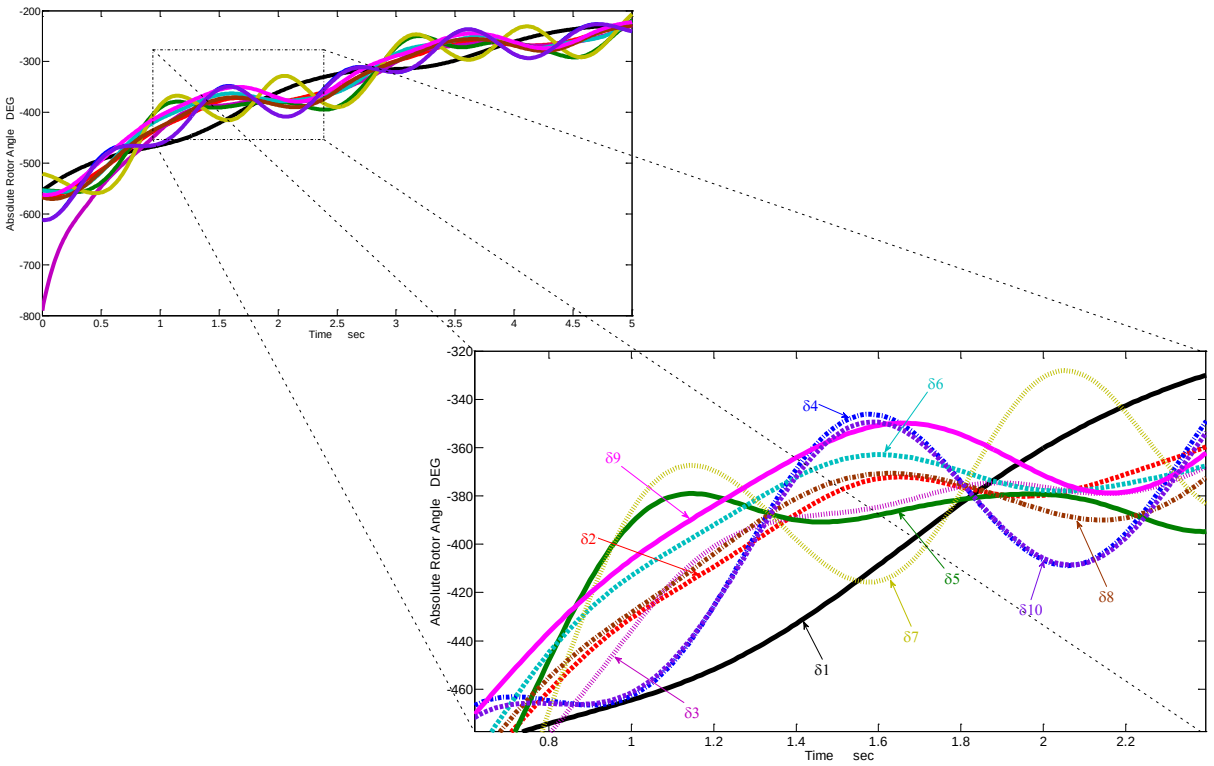

a) Absolute rotor angles

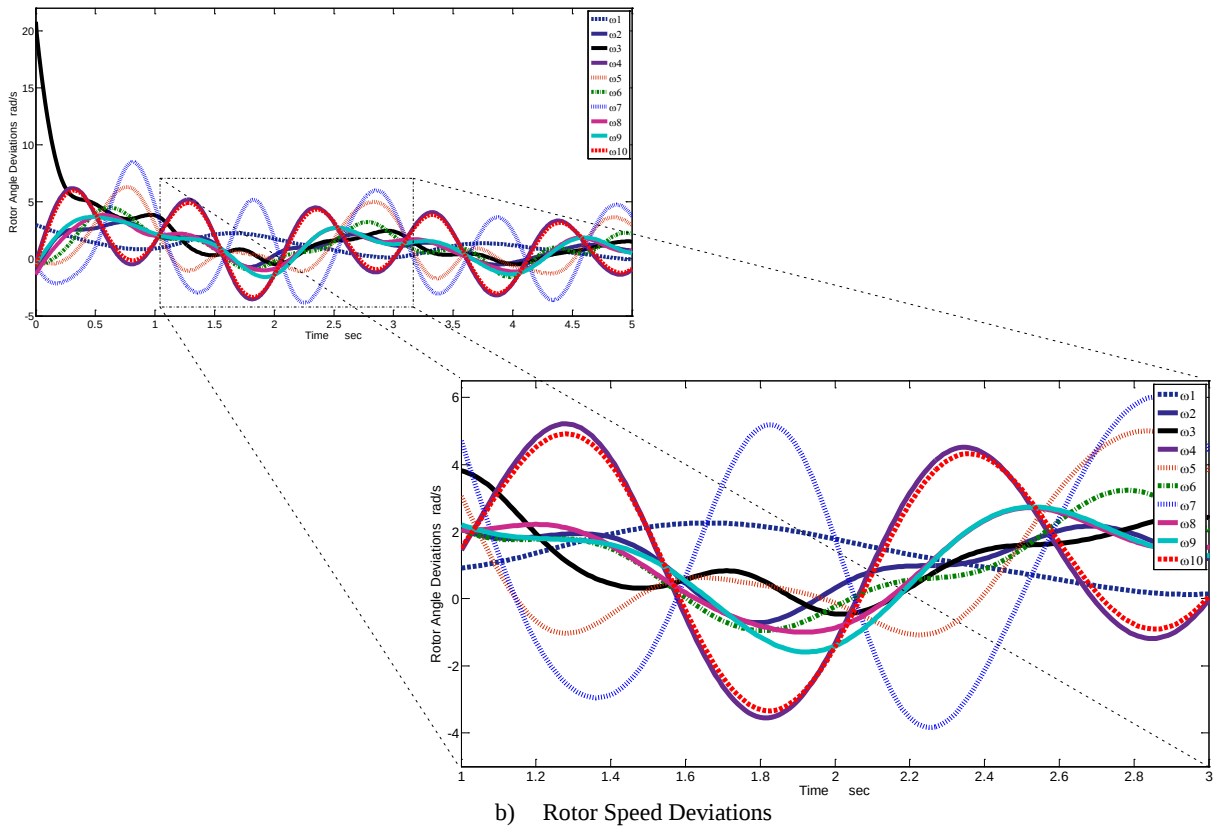

b) Rotor Speed Deviations

Figure 6.25 Time domain nonlinear contributions

6.3.5 Critical Fault Clearance

This experiment is centered on moving the time over which a three phase stub is maintained. The faulted bus is the 30 node, which directly affects to the machine 2. The expected result is that the nonlinearity of the power system goes increasing due to the even longer time of fault application, that is, disturbed and stressing conditions of the system have been assumed. Again, a comparison between the modal series method (MS) with respect to linear approximation (LINA) and full numerical solution (FNS) of the nonlinear system is carried-out. The comparison is established on the variables with higher dynamics during the fault, which in a qualitative way are the rotor angles δ_3 and δ_7 together with ω_3 and ω_7.

As it was studied in Chapter 3, the accuracy of the modal series depends on the stress conditions: when the system is more stressed, the solution obtained by modal series tends to follows a different trajectory with respect to the full numerical solution, which implies that the dynamic of the system cannot be followed due to the stable equilibrium point is moving far away of the equilibrium conditions.

The Figure 6.26 shows the time domain evolution of selected variables when the time clearing is moving. The fault clearing times are: $t_1 = 3T\,s, t_2 = 5T\,s, t_3 = 8T\,s, t_4 = 10T\,s, t_5 = 15T\,s$. Some observations concerning on the experiment can be pointed out:

- When the fault is liberated after $t_1 = 3T\,s$ (Figure 26a), the solutions exhibit identical solutions between MS and FNS while the LINA tends to follow a different trajectory.
- The same situation is observed when $t_2 = 5T\,s$ (Figure 26b) although a small difference between MS and FNS is presented.
- Now, for the time clearing $t_3 = 8T\,s$ (Figure 26c) the difference between MS and FNS solutions has increased, resulting more evident the differences between both solutions with respect to LINA.

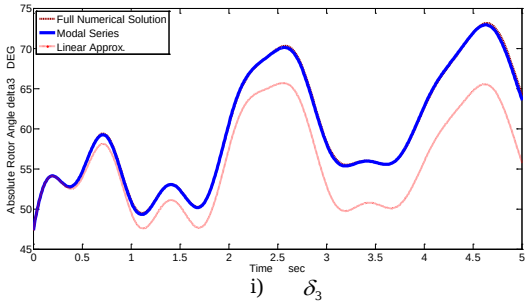

i) δ_3

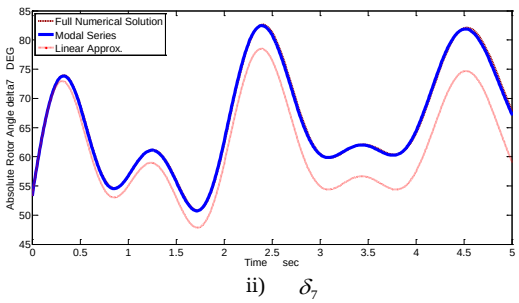

ii) δ_7

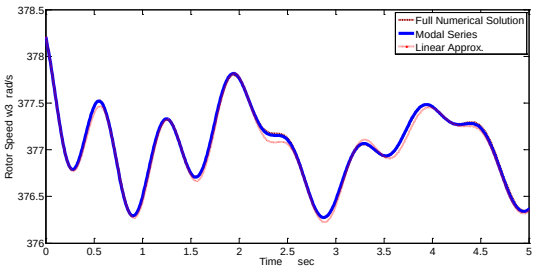

iii) ω_3

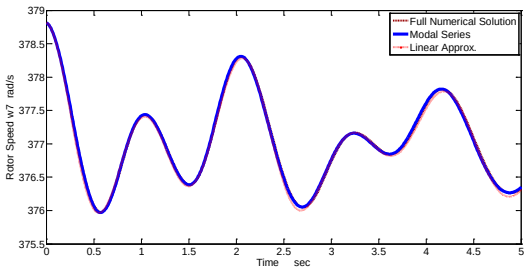

iv) ω_7

a) $t = 3T$ sec (0.05sec)

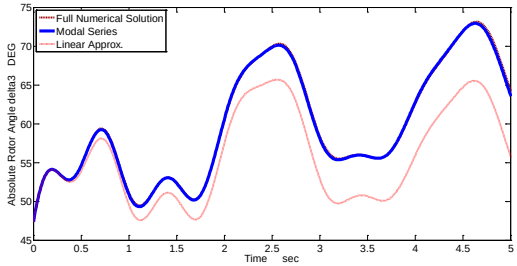

i) δ_3

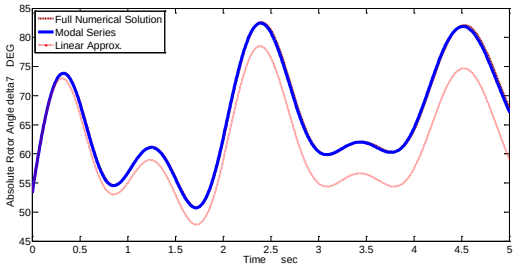

ii) δ_7

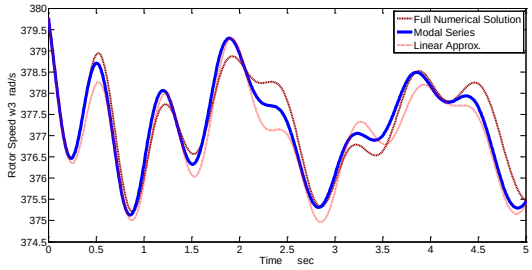

iii) ω_3

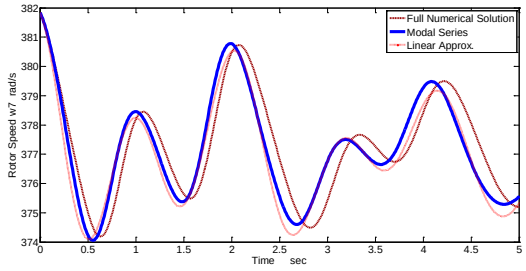

iv) ω_7

b) $t = 5T$ sec (0.0833sec)

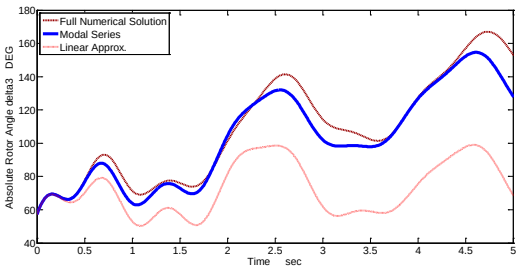

i) δ_3

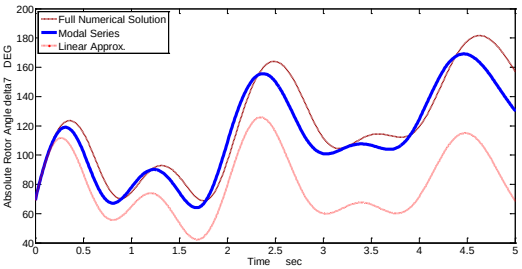

ii) δ_7

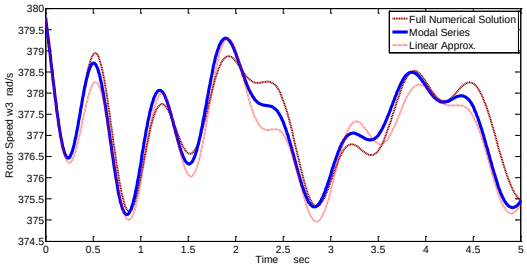

iii) ω_3

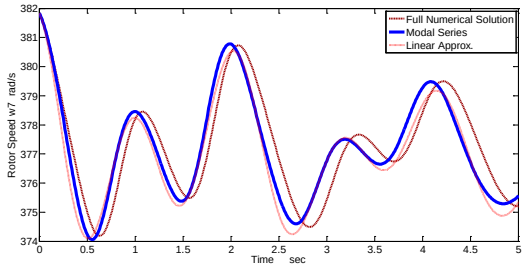

iv) ω_7

c) $t = 8T$ sec (0.1333sec)

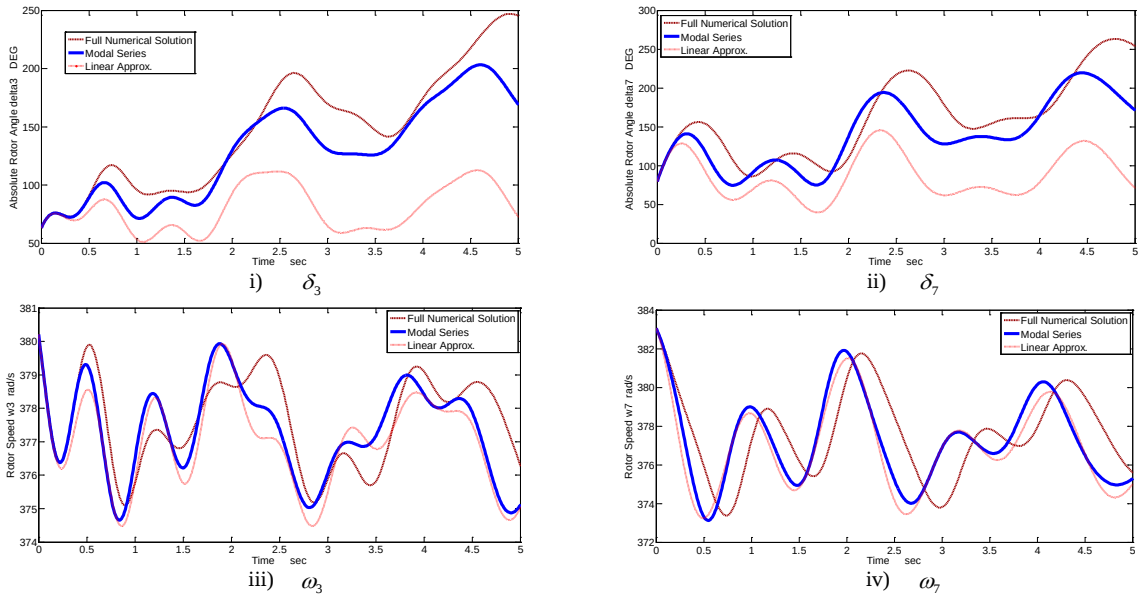

i) δ_3 ii) δ_7

iii) ω_3 iv) ω_7

d) $t = 10T$ sec (0.1667 sec)

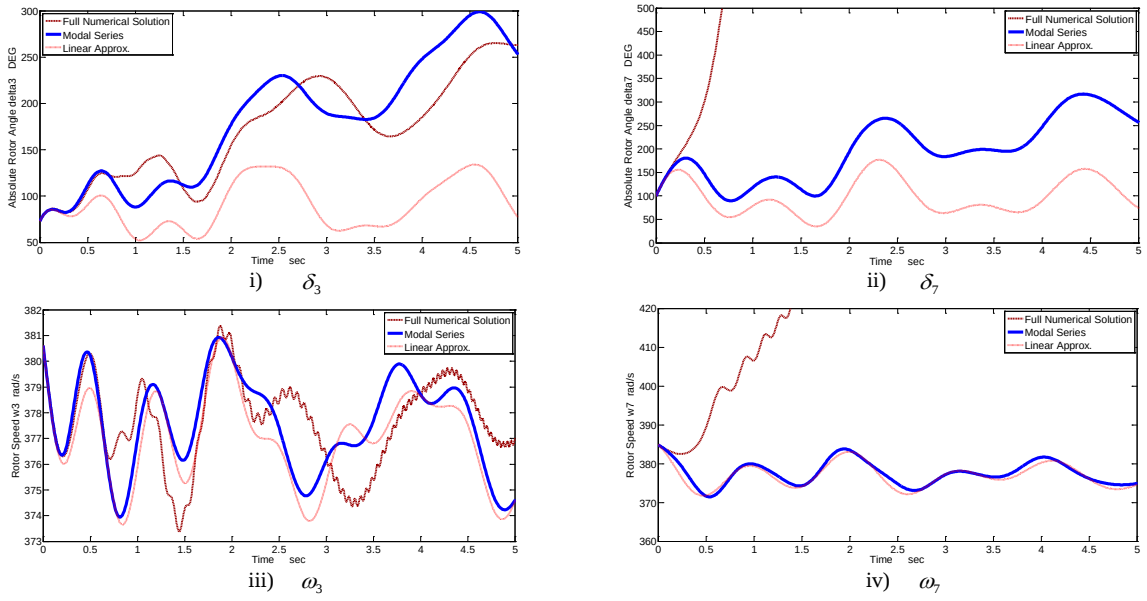

i) δ_3 ii) δ_7

iii) ω_3 iv) ω_7

e) $t = 15T$ sec (0.25 sec)

Figure 6.26 Nonlinear time domain simulation for different time clearing fault

- The case of $t_4 = 10T\,s$ (Figure 26d) demonstrates that the MS and FNS responses tend to separate but maintaining the same dynamics, while LINA is following different trajectories for all the variables here illustrated.
- Finally, the condition of time clearing equal to $t_5 = 15T\,s$ (Figure 26e) exhibits dramatic differences in all the variables: δ_7 and ω_7 have become unstable and not followed by MS and

LINA, while the dynamics of δ_3 and ω_3 calculated by FNS is not the same to that determined by MS and LINA.

The experiment conducts to the next conclusions:

- While the time clearing is changed, the system is approximating to unstable conditions due to the perturbation condition.
- The modal series method can be very accurate for low stress conditions, and under increased stress tends to be more precise than linear approximation approach. The oscillations presented during the transient state are accurately followed by the modal series solution.
- Definitely, the linear approximation cannot reproduced the dynamic of the system. During transient, the oscillations predicted by the linear approximation method are in considerable error with respect to the full numerical solution.

6.4 UNSTABLE CASE STUDY OF THE NEW ENGLAND TEST POWER SYSTEM

It is important to recall that the application of the modal series method is based on determining an stable equilibrium point of the nonlinear power system. However, it is possible to operate the system under instability conditions, which leads the system to eventually loss synchronism.

Table 6.5 Small signal analysis of unstable study case

MODE	EIGENVALUE	FREQ. (Hz)	DAMPING RATIO	ASSOCIATED STATE VARIABLES	PARTICIPATION FACTORS
1,2	-0.5557 + 9.4232i	1.4998	0.0589	$\delta_1, \delta_3, \omega_2, \omega_3$	0.2148, 0.2527
3,4	-0.6530 + 9.3381i	1.4862	0.0698	$\delta_8, \delta_9, \omega_8, \omega_9$	0.2609, 0.1624
5,6	-0.4984 + 9.0567i	1.4414	0.0549	δ_6, ω_6	0.3503
7,8	-0.3226 + 7.8551i	1.2502	0.041	$\delta_4, \delta_{10}, \omega_4, \omega_{10}$	0.2285, 0.2489
9,10	-0.2829 + 7.7129i	1.2275	0.0367	$\delta_2, \delta_3, \omega_2, \omega_3$	0.2018, 0.1817
11,12	-0.2350 + 6.7983i	1.082	0.0345	$\delta_4, \delta_8, \delta_9, \omega_4, \omega_8, \omega_9$	0.0704, 0.1004, 0.1779
13,14	-0.0337 + 5.9727i	0.9506	0.0056	$\delta_4, \delta_5, \delta_{10}, \omega_4, \omega_5, \omega_{10}$	0.0864, 0.1913, 0.0868
15,16	0.3982 + 5.6952i	0.9064	0.0697	$\delta_5, \delta_7, \omega_5, \omega_7, E'_{q7}, E'_{fd7}$	0.0795, 0.2578, 0.0815, 0.0731
20,21	-3.2900 + 4.3688i	0.6953	0.6016	$\delta_7, \omega_7, E'_{q7}, E'_{fd7}$	0.0901, 0.0901, 0.3547, 0.3893
22,23	0.2483 + 3.0600i	0.487	0.0809	δ_1, ω_1	0.1584, 0.1584
24,25	-2.9431 + 3.5629i	0.567	0.6369	E'_{q8}, E_{fd8}	0.3938, 0.4195
29,30	-2.5699 + 2.2984i	0.3658	0.7454	E'_{q2}, E_{fd2}	0.3955, 0.3913
31,32	-2.6842 + 1.9144i	0.3047	0.8141	E'_{q5}, E_{fd5}	0.3757, 0.3744
34,35	-1.7205 + 0.3695i	0.0588	0.9777	$E'_{q4}, E'_{d4}, E'_{d10}, E_{fd4}, E_{fd10}$	0.0988, 0.2713, 0.1293, 0.3364, 0.1188
36,37	-1.3700 + 0.3237i	0.0515	0.9732	$E'_{q10}, E'_{d10}, E_{fd10}$	0.1121, 0.2353, 0.325
41,42	-1.0293 + 0.2047i	0.0326	0.9808	$E'_{q4}, E'_{q10}, E'_{d1}, E'_{d10}, E_{fd10}$	0.0924, 0.1519, 0.142, 0.0943, 0.2052

The main objective of this case study is to simulate the same power system earlier analyzed in Section 6.3, but now operating under unstable conditions. Basically, the instability conditions are obtained when the time constant in the generator 2 is reduced to 0.7, with an addition in the damping speed parameter of generator 1 to $D_1 = 3.5$.

Table 6.5 details the oscillatory modes obtained in this case study, being the modes 15-16 and 22-23 the unstable ones. For the case of modes 15-16, the generators 5 and 7 are involved in the main dynamics, while for the case of modes 22-23 the generator 1 is the most affected.

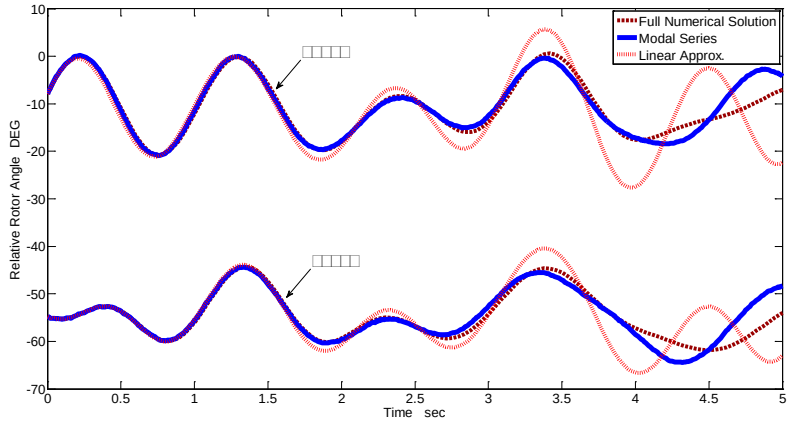

a) Relative rotor angles $\delta_{(4,7)}$ and $\delta_{(2,7)}$

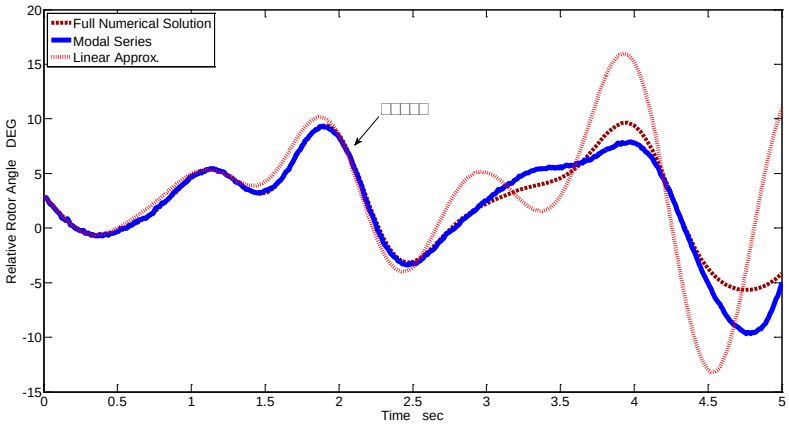

b) Relative rotor angles $\delta_{(7,6)}$

6.27 Relative rotor angles in the unstable case of the New England power system

The dynamics of the system is illustrated in Figures 6.27 to 6.29. In the first place, Figure 6.27 shows the dynamics followed by the relative rotor angle for the selected angles $\delta_{(4,7)}$, $\delta_{(2,7)}$ and $\delta_{(7,6)}$. Over the first 3 seconds of simulation, the solutions obtained by the full numerical approach, modal series and linear approximation, respectively, follow the same trajectory. However, while the time is running up to 3 seconds, appreciable differences between linear approximation with the other solutions

are observed, being more important in the angle $\delta_{(7,6)}$ (Figure 6.27b). In general, while the time of simulation is increasing, the separation between linear approximation, modal series and full numerical solution becomes larger, due to the instability condition and modal interaction.

Continuing the experiment, Figure 6.28 shows the absolute rotor angles of each machine of the system under analysis. The comparison denotes appreciable differences between the angles determined with the linear approximation, which are under and away of the solutions obtained by modal series, and the full numerical solution. That is, the dynamics shown by the linear angles cannot follow the real oscillation of the unstable system; even so, the modal series solution is more accurate since it is maintained closer to the real angles.

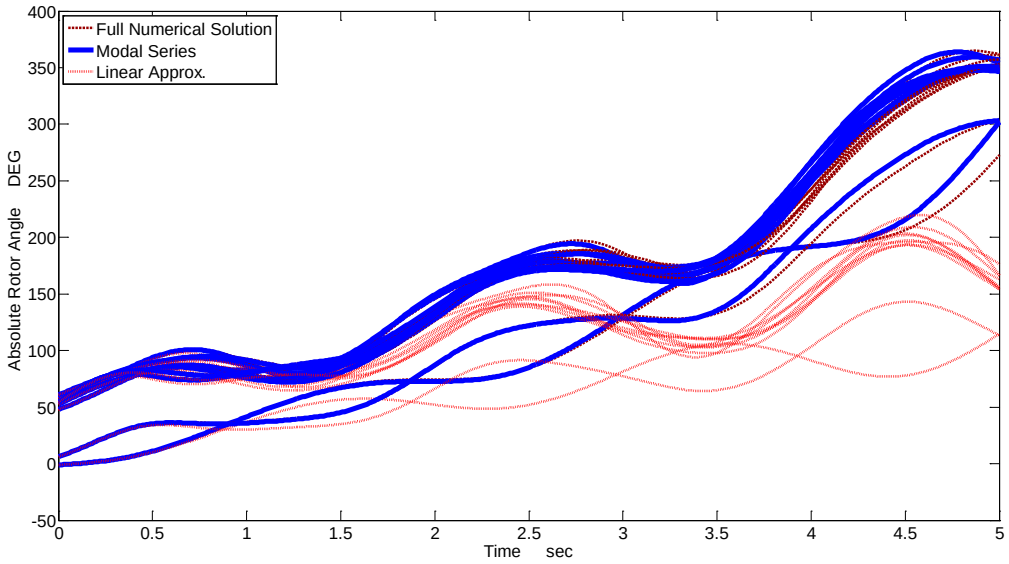

Figure 6.28 Absolute Rotor Angles the unstable case of the New England power system

Finally, the case study is concluded with the rest of state variables analysis. Figure 6.29 shows the oscillatory behavior of the selected variables $\omega_5, \omega_7, E'_{q4}, E'_{q7}, E_{fd3}, E_{fd7}$. Some comments are drawn from the graphs:

- The comparison of the rotor speeds ω_5 and ω_7 describe slow oscillations being the linear approximation solution detached from the trajectory described by modal series and the full numerical solution.
- The oscillations followed by linear approximation, for the case of $E'_{q4}, E'_{q7}, E_{fd3}$ and E_{fd7}, have appreciable differences with respect to the solution obtained with modal series and full numerical solution, respectively. In such case, the nonlinear terms have an important

contribution to the oscillations of these variables, which are not taken into account when the linear approximation is used.

- The generator with the highest contribution to the oscillations is the generator 7. This situation has been graphically observed along the study. Please observe Figures 6.29 d) and f), where the corresponding variables to generator 7 E'_{q7} and E_{fd7} show considerable differences to the solution obtained with linear approximation with respect to the modal series and the full numerical solution.

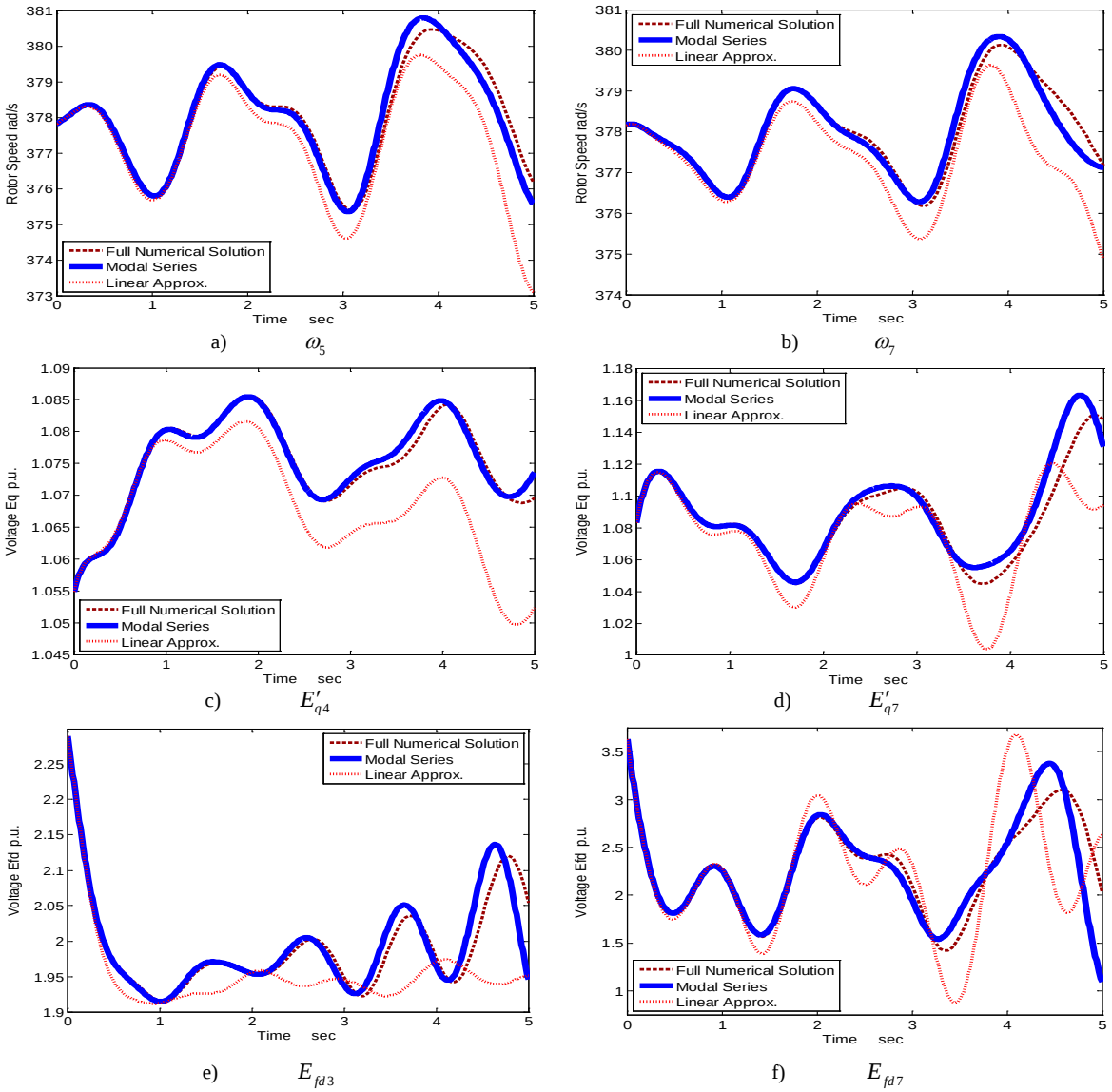

Figure 6.29 Generator selected variables in the unstable case of the New England power system

6.5 DISCUSSION

The Chapter has been focused on the analysis of the two test power systems, *i.e.* the 3 generators-9 buses and the New England 10 generators-39 buses, when are subjected to perturbation and stress conditions. The oscillations observed during the transient followed after the perturbations have been graphically analyzed, and the effects observed on the global state variables involved in the modeling described in detail. The analysis of nonlinear contributions using nonlinear indices and nonlinear participation factors have been considered. The case study has demonstrated that the contribution to the oscillations of nonlinear terms represented with the modal series method, is of great importance, in order to represent and characterize the effects involved during perturbation conditions.

Beside from the visual study of the nonlinear oscillations, the importance of characterize the nonlinear contribution to the nonlinear power system can be concluded. The information that is leaving out of scope is when only the linear approximation is used. One of the most important characteristics of the modal series method relies on the analytical closed form solution, which means a straight form to incorporate nonlinear modal interactions to the nonlinear system analysis. It is of concern how to detail and link this information with the nature of phenomena presented in a real operation of the power system. To be developed further, is the application of the modal series method to large scale systems and systems with more detailed models.

7

INCORPORATION OF FACTS DEVICES: REFERENCE TO THE UPFC MODELLING

7.1 INTRODUCTION

Modern power systems have to be able to operate under a wide range of constraints, new power sources, dynamic loads continuously increasing on type and amount, which moved to the power system to operate among different stability conditions. With respect to small disturbances, small signal models are needed in order to efficiently incorporate, and as a predictive assessment, the new challenges of operating conditions. Following this philosophy, several models have been proposed in the literature concerning flexible AC transmission systems; created to make easier and more versatile the operating conditions of the modern power systems. In parallel, FACTS technology has opened new opportunities to control power and to enhance the usable capacity, thus to control the interrelated power systems parameters that govern the operation of transmission systems, including series impedance, shunt impedance, current, voltage, phase angle and the damping of oscillation at a various frequency levels [Hingorani y Giugyi 2000].

The primary function of the FACTS devices is to control the transmission line power flows. Secondary functions of the FACTS are related to the voltage control, transient stability improvement and oscillation damping.

7.2 UPFC MODELING

The UPFC is a versatile element of the FACTS family that is able to simultaneously provide both series and shunt compensation to a transmission line, providing separate control of the active and reactive power on the transmission lines [Guo *et al.* 2009]. The UPFC here modeled is formed by two VSC's employed in combinations that are used for dynamic compensation and real time control of voltage and power flow in transmission systems [Uzunovic 2001]. The DC terminals of both converters are connected to a common capacitor. Basically, it can be affirmed that an UPFC is a combination of STATCOM (shunt VSC compensator) and a SSSC (series compensator); acting

together conform the UPFC, but each VSC complies with specific functions: STATCOM can absorb or generate reactive power while the SSSC acts as a voltage source, injected in series to the transmission line through the series transformer. Thus, the two branches of the UPFC can generate or absorb the reactive power independent of each other [Uzunovic 2001].

7.3 THE UPFC. GENERAL CHARACTERISTICS

The UPFC is a very versatile controller which has many applications in order to improve power system operation. The UPFC combines two controlled voltage sources that work together linked by a direct current busbar. Figure 7.1 shows the basic structure and operation of the UPFC. Some important operating characteristics of the UPFC that identifies it from other FACTS devices family are the following,

- The series part is normally used to control the power flow over the transmission line, inserting a series voltage source through a series transformer.
- The shunt part of UPFC is generally used to control the AC voltage. This function is achieved by interchange of reactive power, and the direct current voltage control is obtained by interchange of active power.

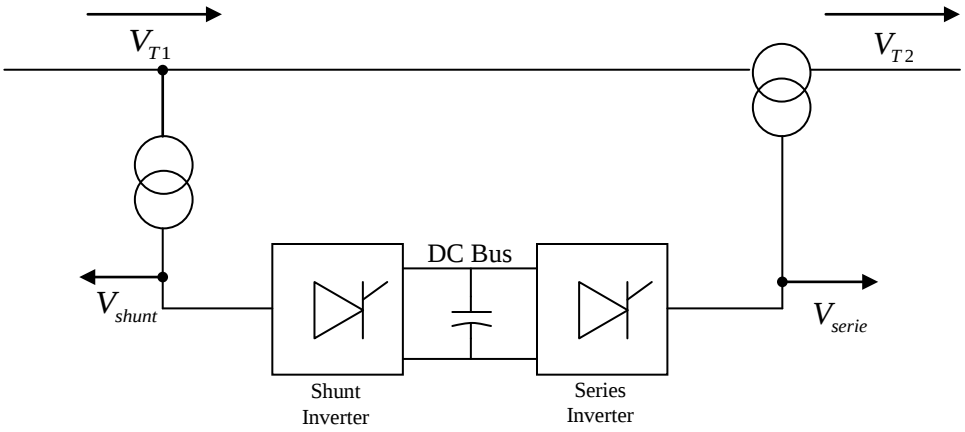

Figure 7.1 Basic operation of the UPFC

At its own part, the series inverter operates according to the diagram shown in Figure 7.2, where the following is observed,

- A voltage can be sourced that it is adjustable on magnitude and phase angle.
- If the active power flow is modified over the transmission line, the series voltage is inserted in such a way that it creates a voltage phase shifting.
- If it is desirable to modify the reactive power flow over the transmission line, the series voltage is injected, in such a way that a change in voltage magnitude is added.

- The possible operating points are governed by two main constraints: the maximum magnitude of series voltage and the minimal magnitude of voltage, in order to control the terminal voltage V_{T2}.

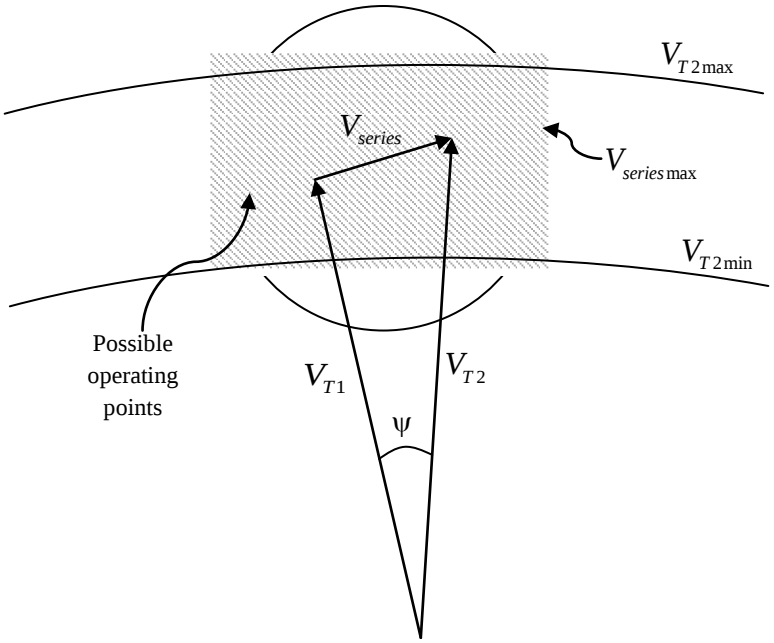

Figura 7.2 Operating principle of UPFC series part

On the other side, the series part performs the following functions:

- Keeps the voltage constant over the direct current bus. This is done by interchanging active power with the network and controlling the phase angle of the shunt converter generated voltage.
- Controls the voltage magnitude over the AC side, through interchange of reactive power with the network, by controlling generated voltage magnitude of the shunt converter.

The diagram of Figure 7.3 illustrates these functions.

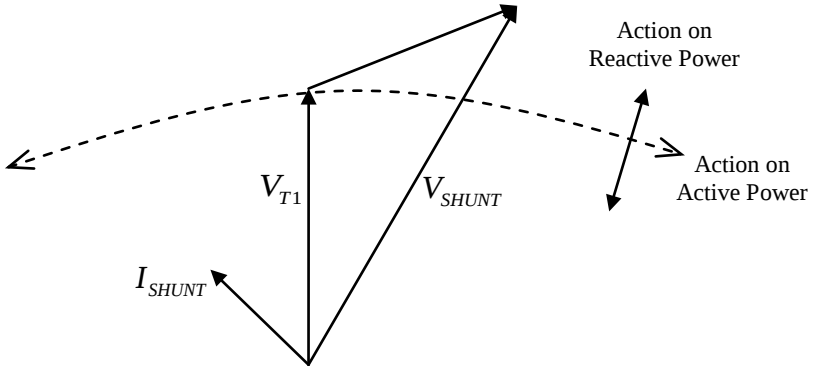

Figure 7.3 Operating principle of the UPFC shunt part

7.4 DETAILED MODEL OF UPFC

In this section, the UPFC steady state and dynamic model is described. The model here selected is one basically described and widely utilized by [Nabavi-Niaki & Iravani 1996] [Wang 1999], however, some other alternative models have been explored as well [Dong *et al*. 2004].

7.4.1 Steady State of UPFC

The UPFC in steady state operation, and not considering converter losses, neither absorbs nor injects active and reactive power to the power system. Physical insight of this operating conditions is due to the fact that the voltage capacitor is maintained over a predetermined constant V_{cd}. [Nabavi-Niaki & Iravani 1996]. Figure 7.4 shows this condition, where controlled voltage sources of the UPFC are represented as constant voltage sources.

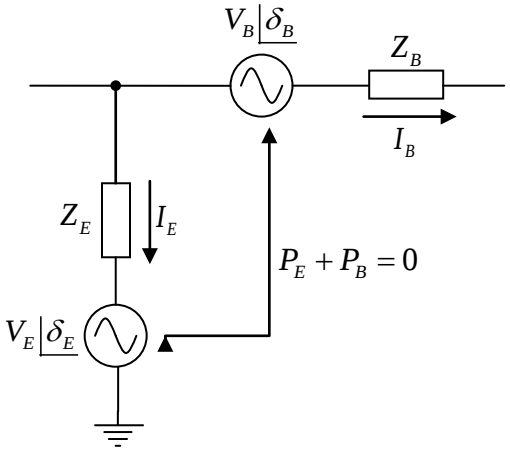

Figure 7.4 UPFC diagram in sinusoidal steady state condition

The constraint $P_E + P_B = 0$ implies that no real power is exchanged between the UPFC and the system; hence, the dc link remains constant and the two voltage sources V_B and V_E are mutually dependent [Nabavi-Niaki 1996]

7.4.2 UPFC power flow

Consider the diagram shown in Figure 7.5 that illustrates the UPFC in parallel with the power system represented as a black box. The UPFC is connected between buses *E* and *B*. Referring to the diagram, please observe that the UPFC is mainly used to maintain a pre-specified power flow from the *E* bus to the *B* bus and to regulate the *B* bus voltage at a pre-specified value [Nabavi-Niaki 1996].

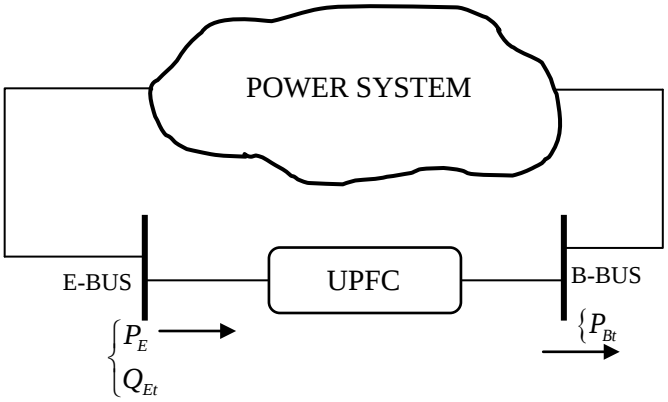

Figure 7.5 UPFC linked to the power system

It should be remarked that δ_B and M_B determine the active power P_{Bt} and V_{Bt}, respectively. In the same way, M_E and δ_E determine the reactive power Q_E and the dc voltage at the capacitor link V_{dc}, respectively.

Taking into account the UPFC operation, the power flow analysis results are used in order to determine the steady state condition of the UPFC through the control variables δ_B, M_B, δ_E, and M_E by solving [Nabavi-Niaki 1996],

$$\begin{aligned} f_1(M_E,\delta_E,M_B,\delta_B) - P_{Et} &= 0 \\ f_2(M_E,\delta_E,M_B,\delta_B) - Q_{Et} &= 0 \\ f_3(M_E,\delta_E,M_B,\delta_B) - P_{Bt} &= 0 \\ f_4(M_E,\delta_E,M_B,\delta_B) - Q_{Bt} &= 0 \end{aligned} \tag{7.1}$$

where f_1 to f_4 are nonlinear functions of the UPFC steady state model. The solution of this set of nonlinear algebraic equations may be obtained with the application of Newton methods (FACTS power flows) [Acha *et al.* 2004].

7.4.3 Dynamic Model of UPFC

The dynamic UPFC is modeled according to [Navabi-Niaki and Iravani 1996], which is based on assuming VSC's without losses and interferences due to commutation effects of IGBT's. The proposed model is developed at fundamental frequency with each VSC (both series and shunt) dependent on modulation indexes and phase angle of each constant voltage source.

Figure 7.6 shows the UPFC diagram connected to an infinite busbar, linked with a synchronous machine and a tie transmission line. In this particular case, the UPFC is controlling the amount of reactive power transmitted from generator to the infinite busbar and viceversa.

Following the model illustrated by Figure 7.6, m_E, m_B, δ_E and δ_B are the modulation indexes and

phase angles, corresponding to the series converter and shunt converter, respectively. These variables may be assumed as the input control variables of the UPFC controller, which rule the characteristics of operation of UPFC connected to the power network. That is,

$$V_{SH} = \frac{m_E v_{dc}}{2}\left(\cos\delta_E + j\sin\delta_E\right) \tag{7.2}$$

Furthermore,

$$V_{SERIES} = \frac{m_B v_{dc}}{2}\left(\cos\delta_B + j\sin\delta_B\right) \tag{7.3}$$

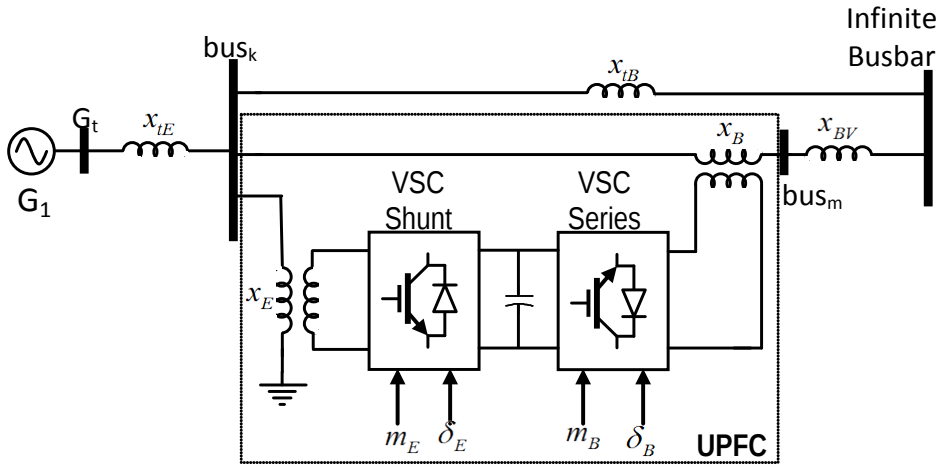

Figura 7.6 Diagram of UPFC connected to an infinite-busbar

In order to obtain the model which will be eventually applied to the nonlinear analysis of the dynamic power system, consider the single phase diagram shown in Figure 7.7, which again describes the same UPFC connected between generator and the infinite busbar, but now shown as an equivalent circuit. If the general Pulse Width Modulation (PWM) is adopted for the IGBT based VSC, the three phase dynamic differential equations of the UPFC are [Song and Johns 1999],

$$\begin{bmatrix} \frac{di_{Ea}}{dt} \\ \frac{di_{Eb}}{dt} \\ \frac{di_{Ec}}{dt} \end{bmatrix} = \begin{bmatrix} -\frac{r_E}{l_E} & 0 & 0 \\ 0 & -\frac{r_E}{l_E} & 0 \\ 0 & 0 & -\frac{r_E}{l_E} \end{bmatrix} \begin{bmatrix} i_{Ea} \\ i_{Eb} \\ i_{Ec} \end{bmatrix} - \frac{m_E v_{dc}}{2l_E} \begin{bmatrix} \cos(\omega t + \delta_E) \\ \cos(\omega t + \delta_E - 120^\circ) \\ \cos(\omega t + \delta_E + 120^\circ) \end{bmatrix} + \begin{bmatrix} \frac{1}{l_E} & 0 & 0 \\ 0 & \frac{1}{l_E} & 0 \\ 0 & 0 & \frac{1}{l_E} \end{bmatrix} \begin{bmatrix} v_{Eta} \\ v_{Etb} \\ v_{Etc} \end{bmatrix} \tag{7.4}$$

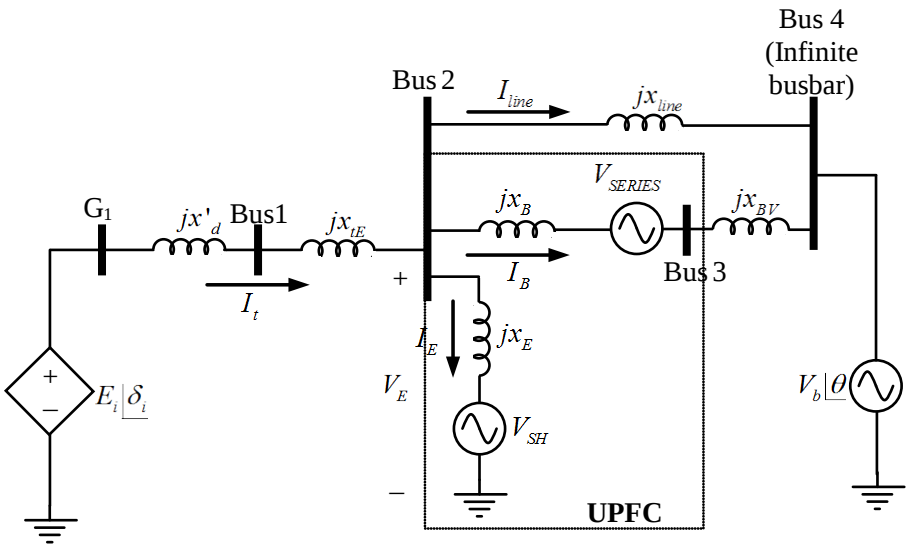

Figure 7.7 Single line of UPFC connected in a synchronous machine infinite busbar power system

$$\begin{bmatrix} \frac{di_{Ba}}{dt} \\ \frac{di_{Bb}}{dt} \\ \frac{di_{Bc}}{dt} \end{bmatrix} = \begin{bmatrix} -\frac{r_B}{l_B} & 0 & 0 \\ 0 & -\frac{r_B}{l_B} & 0 \\ 0 & 0 & -\frac{r_B}{l_B} \end{bmatrix} \begin{bmatrix} i_{Ba} \\ i_{Bb} \\ i_{Bc} \end{bmatrix} - \frac{m_B v_{dc}}{2l_B} \begin{bmatrix} \cos(\omega t + \delta_B) \\ \cos(\omega t + \delta_B - 120^\circ) \\ \cos(\omega t + \delta_B + 120^\circ) \end{bmatrix} + \begin{bmatrix} \frac{1}{l_E} & 0 & 0 \\ 0 & \frac{1}{l_E} & 0 \\ 0 & 0 & \frac{1}{l_E} \end{bmatrix} \begin{bmatrix} v_{Bta} \\ v_{Btb} \\ v_{Btc} \end{bmatrix} \tag{7.5}$$

$$\begin{aligned} \frac{dv_{dc}}{dt} &= \frac{m_E}{2C_{dc}} \begin{bmatrix} \cos(\omega t + \delta_E) & \cos(\omega t + \delta_E - 120^\circ) & \cos(\omega t + \delta_E + 120^\circ) \end{bmatrix} \begin{bmatrix} i_{Ea} \\ i_{Eb} \\ i_{Ec} \end{bmatrix} \\ &+ \frac{m_B}{2C_{dc}} \begin{bmatrix} \cos(\omega t + \delta_B) & \cos(\omega t + \delta_B - 120^\circ) & \cos(\omega t + \delta_B + 120^\circ) \end{bmatrix} \begin{bmatrix} i_{Ba} \\ i_{Bb} \\ i_{Bc} \end{bmatrix} \end{aligned} \tag{7.6}$$

Applying Park's transformation, the dynamic system for the UPFC in $dq0$ coordinates is,

$$\begin{bmatrix} \frac{di_{Ed}}{dt} \\ \frac{di_{Eq}}{dt} \\ \frac{di_{E0}}{dt} \end{bmatrix} = \begin{bmatrix} 0 & \omega & 0 \\ -\omega & 0 & 0 \\ 0 & 0 & 0 \end{bmatrix} \begin{bmatrix} i_{Ed} \\ i_{Eq} \\ i_{E0} \end{bmatrix} + \begin{bmatrix} -\frac{r_E}{l_E} & 0 & 0 \\ 0 & -\frac{r_E}{l_E} & 0 \\ 0 & 0 & -\frac{r_E}{l_E} \end{bmatrix} \begin{bmatrix} i_{Ed} \\ i_{Eq} \\ i_{E0} \end{bmatrix} - \frac{m_E v_{dc}}{2l_E} \begin{bmatrix} \cos\delta_E \\ \sin\delta_E \\ 0 \end{bmatrix} + \begin{bmatrix} \frac{1}{l_E} & 0 & 0 \\ 0 & \frac{1}{l_E} & 0 \\ 0 & 0 & \frac{1}{l_E} \end{bmatrix} \begin{bmatrix} v_{Etd} \\ v_{Etq} \\ v_{Et0} \end{bmatrix} \tag{7.7}$$

$$\begin{bmatrix} \frac{di_{Bd}}{dt} \\ \frac{di_{Bq}}{dt} \\ \frac{di_{B0}}{dt} \end{bmatrix} = \begin{bmatrix} 0 & \omega & 0 \\ -\omega & 0 & 0 \\ 0 & 0 & 0 \end{bmatrix} \begin{bmatrix} i_{Bd} \\ i_{Bq} \\ i_{B0} \end{bmatrix} + \begin{bmatrix} -\frac{r_E}{l_E} & 0 & 0 \\ 0 & -\frac{r_E}{l_E} & 0 \\ 0 & 0 & -\frac{r_E}{l_E} \end{bmatrix} \begin{bmatrix} i_{Bd} \\ i_{Bq} \\ i_{B0} \end{bmatrix} - \frac{m_B v_{dc}}{2 l_B} \begin{bmatrix} \cos\delta_B \\ \sin\delta_B \\ 0 \end{bmatrix} + \begin{bmatrix} \frac{1}{l_E} & 0 & 0 \\ 0 & \frac{1}{l_E} & 0 \\ 0 & 0 & \frac{1}{l_E} \end{bmatrix} \begin{bmatrix} v_{Btd} \\ v_{Btq} \\ v_{Bt0} \end{bmatrix} \tag{7.8}$$

$$\frac{dv_{dc}}{dt} = \frac{3m_E}{4C_{dc}} \begin{bmatrix} \cos\delta_E & \sin\delta_E & 0 \end{bmatrix} \begin{bmatrix} i_{Ed} \\ i_{Eq} \\ i_{E0} \end{bmatrix} + \frac{3m_B}{4C_{dc}} \begin{bmatrix} \cos\delta_B & \sin\delta_B & 0 \end{bmatrix} \begin{bmatrix} i_{Bd} \\ i_{Bq} \\ i_{B0} \end{bmatrix} \tag{7.9}$$

In order to study oscillations in power systems, transient effects due to transformers characteristics and transmission line resistances can be neglected, so that the set of differential equations take the form,

$$\frac{dv_{dc}}{dt} = \frac{3m_E}{4C_{dc}} \begin{bmatrix} \cos\delta_E & \sin\delta_E \end{bmatrix} \begin{bmatrix} i_{Ed} \\ i_{Eq} \end{bmatrix} + \frac{3m_B}{4C_{dc}} \begin{bmatrix} \cos\delta_B & \sin\delta_B \end{bmatrix} \begin{bmatrix} i_{Bd} \\ i_{Bq} \end{bmatrix} \tag{7.10}$$

7.4.4 UPFC Algebraic Model

Consider again the system shown in Figure 7.7 which represents the steady state equivalent circuit of the UPFC connected to an infinite busbar. In this single phase diagram, the synchronous machine is represented as a two order flux decay model. Hence,

$$E_i = E'_d + \left(x'_q - x'_d\right) I_q + jE'_q \tag{7.11}$$

From power flow analysis, the voltage magnitudes and nodal angles are obtained, as well as active power generated and generator terminal voltages. Thus, referring all values of the equivalent circuit to the generator quantities, it yields,

$$I_d + jI_q = I_G e^{-j\left(\delta - \pi/2\right)} \tag{7.12}$$

$$V_d + jV_q = V_t e^{-j\left(\delta - \pi/2\right)} \tag{7.13}$$

Considering the rest of constraints for the network, we have,

$$V_2 \angle \theta_2 = V_E \;\Rightarrow\; V_E e^{-j\left(\delta - \pi/2\right)}$$

In a similar manner,

$$V'_{SH} \Rightarrow V_{SH} e^{-j\left(\delta - \pi/2\right)} \qquad I'_E \Rightarrow I_E e^{-j\left(\delta - \pi/2\right)} \qquad I'_L \Rightarrow I_L e^{-j\left(\delta - \pi/2\right)}$$

$$V'_{SER} \Rightarrow V_{SER} e^{-j\left(\delta - \pi/2\right)} \qquad I'_B \Rightarrow I_B e^{-j\left(\delta - \pi/2\right)} \qquad V'_b \Rightarrow V_b e^{-j\left(\delta - \pi/2\right)} \tag{7.14}$$

Combining equations relationships according to the chosen reference, we have,

$$\begin{aligned} E'_d &= V_d - x'_q I_q \\ E'_q &= V_q + x'_d I_d \end{aligned} \quad \Rightarrow \quad \begin{aligned} V_d &= E'_d + x'_q I_q \\ V_q &= E'_q - x'_d I_d \end{aligned} \tag{7.15}$$

For the sake of simplicity, only the UPFC part of the network is considered, in order to obtain the main relationships of UPFC variables through the simple circuit shown in Figure 7.8, which is basically the same circuit of Figure 7.7 but only showing the UPFC part. Hence,

$$V_E = jx_E I_E + V_{SH} \tag{7.16}$$

$$V_B = jx_B I_B + V_{SERIES} \tag{7.17}$$

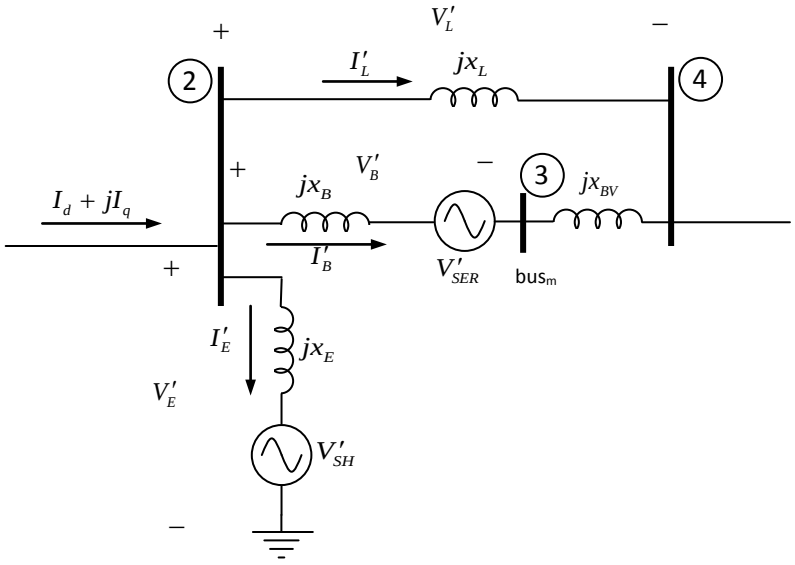

Figure 7.8 One line diagram of UPFC. Equivalent circuit in steady state

From the branch belonging to the shunt converter, we have,

$$V'_E = jx_E I'_E + V'_{SH}$$

or,

$$v_{Ed} + jv_{Eq} = jx_E \left(i_{Ed} + ji_{Eq} \right) + V_{SH} \tag{7.18}$$

Expanding Equation (7.18) and separating into real and imaginary parts, we obtain

$$v_{Ed} = -x_E i_{Eq} + V_{SH\,d} \tag{7.19}$$

$$v_{Eq} = x_E i_{Ed} + V_{SH\,q} \tag{7.20}$$

with,

$$v_{SH\,d} = \frac{m_E v_{dc}}{2} \cos \delta_E \qquad \text{y} \qquad v_{SH\,q} = \frac{m_E v_{dc}}{2} \sin \delta_E$$

Now, taking the branch which contains the series converter and applying KLV gives,

$$V'_B = jx_B I'_B + V'_{SER}$$

Also,

$$v_{Bd} + jv_{Bq} = jx_B\left(i_{Bd} + ji_{Bq}\right) + V_{SER} \tag{7.21}$$

In a similar way for the shunt converter branch, substituting the series converter source given by (7.21) and separating into real and imaginary parts, gives,

$$v_{Bd} = -x_B i_{Bq} + V_{SERd} \tag{7.22}$$

$$v_{Bq} = x_B i_{Bd} + V_{SERq} \tag{7.23}$$

From Equations (7.19)-(7.20) and (7.22)-(7.23), the algebraic matrix representation of voltages and currents for the UPFC is,

$$\begin{bmatrix} v_{Ed} \\ v_{Eq} \end{bmatrix} = \begin{bmatrix} 0 & -x_E \\ x_E & 0 \end{bmatrix}\begin{bmatrix} i_{Ed} \\ i_{Eq} \end{bmatrix} + \begin{bmatrix} \frac{m_E v_{dc}}{2}\cos\delta_E \\ \frac{m_E v_{dc}}{2}\sin\delta_E \end{bmatrix} \tag{7.24}$$

$$\begin{bmatrix} v_{Bd} \\ v_{Bq} \end{bmatrix} = \begin{bmatrix} 0 & -x_B \\ x_B & 0 \end{bmatrix}\begin{bmatrix} i_{Bd} \\ i_{Bq} \end{bmatrix} + \begin{bmatrix} \frac{m_B v_{dc}}{2}\cos\delta_B \\ \frac{m_B v_{dc}}{2}\sin\delta_B \end{bmatrix} \tag{7.25}$$

Now, incorporating these relationships to the transmission line current that is parallel with the UPFC, the line currents are obtained as,

$$I_d + jI_q = \left(I_B + I_E + I_L\right)e^{-j\left(\delta - \pi/2\right)}$$

$$I_d + jI_q = \left[\left(i_{Ed} + i_{Bd} + i_{Ld}\right) + j\left(i_{Ed} + i_{Bd} + i_{Ld}\right)\right]e^{-j\left(\delta - \pi/2\right)} \tag{7.26}$$

Solving for voltages and currents that involve generator variables and not considering saliency effects, the voltage at generator terminals can be expressed as,

$$V_d + jV_q = E'_d + jE'_q - jx'_d\left(I_d + jI_q\right)$$

Also,

$$-\left[E'_d + \left(x'_q - x'_d\right)I_q + jE'_q\right] + j\left(x'_d + x_{tE}\right)\left(I_d + jI_q\right) + \left(v_{Ed} + jv_{Eq}\right)e^{-j\left(\delta - \pi/2\right)} = 0 \tag{7.27}$$

After some algebraic manipulations of (7.18) to (7.27) and solving for internal UPFC currents, the algebraic equations expressed in matrix form for the UPFC connected to the synchronous machine-infinite busbar power system are,

$$\begin{bmatrix} i_{Eq} \\ i_{Bq} \end{bmatrix} = \left[\begin{array}{c|c} -\left(x'_d + x_{tE}\right) - \\ \frac{1}{x_{line}}\left(x'_d + x_{tE}\right)x_E - x_E & -\left(x'_d + x_{tE}\right) \\ \hline --x_E & x_B + x_{BV} \end{array}\right]^{-1} \begin{bmatrix} E'_d \sin\delta + E'_q \cos\delta - \frac{1}{x_{line}}\left(x'_d + x_{tE}\right)\frac{m_E v_{dc}}{2}\cos\delta_E \\ -\frac{1}{x_{line}}\left(x'_d + x_{tE}\right)V_b \cos\theta - \frac{m_E v_{dc}}{2}\cos\delta_E \\ \hline -\frac{m_E v_{dc}}{2}\cos\delta_E + \frac{m_B v_{dc}}{2}\cos\delta_B - V_b \cos\theta \end{bmatrix} \tag{7.28}$$

$$\begin{bmatrix} i_{Ed} \\ i_{Bd} \end{bmatrix} = \left[\begin{array}{c|c} \left(x'_d + x_{tE}\right) + \\ \frac{1}{x_L}\left(x'_d + x_{tE}\right)x_E + x_E & x'_d + x_{tE} \\ \hline -x_E & -\left(x_B + x_{BV}\right) \end{array}\right]^{-1} \begin{bmatrix} -E'_d \cos\delta + E'_q \sin\delta - \frac{1}{x_{line}}\left(x'_d + x_{tE}\right)\frac{m_E v_{dc}}{2}\sin\delta_E \\ +\frac{1}{x_L}\left(x'_d + x_{tE}\right)V_b \sin\theta - \frac{m_E v_{dc}}{2}\sin\delta_E \\ \hline -\frac{m_E v_{dc}}{2}\sin\delta_E + \frac{m_B v_{dc}}{2}\sin\delta_B + V_b \sin\theta \end{bmatrix} \tag{7.29}$$

with,

$$I_d = i_{Ed} + i_{Bd} + i_{Ld}$$

$$I_q = i_{Eq} + i_{Bq} + i_{Lq}$$

7.5 UPFC CONTROL FUNCTIONS

The UPFC control function to be chosen depends on the functions it must perform. For instance, the UPFC may have three control parameters: magnitude and angle of the injected voltage and shunt reactive current. The active and reactive power flow control can be independently controlled by injecting a series voltage with a specified magnitude and angle [Dong *et al.* 2004]. In the reference [Guo *et al.* 2009] a different alternative of UPFC control is proposed, which is based on injecting a series voltage into the line, so that the line powers satisfy certain desired active and reactive power, with respect to the series controller. The shunt control is designated following the same functions as a STATCOM controller, regulating the shunt bus voltage magnitude and maintaining the dc link capacitor voltage.

The UPFC control scheme used in this thesis is basically the one proposed in the study of [Wang 2002]. Although control systems designed for UPFC functionality are more accurate and with solid theoretical basis, the control here used tries to overcome the final goal of damping oscillations. Some other control schemes have been developed such as [Mehraeen *et al.* 2010], [Uzunovic 2001], [Wang 1999] [Huang *et al.* 2000] [Cañizares *et al.* 2004] and oriented to different applications, such as

employing ultracapacitors as a part of the UPFC configuration for controlling interarea oscillations [Zarghami *et al*. 2010].

The UPFC is assigned to operate under basic control functions: power flow and AC voltage control. In order to achieve this, three PI controllers are included, *i.e*. a PI power flow controller, a PI AC voltage controller and a PI DC voltage controller; separately designed to try to ensure close loop system stability and good control performance [Wang 2002]. The scheme of such controller is shown in Figure 7.9. It is necessary to remark that one of the main contributions of this chapter is to demonstrate the modal interaction presented even among control functions of the UPFC. [Wang 2002] has stated that when the three PI controllers associated to the UPFC are in combined operation, poor control performance and even the closed-loop system instability occurs due to existence of the dynamic interactions among controllers. Obviously, when linear approximations are used, this interaction is imputable to linear modes, however when a nonlinear interaction is considered, it gives insight into the nature of control actions between controllers.

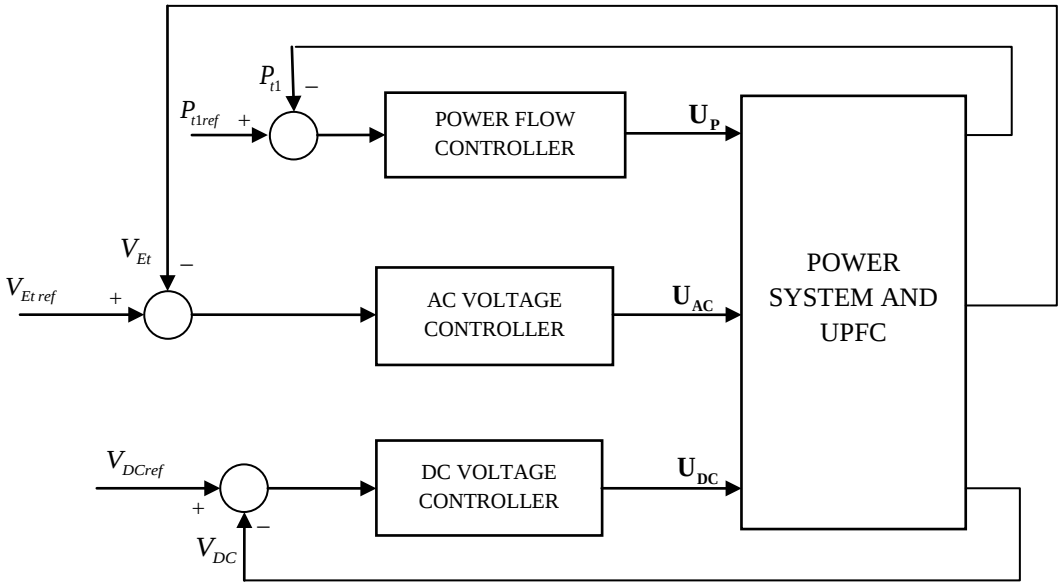

Figure 7.9 UPFC Control functions: Power flow controller, AC voltage and DC voltage controller

The selection of UPFC control is made following the suggested approach from [Wang 2002] which uses two variant selection of output control signals, i.e. $U_p = m_B, U_{AC} = m_E$ and $U_{DC} = \delta_E$ or $U_p = m_E, U_{AC} = m_B$ and $U_{DC} = \delta_E$. The first one is operated with power flow control function for the series part and AC voltage support and DC voltage regulation in the link capacitor for the shunt part; the second option takes the AC voltage controller in the series part, leaving the shunt part with power flow control and DC voltage regulation.

Despite the UPFC controls constitute a multi input-multi-output control (MIMO) problem, it is decomposed into three single input-single output (SISO) problem [Navabi Niaki 1996]. The close loop poles of the overall system are tested against a wide range of operating conditions of the system to ensure the accuracy of the control tuning. Thus, a multivariable PI controller for the UPFC is used to perform the three control functions, with the transfer functions [Wang 2002] given in Table 7.1:

Table 7.1 Transfer Functions PI Controllers of UPFC

OPTION 1	**OPTION 2**
PI power flow controller	PI power flow controller
$m_B = \left(K_P + \frac{K_{PI}}{s}\right)\left(P_{t\,ref} - P_t\right)$	$m_E = \left(K_P + \frac{K_{PI}}{s}\right)\left(P_{t\,ref} - P_t\right)$
PI DC voltage controller	PI DC voltage controller
$\delta_E = \left(K_{DCP} + \frac{K_{DCI}}{s}\right)\left(V_{DC\,ref} - V_{DC}\right)$	$\delta_E = \left(K_{DCP} + \frac{K_{DCI}}{s}\right)\left(V_{DC\,ref} - V_{DC}\right)$
PI AC voltage controller	PI AC voltage controller
$m_E = \left(K_{ACP} + \frac{K_{ACI}}{s}\right)\left(V_{E\,ref} - V_{Et}\right)$	$m_B = \left(K_{ACP} + \frac{K_{ACI}}{s}\right)\left(V_{E\,ref} - V_{Et}\right)$

7.6 UPFC DAMPING APPLICATIONS. SMIB POWER SYSTEM

The UPFC needs the DC voltage across the link capacitor to be kept constant. A generic diagram of the UPFC can be illustrated in Figure 7.10. The block diagram refers to a FACTS device (such as the UPFC or SVC) installed in a power system. Referring to the particular case of a UPFC, the reference signal is the $v_{dc\,ref}$, being the output the variable v_{dc} [Wang *et al.* 1999],

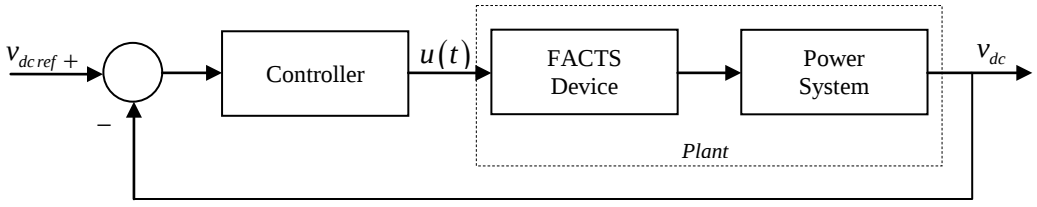

Figure 7.10 Control Diagram of a UPFC Connected to a Power System

To exemplify the behavior of a UPFC interacting with the power system, the experiment is designed in order to describe the next statements:

- To analyze the small signal stability of the system
- To evaluate the nonlinear contributions of the UPFC interacting with the power system

The system to be analyzed is shown in Figure 7.11.

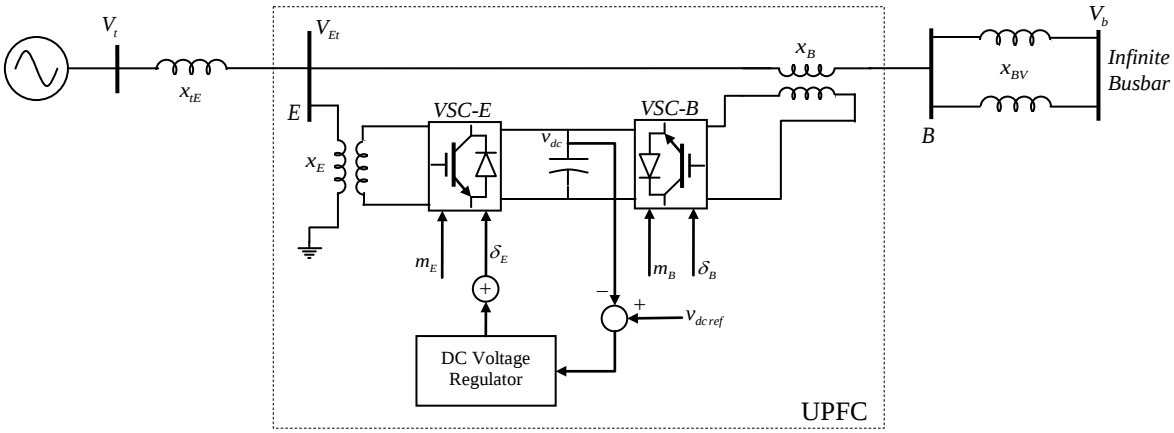

Figure 7.11 UPFC connected to a SMIB test power system for damping oscillations

The DC voltage regulator is basically a PI controller, with the transfer function taken from Table 7.1 with a slight addition,

$$\delta_E(s) = \frac{1}{1+sT_c}\left(K_P + \frac{K_I}{s}\right)\left(v_{dc\,ref} - v_{dc}\right) \tag{7.30}$$

Manipulating (7.30) to obtain a state variable representation, a set of differential equations that represents the voltage regulator is,

$$\frac{d\delta'_E}{dt} = K_I\left(v_{DC\,ref} - v_{DC}\right)$$

$$\frac{d\delta_E}{dt} = \frac{1}{T_C}\left[K_P\left(v_{DC\,ref} - v_{DC}\right) + \delta'_E - \delta_E\right]$$

Thus, the power system integrated with the UPFC and control actions is an eighth order dynamic system. This system is linearized and then, the modal series method is applied such as it was described in Chapter 3.

The steady state diagram in this case study is shown in Figure 7.12. The steady state values are obtained from a power flow study with estimated initial conditions as [Acha *et al.* 2004] [Fuerte-Esquivel and Acha 1997],

<u>VSC B</u>

$$\delta_B = \tan^{-1}\left(\frac{P_t}{C.I.}\right)$$

$$V_E^0 = \left(\frac{x_B}{V_{Bt}^0}\right)\sqrt{P_t^2 + C.I.^2} \tag{7.31}$$

where

$$C.I. = Q_t - \frac{V_{Bt}^0}{x_B}\left(V_{Bt}^0 - V_{Et}^0\right) \qquad \text{if} \qquad V_{Bt}^0 \neq V_{Et}^0$$

$$C.I. = Q_t \qquad \text{if} \qquad V_{Bt}^0 = V_{Et}^0$$

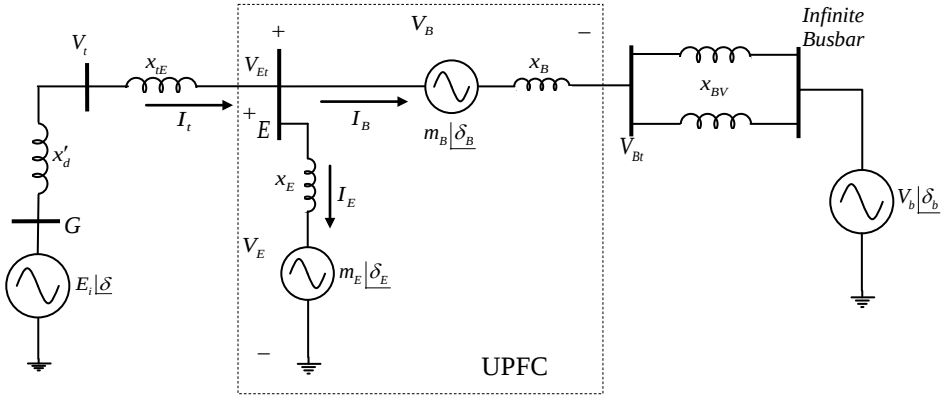

Figure 7.12 Steady state diagram of the UPFC connected to the SMIB study case

$$\underline{\text{VSC E}} \qquad \delta_E = -\sin^{-1}\left\{\frac{\left(V_{Et}^0 - V_{Bt}^0\right) m_B^0 x_E \sin\delta_B^0}{m_E^0 V_{Et}^0 x_B}\right\} \tag{7.32}$$

From power flow analysis, the system under study results in the following UPFC parameters of modulation indices and angles for shunt (m_E, δ_E) and series (m_B, δ_B) VSC's and internal voltage machine (E_i) and rotor angle (δ), that is,

$$E_i|\underline{\delta} = 1.16|\underline{40.0666}\ p.u.$$

$$m_B|\underline{\delta_B} = -0.11385|\underline{-174.949}\ p.u.$$

$$m_E|\underline{\delta_E} = 0.979554|\underline{20.0086}\ p.u.$$

Table 7.2 Eigenvalues and damping ratio for the case study of SMIB-UPFC

Eigenvalues	**Damping Ratio**
−49.831885231975711	1.00
−33.492328635278355	1.00
$-16.673751838802978 \pm 3.740509054841034i$	0.975748485361660
−2.838813683838964	1.00
$-0.771881207091769 \pm 0.395341519956049i$	0.890049105052969
−0.237839096373391	1.00

The small signal analysis is indicated in Table 7.2. There are four oscillatory modes that for the case of the UPFC connected show high values of damping ratios.

The eigenvalues are changing depending on the controller parameters. The list shown in Table 7.3 resumes the eigenvalues obtained for the given constraints.

Table 7.3 Controller parameters variation and Eigenvalues for the case study of SMIB-UPFC

CONTROLLER PARAMETERS	EIGENVALUES
$K_p = -1,\ K_I = -14$	$\mathbf{L} = \begin{bmatrix} -49.798007988217186 \\ -31.775868883313439 \\ -33.368378715993721 \\ -3.816071582811596 \\ -0.357354263976474 + 1.961087561753644i \\ -0.357354263976474 - 1.961087561753644i \\ -1.565026171201958 \\ -0.254070869765097 \end{bmatrix}$
$K_p = -10.5,\ K_I = -1$	$\mathbf{L} = \begin{bmatrix} -49.798229591698757 \\ -33.479633864535877 \\ -24.500358420498447 \\ -10.149186309011327 \\ -2.135545061513665 \\ -0.161309437325926 + 0.048081636278437i \\ -0.161309437325926 - 0.048081636278437i \\ -0.906560617345859 \end{bmatrix}$
$K_p = -0.5,\ K_I = -5$	$\mathbf{L} = \begin{bmatrix} -49.797999386311581 \\ -31.904580188031169 \\ -33.356400692828117 \\ -4.194528651744296 \\ -1.685096756928323 \\ -0.045378617710198 + 1.073813162495645i \\ -0.045378617710198 - 1.073813162495645i \\ -0.262769827991752 \end{bmatrix}$
$K_p = -1.5,\ K_I = -1.5$	$\mathbf{L} = \begin{bmatrix} -49.798027828957636 \\ -31.247817660898104 \\ -33.400468555660680 \\ -4.695880010721426 \\ -1.790892209196046 \\ -0.032587203635567 + 0.514287467647266i \\ -0.032587203635567 - 0.514287467647266i \\ -0.284655543914654 \end{bmatrix}$
$K_p = -15,\ K_I = -15$	$\mathbf{L} = \begin{bmatrix} -49.798305761437945 \\ -33.488382215081415 \\ -16.854376998063390 + 2.143667676639956i \\ -16.854376998063390 - 2.143667676639956i \\ -2.065300049765778 \\ -0.988080406689826 + 0.606543283650125i \\ -0.988080406689826 - 0.606543283650125i \\ -0.255229903464238 \end{bmatrix}$

7.7 SECOND ORDER SMIB-UPFC SOLUTIONS

The SMIB-UPFC system is decomposed into its linear and nonlinear model using the modal series method. The system is given by the next state variables vector,

$$X = \begin{bmatrix} \delta & \omega & E'_q & E'_d & E_{fd} & v_{dc} \end{bmatrix}^T \tag{7.33}$$

The order of the state vector depends on the control actions that are used in order to control de VSC's of the UPFC. The stable equilibrium point of the system is given as,

$$X_{SEP} = \begin{bmatrix} \delta_0 & \omega_0 & E'_{q0} & E'_{d0} & E_{fd0} & v_{dc0} \end{bmatrix}^T \tag{7.34}$$

The linearization and second order of the state variables δ, ω, E'_q, E'_d and E_{fd} have been detailed in this thesis. Emphasis on the dc voltage at the VSC's of the UPFC is deduced in this section. The differential equation that overcomes the dynamics of the dc link in the UPFC operation has characteristics of highly nonlinear nature, since it is dependent on modulation indices and angles of both series and shunt VSC's. Besides the quadrature and direct axis currents are involved, followed by nonlinear interactions of the rotor angle. This may implies the presence of high nonlinear modal interactions, which can be detailed using the modal series method.

Recalling the modal series procedure, applied into this particular case of the differential equation for dc voltage $\dot{v}_{dc}$, a closed form analytical solution can be found based on their linear and nonlinear components; this is obtained with Equation (7.35). It results evident the division of this Taylor expanded equation into linear and nonlinear terms; the variables that are not involved in the state variable are not considered. In order to apply the modal series method, the Jacobian and Hessian matrices of the global test power system have to be calculated, as well as eingenvalues and eigenvectors. As it was pointed-out in the previous section above, the eigenvalues are function on the system parameters, thus resulting necessary the determination of the steady state operation selected for a given control action *i.e.*, constant voltage condition at the VSC shunt, active and reactive power controlled after the series VSC, etc.

$$
\begin{aligned}
\Delta\dot{v}_{dc} = {} & \frac{3m_E}{4C_{dc}}\left[\cos\delta_E\left(\frac{\partial i_{Ed}}{\partial\delta}\Delta\delta+\frac{\partial i_{Ed}}{\partial E'_q}\Delta E'_q+\frac{\partial i_{Ed}}{\partial v_{dc}}\Delta v_{dc}\right)+\sin\delta_E\left(\frac{\partial i_{Eq}}{\partial\delta}\Delta\delta+\frac{\partial i_{Eq}}{\partial v_{dc}}\Delta v_{dc}\right)\right]_{X_{SEP}} \\
& + \frac{3m_B}{4C_{dc}}\left[\cos\delta_B\left(\frac{\partial i_{Bd}}{\partial\delta}\Delta\delta+\frac{\partial i_{Bd}}{\partial E'_q}\Delta E'_q+\frac{\partial i_{Bd}}{\partial v_{dc}}\Delta v_{dc}\right)+\sin\delta_B\left(\frac{\partial i_{Bq}}{\partial\delta}\Delta\delta+\frac{\partial i_{Bq}}{\partial v_{dc}}\Delta v_{dc}\right)\right]_{X_{SEP}} \\
& + \frac{1}{2!}\left\{\begin{array}{l}
\dfrac{3m_E}{4C_{dc}}\left[\begin{array}{l}
\cos\delta_E\left(\begin{array}{l}
\dfrac{\partial^2 i_{Ed}}{\partial\delta\partial\delta}\Delta\delta^2+\dfrac{\partial^2 i_{Ed}}{\partial\delta\partial E'_q}\Delta\delta\Delta E'_q+\dfrac{\partial^2 i_{Ed}}{\partial\delta\partial v_{dc}}\Delta\delta\Delta v_{dc}+ \\
\dfrac{\partial^2 i_{Ed}}{\partial E'\partial\delta}\Delta E'\Delta\delta+\dfrac{\partial^2 i_{Ed}}{\partial E'\partial E'_q}\Delta E'^2_q+\dfrac{\partial^2 i_{Ed}}{\partial E'\partial v_{dc}}\Delta E'\Delta v_{dc}+ \\
\dfrac{\partial^2 i_{Ed}}{\partial v_{dc}\partial\delta}\Delta v_{dc}\Delta\delta+\dfrac{\partial^2 i_{Ed}}{\partial v_{dc}\partial E'_q}\Delta v_{dc}\Delta E'_q+\dfrac{\partial^2 i_{Ed}}{\partial v_{dc}\partial v_{dc}}\Delta {v_{dc}}^2
\end{array}\right) \\
+\sin\delta_E\left(\dfrac{\partial^2 i_{Eq}}{\partial\delta\partial\delta}\Delta\delta^2+\dfrac{\partial^2 i_{Eq}}{\partial\delta\partial v_{dc}}\Delta\delta\Delta v_{dc}+\dfrac{\partial^2 i_{Eq}}{\partial v_{dc}\partial\delta}\Delta v_{dc}\Delta\delta+\dfrac{\partial^2 i_{Eq}}{\partial v_{dc}\partial v_{dc}}\Delta {v_{dc}}^2\right)
\end{array}\right]_{X_{SEP}} + \\
\dfrac{3m_B}{4C_{dc}}\left[\begin{array}{l}
\cos\delta_B\left(\begin{array}{l}
\dfrac{\partial^2 i_{Bd}}{\partial\delta\partial\delta}\Delta\delta^2+\dfrac{\partial^2 i_{Bd}}{\partial\delta\partial E'_q}\Delta\delta\Delta E'_q+\dfrac{\partial^2 i_{Bd}}{\partial\delta\partial v_{dc}}\Delta\delta\Delta v_{dc}+ \\
\dfrac{\partial^2 i_{Bd}}{\partial E'_q\partial\delta}\Delta E'\Delta\delta+\dfrac{\partial^2 i_{Bd}}{\partial E'_q\partial E'_q}\Delta E'^2_q+\dfrac{\partial^2 i_{Bd}}{\partial E'_q\partial v_{dc}}\Delta E'\Delta v_{dc}+ \\
\dfrac{\partial^2 i_{Bd}}{\partial v_{dc}\partial\delta}\Delta v_{dc}\Delta\delta+\dfrac{\partial^2 i_{Bd}}{\partial v_{dc}\partial E'_q}\Delta v_{dc}\Delta E'_q+\dfrac{\partial^2 i_{Bd}}{\partial v_{dc}\partial v_{dc}}\Delta {v_{dc}}^2
\end{array}\right) \\
+\sin\delta_B\left(\dfrac{\partial^2 i_{Bq}}{\partial\delta\partial\delta}\Delta\delta^2+\dfrac{\partial^2 i_{Bq}}{\partial\delta\partial v_{dc}}\Delta\delta\Delta v_{dc}+\dfrac{\partial^2 i_{Bq}}{\partial v_{dc}\partial\delta}\Delta v_{dc}\Delta\delta+\dfrac{\partial^2 i_{Bq}}{\partial v_{dc}\partial v_{dc}}\Delta {v_{dc}}^2\right)
\end{array}\right]_{X_{SEP}}
\end{array}\right\} + \\
\end{aligned}
$$

(7.35)

Although in the development of Taylor series expansion in Equation (7.35) the controller actions are not included, the formulation tries to get insight into the nature of nonlinear contribution based on the UPFC dynamic modeling.

One of the usefulness of the modal series method relies on its capacity to represent the linear and nonlinear expansion in terms of multidimensional Laplace transform. Thus, a closed form solution is given by (7.36), where the linear part (basically expressed in terms on single Laplace variable) and second order terms (as a function of two variables Laplace domain) are easily identified. Please observe in this detailed closed form solution, that there is an explicit relationship between state variables (rotor angle δ and quadrature axis voltage E'_q) with *d* and *q* current components given for both voltage source converters, series and shunt. This represents a very interesting analytical result, since the nonlinear dynamics of the UPFC can be explicitly incorporated using the algebraic and state variables in the analysis.

$$\Delta V_{dc}(s)=\frac{3m_E}{4C_{dc}}\begin{bmatrix} I_{Ed}(s)\cos\delta_E\left(K_{i_{Ed},\delta}\delta(s)+K_{i_{Ed},E'_q}E'_q(s)+K_{i_{Ed},v_{dc}}v_{dc}(s)\right)+\\ I_{Eq}(s)\sin\delta_E\left(K_{i_{Eq},\delta}\delta(s)+K_{i_{Eq},v_{dc}}v_{dc}(s)\right)\end{bmatrix}$$
$$+\frac{3m_B}{4C_{dc}}\begin{bmatrix} I_{Bd}(s)\cos\delta_B\left(K_{i_{Bd},\delta}\delta(s)+K_{i_{Bd},E'_q}E'_q(s)+K_{i_{Bd},v_{dc}}v_{dc}(s)\right)+\\ I_{Bd}(s)\sin\delta_B\left(K_{i_{Bq},\delta}\delta(s)+K_{i_{Bq},v_{dc}}v_{dc}(s)\right)\end{bmatrix}$$
$$+\frac{1}{2!}\left\{\begin{array}{l}\dfrac{3m_E}{4C_{dc}}\left[\begin{array}{l} I_{Ed}(s_1,s_2)\cos\delta_E\left(\begin{array}{l}K^2_{i_{Ed},\delta,\delta}\delta(s_1)\delta(s_2)+K^2_{i_{Ed},\delta,E'_q}\delta(s_1)E'_q(s_2)+K^2_{i_{Ed},\delta,v_{dc}}\delta(s_1)v_{dc}(s_2)+\\ K^2_{i_{Ed},E'_q,\delta}E'_q(s_1)\delta(s_2)+K^2_{i_{Ed},E'_q,E'_q}E'_q(s_1)E'_q(s_2)+K^2_{i_{Ed},E'_q,v_{dc}}E'_q(s_1)v_{dc}(s_2)+\\ K^2_{i_{Ed},v_{dc},\delta}v_{dc}(s_1)\delta(s_2)+K^2_{i_{Ed},v_{dc},E'_q}v_{dc}(s_1)E'_q(s_2)+K^2_{i_{Ed},v_{dc},v_{dc}}v_{dc}(s_1)v_{dc}(s_2)\end{array}\right)+\\ +I_{Eq}(s_1,s_2)\sin\delta_E\left(\begin{array}{l}K^2_{i_{Eq},\delta,\delta}\delta(s_1)\delta(s_2)+K^2_{i_{Eq},\delta,v_{dc}}\delta(s_1)v_{dc}(s_2)+\\ K^2_{i_{Eq},v_{dc},\delta}v_{dc}(s_1)\delta(s_2)+K^2_{i_{Eq},v_{dc},v_{dc}}v_{dc}(s_1)v_{dc}(s_2)\end{array}\right)\end{array}\right]+\\ \dfrac{3m_B}{4C_{dc}}\left[\begin{array}{l} I_{Bd}(s_1,s_2)\cos\delta_B\left(\begin{array}{l}K^2_{i_{Bd},\delta,\delta}\delta(s_1)\delta(s_2)+K^2_{i_{Bd},\delta,E'_q}\delta(s_1)E'_q(s_2)+K^2_{i_{Bd},\delta,v_{dc}}\delta(s_1)v_{dc}(s_2)+\\ K^2_{i_{Bd},E'_q,\delta}E'_q(s_1)\delta(s_2)+K^2_{i_{Bd},E'_q,E'_q}E'_q(s_1)E'_q(s_2)+K^2_{i_{Bd},E'_q,v_{dc}}E'_q(s_1)v_{dc}(s_2)+\\ K^2_{i_{Bd},v_{dc},\delta}v_{dc}(s_1)\delta(s_2)+K^2_{i_{Bd},v_{dc},E'_q}v_{dc}(s_1)E'_q(s_2)+K^2_{i_{Bd},v_{dc},v_{dc}}v_{dc}(s_1)v_{dc}(s_2)\end{array}\right)+\\ +I_{Bq}(s_1,s_2)\sin\delta_B\left(\begin{array}{l}K^2_{i_{Bq},\delta,\delta}\delta(s_1)\delta(s_2)+K^2_{i_{Bq},\delta,v_{dc}}\delta(s_1)v_{dc}(s_2)+\\ K^2_{i_{Bq},v_{dc},\delta}v_{dc}(s_1)\delta(s_2)+K^2_{i_{Bq},v_{dc},v_{dc}}v_{dc}(s_1)v_{dc}(s_2)\end{array}\right)\end{array}\right]\end{array}\right\}+$$

(7.36)

Finally, the closed form solution in the time domain of (7.36) is calculated applying association of variables and inverse Laplace transform, resulting in,

$$x_i(t)=v_{dc}(t)=\sum_{j=1}^{N}\left(u_{ij}y^1_j(0)-\sum_{k=1}^{N}\sum_{l=1}^{N}u_{ij}h^j_{2kl}y^1_k(0)y^1_l(0)\right)e^{\lambda_j t}+\sum_{j=1}^{N}\sum_{k=1}^{N}\sum_{l=1}^{N}u_{ij}h^j_{2kl}y^1_k(0)y^1_l(0)e^{(\lambda_k+\lambda_l)t} \tag{7.37}$$

where,

$$Y_0=U^{-1}\begin{bmatrix}\delta_0 & \omega_0 & E'_{q0} & E'_{d0} & E_{fd0} & v_{dc0}\end{bmatrix}^T$$

The rest of time domain solutions obey the same reasoning. Also, in the nonlinear interaction coefficients h^j_{2kl} are included in the relationships of terms associated to the internal parameters and algebraic equations of the UPFC, as well as the modal characteristics and modal interaction through second order modal combination.

7.8 NONLINEAR OSCILLATIONS ANALYSIS

The system is perturbed increasing the rotor angle from its initial value of $\delta=71^\circ$ to the value of $\delta=81^\circ$ followed by an step increase in the dc voltage reference. Due to the inclusion of the dc voltage dynamics and its control, the UPFC-SMIB power system is highly nonlinear. The waveforms of the experiment are shown in Figure 7.13, where the nonlinear oscillations of rotor angles and rotor speeds

for each generator are shown. Through the analysis of the simulation, it can be resumed that the system describe different oscillations depending on the controller setting parameters, which are reflected on more content of nonlinear contributions. In the same form as the previous case study, the oscillations of rotor angles are charted comparing their response obtained with the modal series method and the linear approximation.

The experiment shows differences between both solutions in phase and amplitude mostly in the case of oscillatory response. Each angle corresponds to the controller parameters according to the Table 7.3.

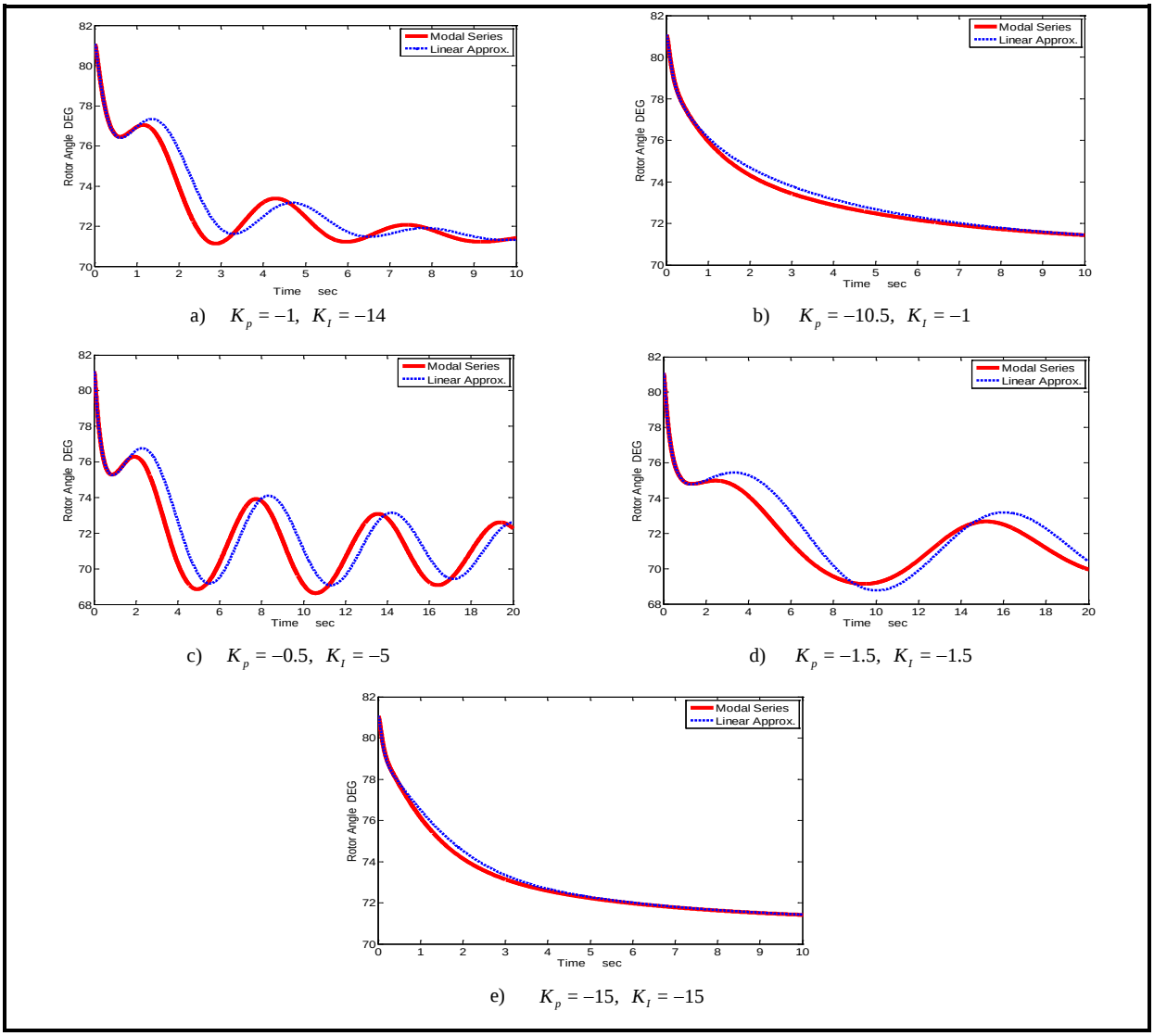

a) $K_p = -1,\ K_I = -14$

b) $K_p = -10.5,\ K_I = -1$

c) $K_p = -0.5,\ K_I = -5$

d) $K_p = -1.5,\ K_I = -1.5$

e) $K_p = -15,\ K_I = -15$

Figure 7.13 Rotor angles for different PI controller parameters in the case study of SMIB-UPFC

It is clear that the correctness setting of the controller reflects into higher damped response after the disturbance; hence, the better controllers are those with values $K_p = -10.5,\ K_I = -1$ (Figure 7.13b)

and $K_p = -15$, $K_I = -15$ (Figure 7.13e). The controllers designed with parameters $K_p = -1$, $K_I = -14$ (Figure 7.13a), $K_p = -0.5$, $K_I = -5$ (Figure 7.13c) and $K_p = -0.5$, $K_I = -5$ (Figure 7.13d) show low frequency oscillations after the transient, which means that the controllers are not able to damp the oscillations due to the disturbance in the power system.

The waveforms of Figure 7.14 complete the analysis of the electromechanical variables involved in the model. In the same way as the rotor angles, the rotor speed also oscillates depending on the controller parameters, reflecting that the most oscillatory cases are when $K_p = -1$, $K_I = -14$ and $K_p = -0.5$, $K_I = -5$. These results are in clear agreement with the eigenvalues detailed in Table 7.3.

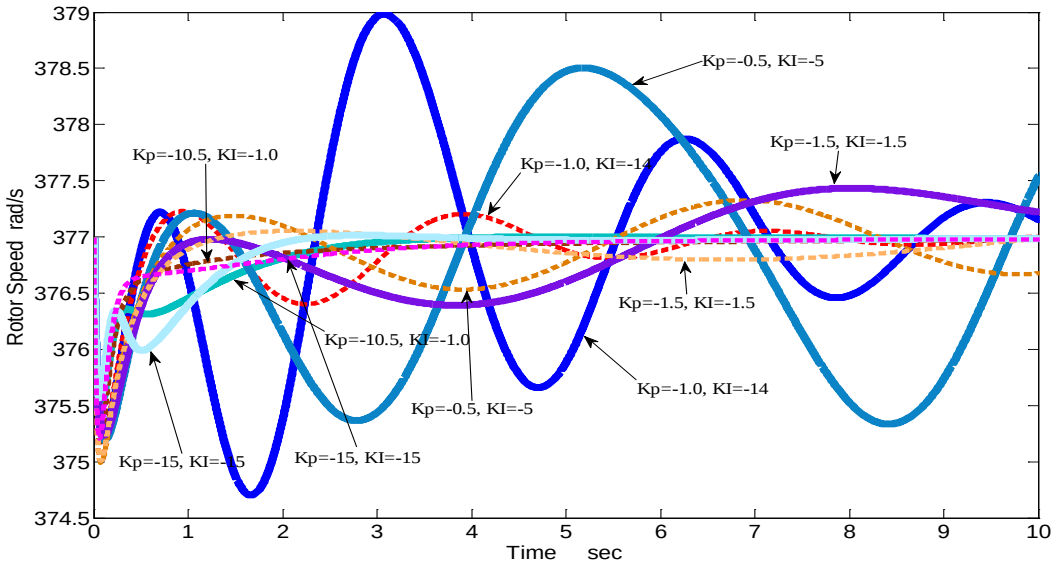

b) Rotor Speed

Figure 7.14 Case study of SMIB-UPFC (Rotor speed variables)

Keeping the same subject followed in this case study, now it is important to analyze the Figure 7.15, which shows the voltages presented in the dc link of the UPFC. Again, each graph corresponds to its controller parameters according to the Table 7.3. It is evident the most oscillatory responses, which agrees with Figures 7.13 and 7.14 for the rotor angle and speed rotor, respectively. However, it is also important to describe the remarkable differences between the linear approximation and the modal series solutions. The differences are observed in both, amplitude and phase shifting, being the worst cases for the most oscillatory responses.

Then, it can be inferred from Figure 7.15 that there is an important nonlinear contribution in the total response related to the modal interaction, which is not included in the linear approximation

method. The dynamic during transient cannot be followed in the same way applying only a linear solution, being relevant the inclusion of a nonlinear method such as the modal series.

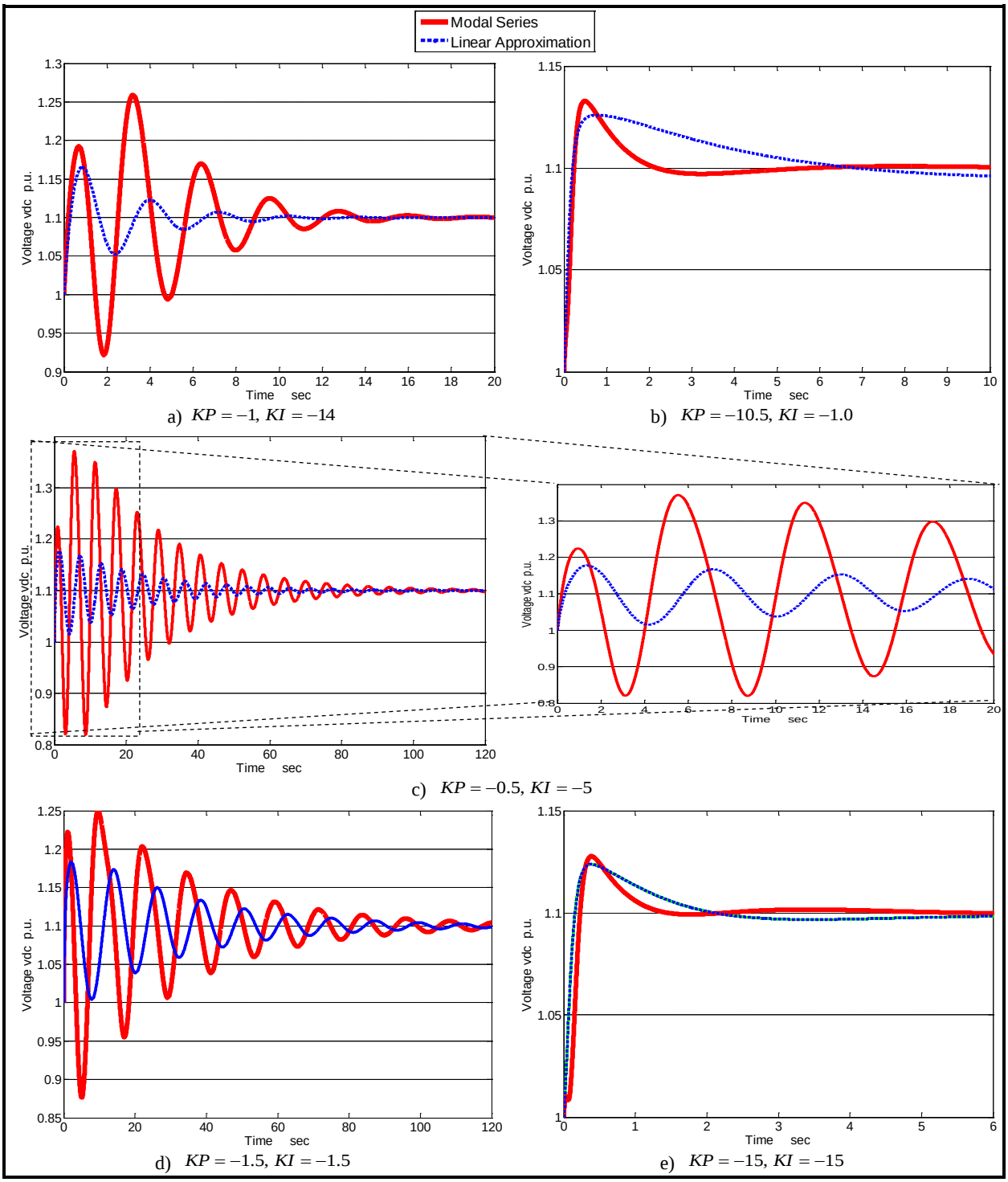

Figure 7.15 Case study of SMIB-UPFC (voltages v_{dc} for each constraint of PI controllers)

The nonlinear contribution described above is remarked through the nonlinear indices analysis shown in the graph diagrams of Figure 7.16. The calculated indices are the same used in Chapter 6, described by Equations (6.1)-(6.4), applied now to this case study. Basically, the bar diagrams indicate the value of each index for the given controller parameters. From this Figure 7.16, the following comments are resumed:

- The case with the higher values for all indices is when the controller parameters have values with $KP = -15,\ KI = -15$ (Figure 7.16e) whose highest index is $I4$, which denotes considerable modal interaction.

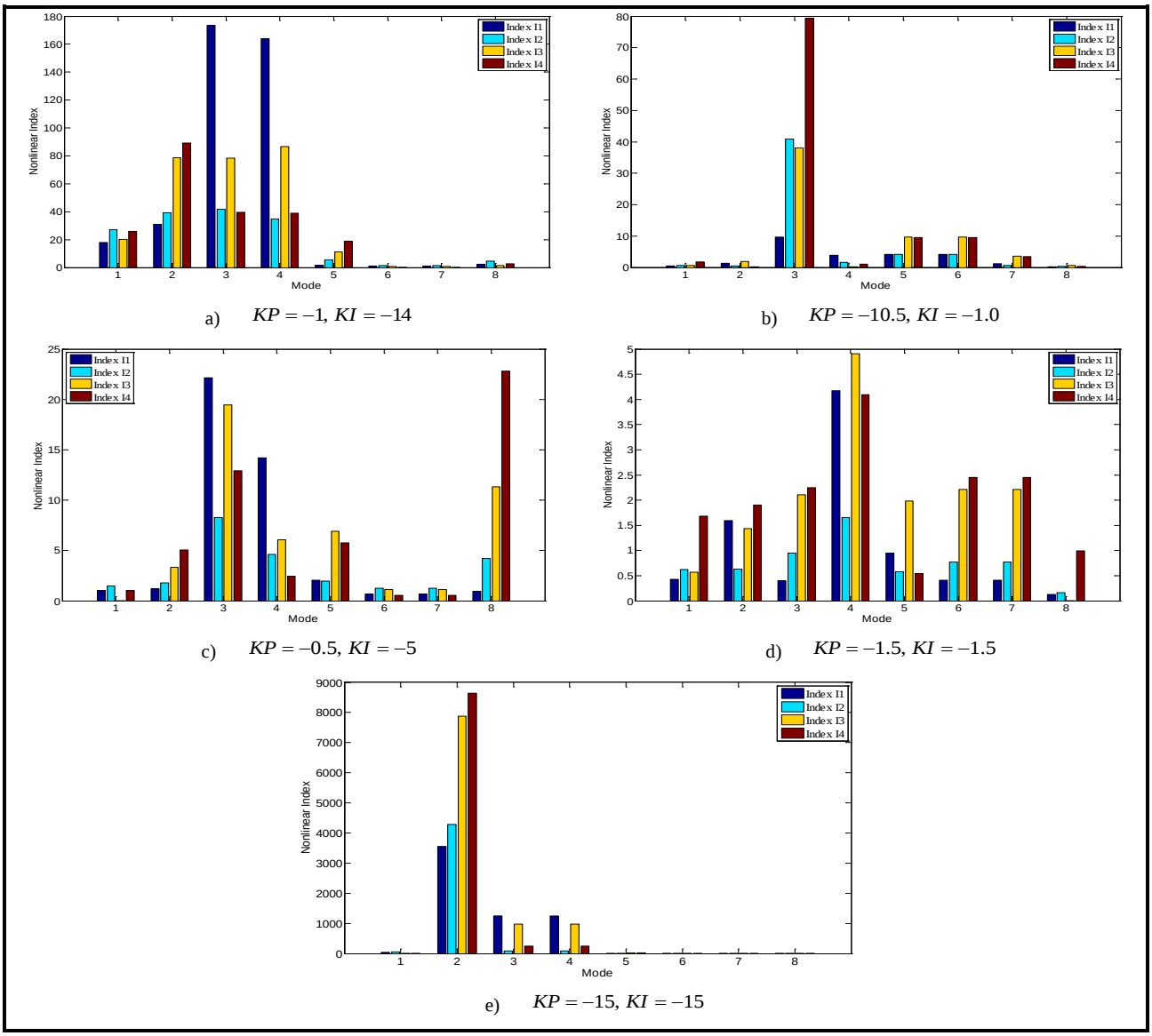

Figure 7.16 Nonlinear indices for the different PI controller parameters

Table 7.4 Linear and nonlinear participation factors for the SMIB-UPFC power system

MODE	Scenario 1				Scenario 2				Scenario 3				Scenario 4				Scenario 5			
	$\max\lvert P1_{jkl}\rvert$	k	$\max\lvert P2_{jkl}\rvert$	k	$\max\lvert P1_{jkl}\rvert$	k	$\max\lvert P2_{jkl}\rvert$	k	$\max\lvert P1_{jkl}\rvert$	k	$\max\lvert P2_{jkl}\rvert$	k	$\max\lvert P1_{jkl}\rvert$	k	$\max\lvert P2_{jkl}\rvert$	k	$\max\lvert P1_{jkl}\rvert$	k	$\max\lvert P2_{jkl}\rvert$	k
1	1.0056	5	0.0027	3	1.0055	5	0.0165	6	1.0056	5	0.0027	3	1.0056	5	0.0027	3	1.0055	5	0.002	3
2	0.8436	2	0.0643	1	1.4182	1	1.3988	1	0.9044	2	0.091	1	0.7022	2	0.2582	6	146.428	8	146.2738	8
3	0.6822	8	0.3719	1	115.8674	6	115.4191	6	0.8676	8	0.0294	1	0.6347	8	0.0274	1	1,853.7	6	1,854.80	6
4	2.1103	4	0.9816	4	109.5481	6	110.5128	6	1.9963	4	1.089	4	1.7871	4	1.0464	4	1,853.7	6	1,854.80	6
5	15.0041	6	15.1588	6	1.7939	6	1.9153	6	1.0413	1	0.3292	1	1.1561	3	0.8856	3	3.2744	5	3.4503	1
6	15.0041	6	15.1588	6	2.6414	6	2.7934	6	7.6002	6	7.7544	6	4.3887	6	4.669	6	8.1927	6	8.516	6
7	2.5018	1	2.0532	6	10.9072	3	2.7934	6	7.6002	6	7.7544	6	4.3887	6	4.669	6	8.1927	6	8.516	6
8	0.6555	3	0.2569	7	10.9072	3	10.3575	3	0.5776	1	0.4552	7	0.4117	3	0.3049	3	0.629	3	0.1183	6

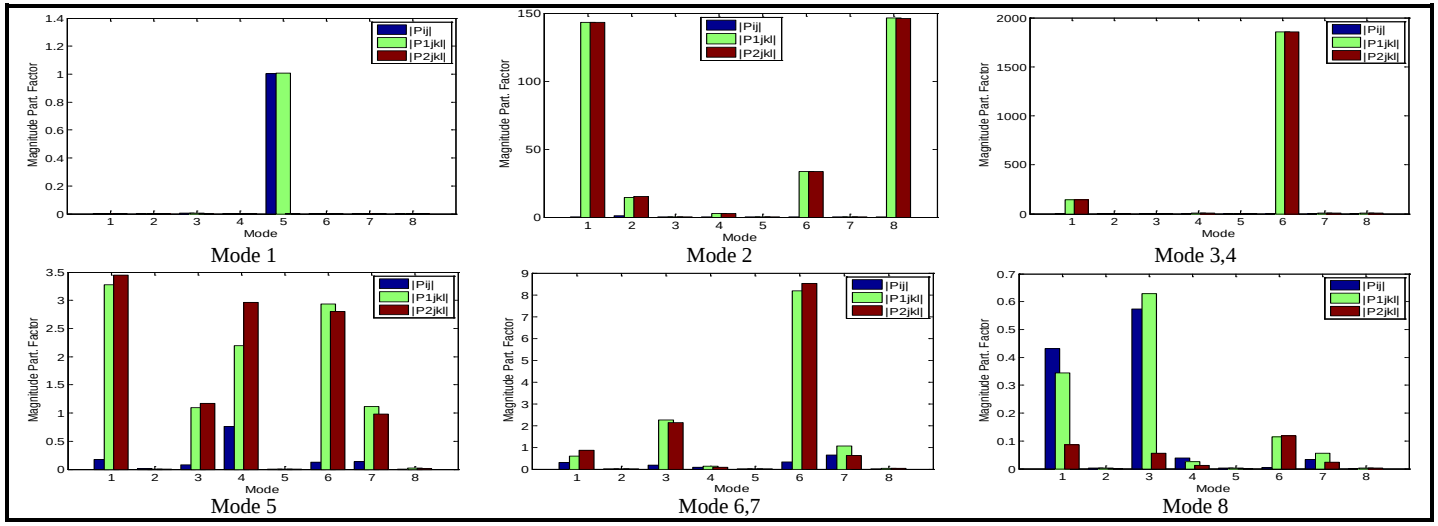

Figure 7.17 Linear and nonlinear participation factors bar graphs for the case of SMIB-UPFC

- The case with the less modal interaction is when the controller parameters are $KP = -1.5,\ KI = -1.5$ (Figure 7.16d) since all the indices have small values.
- The case of $KP = -10.5,\ KI = -1.0$ (Figure 7.16b) has the highest index associated to $I4$. Again, the dynamic of the system under such constraints has an important modal interaction presented in the original state variables.

The case study is completed with the analysis of linear and nonlinear participation factors described in Table 7.4. Here, the maximum linear and nonlinear participation factors as well as the interacting modes are indicated. The most dominant modal interaction is presented when the parameters are $KP = -15,\ KI = -15$, which agrees with Figure 7.15e) for the nonlinear indices. Please observe the annexed bar diagram of Figure 7.17, which visually denotes the modal contribution measured by the participation factors. Here, the linear participation factor defined by Equation (6.5) has the lowest contribution, then being the most important participation those due to the nonlinear interaction coefficients given by (6.15).

7.9 SUMMARY

The conclusion of the case study can be decomposed into two issues: the first one is the damping scenario introduced by the correct setting of controller parameters. As it was mentioned in Section 7.5 above, extensive work has been proposed to determine the correct setting of controller parameters for the UPFC and in general, for any FACTS device. In second place, the case study was focused to get insight into the nature the modal interaction when the UPFC is presented.

It is clear that the idea of including FACTs devices such as the UPFC in the power system open a great variety of work that can be done in future contributions: the setting of controller parameters, the inclusion of one or more UPFC´s into multimachine and large scale power networks, which opens a plenty of research related to the nature of linear and nonlinear modal interactions.

THIS PAGE IS INTENTIONALLY LEFT BLANK

8

CONCLUSIONS AND FUTURE RESEARCH

8.1 CONCLUDING REMARKS

The modal series method studied along this thesis is a systematic procedure that allows the study of a nonlinear system, obtaining decomposed terms, which specify separately the first, second, third, etc. order terms of the nonlinear system.

As it was mentioned, mainly in Chapter 2, the modal analysis represents a very important tool to characterize the oscillation characteristics of a linear system subjected to a small perturbation. However, under a more general set of operating conditions and perturbations, the linear approximation given by the modal analysis may not be enough to determine the nature of nonlinear contributions neither of modal interaction.

Some analytical methods have been developed and tested to get insight into these nonlinear oscillations, *i.e.* the method of Normal Forms of Vector Fields and the method of Modal Series, both studied and compared in this thesis. Each of them have their own properties, although the core the methods are strictly the same, that is, the linearization of the nonlinear system around a stable equilibrium point applying Taylor series expansion and then, the Jordan canonical form. Finally, an analytical closed form solution is obtained, after a nonlinear transformation (for the case of the Normal Forms method) and application of the multidimensional Laplace transform and association of variables theorems (for the case of the Modal Series method).

In chronological order of appearance along the thesis, the next statements draw the main conclusions of this research, based on the study of nonlinear oscillations:

- In this thesis, an analytical methodology based on the modal series technique has been presented. Based on the modal series previously proposed by [Schanechi, *et al.* 2003] [Pariz *et al.* 2003], an extension of the method has been achieved, which consists on generalizing the method using the theorems of multidimensional Laplace transform and the theorems of association of variables, to solve the dynamic nonlinear system as an algebraic problem.

- The application of multidimensional Laplace transform was applied so far only to nonlinear systems using the Volterra series expansion; some kernels in terms of multidimensional Laplace variables are solved to characterize the nonlinear system. In the method of Modal Series, a set of kernels expressed in terms of multidimensional Laplace transform are solved by the association of variables theorems, thus obtaining a single Laplace domain set of kernels.
- A comparison with other methods such as linear approximation has been presented, remarking the main advantages of the method here proposed.
- An application of the Normal Forms (NF) and the Modal Series (MS) methods to nonlinear dynamic systems has been illustrated. When the solution of both methods is compared with respect to the direct numerical integration of differential equations, it is shown that it strongly depends on the initial conditions and parameters of the original system. Selected conditions to start the simulation in both NF and MS, becomes in remarkable differences with respect to the closed form analytic solution for the two methods, reflecting more drastic differences in the NF method.
- The main contribution of the comparative analysis between NF and MS has demonstrated the viability of the application of the modal series method, as an easier and less complex alternative to analyze dynamic systems, rather than Normal Forms, and shown how the initialization of the system also modifies the final solution.
- The application of the multidimensional Laplace transform and association of variables techniques are the core of the Modal Series technique, which allows a closed form analytical solution of the nonlinear system; being the extension of including the control forced response, one of the main contributions of this thesis.
- The solutions obtained with the Modal Series method have been compared with the full numerical solution of the nonlinear set differential equations, in order to establish the numerical validations of the results obtained. For each case study the accuracy of responses has been detailed.
- The forced response solution by the Modal Series technique has been obtained. The analytical solution includes the main characteristics between the nonlinear terms and the input signal function. The basic case is when an impulse function is used as the input signal of the transfer function, however it is possible to apply any input function. The case with the unit step function has been tested as well.
- The method has been successfully simulated through a 9-bus, 3-machines and the New England 10 generators, 39 buses test systems, presenting the results on the principal state variables in the time domain and remarking the main contributions of oscillatory modes. Emphasis is given to

the nonlinear contributions using the Fast Fourier Transform on machines speed deviations, modal analysis, nonlinear interaction indices and nonlinear participation factors.

- A detailed description of the higher order modal series terms have been exemplified with a synchronous machine infinite busbar power system, through the classic model and the one flux dynamic model.
- The nonlinear oscillations produced by a perturbation in the third order model of the synchronous machine have been analyzed
- The detailed theory related to the linear transfer function concepts and its extension to the nonlinear transfer function through the application of the modal series method, as the basis of nonlinear system expansion, and assuming an input force response, have been described
- The method has the great advantage to analyze in both time and frequency domain, in numerical and analytical ways, the transfer functions of nonlinear system
- The examples of application of the nonlinear transfer function definition was focused on applications to simple power systems, such as the SMIB and the 3 machines-9 buses test systems. However, following the same definitions, it is possible to extend the concepts in a straightforward manner to the analysis of large scale power systems. It is clear that dealing with larger-scale systems, the complexity of analysis is increased, thus resulting necessary the inclusion of sparsity techniques, effective algorithms of eigenvalues determination, etc.
- The incorporation of UPFC to the nonlinear power system model has been analyzed. The steady state and dynamic model of the UPFC have been included in the study, detailing their main equations that link its dynamic behavior.
- The modal analysis and the nonlinear contributions to the damping oscillations of the power system operating together with the UPFC have been analyzed. The correct set of UPFC control actions over the damping performance and nonlinear interaction have been performed.

8.2 FUTURE CONTRIBUTIONS

The next issues can be included as some ideas to be developed in a near future based on this research. Most of them are focused on the nonlinear systems analysis, FACTS devices and other analytical and numerical topics.

- Incorporation of algorithms to determine dominant poles in the nonlinear transfer functions. The nonlinear transfer functions concept introduced in this thesis, needs to determine what are the most important poles that originate the modal interaction. Hence, it is proposed to use the techniques developed to determine the most dominant poles [Martins *et al.* 1996] in the nonlinear transfer function concept.

- Power damping devices sintonization applying nonlinear transfer functions and frequency analysis for the nonlinear interactions. Since the modal series method allows the definition of nonlinear transfer function, and the frequency and system stability calculation, it is very useful to determine the damping devices that help to damp the oscillations presented during disturbances.
- Reference [Pagola *et al.* 1989] deals with eigenvalue sensitivities analysis. An extension of this interesting work can be done now assuming the interaction between modes and determining their sensitivities.
- Regarding the study of near resonance conditions presented when modal series method is applied. Despite the demonstrated fact that the modal series method can obtain a closed form solution under resonance condition, there is a lack of work concerning on how to determine the near to resonance conditions. [Zhu *et al.* 2001] describe an approach that incorporates a procedure to determine resonance and near-resonance conditions in the Normal Forms method. Similar procedure can be analyzed in order to find a systematic procedure to be applied in the modal series method.
- A method to establish the relationship between stability zones obtained with bifurcation theory and continuation techniques, can be included in the modal series method to identify the zones where the application of the method is valid.
- Other linearization procedures, such as Carleman linearization can be explored to avoid Taylor series expansion. In the reference [Arroyo 2007], the author proposed the Carleman linearization that modifies the analytical response and analysis obtained with the Normal Forms method. A similar procedure can be followed to determine different characteristics of the closed form solutions obtained with the Modal Series method.
- In the same way as the UPFC was modeled and analyzed in this thesis, other FACTS devices can be easily explored, in order to determine their nonlinear modal interaction when are connected to the power system.
- The linear and nonlinear dynamic analysis of the VSC-HVDC represents an interesting application of the Modal Series method. The topic involves calculation of steady state conditions, dynamic analysis of the control actions and applications to the links of non-conventional energy sources.

APPENDIX A
MULTIDIMENSIONAL LAPLACE TRANSFORM AND ASSOCIATION OF VARIABLES THEOREMS

A.1 ***Theorem 1*** [Crum & Heinen 1974]

The reduction and expansion of a realizable two dimensional Laplace Transform kernel of the form,

$$Z_2(s_1,s_2)=\frac{N_2(s_1,s_2)}{\prod_{i=1}^{II}(s_1+s_2+\alpha_i)\prod_{j=1}^{JJ}(s_1+\beta_j)\prod_{k=1}^{KK}(s_2+\gamma_k)} \tag{A.1}$$

where $N_2(s_1,s_2)$ is a polynomial in s_1 and s_2, yields,

$$\begin{aligned} Z_2(s)=&\sum_{J=1}^{JJ}\sum_{K=1}^{KK}\left\{\frac{\left[(s_1+\beta_J)(s_2+\gamma_K)Z_2(s_1,s_2)\big|_{\substack{s_1=-\beta_J\\ s_2=-\gamma_K}}\right]}{(s+\gamma_K+\beta_J)}\right\}\\ &+\sum_{I=1}^{II}\left\{\frac{\left[\sum_{K=1}^{KK}(s_1+s_2+\alpha_I)(s_2+\gamma_K)Z_2(s_1,s_2)\big|_{\substack{s_1=\gamma_K-\alpha_I\\ s_2=-\gamma_K}}\right]}{(s+\alpha_I)}\right\}\end{aligned} \tag{A.2}$$

The function $Z_2(s_1,s_2)$ represents the second order Laplace term whose variables would be *associated* to the function $Z_2(s)$ that is defined as a single variable problem. Applied to our case, the second order term $Y_2^j(s_1,s_2)$ given by equation (A.2) will be converted into a one dimensional expression $Y_2^j(s)$, as it is explained below.

A.2 ***Theorem 2*** [Crum & Heinen 1974]

The complete reduction and expansion of a realizable *n*-dimensional kernel of the form,

$$\begin{aligned} Z_n(s_1,s_2,\ldots,s_n)=&\frac{N_n(s_1,s_2,\ldots,s_n)}{\prod_{k=1}^{K1}(s_1+s_2+\cdots+s_n+x_k)\prod_{j1=1}^{J11}(s_1+\alpha_{j1})}\cdot\\ &\frac{1}{\prod_{j2=1}^{J22}(s_2+\beta_{j2})\cdots\prod_{jn=1}^{Jnn}(s_n+\omega_{jn})}\end{aligned} \tag{A.3}$$

where, $N_n(s_1, s_2, \ldots, s_n)$ is a polynomial in *n* variables.

The generalization to the n-dimensional case is straightforward [10]:

$$Z_n(s) = \sum_{K=1}^{K1} \left\{ \frac{\left[\sum_{J2=1}^{J22} \cdots \sum_{Jn=1}^{Jnn} \left[\begin{array}{l} (s_1 + s_2 + \cdots + s_n + x_K) \\ \cdot (s_2 + \beta_{J2}) \cdots (s_n + \omega_{Jn}) \\ \cdot Z_n(s_1, s_2, \ldots, s_n) \end{array} \right|_{\substack{s_1 = -x_{K1} + \beta_{J2} \\ \quad + \cdots + \omega_{Jn} \\ s_2 = -\beta_{J2} \\ \vdots \\ s_n = -\omega_{Jn}}} \right]}{(s + x_K)} \right\}$$

$$+ \sum_{J1=1}^{J11} \sum_{J2=1}^{J22} \cdots \sum_{Jn=1}^{Jnn} \left\{ \frac{\left[\begin{array}{l} (s_1 + \alpha_{J1})(s_2 + \beta_{J2}) \cdots \\ (s_n + \omega_{Jn}) \cdot Z_n(s_1, s_2, \ldots, s_n) \end{array} \right|_{\substack{s_1 = -\alpha_{J1} \\ s_2 = -\beta_{J2} \\ \vdots \\ s_n = -\omega_{Jn}}}}{(s + \alpha_{J1} + \beta_{J2} + \cdots \omega_{Jn})} \right\} \qquad \text{(A.4)}$$

APPENDIX B
MODAL SERIES HIGHER ORDER DEDUCTION

B1. SECOND ORDER TERMS

With the terms obtained in Chapter 3, but defining them on terms of s_1 and s_2 yields,

$$Y_k^1(s_1)=\frac{Y_k^1(0)}{(s_1-\lambda_k)} \qquad \text{and} \qquad Y_l^2(s_2)=\frac{Y_l^2(0)}{(s_2-\lambda_l)} \tag{B.1}$$

Then,

$$Y_j^2(s_1,s_2)=\sum_{k=1}^{n}\sum_{l=1}^{n}\frac{1}{(s_1+s_2-\lambda_j)}C_{kl}^j\frac{Y_k^1(0)}{(s_1-\lambda_k)}\frac{Y_l^1(0)}{(s_2-\lambda_l)}$$

which can be also expressed as

$$Y_j^2(s_1,s_2)=\sum_{k=1}^{n}\sum_{l=1}^{n}C_{kl}^jY_k^1(0)Y_l^1(0)\frac{1}{(s_1+s_2-\lambda_j)(s_1-\lambda_k)(s_2-\lambda_l)} \tag{B.2}$$

We can now apply Theorem 1 to associate the variables of the function $Y_j^2(s_1,s_2)$ to $Y_j^2(s)$. Let

$$N_2(s_1,s_2)=\frac{1}{(s_1+s_2-\lambda_j)(s_1-\lambda_k)(s_2-\lambda_l)}$$

$$N_2(s)=\frac{(s_1-\lambda_k)(s_2-\lambda_l)N_s(s_1,s_2)\big|_{\substack{s_1=\lambda_k\\ s_2=\lambda_l}}}{(s-\lambda_k-\lambda_l)}+\frac{(s_1+s_2-\lambda_j)(s_2-\lambda_l)N_s(s_1,s_2)\big|_{\substack{s_1=-\lambda_l+\lambda_j\\ s_2=\lambda_l}}}{(s-\lambda_j)}$$

$$N_2(s)=\frac{1}{(\lambda_k+\lambda_l-\lambda_j)}\left[\frac{1}{(s-\lambda_k-\lambda_l)}-\frac{1}{(s-\lambda_j)}\right]$$

Therefore, the second order-term becomes

$$Y_j^2(s)=\sum_{k=1}^{n}\sum_{l=1}^{n}\left\{C_{kl}^jY_k^1(0)Y_l^1(0)\frac{1}{(\lambda_k+\lambda_l-\lambda_j)}\left[\frac{1}{(s-\lambda_k-\lambda_l)}-\frac{1}{(s-\lambda_j)}\right]\right\} \tag{B.3}$$

Higher order terms could be obtained in like manner.

B2. THIRD ORDER TERMS

Recalling,

$$\begin{aligned}\left(s_1+s_2+s_3\right)Y_j^3\left(s_1,s_2,s_3\right)=\lambda_j Y_j^3\left(s_1,s_2,s_3\right)+\sum_{k=1}^{n}\sum_{l=1}^{n}C_{kl}^{j}\left[Y_k^2\left(s_1,s_2\right)Y_l^1\left(s_3\right)+Y_k^1\left(s_1\right)Y_l^2\left(s_2,s_3\right)\right]\\+\sum_{p=1}^{n}\sum_{q=1}^{n}\sum_{r=1}^{n}D_{pqr}^{j}\left[Y_p^1\left(s_1\right)Y_q^1\left(s_2\right)Y_r^1\left(s_3\right)\right]\end{aligned}\tag{B.4}$$

And also,

$$Y_j^1\left(s_1\right)=\frac{Y_j^1(0)}{\left(s_1-\lambda_j\right)}\qquad\text{and}\qquad Y_j^2\left(s_1,s_2\right)=\sum_{k=1}^{n}\sum_{l=1}^{n}\frac{1}{\left(s_1+s_2-\lambda_j\right)}C_{kl}^{j}Y_k^1\left(s_1\right)Y_l^1\left(s_2\right)\tag{B.5}$$

New indexes are defined in order to conform third order terms. That is,

$$Y_l^1\left(s_3\right)=\frac{Y_l^1(0)}{\left(s_3-\lambda_l\right)}\qquad;\qquad Y_k^1\left(s_1\right)=\frac{Y_k^1(0)}{\left(s_1-\lambda_k\right)}$$

$$Y_p^1\left(s_1\right)=\frac{Y_p^1(0)}{\left(s_1-\lambda_p\right)}\qquad;\qquad Y_q^1\left(s_2\right)=\frac{Y_q^1(0)}{\left(s_2-\lambda_q\right)}\qquad;\qquad Y_r^1\left(s_3\right)=\frac{Y_r^1(0)}{\left(s_3-\lambda_r\right)}$$

In the same way, second order terms are re-indexed as,

$$Y_k^2\left(s_1,s_2\right)=\sum_{p=1}^{n}\sum_{q=1}^{n}\frac{1}{\left(s_1+s_2-\lambda_k\right)}C_{pq}^{k}Y_p^1\left(s_1\right)Y_q^2\left(s_2\right)\tag{B.6}$$

$$Y_l^2\left(s_2,s_3\right)=\sum_{p=1}^{n}\sum_{q=1}^{n}\frac{1}{\left(s_2+s_3-\lambda_l\right)}C_{pq}^{l}Y_p^1\left(s_2\right)Y_q^1\left(s_3\right)\tag{B.7}$$

Substituting,

$$\begin{aligned}&\left(s_1+s_2+s_3\right)Y_j^3\left(s_1,s_2,s_3\right)=\\&\lambda_j Y_j^3\left(s_1,s_2,s_3\right)\\&+\sum_{k=1}^{n}\sum_{l=1}^{n}C_{kl}^{j}\left[\sum_{p=1}^{n}\sum_{q=1}^{n}\frac{1}{\left(s_1+s_2-\lambda_k\right)}C_{pq}^{k}\frac{Y_p^1(0)}{\left(s_1-\lambda_p\right)}\frac{Y_q^1(0)}{\left(s_2-\lambda_q\right)}\frac{Y_l^1(0)}{\left(s_3-\lambda_l\right)}+\right.\\&\left.\frac{Y_k^1(0)}{\left(s_1-\lambda_k\right)}\sum_{p=1}^{n}\sum_{q=1}^{n}\frac{1}{\left(s_2+s_3-\lambda_l\right)}C_{pq}^{l}\frac{Y_p^1(0)}{\left(s_2-\lambda_p\right)}\frac{Y_q^1(0)}{\left(s_3-\lambda_q\right)}\right]\\&+\sum_{p=1}^{n}\sum_{q=1}^{n}\sum_{r=1}^{n}D_{pqr}^{j}\left[\frac{Y_p^1(0)}{\left(s_1-\lambda_p\right)}\frac{Y_q^1(0)}{\left(s_2-\lambda_q\right)}\frac{Y_r^1(0)}{\left(s_3-\lambda_r\right)}\right]\end{aligned}\tag{B.8}$$

$$\left(s_1+s_2+s_3\right)Y_j^3\left(s_1,s_2,s_3\right)=$$
$$\lambda_j Y_j^3\left(s_1,s_2,s_3\right)$$
$$+\sum_{k=1}^{n}\sum_{l=1}^{n}\sum_{p=1}^{n}\sum_{q=1}^{n}C_{kl}^{j}C_{pq}^{k}\frac{1}{\left(s_1+s_2-\lambda_k\right)}\frac{Y_p^1(0)}{\left(s_1-\lambda_p\right)}\frac{Y_q^1(0)}{\left(s_2-\lambda_q\right)}\frac{Y_l^1(0)}{\left(s_3-\lambda_l\right)}+$$
$$\sum_{k=1}^{n}\sum_{l=1}^{n}\sum_{p=1}^{n}\sum_{q=1}^{n}C_{kl}^{j}C_{pq}^{l}\frac{Y_k^1(0)}{\left(s_1-\lambda_k\right)}\frac{1}{\left(s_2+s_3-\lambda_l\right)}\frac{Y_p^1(0)}{\left(s_2-\lambda_p\right)}\frac{Y_q^1(0)}{\left(s_3-\lambda_q\right)}$$
$$+\sum_{p=1}^{n}\sum_{q=1}^{n}\sum_{r=1}^{n}D_{pqr}^{j}\left[\frac{Y_p^1(0)}{\left(s_1-\lambda_p\right)}\frac{Y_q^1(0)}{\left(s_2-\lambda_q\right)}\frac{Y_r^1(0)}{\left(s_3-\lambda_r\right)}\right]$$

$$\left(s_1+s_2+s_3\right)Y_j^3\left(s_1,s_2,s_3\right)=$$
$$\lambda_j Y_j^3\left(s_1,s_2,s_3\right)+$$
$$\sum_{k=1}^{n}\sum_{l=1}^{n}\sum_{p=1}^{n}\sum_{q=1}^{n}C_{kl}^{j}C_{pq}^{k}Y_p^1(0)Y_q^1(0)Y_l^1(0)\left[\frac{1}{\left(s_1+s_2-\lambda_k\right)\left(s_1-\lambda_p\right)\left(s_2-\lambda_q\right)\left(s_3-\lambda_l\right)}\right]+$$
$$\sum_{k=1}^{n}\sum_{l=1}^{n}\sum_{p=1}^{n}\sum_{q=1}^{n}C_{kl}^{j}C_{pq}^{l}Y_k^1(0)Y_p^1(0)Y_q^1(0)\left[\frac{1}{\left(s_2+s_3-\lambda_l\right)\left(s_1-\lambda_k\right)\left(s_2-\lambda_p\right)\left(s_3-\lambda_q\right)}\right]+$$
$$\sum_{p=1}^{n}\sum_{q=1}^{n}\sum_{r=1}^{n}D_{pqr}^{j}Y_p^1(0)Y_q^1(0)Y_r^1(0)\left[\frac{1}{\left(s_1-\lambda_p\right)\left(s_2-\lambda_q\right)\left(s_3-\lambda_r\right)}\right]$$

Hence,

$$Y_j^3\left(s_1,s_2,s_3\right)=\frac{1}{\left(s_1+s_2+s_3-\lambda_j\right)}$$
$$\left\{\sum_{k=1}^{n}\sum_{l=1}^{n}\sum_{p=1}^{n}\sum_{q=1}^{n}C_{kl}^{j}C_{pq}^{k}Y_p^1(0)Y_q^1(0)Y_l^1(0)\left[\frac{1}{\left(s_1+s_2-\lambda_k\right)\left(s_1-\lambda_p\right)\left(s_2-\lambda_q\right)\left(s_3-\lambda_l\right)}\right]+\right.$$
$$\sum_{k=1}^{n}\sum_{l=1}^{n}\sum_{p=1}^{n}\sum_{q=1}^{n}C_{kl}^{j}C_{pq}^{l}Y_k^1(0)Y_p^1(0)Y_q^1(0)\left[\frac{1}{\left(s_2+s_3-\lambda_l\right)\left(s_1-\lambda_k\right)\left(s_2-\lambda_p\right)\left(s_3-\lambda_q\right)}\right]+ \quad \text{(B.9)}$$
$$\left.\sum_{p=1}^{n}\sum_{q=1}^{n}\sum_{r=1}^{n}D_{pqr}^{j}Y_p^1(0)Y_q^1(0)Y_r^1(0)\left[\frac{1}{\left(s_1-\lambda_p\right)\left(s_2-\lambda_q\right)\left(s_3-\lambda_r\right)}\right]\right\}$$

Or,

$$
\begin{aligned}
&Y_j^3(s_1,s_2,s_3) = \\
&\sum_{k=1}^{n}\sum_{l=1}^{n}\sum_{p=1}^{n}\sum_{q=1}^{n} C_{kl}^{j} C_{pq}^{k} Y_p^1(0) Y_q^1(0) Y_l^1(0) \left[\frac{1}{(s_1+s_2+s_3-\lambda_j)(s_1+s_2-\lambda_k)(s_1-\lambda_p)(s_2-\lambda_q)(s_3-\lambda_l)} \right] + \\
&\sum_{k=1}^{n}\sum_{l=1}^{n}\sum_{p=1}^{n}\sum_{q=1}^{n} C_{kl}^{j} C_{pq}^{l} Y_k^1(0) Y_p^1(0) Y_q^1(0) \left[\frac{1}{(s_1+s_2+s_3-\lambda_j)(s_2+s_3-\lambda_l)(s_1-\lambda_k)(s_2-\lambda_p)(s_3-\lambda_q)} \right] + \\
&\sum_{p=1}^{n}\sum_{q=1}^{n}\sum_{r=1}^{n} D_{pqr}^{j} Y_p^1(0) Y_q^1(0) Y_r^1(0) \left[\frac{1}{(s_1+s_2+s_3-\lambda_j)(s_1-\lambda_p)(s_2-\lambda_q)(s_3-\lambda_r)} \right]
\end{aligned}
\tag{B.10}
$$

Third order kernel can be re-defined as,

$$
Y_j^3(s_1,s_2,s_3) = K_1 N_1(s_1,s_2,s_3) + K_2 N_2(s_1,s_2,s_3) + K_3 N_3(s_1,s_2,s_3) \tag{B.11}
$$

Where,

$$
N_1(s_1,s_2,s_3) = \frac{1}{(s_1+s_2+s_3-\lambda_j)(s_1+s_2-\lambda_k)(s_1-\lambda_p)(s_2-\lambda_q)(s_3-\lambda_l)} \tag{B.12}
$$

$$
N_2(s_1,s_2,s_3) = \frac{1}{(s_1+s_2+s_3-\lambda_j)(s_2+s_3-\lambda_l)(s_1-\lambda_k)(s_2-\lambda_p)(s_3-\lambda_q)} \tag{B.13}
$$

$$
N_3(s_1,s_2,s_3) = \frac{1}{(s_1+s_2+s_3-\lambda_j)(s_1-\lambda_p)(s_2-\lambda_q)(s_3-\lambda_r)} \tag{B.14}
$$

B3. ASSOCIATION OF VARIABLES

In order to solve the kernels $N_1(s_1,s_2,s_3)$ and $N_2(s_1,s_2,s_3)$ it is posible to use the corollary proposed by [Crum and Heinen 1974]. The corollary fits to $(i-1)^{\text{st}}$ reduction and expansion of a *n*-dimensional kernels of the form,

$$
\begin{aligned}
Z_n(s_1,s_2,\ldots,s_n) = &\frac{G_n(s_1,s_2,\ldots,s_n)}{\prod_{k1=1}^{K11}(s_1+s_2+\ldots+s_i+x_{k1})} \\
&\cdot \frac{1}{\prod_{k2=K11+1}^{K22}\left(s_1+s_2+\ldots+s_i+\sum_{m>i}s_m+x_{k2}\right)} \\
&\cdot \frac{1}{\prod_{j1=1}^{J11}(s_1+\alpha_{j1})\prod_{j2=1}^{J22}(s_2+\beta_{j2})\cdots\prod_{ji=1}^{Jii}(s_i+\eta_{ji})}
\end{aligned}
\tag{B.15}
$$

where $G_n(s_1, s_2, \ldots, s_n)$ is the ratio of a polynomial in *n* variables to a polynomial in the $n-i$ variables $i+1, i+2, \ldots, n-1$ and *n*, yields

$$
\begin{aligned}
&Z_n(s_1, s_{i+1}, \ldots, s_n) \\
&= \sum_{k1=1}^{K22} \left[\frac{\left\{ \sum_{J2=1}^{J22} \cdots \sum_{Ji=1}^{Jii} \left\{ \left(s_1 + s_2 + \cdots + s_i + x_{k1}\right)\left(s_2 + \beta_{J2}\right)\cdots\left(s_i + \eta_{Ji}\right) \cdot Z_n(s_1, s_2, \ldots, s_n) \right|_{\substack{s_1 = -x_{k1} + \beta_{J2} + \cdots + \eta_{Ji} \\ s_2 = -\beta_{J2} \\ \vdots \\ s_i = -\eta_{Ji}}} \right\}}{\left(s_1 + x_{K1}\right)} \right] \\
&+ \sum_{J1=1}^{J11} \sum_{J2=1}^{J22} \cdots \sum_{Ji=1}^{Jii} \left[\frac{\left\{ \left(s_1 + \alpha_{J1}\right)\left(s_2 + \beta_{J2}\right)\cdots\left(s_i + \eta_{Ji}\right) \cdot Z_n(s_1, s_2, \ldots, s_n) \right|_{\substack{s_1 = -\alpha_{J1} \\ s_2 = -\beta_{J2} \\ \vdots \\ s_i = -\eta_{Ji}}} \right\}}{\left(s_1 + \alpha_{J1} + \beta_{J2} + \cdots + \eta_{Ji}\right)} \right]
\end{aligned}
\tag{B.16}
$$

Where,

$$x_{k1} = \sum_{m>i} s_m + x_{k2}, \qquad K11 < k1 \le K22$$

Hence, applying the corollary to kernels $N_1(s_1, s_2, s_3)$ and $N_2(s_1, s_2, s_3)$, it yields,

$$
\begin{aligned}
N_1(s_1, s_3) = &\frac{\left[\left(s_1 + s_2 + s_3 - \lambda_j\right)\left(s_2 - \lambda_q\right)\left(s_3 - \lambda_l\right) \frac{1}{\left(s_1 + s_2 + s_3 - \lambda_j\right)\left(s_1 + s_2 - \lambda_k\right)\left(s_1 - \lambda_p\right)\left(s_2 - \lambda_q\right)\left(s_3 - \lambda_l\right)} \right|_{\substack{s_3 = \lambda_l \\ s_2 = \lambda_q \\ s_1 = \lambda_j - \lambda_q - \lambda_l}} \Bigg]}{\left(s_1 + s_3 - \lambda_j\right)} \\
&+ \frac{\left[\left(s_1 - \lambda_p\right)\left(s_2 - \lambda_q\right)\left(s_3 - \lambda_l\right) \frac{1}{\left(s_1 + s_2 + s_3 - \lambda_j\right)\left(s_1 + s_2 - \lambda_k\right)\left(s_1 - \lambda_p\right)\left(s_2 - \lambda_q\right)\left(s_3 - \lambda_l\right)} \right|_{\substack{s_3 = \lambda_l \\ s_2 = \lambda_q \\ s_1 = \lambda_p}} \Bigg]}{\left(s_1 - \lambda_p - \lambda_q - \lambda_l\right)}
\end{aligned}
$$

Making algebraic operations, the new kernel is,

$$N_1(s_1, s_3) = \frac{1}{\left(\lambda_j - \lambda_p - \lambda_q - \lambda_l\right)} \left[\frac{1}{\left(\lambda_j - \lambda_l - \lambda_k\right)} \frac{1}{\left(s_1 + s_3 - \lambda_j\right)} - \frac{1}{\left(\lambda_p + \lambda_q - \lambda_k\right)} \frac{1}{\left(s_1 - \lambda_p - \lambda_q - \lambda_l\right)} \right]$$

which is defined in terms of a single Laplace domain by association of variables theorems as,

$$N_1(s)=\frac{1}{\left(\lambda_j-\lambda_p-\lambda_q-\lambda_l\right)}\left[\frac{1}{\left(\lambda_j-\lambda_l-\lambda_k\right)}\frac{1}{\left(s-\lambda_j\right)}-\frac{1}{\left(\lambda_p+\lambda_q-\lambda_k\right)}\frac{1}{\left(s-\lambda_p-\lambda_q-\lambda_l\right)}\right] \tag{B.17}$$

$$N_2(s_1,s_3)=\frac{\left[\left(s_1+s_2+s_3-\lambda_j\right)\left(s_2-\lambda_p\right)\left(s_3-\lambda_q\right)\frac{1}{\left(s_1+s_2+s_3-\lambda_j\right)\left(s_2+s_3-\lambda_l\right)\left(s_1-\lambda_k\right)\left(s_2-\lambda_p\right)\left(s_3-\lambda_q\right)}\Big|_{\substack{s_3=\lambda_q\\ s_2=\lambda_p\\ s_1=\lambda_j-\lambda_p-\lambda_q}}\right]}{\left(s_1+s_3-\lambda_j\right)}$$

$$+\frac{\left[\left(s_1-\lambda_k\right)\left(s_2-\lambda_p\right)\left(s_3-\lambda_q\right)\frac{1}{\left(s_1+s_2+s_3-\lambda_j\right)\left(s_2+s_3-\lambda_l\right)\left(s_1-\lambda_k\right)\left(s_2-\lambda_p\right)\left(s_3-\lambda_q\right)}\Big|_{\substack{s_3=\lambda_k\\ s_2=\lambda_p\\ s_1=\lambda_q}}\right]}{\left(s_1-\lambda_k-\lambda_p-\lambda_q\right)}$$

$$N_2(s_1,s_3)=\frac{1}{\left(\lambda_j-\lambda_p-\lambda_q-\lambda_k\right)}\frac{1}{\left(\lambda_p+\lambda_q-\lambda_l\right)}\left[\frac{1}{\left(s_1+s_3-\lambda_j\right)}-\frac{1}{\left(s_1-\lambda_p-\lambda_q-\lambda_k\right)}\right]$$

which is defined in terms of a single Laplace domain by association of variables theorems as,

$$N_2(s_1,s_3)=\frac{1}{\left(\lambda_j-\lambda_p-\lambda_q-\lambda_k\right)}\frac{1}{\left(\lambda_p+\lambda_q-\lambda_l\right)}\left[\frac{1}{\left(s-\lambda_j\right)}-\frac{1}{\left(s_1-\lambda_p-\lambda_q-\lambda_k\right)}\right] \tag{B.18}$$

Finally, the kernel $N_1(s_1,s_2,s_3)$ is reduced following the next approach:

Recalling (B.14),

$$N_3(s_1,s_2,s_3)=\frac{1}{\left(s_1+s_2+s_3-\lambda_j\right)\left(s_1-\lambda_p\right)\left(s_2-\lambda_q\right)\left(s_3-\lambda_r\right)}$$

From [Lubbock and Bansal 1968],

$$\frac{k}{\left(s_1+a_1\right)\left(s_2+a_2\right)\ldots\left(s_m+a_m\right)\left(s_1+s_2+\ldots+s_m+\alpha\right)} \tag{B.19}$$

It is associated as,

$$\frac{k}{\left(s+\alpha\right)\left(s+a_1+a_2+\ldots+a_m\right)} \tag{B.20}$$

Therefore,

$$N_3(s) = \frac{1}{(s-\lambda_j)(s-\lambda_p-\lambda_q-\lambda_r)} \tag{B.21}$$

Decomposing (B.21) in partial fractions expansion, results in,

$$N_3(s) = \frac{1}{(\lambda_j-\lambda_p-\lambda_q-\lambda_r)}\left[\frac{1}{(s-\lambda_j)} - \frac{1}{(s-\lambda_p-\lambda_q-\lambda_r)}\right] \tag{B.22}$$

Thus, the final solution of third order terms expressed as a single Laplace transform variable is,

$$Y_j^3(s) = K_1 N_1(s) + K_2 N_2(s) + K_3 N_3(s)$$

$$\begin{aligned} Y_j^3(s) = {} & K_1 \frac{1}{(\lambda_j-\lambda_p-\lambda_q-\lambda_l)}\left[\frac{1}{(\lambda_j-\lambda_l-\lambda_k)}\frac{1}{(s-\lambda_j)} - \frac{1}{(\lambda_p+\lambda_q-\lambda_k)}\frac{1}{(s-\lambda_p-\lambda_q-\lambda_l)}\right] \\ & + K_2 \frac{1}{(\lambda_j-\lambda_p-\lambda_q-\lambda_k)}\frac{1}{(\lambda_p+\lambda_q-\lambda_l)}\left[\frac{1}{(s-\lambda_j)} - \frac{1}{(s_1-\lambda_p-\lambda_q-\lambda_k)}\right] \\ & + K_3 \frac{1}{(\lambda_j-\lambda_p-\lambda_q-\lambda_r)}\left[\frac{1}{(s-\lambda_j)} - \frac{1}{(s-\lambda_p-\lambda_q-\lambda_r)}\right] \end{aligned}$$

$$\begin{aligned} Y_j^3(s) = {} & \\ & C_{kl}^j C_{pq}^k Y_p^1(0) Y_q^1(0) Y_l^1(0) \cdot \\ & \sum_{k=1}^{n}\sum_{l=1}^{n}\sum_{p=1}^{n}\sum_{q=1}^{n} \frac{1}{(\lambda_j-\lambda_p-\lambda_q-\lambda_l)}\left[\frac{1}{(\lambda_j-\lambda_l-\lambda_k)}\frac{1}{(s-\lambda_j)} - \frac{1}{(\lambda_p+\lambda_q-\lambda_k)}\frac{1}{(s-\lambda_p-\lambda_q-\lambda_l)}\right] + \\ & C_{kl}^j C_{pq}^l Y_k^1(0) Y_p^1(0) Y_q^1(0) \cdot \\ & \sum_{k=1}^{n}\sum_{l=1}^{n}\sum_{p=1}^{n}\sum_{q=1}^{n} \frac{1}{(\lambda_j-\lambda_p-\lambda_q-\lambda_k)}\frac{1}{(\lambda_p+\lambda_q-\lambda_l)}\left[\frac{1}{(s-\lambda_j)} - \frac{1}{(s_1-\lambda_p-\lambda_q-\lambda_k)}\right] + \\ & \sum_{p=1}^{n}\sum_{q=1}^{n}\sum_{r=1}^{n} D_{pqr}^j Y_p^1(0) Y_q^1(0) Y_r^1(0) \frac{1}{(\lambda_j-\lambda_p-\lambda_q-\lambda_r)}\left[\frac{1}{(s-\lambda_j)} - \frac{1}{(s-\lambda_p-\lambda_q-\lambda_r)}\right] \end{aligned} \tag{B.23}$$

THIS PAGE IS INTENTIONALLY LEFT BLANK

APPENDIX C
TEST POWER SYSTEMS DATA

C.1 3 GENERATORS, 9 BUSES TEST POWER SYSTEM

Table C1. Line Bus Data

SENDING BUS	RECEIVING BUS	RESISTANCE	REACTANCE	SHUNT SUSCEPTANCE	TAP RATIO
2	7	0	0.0625	0	1
7	8	0.0085	0.072	0.149	1
8	9	0.0119	0.1008	0.209	1
9	3	0	0.0586	0	1
9	6	0.039	0.17	0.358	1
6	4	0.017	0.092	0.158	1
4	5	0.01	0.085	0.176	1

Table C2. Machine Dynamic Data

MACHINE	x_ℓ	r_a	x_d	x'_d	T'_{d0}	x_q	x'_q	T'_{q0}	H	D
G1	0.2	0	0.146	0.0608	8.96	0.0969	0.0608	0.31	23.64	0.0125
G2	0.2	0	0.8958	0.1198	6	0.8645	0.1198	0.535	6.4	0.0068
G3	0.2	0	1.3125	0.1813	5.89	1.2578	0.1813	0.6	3.01	0.0048

Table C3. Power Flow Data

BUS	$\lvert V\rvert$	θ	P_G	Q_G	P_L	Q_L
1	1.04	0	0.716	0.27	0	0
2	1.025	0.1623	1.63	0.067	0	0
3	1.025	0.082	0.85	-0.109	0	0
4	1.026	-0.0384	0	0	0	0
5	0.996	-0.0698	0	0	1.25	0.5
6	1.013	-0.0646	0	0	0.9	0.3
7	1.026	0.0646	0	0	0	0
8	1.016	0.0122	0	0	1	0.35
9	1.032	0.0349	0	0	0	0

C.2 10 GENERATORS, 39 BUSES NEW ENGLAND TEST POWER SYSTEM

Table C4. Line Bus Data

SENDING BUS	RECEIVING BUS	RESISTANCE	REACTANCE	SHUNT SUSCEPTANCE	TAP RATIO
39	30	0.0035	0.0411	0.6987	1
39	1	0.001	0.025	0.75	1
30	37	0.0013	0.0151	0.2572	1
30	25	0.007	0.0086	0.146	1
37	31	0.0013	0.0213	0.2214	1
37	18	0.0011	0.0133	0.2138	1
31	34	0.0008	0.0128	0.1342	1
31	14	0.0008	0.0129	0.1382	1
34	33	0.0002	0.0026	0.0434	1
34	36	0.0008	0.0112	0.1476	1
33	38	0.0006	0.0092	0.113	1
33	11	0.0007	0.0082	0.1389	1
38	36	0.0004	0.0046	0.078	1
36	35	0.0023	0.0363	0.3804	1
35	1	0.001	0.025	1.2	1
32	11	0.0004	0.0043	0.0729	1
32	13	0.0004	0.0043	0.0729	1
13	14	0.0009	0.0101	0.1723	1
14	15	0.0018	0.0217	0.366	1
15	16	0.0009	0.0094	0.171	1
16	17	0.0007	0.0089	0.1342	1
16	19	0.0016	0.0195	0.304	1
16	21	0.0008	0.0135	0.2548	1
16	24	0.0003	0.0059	0.068	1
17	18	0.0007	0.0082	0.1319	1
17	27	0.0013	0.0173	0.3216	1
21	22	0.0008	0.014	0.2565	1
22	23	0.0006	0.0096	0.1846	1
23	24	0.0022	0.035	0.361	1
25	26	0.0032	0.0323	0.513	1
26	27	0.0014	0.0147	0.2396	1
26	28	0.0043	0.0474	0.7802	1
26	29	0.0057	0.0625	1.029	1
28	29	0.0014	0.0151	0.249	1
12	11	0.0016	0.0435	0	1
12	13	0.0016	0.0435	0	1
33	4	0	0.025	0	1
32	10	0	0.02	0	1
19	6	0.0007	0.0142	0	1
20	5	0.0009	0.018	0	1
22	9	0	0.0143	0	1
23	8	0.0005	0.0272	0	1
25	3	0.0006	0.0232	0	1
30	2	0	0.0181	0	1
29	7	0.0008	0.0156	0	1
19	20	0.0007	0.0138	0	1

Table C6. Power Flow Data

BUS	$\|V\|$	θ	P_G	Q_G	P_L	Q_L
1	1.03	-11.13	10	0.904	11.04	2.5
2	1.0475	-4.61	2.5	1.5114	0	0
3	1.0278	1.15	5.4	0.0773	0	0
4	0.982	0	5.7356	2.0889	0.092	0.046
5	1.0123	0.61	5.08	1.6827	0	0
6	0.9972	2.05	6.32	1.1171	0	0
7	1.0265	6.65	8.3	1.0451	0	0
8	1.0635	6.72	5.6	1.0221	0	0
9	1.0493	4.03	6.5	2.1423	0	0
10	0.9831	1.6	6.5	2.0786	0	0
11	1.0121	-7.21	0	0	0	0
12	0.9995	-7.23	0	0	0.085	0.88
13	1.0137	-7.11	0	0	0	0
14	1.011	-8.78	0	0	0	0
15	1.0147	-9.2	0	0	3.2	1.53
16	1.0311	-7.79	0	0	6.29	1.323
17	1.032	-8.79	0	0	0	0
18	1.0296	-9.64	0	0	1.58	0.3
19	1.0496	-3.17	0	0	0	0
20	0.9907	-4.58	0	0	6.8	1.03
21	1.0313	-5.39	0	0	2.74	1.15
22	1.0495	-0.93	0	0	0	0
23	1.0445	-1.13	0	0	2.475	0.846
24	1.0367	-7.68	0	0	3.086	0.922
25	1.0559	-5.64	0	0	2.24	0.472
26	1.0464	-6.89	0	0	1.39	0.47
27	1.0339	-8.93	0	0	2.81	0.755
28	1.0389	-3.3	0	0	2.06	0.276
29	1.0372	-0.47	0	0	2.835	1.269
30	1.0479	-7.03	0	0	0	0
31	1.003	-10.67	0	0	5	1.84
32	1.0166	-6.4	0	0	0	0
33	1.0069	-8.78	0	0	0	0
34	1.0045	-9.49	0	0	0	0
35	1.0279	-11.32	0	0	0	0
36	0.9953	-11.5	0	0	5.22	1.76
37	1.0292	-9.88	0	0	3.22	1.224
38	0.9962	-10.99	0	0	2.338	0.84
39	1.0471	-9.59	0	0	0	0

Table C5. Machine Dynamic Data

MACHINE	x_ℓ	r_a	x_d	x'_d	T'_{d0}	x_q	x'_q	T'_{q0}	H	D
G1	0.003	0	0.02	0.06	7	0.019	0.06	0.7	500	0
G2	0.0125	0	0.1	0.031	10.2	0.069	0.031	1.5	42	0
G3	0.028	0	0.29	0.057	6.7	0.28	0.057	0.41	24.3	0
G4	0.035	0	0.295	0.0697	6.56	0.282	0.0697	1.5	30.3	0
G5	0.054	0	0.67	0.132	5.4	0.62	0.132	0.44	26	0
G6	0.0295	0	0.262	0.0436	5.69	0.258	0.0436	1.5	28.6	0
G7	0.0298	0	0.2106	0.057	4.79	0.205	0.057	1.96	34.5	0
G8	0.0322	0	0.295	0.049	5.66	0.292	0.049	1.5	26.4	0
G9	0.0224	0	0.254	0.05	7.3	0.241	0.05	0.4	34.8	0
G10	0.0304	0	0.2495	0.0531	5.7	0.237	0.0531	1.5	35.8	0

Table C7. Excitation System Data

Generator No.	T_A	K_A
1	0.02	40
2	0.6	40
3	0.2	40
4	0.05	6.2
5	0.2	40
6	0.06	5
7	0.02	5
8	0.02	40
9	0.02	5
10	0.06	5

APPENDIX D
INITIAL CONDITIONS CALCULATIONS
3 SM-9 BUSES TEST POWER SYSTEM

The admittance matrix $\mathbf{Y}_{BUS}$ and the intermediate matrix admittances are calculated among reduced admittance matrix $\mathbf{Y}_{red}$. The numerical matrices obtained are,

$\mathbf{Y}_{BUS}$ =

-17.3611i	0	0	17.3611i	0	0	0	0	0
0	-16.0000i	0	0	0	0	16.0000i	0	0
0	0	-17.0648i	0	0	0	0	0	0 +17.0648i
17.3611i	0	0	3.3074 - 39.3089i	-1.3652 +11.6041i	-1.9422 +10.5107i	0	0	0
0	0	0	-1.3652 +11.6041i	3.8138 - 17.8426i	0	-1.1876 + 5.9751i	0	0
0	0	0	-1.9422 +10.5107i	0	4.1018 - 16.1335i	0	0	-1.2820 + 5.5882i
0	16.0000i	0	0	-1.1876 + 5.9751i	0	2.8047 - 35.4456i	-1.6171 +13.6980i	0
0	0	0	0	0	0	-1.6171 +13.6980i	3.7412 - 23.6424i	-1.1551 + 9.7843i
0	0	17.0648i	0	0	-1.2820 + 5.5882i	0	-1.1551 + 9.7843i	2.4371 - 32.1539i

which is the admittance matrix conformed by the multimachine parameters (basically transmission lines). The matrices that complement the total matrix of the power system are the loads and internal generators parameters, that is,

$$\mathbf{Y}_G = \begin{bmatrix} -16.4474\text{i} & 0 & 0 \\ 0 & -8.3472\text{i} & 0 \\ 0 & 0 & -5.5157\text{i} \end{bmatrix}$$

$$\mathbf{Y}_{LOAD} = \begin{bmatrix} 0 \\ 0 \\ 0 \\ 0 \\ 1.2610 - 0.5044i \\ 0.8776 - 0.2925i \\ 0 \\ 0.9690 - 0.3391i \\ 0 \end{bmatrix}$$

Hence, the complete admittance matrix that includes transmission line parameters, loads and internal generators admittances is,

$\left[\mathbf{Y}_{BUS} + \mathbf{Y}_{LOAD} + \mathbf{Y}_{G}\right] =$

-33.8085i	0	0	17.3611i	0	0	0	0	0
0	-24.3472i	0	0	0	0	16.0000i	0	0
0	0	-22.5806i	0	0	0	0	0	17.0648i
17.3611i	0	0	3.3074 -39.3089i	-1.3652 +11.6041i	-1.9422 +10.5107i	0	0	0
0	0	0	-1.3652 +11.6041i	3.8138 -17.8426i	0	-1.1876 + 5.9751i	0	0
0	0	0	-1.9422 +10.5107i	0	4.1018 -16.1335i	0	0	-1.2820 + 5.5882i
0	16.0000i	0	0	-1.1876 + 5.9751i	0	2.8047 -35.4456i	-1.6171 +13.6980i	0
0	0	0	0	0	0	-1.6171 +13.6980i	3.7412 -23.6424i	-1.1551 + 9.7843i
0	0	17.0648i	0	0	-1.2820 + 5.5882i	0	-1.1551 + 9.7843i	2.4371 -32.1539i

Following the augmented admittance matrix given by Equation (4.13) it yields,

$\mathbf{Y}_{AUG} =$

-16.4474i	0	0	16.4474i	0	0	0	0	0	0	0	0
0	-8.3472i	0	0	8.3472i	0	0	0	0	0	0	0
0	0	-5.5157i	0	0	5.5157i	0	0	0	0	0	0
16.4474i	0	0	-33.8085i	0	0	17.3611i	0	0	0	0	0
0	8.3472i	0	0	-24.3472i	0	0	0	0	16.0000i	0	0
0	0	5.5157i	0	0	-22.5806i	0	0	0	0	0	17.0648i
0	0	0	17.3611i	0	0	3.3074 -39.3089i	-1.3652 +11.6041i	-1.9422 +10.5107i	0	0	0
0	0	0	0	0	0	-1.3652 +11.6041i	3.8138 -17.8426i	0	-1.1876 + 5.9751i	0	0
0	0	0	0	0	0	-1.9422 +10.5107i	0	4.1018 - 16.1335i	0	0	-1.2820 +5.5882i
0	0	0	0	16.0000i	0	0	-1.1876 +5.9751i	0	2.8047 - 35.4456i	-1.6171 +13.6980i	0
0	0	0	0	0	0	0	0	0	-1.6171 +13.6980i	3.7412 -23.6424i	-1.1551 +9.7843i
0	0	0	0	0	17.0648i	0	0	-1.2820 +5.5882i	0	-1.1551 +9.7843i	2.4371 -32.1539i

with reduced admittance matrix agreeing with (4.14),

$\mathbf{Y}_{red} =$

0.8455 - 2.9883i	0.2871 + 1.5129i	0.2096 + 1.2256i
0.2871 + 1.5129i	0.4200 - 2.7239i	0.2133 + 1.0879i
0.2096 + 1.2256i	0.2133 + 1.0879i	0.2770 - 2.3681i

After the calculations of the admittance matrix, steady state initial conditions are necessary before the dynamic analysis. The next set of numerical calculations were obtained with the application of the approach detailed in Section 4.4 (Equations (4.42)-(4.62)), thus resulting,

$$\mathbf{V} = \begin{bmatrix} 1.04 \\ 1.0116 + 0.1653i \\ 1.0216 + 0.0834i \end{bmatrix} \qquad \mathbf{I}_G = \begin{bmatrix} 0.6889 - 0.2601i \\ 1.5799 + 0.1924i \\ 0.8179 + 0.1730i \end{bmatrix}$$

$$\mathbf{E}_i = \begin{bmatrix} 1.0652 + 0.0668i \\ 0.8453 + 1.5311i \\ 0.8040 + 1.1121i \end{bmatrix} \qquad \hat{\delta}_i = \begin{bmatrix} 3.5857 \\ 61.0984 \\ 54.1366 \end{bmatrix}$$

$$\mathbf{I}_d = \begin{bmatrix} 0.3026 \\ 1.2901 \\ 0.5615 \end{bmatrix} \qquad \mathbf{I}_q = \begin{bmatrix} 0.6712 \\ 0.932 \\ 0.6194 \end{bmatrix}$$

$$\mathbf{V}_d = \begin{bmatrix} 0.065 \\ 0.8057 \\ 0.7791 \end{bmatrix} \qquad \mathbf{V}_q = \begin{bmatrix} 1.038 \\ 0.6336 \\ 0.6661 \end{bmatrix}$$

$$\mathbf{E}'_{d0} = \begin{bmatrix} 0.0242 \\ 0.6941 \\ 0.6668 \end{bmatrix} \qquad \mathbf{E}'_{q0} = \begin{bmatrix} 1.0564 \\ 0.7882 \\ 0.7679 \end{bmatrix}$$

$$\mathbf{E}_{fd0} = \begin{bmatrix} 1.0821 \\ 1.7893 \\ 1.403 \end{bmatrix} \qquad V_{texc0} = \begin{bmatrix} 1.04 \\ 1.025 \\ 1.025 \end{bmatrix}$$

$$V_{ref0} = \begin{bmatrix} 1.0941 \\ 1.1145 \\ 1.0951 \end{bmatrix} \qquad P_{mi} = \begin{bmatrix} 0.7164 \\ 1.63 \\ 0.85 \end{bmatrix}$$

$$Q_{mi} = \begin{bmatrix} 0.2705 \\ 0.0665 \\ -0.1086 \end{bmatrix} \qquad \hat{\omega}_0 = \begin{bmatrix} 376.9911 \\ 376.9911 \\ 376.9911 \end{bmatrix}$$

$$\mathbf{x}_0 = \begin{bmatrix} 0.0626 \\ 1.0664 \\ 0.9449 \\ 376.9911 \\ 376.9911 \\ 376.9911 \\ 1.0564 \\ 0.7882 \\ 0.7679 \\ 0.0242 \\ 0.6941 \\ 0.6668 \\ 1.0821 \\ 1.7893 \\ 1.403 \end{bmatrix}$$

All quantities are expressed in per unit, except angles which are expressed in degrees and angular speed in radians per second.

REFERENCES

[Abed and Varaiya 1984]

E. H. Abed and P. P. Varaiya, "Nonlinear oscillations in power systems", International Journal on Electric Power and Energy Systems, Vol. 6, 1984, pp. 37-43

[Acha *et al.* 2004]

E. Acha, C.R. Fuerte-Esquivel, H. Ambriz P. C.A. Camacho, Facts: Modeling and Simulation in Power Networks, John Wiley & Sons, 2004

[Ajjarapu and Lee, 1992]

V. Ajjarapu, B. Lee, "Bifurcation Theory and Its Application to Nonlinear Dynamical Phenomena in an Electrical Power System", IEEE Transactions on Power Systems, Vol.7, No.1, February 1992, pp. 424-431

[Amano 2006]

H. Amano, T. Kumano, H. Inoue, "Nonlinear stability indexes of power swing oscillation using normal form analysis", IEEE Transactions on Power Systems, vol. 21, no. 2, 2006, pp. 825-834.

[Anderson and Fouad 2003]

P.M. Anderson, A.A. Fouad, Power System Control, and Stability, IEEE PRESS, John Wiley & Sons, Second Edition, 2003

[Arroyo 2007]

Jaime Arroyo Ledesma, Non-Linear Analysis of Inter-Area Oscillations Using Normal Form Theory and Carleman Linearization, Doctor of Science Thesis, Centro de Investigación y de Estudios Avanzados del I.P.N. Unidad Jalisco, June 2007

[Arroyo *et al.* 2006]

J. Arroyo, E. Barocio, R. Betancourt, A. R. Messina, "A bilinear analysis technique for the detection and quantification of nonlinear modal interaction in power systems", *IEEE PES General Meeting* 2006, Montreal, Quebec, CA., 18-22 June 2006

[Arrowsmith and Place 1994]

D. K. Arrowsmith, C. M. Place, An Introduction to Dynamical Systems, Cambridge University Press, 1994

[Barocio 2003]

Emilio Barocio Espejo, Assessment of Nonlinear Modal Interaction in Stressed Power Systems Using Normal Forms, Doctor of Science Thesis, CINVESTAV Guadalajara, March 2003

[Barocio and Messina 2002]

Barocio, E.; Messina, A.R., "Analysis of nonlinear modal interaction in stressed power systems with SVCs**",** Power Engineering Society Winter Meeting, 2002, IEEE, Volume 2, Jan. 2002 Page(s):1164 - 1169 vol.2

[Barocio and Messina 2002 a]

E. Barocio, A.R. Messina, "Assessment of Nonlinear Modal Interactions in Stressed Power Systems with FACTS Controllers", 14th PSCC, Sevilla, España, 24-28 June 2002, Session 22, Paper 3

[Barocio and Messina 2003]

E. Barocio, A.R. Messina, "Normal form analysis of stressed power systems: Incorporation of SVC models", *Electrical Power and Energy Systems*, vol. 25, 2003, pp. 79-90.

[Barocio *et al.* 2004]

E. Barocio, A.R. Messina, J. Arroyo, "Analysis of Factors Affecting Power System Normal Form Results", Electric Power Systems Research, Vol. 70, 2004, pp. 223-236

[Betancourt *et al.* 2006]

R. J. Betancourt, E. Barocio, J. Arroyo, A.R. Messina, "A Real Normal Form Approach to the Study of Resonant Power Systems", IEEE Transactions on Power Systems, Vol. 21, No.1, February 2006, pp. 431-432

[Betancourt *et al.* 2009]

R.J. Betancourt, E. Barocio, A.R. Messina, I. Martinez, "Modal analysis of inter-area oscillations using the theory of normal modes", Electric Power Systems Research, Volume 79, Issue 4, April 2009, Pages 576-585

[Bussgang *et al.* 1974]

Julian J. Busggang, Leonard Ehrman, James W. Graham, "Analysis of Nonlinear Systems with Multiple Inputs", Proceedings IEEE, Vol. 62, No. 8, August 1974, pp. 1088-1119

[Cañizares *et al.* 2004]

Claudio Cañizares, Edvina Uzunovic, John Reeve, "Transient Stability and Power Flow Models of the Unified Power Flow Controller for Various Control Strategies", Technical Report #2004-09, Department of Electrical and Computer Engineering, University of Waterloo

[Chen and Chiu 1973]

C.F. Chen, R.F. Chiu, "New Theorems of Association of Variables in Multiple Dimensional Laplace Transform", *Int. J. Systems Sci*., Vol.4, No.4, pp. 647-664, 1973

[Chua and Kokubu, 1988]

Leon O.Chua, Hiroshi Kokubu, "Normal Forms for Nonlinear Vector Fields-Part I: Theory and Algorithm", IEEE Transactions on Circuits and Systems, Vol.35, No.7, July 1988, pp. 863-880

[Chua and Oka, 1988]

Leon O.Chua, Hiroe Oka, "Normal Forms for Constrained Nonlinear Differential Equations-Part I: Theory", IEEE Transactions on Circuits and Systems, Vol.35, No.7, July 1988, pp. 881-901

[Crum and Heinen 1974]

L.A. Crum, J.A. Heinen, "Simultaneous Reduction and Expansion of Multidimensional Laplace Transform Kernels", *SIAM J. Appl. Math*., Vol.26, No.4, pp. 753-771, June 1974

[Debnath 1989]

Joyati Debnath, Narayan Chandra Debnath, "Theorems on Association of Variables in Multidimensional Laplace Transforms", International Journal on Mathematics & Sciences, Vol.12, No.2, pp. 363-376, 1989

[Dobson 2001]

Ian Dobson, "Strong Resonance Effects in Normal Form Analysis and Subsynchronous Resonance", Proceedings of Bulk Power System Dynamics and Control V, Agosto 26-31 de 2001, Onomichi, Japon

[Dobson and Barocio, 2004]

Ian Dobson, Emilio Barocio, "Scaling of Normal Form Analysis Coefficients Under Coordinate Change", IEEE Transactions on Power Systems, Vol.19, No.3, August 2004, pp.1438-1444

[Dong *et al.* 2004]

L. Dong, M.L. Crow, Z. Yang, C. Shen, L. Zhang, S. Atcitty, "A Reconfigurable FACTS System for University Laboratories", IEEE Transactions on Power Systems, Vol. 19, No. 1, February 2004, pp. 120-128

[Fuerte-Esquivel and Acha 1997]

C. R. Fuerte-Esquivel, E. Acha. "Unified power flow controller: a critical comparison of Newton-Raphson UPFC algorithms in power flow studies", IEE Proceedings Generation, Transmission and Distribution, Vol. 144, No. 5, September 1997, pp. 437-444

[George 1959]

Donald A. George, Continuous Nonlinear Systems, Technical Report 355, Massachusetts Institute Of Technology, Research Laboratory Of Electronics, Cambridge, Massachusetts, July 24, 1959

[Gomes Jr. *et al.* 2001]

Gomes, S., Jr.; Martins, N.; Portela, C.; , "Modal Analysis Applied to s-Domain Models of AC Networks," *IEEE Power Engineering Society Winter Meeting, 2001*, vol.3, pp.1305-1310, 2001

[Gomes Jr. *et al.* 2009]

Sergio Gomes Jr., Nelson Martins, Carlos Portela, "Sequential Computation of Transfer Function Dominant Poles of s-Domain System Models", IEEE Transactions on Power Systems, Vol.24, No. 2, May 2009, pp. 776-784

[Guckenheimer and Holmes 1983]

John Guckenheimer, Philip Holmes, Nonlinear Oscillations, Dynamical Systems, and Bifurcations of Vector Fields,Springer-Verlag New York Inc, 1983

[Guo *et al.* 2009]

J. Guo, M.L. Crow, Jagannathan Sarangapani, "An Improved UPFC Control for Oscillation Damping", IEEE Transactions on Power Systems, Vol.24, No. 1, February 2009, pp. 288-296

[Halás *et al.* 2008]

Miroslav Halás, Ulle Kotta, Claude H. Moog, "Transfer Function Approach to the Model Matching Problem of Nonlinear Systems", Proceedings of the 17th World Congress The International Federation of Automatic Control, Seoul, Korea, July 6-11, 2008, pp. 15197-15202

[Hingorani y Giugyi 2000]

N.G. Hingorani, L. Gyugyi, Understanding Facts: Concepts and Technology of flexible AC transmission systems, IEEE Press, 2000

[Huang *et al.* 2000]

Zhengyu Huang, Yixin Ni, C. M. Shen, Felix F. Wu, Shousun Chen, Baolin Zhang, "Application of Unified Power Flow Controller in Interconnected Power Systems-Modeling, Interface, Control Strategy and Case Study", IEEE Transactions on Power Systems, Vol. 15, No. 2, May 2000, pp. 817-824

[Isidori 1989]

Alberto Isidori, Nonlinear Control Systems: An Introduction, Springer Verlag Berlin, Second Edition, 1989

[Jang *et al.* 1998]

Gilsoo Jang, Vijay Vittal, Wolfang Kliemann, "Effect of Nonlinear Modal Interaction on Control Performance: Use of Normal Forms Technique in Control Design", Part I and II, IEEE Transactions on Power Systems, Vol. 13, No. 2, May 1998, pp. 401-407

[Kahn and Zarmi 1998]

Peter Khan, Yair Zarmi, Nonlinear Dynamics Exploration Through Normal Forms, John Wiley & Sons, 1998

[Karmakar 1979]

S. B. Karmakar, "Solution of Nonlinear Differential Equations by Using Volterra Series", Indian J. Pure App. Math, 10(4), pp. 421.425, April 1979

[Klein *et al.* 1991]

M. Klein, G.J. Rogers, P. Kundur, "A Fundamental Study of Interarea Oscillations in Power Systems", IEEE Transactions on Power Systems, Vol.6, No. 3, August 1991, pp. 914-921

[Kshatriya 2003]

Niraj Kshatriya, Improving the Accuracy of Normal Form Analysis, Thesis for degree of master of science, Department of Electrical and Computer Engineering, University of Manitoba, December 2003

[Kshatriya *et al.* 2005]

Niraj Kshatriya, Udaya D. Annakkage, A.M. Gole, Ioni Fernando, "Improving the Accuracy of Normal Form Analysis", IEEE Transactions on Power Systems, Vol.20, N0.1, February 2005, pp.286-293

[Kundur 1994]

Prabha Kundur, Power System Stability and Control, McGraw-Hill, 1994

[Kundur and Wang 2002]

Kundur, P.; Lei Wang; , "Small signal stability analysis: experiences, achievements, and challenges," Power System Technology, 2002. Proceedings. PowerCon 2002. International Conference on , vol.1, no., pp. 6- 12 vol.1, 13-17 Oct 2002

[Lazaro-Castillo 2008]

Isidro I. Lazaro-Castillo, Ingeniería de Sistemas de Control Contínuo, Universidad Michoacana de San Nicolás de Hidalgo, Secretaría de Difusión Cultural y Extensión Universitaria, Second Edition, 2011

[Lin, *et al.* 1996]

Chih-Ming Lin, V.Vittal, W.Kliemann, A.A.Fouad, "Investigation of Modal Interaction and Its Effects on Control Performance in Stressed Power Systems Using Normal Forms of Vector Fields", IEEE Transactions on Power Systems, Vol.11, No.2, May 1996, pp. 781-787

[Liu *et al.* 2004]

S. Liu, A.R. Messina, V. Vittal, "Characterization of Nonlinear Modal Interaction Using Normal Forms and Hilbert Analysis", Power System Conference and Exposition 2004, IEEE PES, 10-13 Oct. 2004, pp. 1113-1118, Vol.2

[Liu, *et al.* 2005]

Shu Liu, A.R. Messina, Vijay Vittal, "Assesing Placement of Controllers and Nonlinear Behaviour Using Normal Form Analysis", IEEE Transactions on Power Systems, Vol.20, No.3, August 2005, pp.1486-1495

[Liu *et al.* 2006]

Liu, S.; Messina, A.R.; Vittal, V., "A Normal Form Analysis Approach to Siting Power System Stabilizers (PSSs) and Assessing Power System Nonlinear Behavior"**,** IEEE Transactions on Power Systems,Volume 21,No. 4, Nov. 2006 Page(s):1755 – 1762

[Liu 2006]

Shu Liu, Assesing Placement of Controllers and Nonlinear Behaviour of Electrical Power System Using Normal Form Information, Thesis of Doctor of Philosophy, Iowa State University, 2006

[Lubbock and Bansal 1969]

J. K. Lubbock, V. S. Bansal, "Multidimensional Laplace Transforms for Solution of Nonlinear Equations", Proceedings IEE, Vol. 116, No. 12, December 1969, pp. 2075-2082

[Martinez *et al.* 2004]

I. Martínez, A.R. Messina, E. Barocio, "Higher-Order Normal Form Analysis of Stressed Power Systems: A Fundamental Study", Electric Power Components and Systems, Taylor & Francis Inc., Vol. 32, pp. 1301-1317, 2004

[Martinez *et al.* 2004*a*]

I. Martínez, A. R. Messina, E. Barocio, "Perturbation analysis of power systems: effects of second and third-order nonlinear terms on system dynamic behavior", *Electric Power Systems Research*, vol. 71, no. 2, 2004, pp. 159-167.

[Martínez 2006]

Irma Martínez Carrillo, A Structure-Preserving Approach to Normal Form Analysis of Power Systems", Doctor of Science Thesis, Centro de Investigación y de Estudios Avanzados del I.P.N. Unidad Jalisco, January 2008

[Martínez *et al.* 2007]

Martinez, I.; Messina, A.R.; Vittal, V.; "Normal Form Analysis of Complex System Models: A Structure-Preserving Approach," *Power Systems, IEEE Transactions on* , vol.22, no.4, pp.1908-1915, Nov. 2007

[Martins *et al.* 1996]

Nelson Martins, Leonardo T. G. Lima, Herminio J. P. Pinto, "Computing Dominant Poles of Power System Transfer Functions", IEEE Transactions on Power Systems, Vol. 11, No. 1, February 1996, pp. 162-170

[Martins *et al.* 2007]

Nelson Martins, Paulo C. Pellanda, Joost Rommes, “Computing of Transfer Function Dominant Zeros with Applications to Oscillation Damping Control of Large Power Systems”, IEEE Transactions on Power Systems, Vol. 22, No. 4, November 2007, pp. 1657-1664

[Martins and Quintao 2003]

Nelson Martins, Paulo E. Quintao, “Computing Dominant Poles of Power System Multivariable Transfer Functions”, IEEE Transactions on Power Systems, Vol. 18, No. 1, February 2003, pp. 152-159

[Mehraeen *et al.* 2010]

Shahab Mehraeen, S. Jagannathan, Mariesa L. Crow, “Novel Dynamic Representation and Control of Power Systems with FACTS Devices”, IEEE Transactions on Power Systems, Vol. 25, No. 3, August 2010, pp. 1542-1554

[Messina, *et al.* 2003]

A.R. Messina, E.Barocio, J.Arroyo, “Analysis of Modal Interaction in Power Systems with FACTS Controllers Using Normal Forms”, IEEE PES General Meeting 2003, Toronto, Canada.

[Messina y Barocio 2002]

A.R. Messina, E. Barocio, “Nonlinear Analysis of Inter-Area Oscillations: Effect of SVC Voltage Support”, Electric Power Systems Research, Vol. 64, 2003, pp. 17-26

[Messina and Vittal 2006]

A. R. Messina, Vijay Vittal, “Nonlinear, Non-Stationary Analysis of Interarea Oscillations Via Hilbert Spectral Analysis”, IEEE Transactions on Power Systems, Vol. 21, No. 3, August 2006, pp. 1234-1241

[Mohler 1991]

Ronald R. Mohler, Nonlinear Systems: Applications to Bilinear Control, Prentice Hall, 1991

[Naghshbandy *et al.* 2010]

Ali H. Naghshbandy, Hasan Modir Shanechi, Ahad Kazemi, Iman Pourfar, “Study of Fault Location Effect on the Interarea Oscillations in Stressed Power Systems Using Modal Series Method”, Electric Engineering 92, Springer-Verlag, pp. 17-26, 2010

[Navabi-Niaki 1996]

Seyed Ali Navabi-Niaki, Modelling and Applications of Unified Power Flow Controller (UPFC) for Power Systems, PhD Thesis, University of Toronto, 1996

[Navabi-Niaki and Iravani 1996]

A. Navabi-Niaki, M.R. Iravani, “Steady-state and dynamic models of unified power flow controller (UPFC) for power system studies”, IEEE Transactions on power systems, Vol.11, No.4, November 1996, pp. 1937-1943

[Nayfeh 1993]

Ali H. Nayfeh, Method of Normal Forms, John Wiley & Sons, 1993

[Pagola *et al.* 1989]

Pagola, F.L.; Perez-Arriaga, I.J.; Verghese, G.C.; "On Sensitivities, Residues and Participations: Applications to Oscillatory Stability Analysis and Control", IEEE Transactions on Power Systems, Vol. 4, Issue 1, Feb 1989, Pages 278 - 285

[Pai 1989]

M. A. Pai, Energy Function Analysis for Power System Stability, Kluwer Academic Publishers, Norwell MA., 1989

[Pariz *et al.* 2003]

Naser Pariz, Hasan Modir Schanechi, Ebrahim Vaahedi, “Explaining and Validating Stressed Power Systems Behavior Using Modal Series”, IEEE Transactions on Power Systems, Vol. 18, No.2, May 2003, pp. 778-785

[Pérez-Arriaga *et al.* 1982]

Perez-Arriaga, I.J.; Verghese, G.C.; Schweppe, F.C.; "Selective Modal Analysis with Applications to Electric Power Systems, PART I and II", *IEEE Transactions on Power Apparatus and Systems*, Vol. PAS-101, No.9, pp.3117-3134, Sept. 1982

[Rodríguez *et al.* 2007]

Osvaldo Rodríguez, C. R. Fuerte-Esquivel, Aurelio Medina, "*A Comparative Analysis of Methodologies for the Representation of Nonlinear Oscillations in Dynamic Systems*", IEEE Power Tech 2007, July 2007, Lausanne, Switzerland

[Rodríguez *et al.* 2009]

Osvaldo Rodríguez, Aurelio Medina, A. Román-Messina, Claudio R. Fuerte Esquivel, "*The Modal Series Method and Multi-Dimensional Laplace Transforms for the Analysis of Nonlinear Effects in Power Systems Dynamics*", IEEE General Meeting 2009, Calgary, Alberta, Canada, July 2009

[Rodríguez and Medina 2010]

Rodriguez, Osvaldo; Medina, Aurelio; "Stressed power systems analysis by using higher order modal series method: A basic study," *Transmission and Distribution Conference and Exposition, 2010 IEEE PES* , pp.1-7, 19-22 April 2010

[Rogers 2000]

Graham Rogers, Power System Oscillations, Kluwer Academic Publishers, 2000

[Rommes and Martins 2006]

Joost Rommes, Nelson Martins, "Efficient Computation of Transfer Function Dominant Poles Using Subspace Acceleration", IEEE Transactions on Power Systems, Vol. 21, No.3, August 2006, pp.1218-1226

[Rommes and Martins 2006a]

Joost Rommes, Nelson Martins, "Efficient Computation of Multivariable Transfer Function Dominant Poles Using Subspace Acceleration", IEEE Transactions on Power Systems, Vol. 21, No.4, November 2006, pp.1471-1483

[Rugh 1981]

Wilson J. Rugh, Nonlinear System Theory. The Volterra/Wiener Approach, The Johns Hopkins University Press, 1981

[Saha *et al.* 1997]

S. Saha, A.A. Fouad, W.H. Kliemann, V. Vittal, "Stability Boundary Approximation of a Power System Using the Real Normal Form of Vector Field", IEEE Transactions on Power Systems, Vol.12, No.2, May 1997, pp. 797-802

[Sanchez-Gasca *et al.* 2005]

J. J. Sanchez-Gasca,V.Vittal, M.J. Gibbard, A.R. Messina, D. J. Vowles, S. Liu, U. D. Annakage, "Inclusion of higher-order terms for small-signal (modal) analysis: committee report –task force on assessing the need to include higher order terms for small-signal (modal) analysis", *IEEE Transactions on Power Systems*, vol. 20, no. 4, pp. 1886-1904, November 2005

[Sauer and Pai 1998]

Peter Sauer, M.A. Pai, Power System Dynamics and Stability, Prentice Hall, 1998.

[Schanechi, *et al.* 2003]

Hasan Modir Shanechi, Naser Pariz, Ebrahim Vaahedi, "General Nonlinear Modal Representation of Large Scale Power Systems", IEEE Transactions on Power Systems, Vol.18, No.3, August 2003, pp 1103-1109

[Schetzen 1980]

M. Schetzen, The Volterra and Wiener Theories of Nonlinear Systems, John Wiley, New York, 1980

[Shmaliy 2007]

Yuriy Shmaliy, Continuous Time Systems, Springer, 2007

[Smith *et al.* 1993]

Smith, J.R.; Fatehi, F.; Woods, C.S.; Hauer, J.F.; Trudnowski, D.J.; "Transfer function identification in power system applications", IEEE Transactions on Power Systems, vol.8, no.3, pp.1282-1290, August 1993

[Starret, S. K. 1994]

Shelli Kay Starret, Application of Normal Forms of Vector Fields to Stressed Power Systems, Doctor of Philosophy Thesis, Iowa State University, Ames, Iowa, 1994

[Starret y Fouad 1998]

S.K. Starret, A.A. Fouad, "Nonlinear Measures of Mode Machine Participation", IEEE Transactions on Power Systems, Vol. 13, No. 2, Mayo de 1998, págs.389-394

[Song and Johns 1999]

Yong-Hua Song, A. T. Johns, Flexible AC Transmission Systems (FACTS), IEE Power Series, 1999

[Tambey y Kotari 2003]

N. Tambey, M.L. Kotari, "Damping of power oscillations with unified power flow controller (UPFC)", IEE Proc. Generation Transmission and Distribution, Vol. 150, No.2, March 2003, pp. 129-140

[Thapar *et al.* 1997]

Jyotika Thapar, Vijay Vital, Wolfang Kliemann, A.A.Fouad, "Application of the Normal Form of Vector Fields to Predict Intearea Separation in Power Systems", IEEE Transactions on Power Systems, Vol.12, No.2, May 1997, pp. 844-850

[Trudnowski *et al*. 1991]

D. J. Trudnowski, J. R. Smith, T. A. Short, and D. A. Pierre, "An Application of Prony Methods in PSS Design for Multimachine Systems", IEEE Transactions *on* Power Systems, Vo1.6, No.1, February 1991, pp. 118-126

[Uzunovic 2001]

Edvina Uzinovic, "EMTP, Transient Stability and Power Flow Models and Controls of VSC Based FACTS Controllers", Doctor of Philosophy Thesis, University of Waterloo, 2001

[Vittal *et al.* 1991]

V. Vittal, N. Bhatia, A. A. Fouad, "Analysis of the inter-area mode phenomenon in power systems following large disturbances", *IEEE Transactions on Power Systems*, vol. 6, no. 4., pp. 1515-1521, November, 1991

[Vittal *et al.* 1998]

V. Vittal, W. Kliemann, D.G.Chapman, A.D. Silk, Y.X.Ni, D.J. Sobajic, "Determination of Generator Groupings for an Island Scheme in the Manitoba Hydro System Using the Method of Normal Forms", IEEE Transactions on Power Systems, Vol.13, No.4, pp. 1345-1351, November 1998

[Yorino *et al.* 1989]

N. Yorino, H. Sasaki, Y. Tamura, R. Yokoyama, "A generalized Analysis Method of Auto-Parametric Resonants in Power Systems", IEEE Transactions in Power Systems, Vol.4, No.3, August 1989, pp. 1057-1064

[Zarghami *et al.* 2010]

M. Zarghami, M. L. Crow, S. Jagannathan, Y. Liu, S. Atcitty, "A Novel Approach to Interarea Oscillation Damping by Unified Power Flow Controllers Utilizing Ultracapacitors", IEEE Transactions on Power Systems, Vol. 25, No. 1, February 2010, pp. 404-412

[Zhu *et al.* 1995]

Xiong-Zhu, Ming-Wu Zhu and Mao-Jun Fan, "The Study of Dynamic Characteristics in Nonlinear Systems", IEEE Transactions on Instrumentation and Measurement, Vol. 44, No. 3, June 1995, pp. 652-656.

[Zhu, *et al.* 2001]

Songzhe Zhu, Vijay Vittal, Wolfang Kliemann, "Analyzing Dynamic Performance of Power Systems Over Parameter Space Using Normal Forms of Vector Fields-Part I and II", IEEE Transactions on Power Systems, Vol.16, No.3, August 2001, pp. 444-450

[Zou *et al.* 2005]

Z.Y. Zou, Q.Y. Jiang, Y.J. Cao, H.F. Wang, "Normal Form Analysis of Interactions Among Multiple SVC Controllers in Power Systems", IEE Proc.-Generation, Transm. Distrib., Vol. 152, No. 4, July 2005, pp. 469-474

[Wang 1997]

Xiaobo Wang, Modal Analysis of Large Interconnected Power Systems, Fortschritt-Berichte VDI, Reihe 6, Nr. 380, Düsseldorf: VDI Verlag, 1997

[Wang 1999]

H.F. Wang, "Damping function of unified power flow controller", IEE Proc. Gener. Transm. Distrib., Vol. 146, No.1, January 1999, pp. 81-87

[Wang *et al.* 1999]

H. F. Wang, F. Li, R. G. Cameron, "Facts Control Design Based on Power System Nonparametric Models", IEE Proceedings Generation, Transmission and Distribution, Vol. 146, No. 5, September 1999, pp. 409-415

[Wang 2000]

Hai Feng Wang, "A Unified Model for the Analysis of FACTS Devices in Damping Power System Oscillations-Part III: Unified Power Flow Controller", IEEE Transactions on Power Delivery, Vol. 15, No. 3, July 2000, pp. 978-983

[Wang 2002]

H.F. Wang, "Interactions and multivariable design of multiple control functions of a unified power flow controller", Electrical Power and Energy Systems, No. 24, 2002, pp. 591-600

[Wu *et al.* 2007]

F.X.Wu; H.Wu; Z.X.Han; D.Q.Gan; "Validation of Power System Nonlinear Modal Methods", Electric Power Systems Research, 77(10), pp. 1418-1424, 2007